



National Library
of Canada

Bibliothèque nationale
du Canada

Ottawa, Canada
K1A 0N4

TC -

0-315-24092-X

CANADIAN THESES ON MICROFICHE SERVICE - SERVICE DES THÈSES CANADIENNES SUR MICROFICHE

PERMISSION TO MICROFILM - AUTORISATION DE MICROFILMER

• Please print or type - Écrire en lettres moulées ou dactylographier

AUTHOR - AUTEUR

Full Name of Author - Nom complet de l'auteur

Amr Waguih Sadek

Date of Birth - Date de naissance

January 13, 1954

Canadian Citizen - Citoyen canadien

☐ Yes - Oui

☒ No - Non

Country of Birth - Lieu de naissance

United Arab Republic

Permanent Address - Résidence fixe

Cairo University,
Guiza, United Arab Republic

THESIS - THÈSE

Title of Thesis - Titre de la thèse

Seismic Response of Inelastic Structures Subjected to

B1 Directional Excitations

Degree for which thesis was presented
Grade pour lequel cette thèse fut présentée

Ph.D.

Year this degree conferred,
Année d'obtention de ce grade

1985

University - Université

McMaster

Name of Supervisor - Nom du directeur de thèse

Dr. W.K. Tso

AUTHORIZATION - AUTORISATION

Permission is hereby granted to the NATIONAL LIBRARY OF CANADA to
microfilm this thesis and to lend or sell copies of the film.

The author reserves other publication rights, and neither the thesis nor extensive
extracts from it may be printed or otherwise reproduced without the
author's written permission.

L'autorisation est, par la présente, accordée à la BIBLIOTHÈQUE NATIONALE
DU CANADA de microfilmer cette thèse et de prêter ou de vendre des ex-
emplaires du film.

L'auteur se réserve les autres droits de publication; ni la thèse ni de longs ex-
traits de celle-ci ne doivent être imprimés ou autrement reproduits sans
l'autorisation écrite de l'auteur.

ATTACH FORM TO THESIS - VEUILLEZ JOINDRE CE FORMULAIRE À LA THÈSE

Signature

Date

July 5, 1985.

NL 91 (1-84/03)

Canada

SEISMIC RESPONSE OF INELASTIC STRUCTURES
SUBJECTED TO BIDIRECTIONAL EXCITATIONS

by

© AMR WAGIH SADEK, B.Sc., M.Eng.

A Thesis

Submitted to the School of Graduate Studies
in Partial Fulfillment of the Requirements
for the Degree
Doctor of Philosophy

McMaster University

May 1985

SEISMIC RESPONSE OF INELASTIC STRUCTURES
SUBJECTED TO BIDIRECTIONAL EXCITATIONS

DOCTOR OF PHILOSOPHY (1985)
(Civil Engineering and
Engineering Mechanics)

McMASTER UNIVERSITY
Hamilton, Ontario

TITLE: Seismic Response of Inelastic Structures Subjected to
Bidirectional Excitations

AUTHOR: Amr Wagih Sadek, B.Sc. (Cairo University)
M.Eng. (McMaster University)

SUPERVISOR: Dr. W. K. Tso

NUMBER OF PAGES: xx, 215

TO MY KIND PARENTS

ABSTRACT

A study has been made of the inelastic seismic response of single story structures having symmetrical as well as asymmetrical configurations and subjected to bidirectional excitations. The intent of this investigation was (i) to assess the significance of force interaction in yielding of columns in the analysis of inelastic structures, (ii) to provide guidelines as how to account for the bidirectionality of the ground motion, and (iii) to clarify the role of "eccentricity" in the lateral-torsional response of inelastic asymmetrical systems.

The elasto-plastic responses of symmetrical systems with interaction effect included or ignored are presented for sinusoidal base motions as well as earthquake ground motions. The latter excitation consisted of five pairs of recorded earthquake ground motions. It is found that the interaction effect is significant for stiff structures with low yield strength and it increases the response. The increase becomes substantial for very stiff structures. For this type of structure, an elasto-plastic analysis using uniaxial excitation could seriously underestimate the displacement ductility demand. It is recommended herein that such structures be designed to remain elastic or almost elastic under expected earthquake disturbances. Taking the interaction effect and the critical orientation of ground motion components into account, the ductility demand can be up to 40% larger than estimates calculated otherwise.

An inelastic analysis of single mass monosymmetrical structural models subjected to the two horizontal components of ground motion is performed. A new concept of eccentricity based on the yield properties of the resisting elements is proposed as a better index to denote the severity of torsion on the inelastic response of asymmetric systems. The ductility demand of asymmetric structures with uniform strength distribution, i.e. with zero plastic eccentricity, are found to be not much different from those of symmetric structures.

ACKNOWLEDGEMENTS

I would like to express my sincere gratitude and indebtedness to my research supervisor, Dr. W. K. Tso, for his consistent guidance, interest, and continuous encouragement throughout the course of this study. It has been a privilege and a pleasure to work under his supervision.

I am greatly indebted to Drs A. C. Heidebrecht, F. A. Mirza, and D. Weaver, members of my supervisory committee, for their valuable comments and suggestions.

I wish to thank my colleagues A.M. Elhossieny, A.Sh. Essawy, and A.E. Elzawahry for their sincere cooperation.

Special thanks are due to my wife for her help, patience, deep understanding, and encouragement towards the completion of this thesis.

Finally, praise be to God who bestowed on me the faith which has been the nourishing source of all my activities including this present work.

TABLE OF CONTENTS

	PAGE
ABSTRACT	iv
ACKNOWLEDGEMENTS	vi
TABLE OF CONTENTS	vii
LIST OF FIGURES	ix
LIST OF TABLES	xiv
LIST OF SYMBOLS	xv
 CHAPTER 1 INTRODUCTION	
1.1 General	1
1.2 Literature Survey	3
1.2.1 Planar Modelling	4
1.2.2 Three Dimensional Modelling	6
1.2.3 Rules of Spatial Combination	8
1.2.4 Effects of Asymmetry	10
1.3 Objectives and Scope	15
 CHAPTER 2 SINUSOIDAL RESPONSE OF INELASTIC COLUMNS SUBJECTED TO BIAXIAL BENDING	
2.1 Introduction	17
2.2 Yielding in Columns Under Biaxial Bending	18
2.2.1 Yield Curves	18
2.2.2 Stiffness Matrix, $[S]^{ep}$	27
2.3 Sinusoidal Response of Columns	30
2.3.1 Equations of Motion	30
2.3.2 Interaction Effects	40
2.3.3 Energy Input	55
2.3.4 Effects of Phase Angle	55
2.3.5 Response of Typical I-Sections	61
2.4 Summary and Conclusions	67
 CHAPTER 3 RESPONSE OF SYMMETRIC STRUCTURES TO EARTHQUAKE EXCITATIONS	
3.1 Introduction	70
3.2 Equations of Motion	71
3.3 Energy Calculations	80
3.4 Effects of Interaction	81

Table of Contents(cont'd)

PAGE

3.4.1.	Ductility Ratio Responses	82
3.4.2	Axisymmetric Properties of the EPI System	93
3.4.3	Energy Input	100
3.4.4	Response to Ensemble of Earthquakes	108
3.5	Approximate Estimates of Ductility Demand	125
3.5.1	Elasto-Plastic Estimators	127
3.5.2	Elastic Estimators	128
3.6	Symmetric Structures with Unequal Periods Along Two Principal Directions	135
3.6.1	Effect on Ductility Demand μ_x	135
3.6.2	Orientation of Ground Motion	137
3.7	Summary and Conclusions	145
CHAPTER 4	RESPONSE OF ECCENTRIC STRUCTURES TO EARTHQUAKE EXCITATIONS	
4.1	Introduction	149
4.2	Formulation and Model Parameters	150
4.3	Effects of Interaction	155
4.4	Plastic Eccentricity Concept	160
4.4.1	Background	160
4.4.2	Definition	162
4.4.3	Effects on Asymmetric Structures	165
4.5	Mass vs Stiffness Unbalanced Eccentric Structures	179
4.6	Edge Displacement	185
4.7	Summary and Conclusions	188
CHAPTER 5	SUMMARY AND CONCLUSIONS	
5.1	SUMMARY	192
5.2	CONCLUSIONS	193
REFERENCES		201
APPENDIX A	DERIVATION OF THE STIFFNESS MATRIX OF AN ELASTO-PLASTIC ELEMENT INCLUDING THE INTERACTION EFFECT	206
APPENDIX B	NUMERICAL INTEGRATION	209

LIST OF FIGURES

FIGURE		PAGE
2.1	Actual and Idealized Geometry of an I-Section	20
2.2	Major and Minor Axes of Shear and Bending	20
2.3	Yield Curves of the Idealized I-Section and Two Typical I-Sections	26
2.4	Yield Curves	28
2.5	Variation of the Stiffness Matrix Coefficients with Angle θ for an Elasto-Plastic Element With Interaction Effect Included	31
2.6	Column Model	33
2.7	Uniaxial Load-Deflection Curves of the Column in Two Directions	34
2.8a	Time Variation of the Displacement Components in the 1-1 and 2-2 Directions of EP Model	41
2.8b	Time Variation of the Displacement Components in the 1-1 and 2-2 Directions of EPI Model	42
2.9	Hysteretic Behavior and f_1 - f_2 Response Curve	43
2.10a	Force Level at First-Time Yield for Different Yield Curves	45
2.10b	Steady State Displacement Amplitudes b_1 and b_2 ; Phase Angle= 0	46
2.11	f_1 - f_2 Response Curves of Models with Different Yield Curves; Phase Angle=90	48
2.12	Steady State Displacement Amplitudes b_1 and b_2 ; Phase Angle=90	49
2.13	Steady State Hysteretic Loops and Plastic Energy Dissipated per Cycle; Phase Angle= 90	51
2.14a	Frequency Response Curves of the Steady State Displacement Amplitudes; $r=0.7$ and $\rho=90$	53

List of Figures (cont'd)

2.14b	Frequency Response Curves of the Steady State Displacement Amplitudes; $r=1.0$ and $\rho=90$	54
2.15a	Frequency Response Curves of the Input Energy per Cycle; $r=0.7$ and $\rho=90$	56
2.15b	Frequency Response Curves of the Input Energy per Cycle; $r=1.0$ and $\rho=90$	57
2.16	Variation of the Steady State Displacement Amplitude Components with ρ ; $r=1.0$ and $\eta^2=0.8$	59
2.17	Locus of the Base Motion and the Top Mass Motion in Plan	60
2.18	Variation of Ratio b_m/b with η^2	62
2.19a	Comparison of Frequency Response Curves of the Light I-Section (W14x82); $\eta=0.7, 1.0$ and $\rho=0$	65
2.19b	Comparison of Frequency Response Curves of the Heavy I-Section (W14x370); $r=0.7, 1.0$ and $\rho=0$	66
3.1	Symmetric Structural Model	73
3.2	Variation of Different Ground Motion Characteristics with Structural Period	76
3.3	Elastic Smooth Spectrum S_a^*/\ddot{u}_{gm}	78
3.4	Ductility Demand μ_x of the EP and EPI Models; $R=5$	83
3.5	Displacement Time History of the EP and EPI Models; $T=2.2$ sec and $R=5$	84
3.6	Displacement Time History of the EP and EPI Models; $T=0.1$ sec and $R=5$	85
3.7	Hysteretic Behavior of the EP and EPI models; $T=2.2$ sec and $R=5$	87
3.8	Hysteretic Behavior of the EP and EPI Models; $T=0.1$ sec and $R=5$	88
3.9	Ductility Demand μ_x of the EP and EPI Models; $R=3, 5$	90
3.10	Ductility Demand μ_x of the EP and EPI Models; $R=5$ 1940 El Centro Ground Motion	91

List of Figures (cont'd)

3.11	Elastic Acceleration Spectrum of the NS and EW Components of the 1940 El Centro Ground Motion; $\xi=0.5\%$	92
3.12	Orientation of the Ground Motion Directions Relative to the Structural Axes	94
3.13	Axisymmetric Resistance Functions of Stiffness and Strength	94
3.14	Time History of the Displacement Components $u_x(t)$ and $u_y(t)$ of the EPI Model; $\theta_g=0, 30, 60$ and $T=1$ sec	96
3.15a	Time History of the radial Displacement $ u_r(t) $ of the EPI Model; $\theta_g=0, 30, 60$ and $T=1$ sec	98
3.15b	Time History of the radial Displacement $ u_r(t) $ of the EP Model; $\theta_g=0, 30, 60$ and $T=1$ sec	98
3.16	Variation of the Radial Ductility Demand μ_r with θ_g in the EP and EPI Models; $R=5$ and $T=1$ sec	99
3.17	Comparison of Ductility Demand Estimates μ_r^* and μ_x ; $R=5$	101
3.18a	Time History of the Energy Input E_I of the EPI Model; $\theta_g=0, 30, 60$ and $T=1$ sec	102
3.18b	Time History of the Energy Input E_I of the EP Model; $\theta_g=0, 30, 60$ and $T=1$ sec	103
3.19	Variation of the Energy Input E_I^* with θ_g in the EP and EPI Models; $R=5$ and $T=1$ sec	104
3.20	Comparison of the Energy Input E_I^* in the EP and EPI Models; $R=3, 5$ and 1952 Taft Ground Motion	105
3.21	Comparison of Estimates of the Energy Input E_I^* ; $R=5$ and 1952 Taft Ground Motion	107
3.22	Mean Elastic Acceleration Spectrum of the Ensemble of Earthquakes Records; $\xi=0.5\%$	111
3.23	C.O.V. of the Elastic Responses to the Ensemble of the Earthquakes Records	112
3.24	Average Ductility Demand μ_x in the EP and EPI Models; $R=3, 5$	113
3.25	Average Ductility Demand μ_y in the EP and EPI Models; $R=3, 5$	114

List of Figures (cont'd)

3.26	Average Ductility Demand μ_r in the EP and EPI Models; $R=3,5$	115
3.27	Variation of the Ductility Demand μ_x with Reduction Factor R in the EP Model; $T=0.1$ sec	118
3.28	Average Radial Permanent Set μ_p in the EP and EPI Models; $R=3,5$	120
3.29	C.O.V. of the Inelastic Responses to the Ensemble of the Earthquakes Records; $R=3, 5$	121
3.30	Mean Values of the Ratio of Ductility Estimates (μ_r^*/μ_x); $R=3, 5$	124
3.31	Ratio of the Energy Input E_I^* in the EPI and EP Models; $R=3,5$	126
3.32	Ratio of Accurate to Approximate Estimates of Ductility Demand (EP-Estimator); $R=3, 5$	129
3.33	Variation of the Amplification Factor $\Gamma(n)$ with Lateral Period T ; $n=3, 5$	132
3.34	Comparison of the Accurate and Approximate Estimates of Ductility Demand (E-Estimator); $R=3$	133
3.35	Comparison of the Accurate and Approximate Estimates of Ductility Demand (E-Estimator); $R=5$	134
3.36	Ductility Demand μ_x of the EPI Models ; $T_y=T_x$, $T_y=(2/3)T_x$, and $T_y=(4/3)T_x$; $R=5$	136
3.37	Variation of the Radial Ductility Demand with θ_g in the EPI Model; $T_x=1$ sec and $T_y=0.67$ sec	139
3.38	Comparison of the Effective Elastic Spectra at $\theta_g=45$ and 135 ; 1940 El Centro and 1952 Taft; $\xi=0.5\%$	140
3.39	Ratio $\mu_r/\mu_r^{(90)}$ in the EPI Models; $T_y=(2/3)T_x$; $R=5$	142
4.1	Symmetric and Monosymmetric Single Mass Structural Models	156
4.2	Ductility Demand on Column 1 in Symmetric and Monosymmetric Configurations of the EP and EPI Models; $R=5$; 1952 Taft Ground Motion	157
4.3	Ratio of the Ductility Demand on Column 1 in the EPI Model to that in the EP Model; Symmetric and Monosymmetric Configurations; $R=5$	158

List of Figures (cont'd)

4.4	Time History of the Deformation Components at CM; System Properties: $e_p=0.2D$, $e=0$, $T_x=1.0$ sec, and $R=5$	164
4.5	Properties of the S and SP Models	166
4.6	Comparison of Rotation $u_{\theta m}$ in the S and SP Models; $R=5$	168
4.7	Comparison of Translation u_{xm} in the S and SP Models; $R=5$	169
4.8	Comparison of the Ductility Demand on Column 1 in the S and SP Models; $R=5$	170
4.9a	Comparison of Rotation $u_{\theta m}$ of Models with Different Values of e_p and e_s ; Left: $e_s=0.2D$ and $e_p=0, 0.1D, 0.2D$; Right: $e_p=0.2D$ and $e_s=0, 0.1D, 0.2D$; $R=5$; 1952 Taft	173
4.9b	Comparison of Rotation $u_{\theta m}$ of Models with Different Values of e_p and e_s ; Left: $e_s=0.2D$ and $e_p=0, 0.1D, 0.2D$; Right: $e_p=0.2D$ and $e_s=0, 0.1D, 0.2D$; $R=5$; 1940 El Centro	174
4.10a	Comparison of Ductility Demand on Column 1 in Models with Different Values of e_p and e_s Including the Symmetric Case, ($e_p=e_s=0$); $R=5$, 1952 Taft	175
4.10b	Comparison of the Ductility Demand on Column 1 in Models with Different Values of e_p and e_s Including the Symmetric Case ($e_p=e_s=0$); $R=5$, 1940 El Centro	176
4.11	Structural Plans	180
4.12	Properties of the M and MP Models	182
4.13	Comparison of Translation u_{xm} and Rotation $u_{\theta m}$ of the MP and SP Models; $R=5$; 1940 El Centro and 1952 Taft	183
4.14	Comparison of the Ductility Demand on Column 1 in the MP and SP Models; $R=5$; 1940 El Centro and 1952 Taft	184
4.15a	Comparison of the Ratio (Δ_x/Δ_{x0}) of Stiffness or Mass Unbalanced Models with Uniform or Nonuniform Strength Distributions; $R=5$; 1952 Taft	186
4.15b	Comparison of the Ratio (Δ_x/Δ_{x0}) of Stiffness or Mass Unbalanced Models with Uniform or Nonuniform Strength Distributions; $R=5$; 1940 El Centro	187

LIST OF TABLES

TABLE		PAGE
2.1	The Variation of the Bracketed Term in Eq (2.6) with Ratio α	23
2.2	Dimensions of Two I Sections (inches)	64
3.1	Information on the Ensemble of Recorded Earthquake Ground Motions	110
3.2	Average Values of COV of Different Response Parameters	123
3.3	Ratios of Accurate to Approximate Estimates of the Ductility Demand	144

LIST OF SYMBOLS

a	spacing between columns
A	amplitude of the acceleration sinusoidal wave
A_F, A_W	area of the flange and the web, respectively, of an I-section
A_y	yield acceleration
$2B$	width of the flange of an I-section
b_1, b_2	steady state displacement amplitudes
b_m	maximum displacement amplitude due to varying phase angle
b_r	maximum radial displacement amplitude in the steady state
$[C]$	damping matrix
CM	center of mass
COV	coefficient of variation
CP	center of yield strength
CS	center of stiffness
D	plan dimension of the slab
$[D]_i$	position matrix of column i
e_m	mass eccentricity
e_p	plastic eccentricity
e_s	stiffness eccentricity
e_y	structural eccentricity in the y direction
E_{ei}	elastic energy capacity in direction i
E_{ii}	input energy to the system in direction i
E_I	total energy input to the system at the end of excitation
E_{ki}, E_{si}, E_{pi}	kinetic, strain, and dissipated plastic energy quantities

List of Symbols (cont'd)

EP	symbol denoting elasto-plastic response
EPI	symbol denoting elasto-plastic response with interaction
$\{f\}$	vector of normalized column forces
f_1, f_2	normalized column forces
F_x, F_y, F_θ	system yield strength in translations and rotation
$\{F_U\}^{(k)}$	vector of unbalanced forces in kth iteration
$\{F_D\}$	vector of damping forces
$\{G\}$	excitation term
h	column height
2H	depth of an I-section
$[I]$	identity matrix
k_1, k_2	elastic stiffness values of a column in local coordinates
K_x, K_y, K_θ	elastic stiffness of the system in translations and rotation
$[K_t]$	tangential global stiffness matrix
$[\bar{K}_t]$	$[K_t]/K_x$
$[K^*]$	effective dynamic stiffness matrix
$[L]_i$	transformation matrix of column i
m	mass of the rigid deck
$[M]$	mass matrix
M_1, M_2	biaxial bending moment with reference to 1-1 and 2-2 axes
M_x, M_y	biaxial bending moment with reference to x and y axes
M_{p1}, M_{p2}	plastic moments with reference to 1-1 and 2-2 axes
M_{px}, M_{py}	plastic moments with reference to x and y axes
m_x, m_y	$M_x/M_{px}, M_y/M_{py}$

List of Symbols (cont'd)

M_L	local magnitude of an earthquake
n	ratio of two reduction factors
$\{n\}$	vector normal to the yield curve
$N(x)$	equation of the neutral axis
$P(t)$	modulus in the polar representation of the bidirectional ground motion as defined in Eq (3.12)
$\{P(t)\}$	vector of applied forces
$\{P^*\}$	effective load vector
p, q	exponents in the interaction expression
$\{q\}$	vector of generalized displacements
q_x, q_y, q_θ	lateral and rotational components of deformation at CM
Q_{ij}	j th effect due to application of the i th component of the ground motion
$\{Q\}$	restoring force vector
Q_x, Q_y, Q_θ	shearing and torque restoring forces at CM
r	excitation level parameter (chapter 2)
r	radius of gyration of the slab about center of mass
R	strength reduction factor defined in Eq (3.6)
$[S]_i$	general stiffness matrix of column i
$[S]^e$	elastic stiffness matrix of the column
$[S]^p$	plastic stiffness matrix of the column
$[S]^{ep}$	elasto-plastic stiffness matrix of the column
S_a	elastic spectral acceleration
S_{ap}	inelastic spectral acceleration
S_a^*	smooth elastic acceleration spectrum

List of Symbols (cont'd)

$S_a(\theta g)$	effective elastic response spectrum
t	time variable in seconds
t_f	depth of the flange of an I-section
T_x, T_y	uncoupled natural periods of the system in lateral directions
$\{u\}$	displacement vector
$\{u\}^e, \{u\}^p$	elastic and plastic components of displacement vector
u_1, u_2	normalized column displacements
u_{p1}, u_{p2}	permanent deformations during the steady state response
$u_x(t), u_y(t)$	lateral deformations of the system
$u_\theta(t)$	rotational deformation of the system
$u_{xm}, u_{\theta m}$	maximum absolute values of $u_x(t)$ and $u_\theta(t)$
$u_r(t)$	radial displacement
$\{\ddot{u}_g(t)\}$	vector containing the horizontal components of the ground motion
$\ddot{u}_g(t)$	$\ddot{u}_g(t)/S_a^*$
\ddot{u}_{gm}	peak ground acceleration
\ddot{u}_{rms}	root mean square acceleration
$\{v\}$	vector of column displacements
$\{v\}^e, \{v\}^p$	elastic and plastic components of displacement vector
V_1, V_2	column shearing forces in two orthogonal directions
V_{p1}, V_{p2}	plastic shear capacity of a section in principal directions
w^p	plastic work
x, y	coordinate axes
x_i, y_i	position coordinates of column i

List of Symbols (cont'd)

x_s, y_s	position coordinates of center of stiffness
x_p, y_p	position coordinates of center of yield strength
α	t_f/H
α_j	factors for combining spatial effects in Eq (1.2)
β, γ	$F_y/F_x, \omega_y/\omega_x$
β_c, γ_c	$V_{p2}/V_{p1}, \omega_2/\omega_1$
δ_1, δ_2	yield deformations of the column in its principal axes
Γ	amplification factors defined in Eqs (3.21) and (3.22)
$\delta_x, \delta_y, \delta_\theta$	overall yield deformations of the system in translations and rotation
η	exciting to system frequency ratio
$\theta(t)$	phase angle defined in Eq (3.12)
θ_g	angle of orientation of the ground motion horizontal components with respect to the structural axes
λ	positive scalar defined in Eq (A.8)
μ_x, μ_y	displacement ductility demand in x and y directions
μ_{px}, μ_{py}	permanent deformations in x and y directions at the end of excitation
μ_r	radial ductility ratio
μ_r^*	radial ductility ratio that is invariant to θ_g
μ_x^*, μ_y^*	maximum values of the ductility demand in the long and short period directions due to orientation of ground motion
μ_{E1}, μ_{E2}	approximate estimates of ductility demand
ν	slope of the neutral axis
ξ	fractional critical damping
ρ	phase angle

List of Symbols (cont'd)

σ_y	yield stress
τ	nondimensional time variable
ϕ	yield function
ω_1, ω_2	uncoupled natural frequencies of the column
$\omega_x, \omega_y, \omega_\theta$	uncoupled natural frequencies of the system in translations and rotation
ω_s	frequency of the sinusoidal wave
Ω	torsional to lateral uncoupled frequencies ratio
$\Delta_x(t)$	edge displacement
Δ_x	maximum edge displacement
Δ_{x0}	maximum edge displacement in a symmetric system
$\Delta(.)$	incremental quantity

CHAPTER 1

INTRODUCTION

1.1 GENERAL :

In dynamic analysis of buildings subjected to earthquake excitations, it has been customary to consider planar models of the structure along its orthogonal principal planes of resistance subjected to components of the ground motion one at a time. This approach requires less effort and cost as compared to a more elaborate three dimensional analysis of the same problem. Nevertheless, one should keep in mind that a building located in a seismic area is generally subjected to the simultaneous action of the multicomponent excitation consisting of three orthogonal translational components and as many rotational components. It is important then that the planar modelling of the problem be justified based on the characteristics and configuration of the building under consideration, in plan as well as in elevation.

For buildings which are regular in elevation, the inclusion of the vertical component of the ground motion is only of secondary importance. This is because this component is less severe as compared to the other horizontal components and at the same time buildings usually possess substantial strength in the vertical direction to resist the gravity loads. It was also shown (25) that the vertical component has a minor effect on the lateral deformations of a structure. Furthermore, the rotational components of the ground motion are usually

ignored because there is little available data on them. Therefore, horizontal components of earthquake ground motions, applied either simultaneously or one at a time, represent the most commonly used input to simulate the earthquake effect on buildings.

To analyze the building under the effect of the two horizontal components, planar modelling can be used provided (i) the building has a symmetric plan, i.e. with coincident centers of mass and rigidity, and (ii) the building remains elastic. In other words, planar modelling is strictly valid for elastic symmetric systems only. However, not many structures in practice qualify for such descriptions. On one hand, it is not economical to design ordinary structures to remain elastic when subjected to severe but rare earthquake excitations and hence inelastic behavior can be expected under such excitations. In the inelastic range, even for symmetric structures, the simultaneous application of the two horizontal components can be significant since the two components can be equally damaging to the structure. To properly account for such effect, the interaction of effects caused by the two components acting on the yielding structure should be considered by extending the uniaxial nonlinear models of resisting elements to the two dimensional case. Since such studies are often costly, they should be only used when the effect of interaction is significant. Therefore, an investigation which examines the significance of such interaction is desirable. Furthermore, the two horizontal components used in the input need not coincide with the ground motions along the principal directions of the structural resistance. In fact, their orientation with respect to the structural axes should be regarded as a random parameter. In

deterministic analyses, the critical orientation that gives a maximum value to a certain response parameter should be considered. Therefore, information on how to incorporate such effect within the framework of planar modelling is required.

A third factor that complicates the situation is that most buildings have some irregularity in plan. Due to this asymmetry, their lateral and torsional deformations are coupled because the centers of floor masses and centers of resistance do not coincide. For such systems, a nonplanar analysis should be considered. Most studies on the lateral-torsional responses assume the structure remains in elastic condition. However for reasons mentioned above and under strong shaking, it is likely that many of the resisting elements will be excited beyond their elastic limits and hence a devoted inelastic analysis of asymmetrical buildings is important.

1.2 LITERATURE SURVEY :

The analysis of the inelastic response of structures to seismic excitations is a very wide subject and the relevant published literature is voluminous. The objective of this survey is to highlight some of the published work that is related to the specific areas of the present study and to introduce to the reader some of the concepts discussed in the subsequent chapters. These areas are the modelling of inelasticity, the representation of the ground motions, and the effects of torsional coupling on the inelastic response of structures. The organization of this survey follows the same logic according to which

the research developed in the subject of inelastic response of structures. For this purpose, the survey is divided into the following sections: (i) planar modelling; (ii) three dimensional modelling; (iii) spatial combination rules; and (iv) effects of asymmetry.

The first section reviews the early studies on the inelastic response of structures to seismic excitations. These planar analyses simplified the problem by assuming that it was sufficient to independently analyze the structure along its principal axes of resistance subjected to horizontal ground motion acting one at a time. However, recognizing that such assumption might be an oversimplification and it might lead to underestimate the response, more elaborate analyses which consider the simultaneous action of the different components of the ground motion on three dimensional structural models have been reported. These studies are reviewed in the second section. Another approach to complement the findings of the planar modelling analyses was to devise approximate schemes to combine the independently obtained planar responses so as to estimate the total response. The development of such schemes is discussed in the section on spatial combination rules.

Asymmetric structures with torsional coupling are one example in which planar modelling is inadequate. Analyses examining the effects of asymmetry on the inelastic response of structures are reviewed in the last section of this survey.

1.2.1 PLANAR MODELLING :

Planar modelling of the problem of the seismic response of inelastic structures has been the subject of many studies either on single story or multi story structures. In such modelling, only one horizontal component of the ground motion is applied to the structural model. Even with the reduction in the amount of calculation by virtue of assuming a planar model, the complexity of the problem requires further simplifying assumptions. Among the assumptions which are common to many studies (40, 54, 55) are the following : (i) the shear beam idealization, in other words, floors are assumed to be rigid and the inelastic action is confined to the columns; (ii) the lumped plasticity assumption, under which the formation of a plastic hinge is restricted to specified sections along the column height, usually the end sections, where maximum stresses are likely to occur; and (iii) the elasto-plastic idealization of the nonlinear behavior of elements.

Less restrictive assumptions were adopted by other studies. Clough et al (10) examined a tall building in which both columns and girders undergo inelastic deformations. They indicated the effectiveness of the strong-column-weak-girder design approach in reducing the ductility demand. According to this approach, columns are designed to remain essentially elastic while girders are designed to be responsible for dissipating the input energy through inelastic behavior.

Instead of restricting the inelastic action to the formation of a plastic hinge, Wen et al (56) allowed the spread of plasticity over a finite length of an inelastic cantilever beam. As a result they observed some reduction in the amount of the plastic drift. However, it was concluded that the system response did not seem to be overly

sensitive to such parameter.

Insofar as the idealization of the material nonlinearity, a general class of inelastic behavior which is similar to the Ramberg Osgood relationship was proposed by Jennings (18). It includes the elasto plastic and the bilinear relationships as special cases. These models can best describe the inelastic cyclic behavior of steel structures. For reinforced concrete elements which exhibit stiffness deterioration with load reversals, simplified degrading stiffness models were proposed (11) and the effect of this feature on response was examined (9,11).

Within the framework of planar modelling it is possible to include other effects in addition to the single horizontal component of the ground motion. Lopez and Chopra (25) considered the simultaneous action of one horizontal component and the vertical component of earthquake excitations on a single story inelastic structure. They concluded that the vertical component has little effect on the lateral deformations of the structure. Gravity effects, or P- Δ effect, however, could be an influential parameter in enhancing the collapse of yielding structures under certain conditions as shown by Jennings and Husid (19). For tall structures with low design strength, there is a high potential of collapse due to the P- Δ effect.

1.2.2 THREE DIMENSIONAL MODELLING :

Planar analyses assume implicitly from the outset that the effect of the simultaneous action of the two horizontal components of the ground motion together with the interaction of the resistance

properties in the plane perpendicular to the one being analyzed are insignificant. While this may be valid in the case of the simultaneous action of one horizontal component and the vertical component as was shown by Lopez and Chopra (25), it is not expected to be the case when considering the two horizontal components. Since these two components can be equally severe, then their simultaneous application can cause simultaneous yielding of some resisting elements.

To study the force interaction effect on the inelastic behavior of structural elements, Nigam (34-36) in his leading work attracted the attention to the fact that, even for simple inelastic elements, ignoring interaction effects is unrealistic. In (34), his main contribution was to bridge the gap between the general theory of inelastic members under combined stresses presented by Hodge (15) and its application to the case of dynamic loadings. In this theory, the concept of a yield surface or a plastic potential is used. The yield surface expression is a function of the generalized forces acting on the element. In addition to the existence of a yield surface, a flow rule which controls the growth of the plastic deformations should be assumed before the stiffness matrix relating the incremental forces and displacements can be found. The reader is referred to Appendix A for more details on the derivation of such matrix.

Nigam also considered the response of single mass two degrees of freedom systems to two horizontal components of base excitation. Under sinusoidal base excitations, he observed that including interaction enhances the energy dissipation capacity of the system and as a result

the steady state displacement response is reduced for most of the range of the exciting to system frequencies ratio. Using an ensemble of five pairs of artificial earthquakes records, the mean displacement response was presented for systems of natural periods ranging between 0.25 to 2.5 sec. Over most of the period range, the effect of interaction was not pronounced as compared to the standard elastoplastic response. More discussion on Nigam's work can be found in the subsequent chapters.

Subsequent to Nigam's work, a number of research papers were published (24, 27, 37-39) addressing the problem of inelastic space frames. A formulation based on the kinematic workhardening flow rule is presented in (24, 37). Mora (39) also simulated the gravity effects by assuming a worksoftening material.

In recognition to the severe damage to the reinforced concrete structures during the 1971 San Fernando earthquake (38) which could not be explained using inelastic planar analyses, extensive work has been done on the biaxial bending of inelastic reinforced concrete columns (1-3, 46). The main effort is on extending the available degrading stiffness uniaxial models (11) into the two dimensional case.

1.2.3 RULES OF SPATIAL COMBINATION :

One design approach to find the maximum response of a structure to a multicomponent excitation is first to evaluate independently the response to each component excitation deemed significant and then combine these spatial effects using some approximate scheme. This is analogous to combining the modal responses of an elastic multidegree of freedom system using the modal combination rules. While the latter has

been receiving considerable attention (57), it was only recently, with the growing concern over the effect of the simultaneous action of the different components of the ground motion, that the spatial combination rules started to attract some attention (4).

The SRSS rule, widely used for modal combination, was the first to be proposed for combining the spatial effects (33). If Q_{ij} is the i th response parameter (displacement, moment, etc.) due to the independent application of the component j of the ground motion, then the combined response Q_i is given by

$$Q_i = \left(\sum_{j=1}^m Q_{ij}^2 \right)^{1/2} \quad (1.1)$$

where m is the number of components considered in the analysis. This rule is based on the stochastic treatment of the problem. Assuming the input motions to be Gaussian processes with zero mean which are statistically independent, then the responses of an elastic system to such disturbances will be of the same nature and the mean square deformation is proportional to the variance. Under these assumptions, the variances of the effects of the different components are additive and so are the squares of the responses.

If, in a two dimensional case, the two horizontal components are further assumed to be of equal intensity and to have identical spectral shapes, identical effects Q_j ($j=1,2$) are obtained. Then it follows from the SRSS rule that the combined response Q is equal to the response to one component Q_1 times $\sqrt{2}$. In other words, the two dimensional nature can be accounted for by increasing the unidirectional response by 40%.

Rosenblueth (44) replaced the quadratic expression in Eq (1.1),

which defines an ellipsoid in the response space, with a linear expression

$$Q = \sum_j \alpha_j Q_j \quad (1.2)$$

In which the combined response is given by a linear combination of the responses to the individual components j . Factors α_j are obtained so as to minimize the error due to the linearization of the quadratic expression and are found to be given by

$$\alpha_1 = 1 ; \alpha_j = 0.3 \text{ for } j \geq 2$$

According to this rule, the combined response is equal to the maximum response due to one component plus 30% of the responses due to other components.

It should be pointed out that these rules are based on the assumption of the statistical independence among the different components of the ground motion which was first introduced by Penzien and Watabe (41). Hence these rules do not account for any correlation that exists in actual recorded ground motions. In addition, the combination rules are derived on the basis of elastic response conditions. Nevertheless, they have been applied to the cases in which inelastic action takes place. The consequences of such application remain an open question.

1.2.4 EFFECTS OF ASYMMETRY:

It is well known that both translational and rotational motions

are induced in asymmetrical structures when subjected to seismic ground motions. Most studies on the lateral-torsional response problems assume the system remains in the elastic range (20, 21, 50). Under strong shaking, it is likely that many of the resisting elements will be excited into the inelastic range and the nonlinear hysteretic effect from inelastic action will affect the lateral-torsional responses of the system. The onset of yielding markedly influences the response of asymmetric structures by : (1) lengthening of the structure periods due to reductions in its stiffness, (2) formation of hysteresis that leads to absorbing energy, and (3) migration of the centre of resistance of the structure with respect to time. The complex interaction between these effects is compounded by the irregular nature of the earthquake excitation.

Little work has been done on this subject using single story models (6, 16, 22, 23, 45, 47, 49, 51-53, 58), and even less has been done to address the full scale problem of multistory buildings (5). The prime concern of these studies is to evaluate the peak ductility demand of the resisting elements. Edge displacement, as an index of the nonstructural damage, is also investigated (6, 51).

The models used in these studies can be broadly classified into two groups :

(1) uniaxial strength models (6, 16, 49, 51, 53) in which the resisting elements can offer resistance only in one direction. The contribution and the interaction of the resistance in the perpendicular direction are ignored.

(2) biaxial strength models (13, 45) in which each column is represented by two independent piecewise linear springs. It was pointed out (45) that the occurrence of yielding in one direction affects the response in the other direction. Based on this observation, the interaction between column forces in yielding is considered in (52, 58), and the concept of the yield surface is used as the yield criterion.

The main findings of these studies are discussed in the following.

(i) Effects of Interaction:

Kan and Chopra (23) replaced the multi element eccentric structure with an equivalent single element model for inelastic torsional response calculation. The single element is located at the initial location of the center of stiffness of the original multi element system. For this single element, an interaction expression is obtained in terms of the overall torque and shear at the element's location. The main effort of this study was to simplify the multi-column problem to the single element model. Clarification of the effects of interaction on the overall system responses was only their secondary objective. Yamazaki (58) considered a four column eccentric model subjected to the two horizontal components of recorded ground motions. Comparing the elasto-plastic and the elasto-plastic with interaction responses he concluded that interaction does not necessarily lead to larger ductility ratios as compared to the case when interaction is ignored.

(ii) Excitation Level :

The displacement response of an inelastic asymmetric structure is an increasing function of the excitation level.

(iii) Pseudo Resonance :

Assuming elastic behavior, this refers to the amplification of the rotational response if the uncoupled torsional to lateral frequency ratio is close to unity provided the system eccentricity is small (20). This phenomenon however seems to lose its impact on the response in the presence of inelastic action. It is shown (6, 51, 53) that this case does not lead to extra large values of the ductility demand in the inelastic response of asymmetric structures. The reason (51) is that due to yielding in the system, the "effective" frequencies of the system are detuned even though the initial uncoupled frequencies are equal.

This observation however differs from the finding given in (22). Kan and Chopra (22) have carried out a parametric study to compare the elastic and inelastic responses of a single mass monosymmetric system under horizontal earthquake (El Centro 1940) ground excitation and concluded that the torsional coupling effect depends significantly on the uncoupled torsional to lateral frequency ratio, being most pronounced for systems with this ratio close to unity.

(iv) Nominal Eccentricity :

Tso and Sadek (51) examined the inelastic response of a single story model consisting of a rigid slab supported on three different frames whose stiffness properties control the value of the system eccentricity. Using two actual earthquake records (1940 El Centro and 1952 Taft), it was found that eccentricity has the effect of increasing the ductility demand by a factor of two and the edge displacement by a factor of three as compared to that of a symmetrical system. Bozorgnia

and Tso (6), using a similar model to the one described above, further indicated that the effect of eccentricity becomes very significant in the case of stiff structures with low design yield strength.

Irvine and Kountouris (16) studied the inelastic response of a simple torsionally unbalanced model consisting of two identical frames supporting a diaphragm and the eccentricity is obtained therein by shifting the center of mass of the diaphragm. They reported that the ductility demand on the most stressed frame is rarely more than 30% greater than that in a similar but symmetric structure and they reached the conclusion that the peak ductility demand and the eccentricity of the structure are only weakly correlated.

There does not appear to be a common concensus regarding the importance of eccentricity on ductility demand at the present time.

(v) Frequency Content of the Ground Motion :

Tso and Sadek (53) pointed out that the ductility demand depends to a great extent on the frequency content of the ground motions, particularly in the period range beyond the elastic period of the structure. This is consistent with the observation that the effective natural periods of systems which are excited well into the inelastic range will be elongated beyond their initial elastic period.

In the light of this information it is possible to characterise ground motions based on the general shape of the associated elastic acceleration response spectra. Bozorgnia and Tso (6) examined the inelastic response of asymmetric structures to two types of ground motions. Ground motions of the first type are those which exhibit very

irregular accelerograms and whose frequency content decreases in the long period range. The other group consists of ground motions having some predominant long period components and as a result their elastic response spectrum exhibit pronounced peaks in the long period range. Since inelastic action leads to elongation of the system period, Bozorgnia and Tso concluded that excitations of the second type will induce substantial deformations in the yielding structure. The 1966 Parkfield and the 1977 Romania earthquake records are used as examples of the second type.

1.3 OBJECTIVES AND SCOPE :

Based on the remarks in Section 1.1 and after reviewing the available literature in Section 1.2, the following objectives are set forth for the present investigation.

(1) To clarify the effects and assess the significance of including the interaction effect in the inelastic analysis of structures so that the designer becomes better informed about the limitations of the inelastic planar modelling. *U*

(2) To provide guidelines as how to account for the bidirectionality of the excitation using uniaxial planar responses.

(3) To clarify the role of the system's parameters of asymmetrical buildings in their inelastic lateral-torsional responses.

The scope of the present study is confined to single story buildings subjected to the two horizontal components of the ground motion. Buildings with both symmetrical as well as monosymmetrical

configurations in plan are studied. To accomplish the stated objectives, the study is organized as follows. In Chapter 2, the behavior of inelastic columns under biaxial bending is discussed using sinusoidal excitation. The concept and the significance of the interaction effect is first introduced using an idealized ground motion. In Chapter 3, the effects of the interaction effect are discussed for inelastic symmetrical systems subjected to earthquake ground motions. In Chapter 4, the inelastic response of asymmetrical buildings subjected to earthquake excitations is discussed. At the end of each chapter, a brief summary of the analysis is presented together with the conclusions obtained pertaining to that particular chapter. Chapter 5 provides an overall review of the work done and the conclusions obtained in this investigation.

CHAPTER 2
SINUSOIDAL RESPONSE OF INELASTIC COLUMNS
SUBJECTED TO BIAXIAL BENDING

2.1 INTRODUCTION :

Columns in low rise buildings can be often modelled as members subjected to biaxial bending only. Axial loads caused by overturning moments are often small and can be ignored. In this chapter, the steps of calculating the response of inelastic columns subjected to biaxial bending are presented. These steps are : (i) the derivation of the yield criterion that takes into account the interaction between the two acting bending moments; and (ii) the formulation of the associated stiffness matrices. Columns of both circular and I sections are considered in this chapter.

The sinusoidal response of the inelastic columns with the interaction effect included or ignored is examined. The present work is based on the study by Nigam (34, 35) with the objective of substantiating its findings on the significance of interaction. The equations of motion are presented in normalized form and the controlling parameters are identified to be: (i) the sinusoidal input frequency to system frequency ratio; (ii) excitation level; and (iii) the phase angle between the two input motions along the principal structural axes. The effects of these parameters are discussed. The conservatism of simple strength interaction formula in design codes is discussed as

applied to the dynamic response of typical I sections.

2.2 YIELDING IN COLUMNS UNDER BIAXIAL BENDING :

Columns in actual buildings are usually subjected to a combination of straining actions. For example, at the joint of two intersecting frames, the column is subjected to biaxial bending, torsional moments, and axial loads. In theory, all these straining actions should be incorporated into the yield criterion of the column. For low rise buildings, the effect of the axial loads on columns is less important as compared to that of bending moments and it is permissible to model the inelastic behaviour of the column by taking into account the biaxial bending only. This simplification is adopted in the present study and yielding caused by biaxial bending moments is considered for a member with an idealized I section and a circular section.

2.2.1 YIELD CURVES :

The column is assumed to be subjected to bending moments M_1 and M_2 along its two principal axes. If the column is assumed to be fixed at both ends, shearing force along one direction is given by $V_i = 2M_i/h$ ($i=1,2$); where h is the column height. Let M_{pi} be the plastic moment capacity of the section in the i^{th} direction. Then the plastic shear capacity can be defined as $V_{pi} = 2M_{pi}/h$. The interaction expressions are most conveniently presented in terms of f_1 and f_2 which are the normalized shearing forces with respect to their respective plastic capacities V_{p1} and V_{p2} . Other straining effects such as axial forces and torsional moments are ignored.

Several assumptions need to be made to simplify the analysis. These assumptions are: (1) the partial plastification of the section is ignored. In other words, the section is assumed to change from the elastic state into the fully plastic state or vice versa. (2) Material is assumed to be elasto-plastic with no work hardening properties. The significance of the work hardening becomes less important in a dynamic analysis than in a static one. This is mainly due to the presence of the inertial forces whose contribution dominates over the contribution of the stiffness-related forces. (3) A stable plastic material is assumed according to Drucker's definition (12). (4) The material is assumed to show neither stiffness nor strength deteriorations when subjected to load reversals.

IDEALIZED I-SECTION

The computation of the yield curve for an actual I section can be greatly simplified by considering an idealized section as shown in Fig (2.1). This idealized section is obtained by ignoring the web and assuming the flanges to be rectangular sections. The consequences of ignoring the web on the interaction expression will be discussed later in this section. For this idealized section, the lower bound approach (15) is employed to derive the yield function ϕ . In this approach, a fully plastic stress distribution is assumed and then the stress resultants satisfying this distribution are found. Assuming zero axial forces, the neutral axis (NA) passes through the centroid of the cross

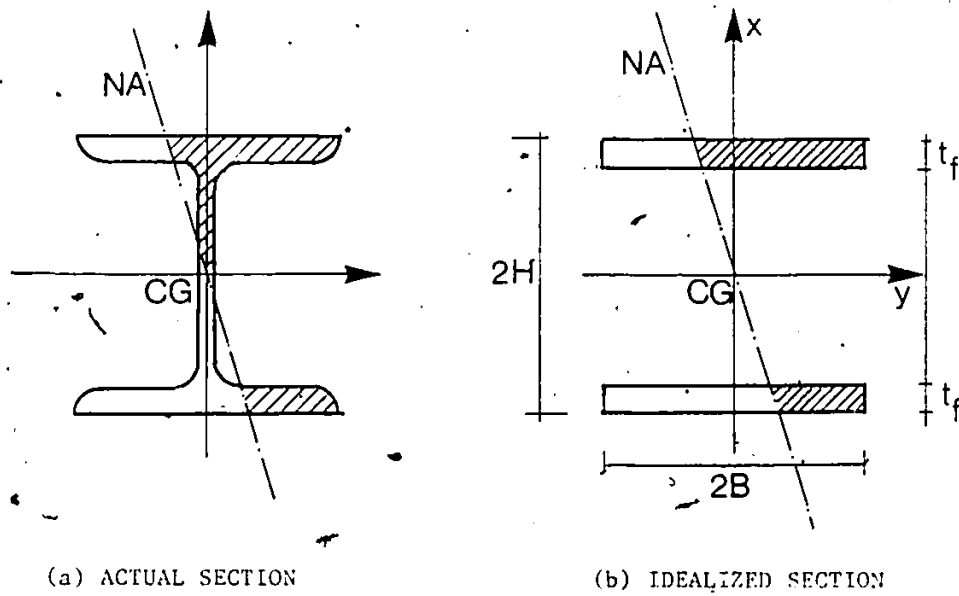


Fig (2.1) Actual and Idealized Geometry of an I-Section

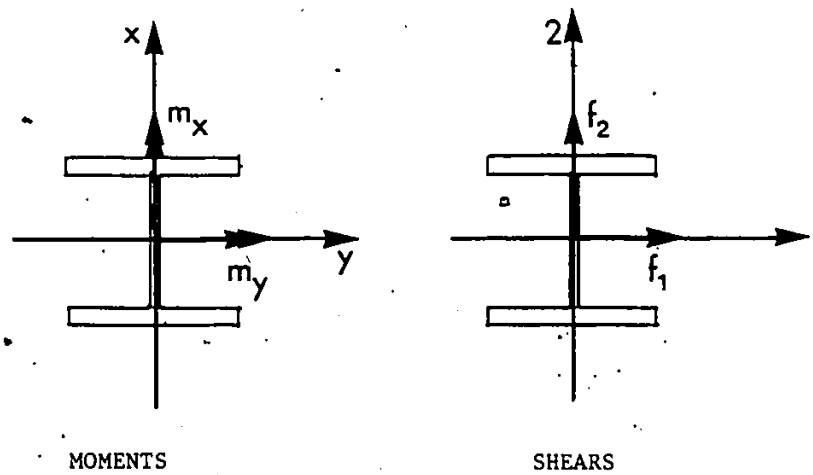


Fig (2.2). Major and Minor Axes of Shear and Bending

section (CG) and divides the cross sectional area into two equal areas. On either side of NA, the yield stress σ_y is uniformly acting in compression or in tension. For any orientation of NA which intersects the flanges, the following expressions of moments M_x and M_y are obtained

$$M_x = \int_{-H}^{-(1-\alpha)H} \left[\int_{-B}^{N(x)} (-\sigma_y) y \, dy + \int_{N(x)}^B (\sigma_y) y \, dy \right] dx + \int_{(1-\alpha)H}^H \left[\int_{-B}^{N(x)} (-\sigma_y) y \, dy + \int_{N(x)}^B (\sigma_y) y \, dy \right] dx \quad (2.1)$$

$$M_y = \int_{-H}^{-(1-\alpha)H} \left[\int_{-B}^{N(x)} (-\sigma_y) x \, dy + \int_{N(x)}^B (\sigma_y) x \, dy \right] dx + \int_{(1-\alpha)H}^H \left[\int_{-B}^{N(x)} (-\sigma_y) x \, dy + \int_{N(x)}^B (\sigma_y) x \, dy \right] dx$$

where $N(x)$ is the equation of NA and is given by vx where v is the slope of NA, and $\alpha = t_f/H$ where t_f is the depth of the flange and $2H$ is the web depth. Performing the integration with respect to y gives

$$M_x = \sigma_y \int_{(1-\alpha)H}^H (B^2 - (N(x))^2) \, dx \quad (2.2)$$

$$M_y = -4 \sigma_y \int_{(1-\alpha)H}^H x N(x) \, dx$$

Substituting with $N(x)=vx$ into Eq (2.2), and integrating with respect to x , there is obtained

$$\begin{aligned}
 M_x &= \frac{2}{3} \sigma_y H^3 [3\alpha(B/H)^2 - v^2(1-(1-\alpha)^3)] \\
 M_y &= -\frac{4}{3} \sigma_y v H^3 [1-(1-\alpha)^3]
 \end{aligned}
 \tag{2.3}$$

Let the plastic moments M_{px} and M_{py} of the idealized section be given by

$$\begin{aligned}
 M_{px} &= 2 \sigma_y \alpha H B^2 \\
 M_{py} &= 2 \sigma_y H^2 B \alpha (2-\alpha)
 \end{aligned}
 \tag{2.4}$$

Normalizing M_x and M_y in Eq (2.3) using M_{px} and M_{py} respectively gives

$$\begin{aligned}
 m_x &= 1 - \frac{1}{3} \frac{v^2}{(H/B)^2} \frac{1-(1-\alpha)^3}{\alpha} \\
 m_y &= \frac{2}{3} \frac{v}{(H/B)} \frac{1-(1-\alpha)^3}{\alpha(2-\alpha)}
 \end{aligned}
 \tag{2.5}$$

where m_x and m_y are the normalized acting moments. Eliminating v from both equations in Eq (2.5) gives the following interaction expression

$$m_x + \left\{ \frac{3}{4} \frac{\alpha(2-\alpha)^2}{1-(1-\alpha)^3} \right\} m_y^2 = 1
 \tag{2.6}$$

The value of the bracketed term in Eq (2.6) is presented in Table (2.1) as a function of $\alpha = t_f/H$. It can be seen that sufficient accuracy is maintained if the bracketed term in Eq (2.6) is replaced by unity. Thus Equation (2.6) reduces to

$$m_x + m_y^2 = 1
 \tag{2.7}$$

Next it is required to express the interaction equation in terms of the

Table 2.1 The Variation of the Bracketed Term in Eq (2.6)
with Ratio α

$\alpha = t_f/H$	$\left\{ (3/4) - \frac{\alpha(2-\alpha)^2}{1-(1-\alpha)^3} \right\}$
0.1	0.999
0.2	0.996
0.3	0.99
0.4	0.98
0.5	0.96

normalized shear forces acting on the column. Let the 1-1 and 2-2 axes be the local axes of the column cross section along which the normalized shear forces f_1 and f_2 act respectively. As shown in Fig (2.2), the f_1 and f_2 components will produce the minor and major bending moments m_x and m_y respectively. Thus Equation (2.7) can be written as follows

$$|f_1| + f_2^2 = 1 \quad (2.8)$$

The modulus sign in Eq (2.8) accounts for the negative values of f_1 . The derived expression has the simple form

$$f_1^p + f_2^q = 1$$

which describes a family of yield curves. Exponents p and q depend on the geometry of the cross section. For the idealized I section, $p=1$ and $q=2$. In general, the direction having the larger exponent, direction 2 in this case, corresponds to the strong axis bending. Since f_2 is always less than unity, then by raising it to a higher power, its contribution in the interaction expression decreases. This is to reflect the larger resistance in this direction.

EFFECT OF IGNORING THE WEB

The ratio of the area of the web (A_w) to the area of the flanges (A_f) is used as a measure of the relative importance of the web in the evaluation of the plastic capacity of the section. For the idealized section in which the web is completely ignored, this ratio (A_w/A_f) is equal to zero. Chen and Atsuta (8) considered the web in their more

elaborate analysis of I sections. They presented interaction expressions for two sections, a light section W8x31 with ratio $A_w/A_f = 0.3$, and a heavier section W14x426 with ratio $A_w/A_f = 0.23$. For both sections, $p=1$, however q was found to be equal to 2.45 and 2.18 for the light and the heavy sections respectively. As expected, including the web leads to larger values of the exponent q in the interaction expression. This implies that including the web contribution makes the difference in strength in the two principal directions more distinct. The interaction curves of these two sections (8) together with that of the idealized section are shown in Fig (2.3). It can be seen that the error introduced due to ignoring the web is not large particularly for the heavy I section. Moreover, the approximate expression predicts lower strength capacity, hence it is more conservative at least from the static point of view.

CIRCULAR SECTIONS

For circular sections, solid or hollow, the interaction expression is available in the literature (34) and is given by

$$f_1^2 + f_2^2 = 1 \quad (2.9)$$

LOWER BOUND AND UPPER BOUND YIELD CURVES

The lower bound yield curve is the one that admits the maximum possible interaction and it can be obtained based on Drucker's definition of a stable plastic material as one exhibiting a

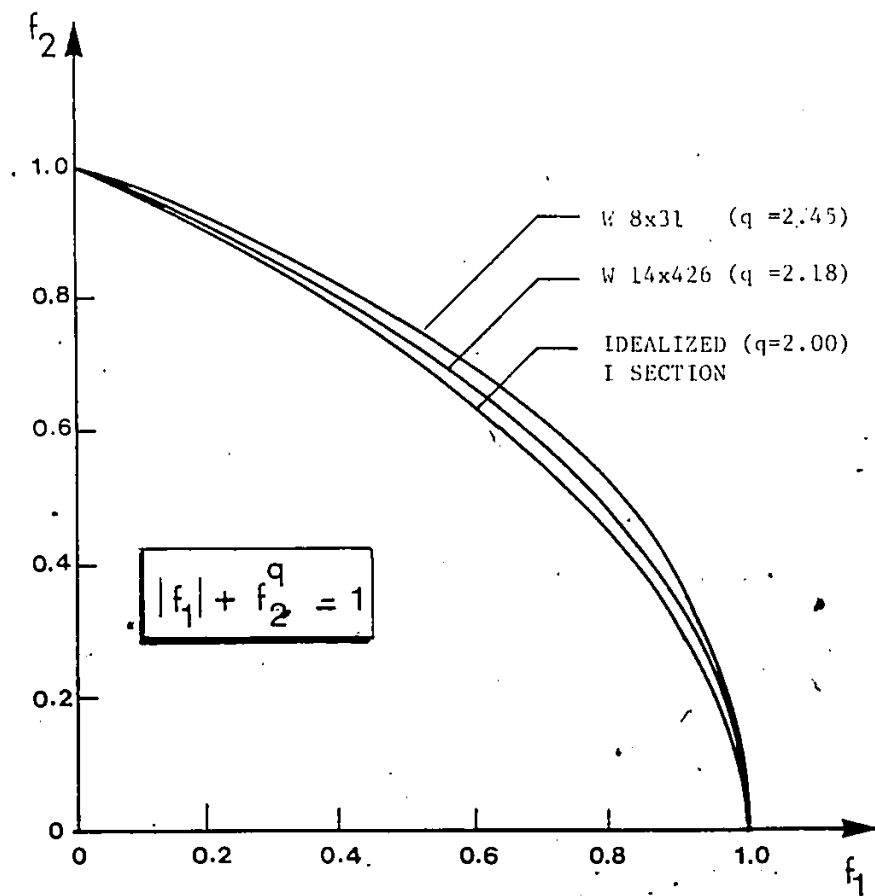


Fig (2.3) Yield Curves of the Idealized I-Section and Two Typical I-Sections

convex yield curve. Therefore, the lower bound yield curve is composed of straight line segments, i.e. of zero curvature, connecting points $f = \pm 1$ as shown in Fig (2.4). Also in the same Figure, the upper most yield curve is shown. It corresponds to the case of no interaction, in other words the element is allowed to reach its full plastic capacity in each direction independent of the state of loading in the other direction. The yield curves for symmetrical sections of different shapes are bounded by these two curves. Therefore, they will be referred to as the lower and upper bound yield curves in this study for ease of identification.

2.2.2 STIFFNESS MATRIX $[S]^{ep}$

It is essential for response calculation purposes to derive the stiffness matrix which relates the incremental forces and displacements at the ends of the inelastic column.

In planar formulations, i.e. when interaction is ignored, the stiffness matrix of an elasto-plastic element is given by the following diagonal matrix

$$[S] = \begin{bmatrix} s_1 & 0 \\ 0 & s_2 \end{bmatrix}$$

where the coefficient s_i ($i=1,2$) either takes on the value of the elastic stiffness k_i when the force in direction i is lower than the uniaxial strength of the element in the same direction, or it is equal to zero otherwise.

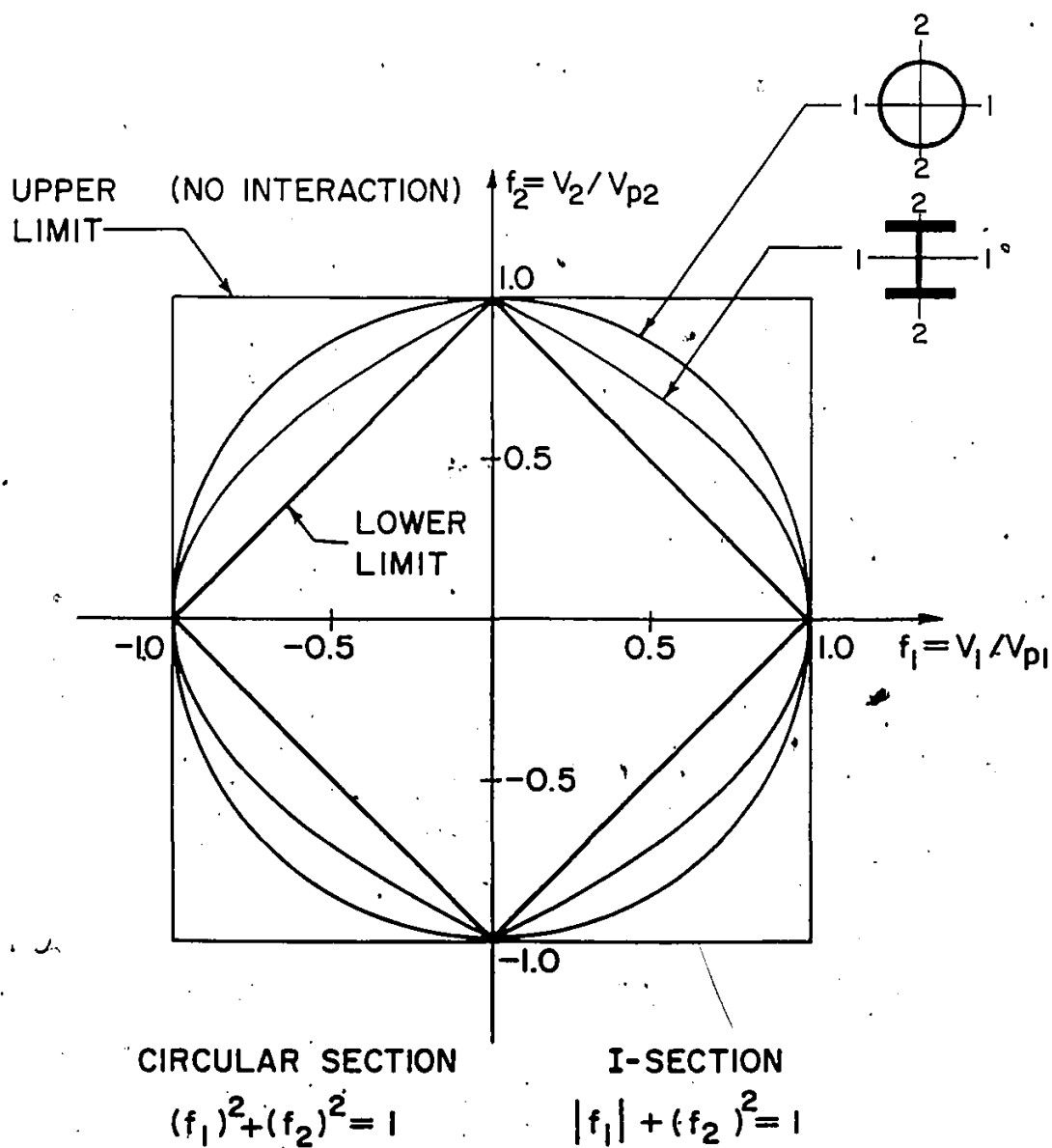


Fig (2.4) Yield Curves

If interaction is included in the formulation, the elasto-plastic stiffness matrix $[S]^{ep}$ can only be obtained after deriving the interaction expression ϕ which defines the yield properties of a section in terms of force components. The theoretical basis of this formulation is outlined in a general form in (15), and is applied in (34). For completeness, the formulation of matrix $[S]^{ep}$ is included in Appendix A in the present thesis. It is given in terms of the derivatives of ϕ with respect to the force components as follows

$$[S]^{ep} = \begin{bmatrix} s_{11} & s_{12} \\ s_{21} & s_{22} \end{bmatrix} = \frac{k_1 k_2}{k_1 \left(\frac{\partial \phi}{\partial V_1} \right)^2 + k_2 \left(\frac{\partial \phi}{\partial V_2} \right)^2} \begin{bmatrix} \left(\frac{\partial \phi}{\partial V_1} \right)^2 & -\left(\frac{\partial \phi}{\partial V_1} \right) \left(\frac{\partial \phi}{\partial V_2} \right) \\ -\left(\frac{\partial \phi}{\partial V_1} \right) \left(\frac{\partial \phi}{\partial V_2} \right) & \left(\frac{\partial \phi}{\partial V_2} \right)^2 \end{bmatrix} \quad (2.10)$$

where V_j ($j=1,2$) are shear forces in the column in the 1-1 and 2-2 directions. It can be shown that determinant $|[S]^{ep}|$ is invariant and is equal to zero. This is a manifestation of the no workhardening assumption used in this study. Under this assumption, values of ϕ larger than one are inadmissible, i.e. $\Delta\phi = 0$, when continuing plastic loading is taking place. Determinant $|[S]^{ep}|$ would have taken on positive or negative values if workhardening or worksoftening, respectively, was assumed in the formulation (39).

In the special case when the elastic stiffness in the two directions are the same, i.e. $k_1=k_2=k$, the sum of the diagonal terms which is given by

$$s_1+s_2 = \frac{k_1 k_2}{k_1 \left(\frac{\partial \phi}{\partial v_1} \right)^2 + k_2 \left(\frac{\partial \phi}{\partial v_2} \right)^2} \left(\left(\frac{\partial \phi}{\partial v_1} \right)^2 + \left(\frac{\partial \phi}{\partial v_2} \right)^2 \right) \quad (2.11)$$

also becomes invariant for all inclinations of the force vector \mathbf{V} in the force space, and the sum reduces to $s_1+s_2=k$.

The variation of the stiffness coefficients with the angle of inclination θ of the force vector \mathbf{f} in the force space, can be demonstrated most conveniently by considering a column with a circular section whose yield curve is also circular. The stiffness coefficients can be represented in terms of θ using the following relationships

$$f_1/\phi = \cos \theta ; \text{ and } f_2/\phi = \sin \theta$$

Then s_1 and s_2 can be shown to vary proportional to $\sin^2 \theta$ and $\cos^2 \theta$ respectively, and s_{12} varies as $(-\sin \theta \cos \theta)$. The variations of these functions are shown in Fig (2.5). It can be seen that including interaction leads to considerable variations in the coefficients of the stiffness matrix as contrasted to the case when interaction is ignored.

2.3 SINUSOIDAL RESPONSE OF COLUMNS :

2.3.1 EQUATIONS OF MOTION :

A simple structural model consisting of a massless inextensible column carrying a rigid mass m at the top, is used as an example for

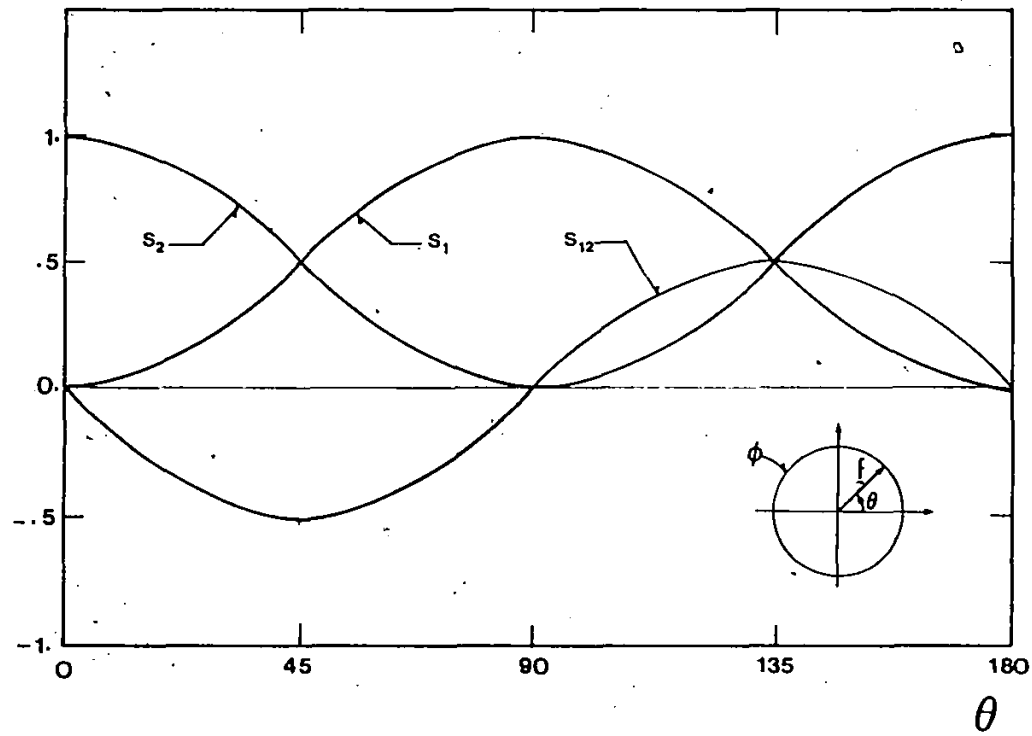


Fig (2.5) Variation of the Stiffness Matrix Coefficients with Angle θ for an Elasto-Plastic Element With Interaction Effect Included

response calculation due to the bidirectional dynamic base excitation as shown in Fig (2.6a). The column is assumed to be clamped at both ends; the deformed shape of the column in one plane is illustrated in Fig (2.6b).

The motion of the mass due to base excitation \ddot{u}_{g1} and \ddot{u}_{g2} along the principal axes of the column, can be adequately described in terms of the generalized displacements v_1 and v_2 as follows

$$\begin{bmatrix} m & 0 \\ 0 & m \end{bmatrix} \begin{Bmatrix} \ddot{v}_1 \\ \ddot{v}_2 \end{Bmatrix} + \begin{Bmatrix} v_1 \\ v_2 \end{Bmatrix} = -m \begin{Bmatrix} \ddot{u}_{g1}(t) \\ \ddot{u}_{g2}(t) \end{Bmatrix} \quad (2.12)$$

where \mathcal{V} is the restoring force vector. In incremental form, forces and displacements are related as follows

$$\Delta \mathcal{V} = [S] \Delta \mathcal{V} \quad (2.13)$$

where $[S]$ is the column stiffness matrix which is dependent on the resistance function assumed and the state of stresses. Two types of inelastic behavior are considered herein.

Type(1): Elasto-Plastic with No Interaction (EP)

In this case the column can be modelled as two independent elasto-plastic springs in the 1-1 and 2-2 directions, characterized by load deflection curves as shown in Fig (2.7). The column stiffness matrix is given by

$$[S] = \begin{bmatrix} s_1 & 0 \\ 0 & s_2 \end{bmatrix} \quad (2.14)$$

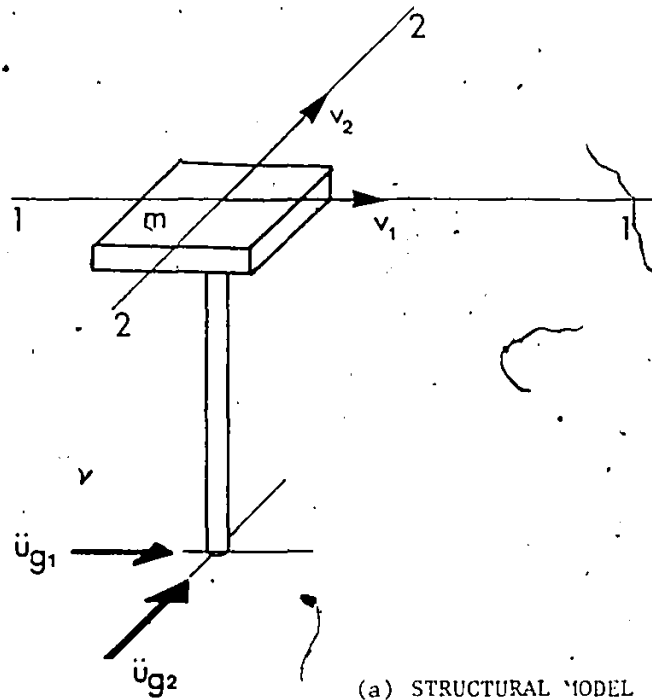


Fig (2.6) Column Model

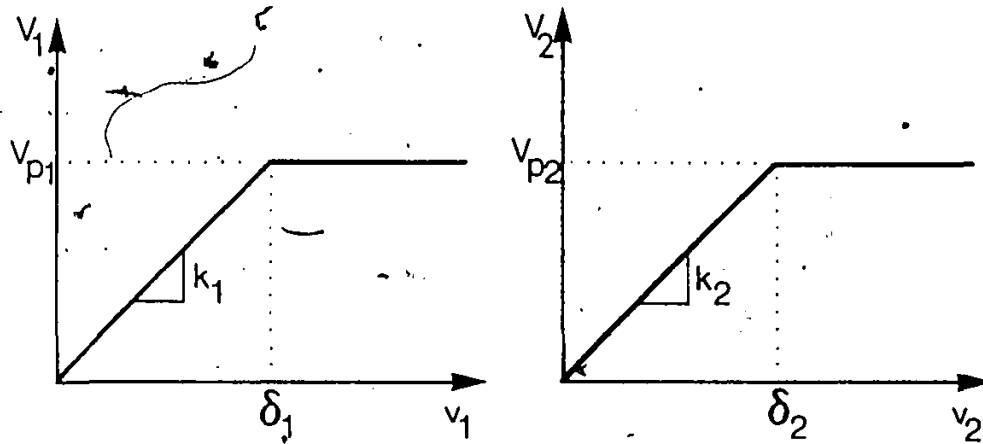


Fig (2.7): Uniaxial Load-Deflection Curves of the Column in Two Directions

where $s_i = k_i$ or 0 depending on whether V_i is less than or equal to V_{pi} respectively.

Type(2) Elasto-Plastic with Interaction (EPI).

If the interaction between the two lateral components of the shearing force V_1 and V_2 is considered, the yield criterion is given by the yield curve ϕ . The column can be in one of the following conditional states:

(i) Elastic: the column is said to be elastic if $\phi < 1$

$$[S] = [S]^e = \begin{bmatrix} k_1 & 0 \\ 0 & k_2 \end{bmatrix} \quad (2.15)$$

(ii) Plastic: if $\phi = 1$ and the incremental plastic work is positive, then the fully plastic state is assumed for which

$$[S] = [S]^{ep} = [S]^e - [S]^p$$

where

$$[S]^p = \frac{1}{k_1 \left(\frac{\partial \phi}{\partial V_1} \right)^2 + k_2 \left(\frac{\partial \phi}{\partial V_2} \right)^2} \begin{bmatrix} k_1^2 \left(\frac{\partial \phi}{\partial V_1} \right)^2 & k_1 k_2 \left(\frac{\partial \phi}{\partial V_1} \right) \left(\frac{\partial \phi}{\partial V_2} \right) \\ k_1 k_2 \left(\frac{\partial \phi}{\partial V_1} \right) \left(\frac{\partial \phi}{\partial V_2} \right) & k_2^2 \left(\frac{\partial \phi}{\partial V_2} \right)^2 \end{bmatrix} \quad (2.16)$$

As for the excitation to the system, the ground motion is given by two lateral components of sinusoidal waves along orthogonal directions. The two waves have identical acceleration amplitudes, A ,

and frequencies, ω_s . The wave along the 2-2 direction lags the one in the 1-1 direction by an angle ρ . These components are expressed as follows

$$\begin{aligned}\ddot{u}_{g1}(t) &= A \sin(\omega_s t) \\ \ddot{u}_{g2}(t) &= A \sin(\omega_s t + \rho)\end{aligned}\quad (2.17)$$

Equation (2.12) can be put into a nondimensional form by dividing the first and the second rows by $V_{p1} = k_1 \delta_1$ and $V_{p2} = k_2 \delta_2$ respectively, there is obtained

$$\begin{bmatrix} 1 & 0 \\ 0 & 1/\gamma_c^2 \end{bmatrix} \begin{Bmatrix} \ddot{u}_1 \\ \ddot{u}_2 \end{Bmatrix} + \omega_1^2 \begin{Bmatrix} f_1 \\ f_2 \end{Bmatrix} = -\omega_1^2 \begin{Bmatrix} r \sin(\omega_s t) \\ (r/\beta_c) \sin(\omega_s t + \rho) \end{Bmatrix} \quad (2.18)$$

where

$$u_1, u_2 = v_1/\delta_1, v_2/\delta_2;$$

$$f_1, f_2 = V_1/V_{p1}, V_2/V_{p2};$$

$$\omega_1, \omega_2 = \sqrt{k_1/m}, \sqrt{k_2/m};$$

$$\gamma_c = \omega_2/\omega_1; \text{ and } \beta_c = V_{p2}/V_{p1}.$$

The nondimensional amplitude r is given by A/A_{y1} , where A_{y1} is an acceleration value which will cause the column to just reach yield in direction 1-1, independent of direction 2-2. In other words, $A_{y1} = V_{p1}/m$. The ratio r serves as a measure of the intensity of the excitation.

Furthermore, if a nondimensional time variable $\tau = \omega_1 t$ is introduced, then Eq (2.18) can be rewritten as follows

$$\begin{bmatrix} \ddot{u}_1 \\ \ddot{u}_2 \end{bmatrix} + \begin{Bmatrix} f_1 \\ \gamma_c^2 f_2 \end{Bmatrix} = - \begin{Bmatrix} r \sin(\eta \tau) \\ (\gamma_c^2 / \beta_c) r \sin(\eta \tau + \rho) \end{Bmatrix} \quad (2.19)$$

where η is the excitation frequency to the column natural frequency ratio, and dots represent differentiation with respect to τ .

SYSTEM PARAMETERS :

For a column of circular cross section, the column has identical stiffness and plastic capacity in the 1-1 and 2-2 directions, i.e. $\gamma_c=1$ and $\beta_c=1$, then Equation (2.19) indicates that the controlling parameters are

- (1) Excitation level parameter r ; its value ranges from 0.5 to 1.0 in this study.
- (2) Excitation to system frequency ratio η ; values of η^2 in this study range from 0.1 to 2.0.
- (3) Phase angle ρ ; values between 0° and 90° are assigned to ρ .

ENERGY CALCULATIONS :

From Eq (2.12), the equilibrium of forces in one direction i can be expressed as follows

$$m\ddot{v}_i + V_i = -m\ddot{u}_{gi} \quad (2.20)$$

The present model has a movable base which is excited by \ddot{u}_{gi} . However, the above equation which is expressed in terms of the relative displacement coordinate v_i , can as well describe a system with an immovable base and whose mass is acted upon by a force $(-m\ddot{u}_{gi})$. Hence the following energy calculation accounts for the relative energy

quantities only. Let the system of forces in Eq (2.20) undergo an incremental displacement dv_i , then the work done by the system is given by

$$m\ddot{v}_i dv_i + V_i dv_i = -m\ddot{u}_{gi} dv_i \quad (2.21)$$

Integrating Eq(2.21) from at-rest conditions to the point that the displacement of the system is equal to v_i yields the following energy equation

$$\int_0^{v_i} m\ddot{v}_i dv_i + \int_0^{v_i} V_i dv_i = \int_0^{v_i} -m\ddot{u}_{gi} dv_i \quad (2.22)$$

In this equation, the first term represents the kinetic energy \bar{E}_{ki} , and the second term is equal to the sum of the strain energy stored in the system \bar{E}_{si} and the energy dissipated by plastic deformations \bar{E}_{pi} . The right hand side of the equation gives the energy imparted to the system in direction i , \bar{E}_{ii} . Hence, the equation of energy balance in direction i , which should be satisfied at any time instant, is given by

$$\bar{E}_{ki} + (\bar{E}_{si} + \bar{E}_{pi}) = \bar{E}_{ii} \quad (2.23)$$

To facilitate the evaluation of the energy integrals, the following change of variables is made

$$\bar{E}_{ki} = \int_0^{v_i} m\dot{v}_i dv_i$$

$$\bar{E}_{si} + \bar{E}_{pi} = \int_0^{v_i} V_i (dv_i^e + dv_i^p) \quad (2.24)$$

$$\bar{E}_{ii} = \int_0^t m\ddot{u}_{gi} \dot{v}_i dt$$

In the second integral, the incremental displacement dv_i is decomposed into its elastic and plastic components to allow the separation of the strain energy and the plastic energy quantities. Substituting $dv_i^e = dV_i/k_i$ and simplifying the above integrals gives

$$\begin{aligned}\bar{E}_{ki} &= m\dot{v}_i^2/2 \\ \bar{E}_{si} &= v_i^2/2k_i \\ \bar{E}_{pi} &= \int_0^{v_i^p} V_i dv_i^p\end{aligned}\quad (2.25)$$

Normalizing the above expressions with respect to the elastic energy capacity in direction i , $E_{ei} = k_i \delta_i^2/2$, and recognizing that $u_i = v_i/\delta_i$ and $f_i = V_i/k_i \delta_i$, gives

$$\begin{aligned}E_{ki} &= (\dot{u}_i/\omega_i)^2 \\ E_{si} &= f_i^2 \\ E_{pi} &= 2 \int_0^{u_i^p} f_i du_i^p\end{aligned}\quad (2.26)$$

Also normalizing \bar{E}_{ii} with E_{ei} and writing $\bar{u}_{gi} = A \sin \omega_i t$ gives

$$E_{ii} = 2 \int_0^t r \sin \omega_i t \dot{u}_i dt \quad (2.27)$$

The energy expressions in Eqs (2.26) and (2.27) can be expressed in terms of τ and its derivatives as follows

$$\begin{aligned}E_{ki} &= \dot{u}_i^2 \\ E_{si} &= f_i^2 \\ E_{pi} &= 2 \int_0^{u_i^p} f_i du_i^p\end{aligned}\quad (2.28)$$

$$E_{11} = 2 \int_0^{\tau} r \sin \eta \tau \dot{u}_1 d\tau$$

The energy integrals are numerically evaluated using the trapezoidal rule.

2.3.2 INTERACTION EFFECTS :

To study the interaction effect, the sinusoidal response of the single mass system with a column of a circular cross section is computed, first with interaction included (EPI) and then with interaction effect ignored (EP). Other parameters of the model are $\eta^2=0.8$, $r=1$, and $\rho=30^\circ$. At the steady state stage, the displacement responses u_1 and u_2 can be expressed as follows

$$\begin{aligned} u_1 &= b_1 \sin(\eta \tau) + u_{p1} \\ u_2 &= b_2 \sin(\eta \tau + \rho) + u_{p2} \end{aligned}$$

where displacement amplitudes b_1 , b_2 and permanent sets u_{p1} , u_{p2} are illustrated in Fig (2.8). With no interaction, the steady state response in directions 1-1 and 2-2 are identical except for phase differences due to the nonzero value of the phase angle ρ in the input motion. Including interaction however leads to significantly different responses in the two directions as shown in Fig (2.8b). Figure (2.9) compares the hysteretic behavior in the two cases. With no interaction, the top figures show the well known elasto-plastic hysteretic behavior. On the other hand, the bottom figures show that interaction influences

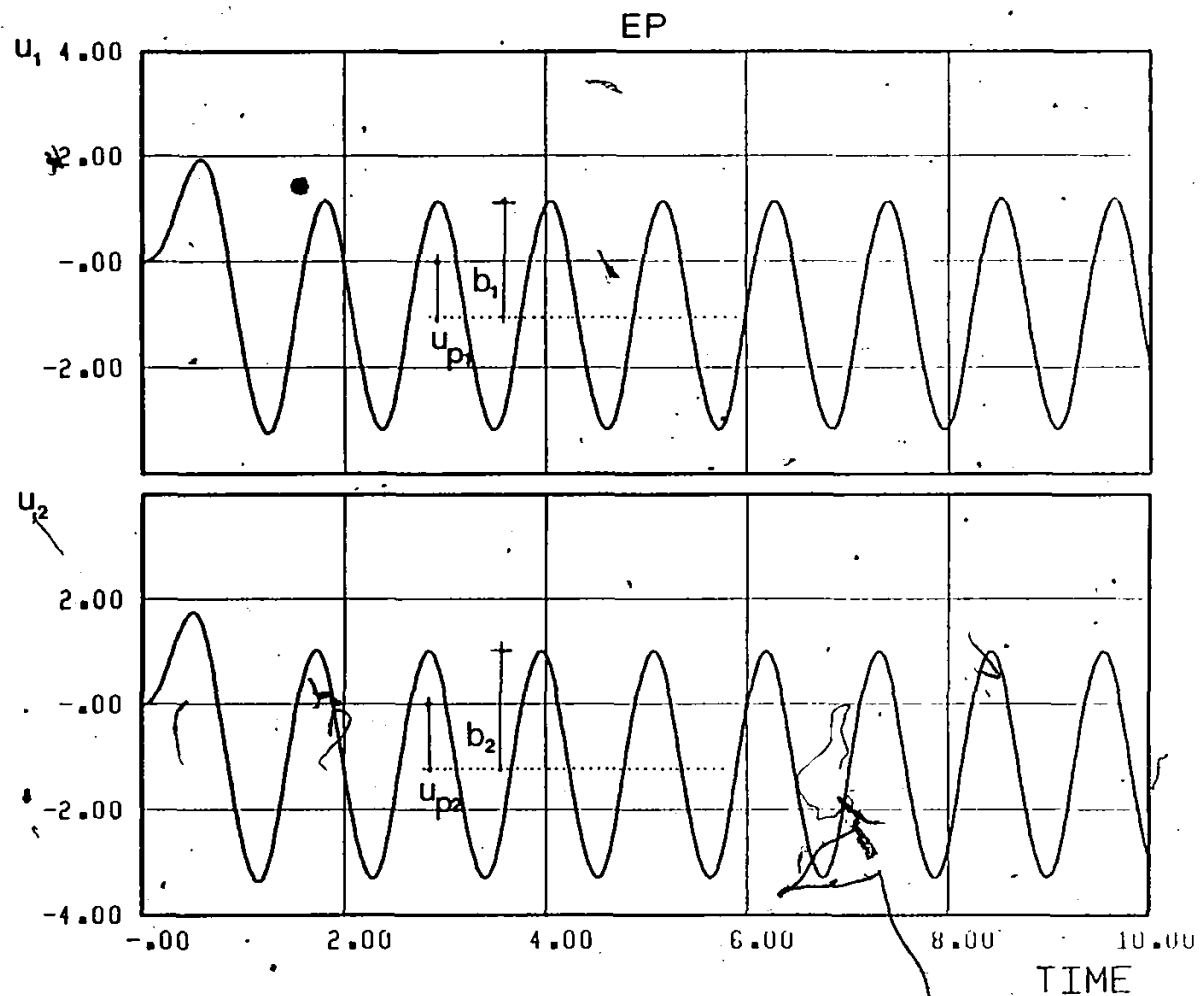


Fig (2.8a) Time Variation of the Displacement Components in the 1-1 and 2-2 Directions of EP Model.

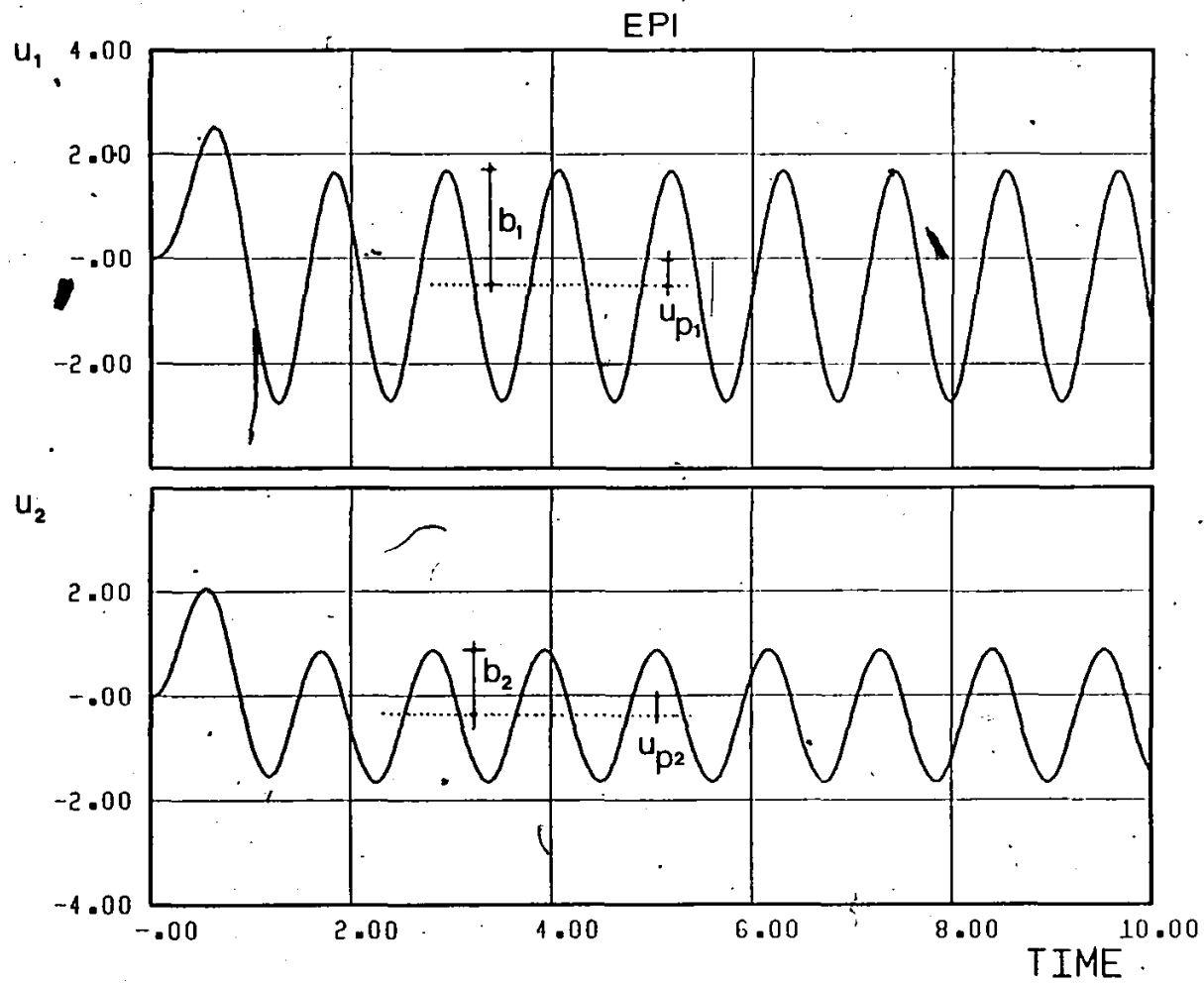
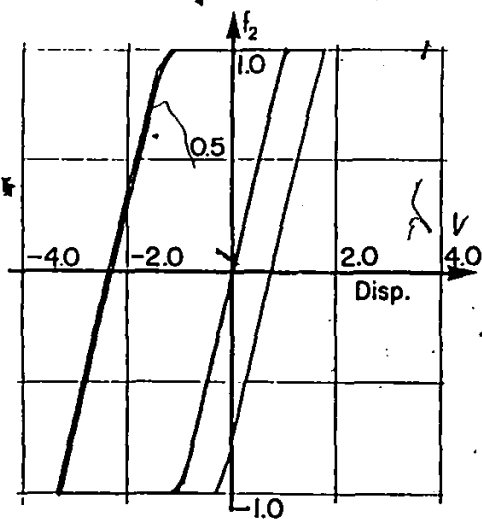
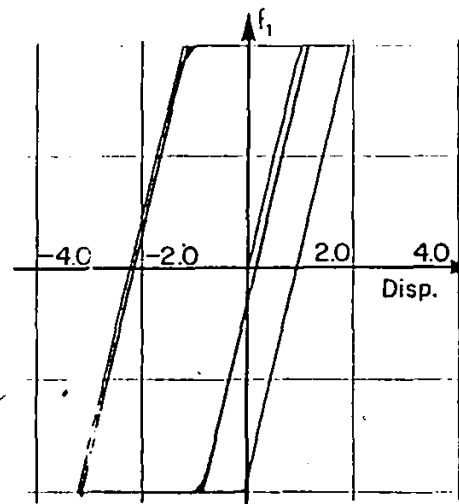


Fig (2.8b) Time Variation of the Displacement Components in the 1-1 and 2-2 Directions of EPI Model



I. NO INTERACTION
 SINUSOIDAL EXCITATION
 Phase Angle = 30.0



II. INTERACTION

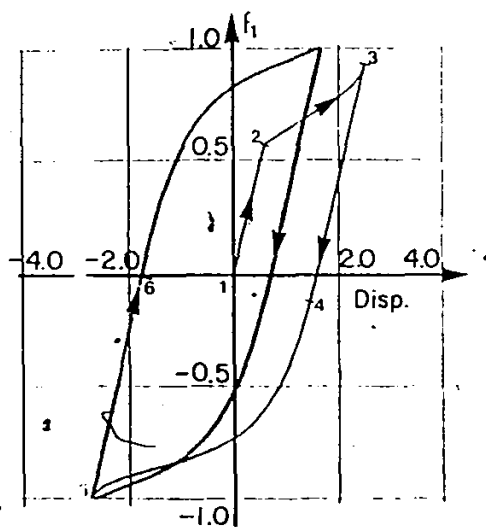
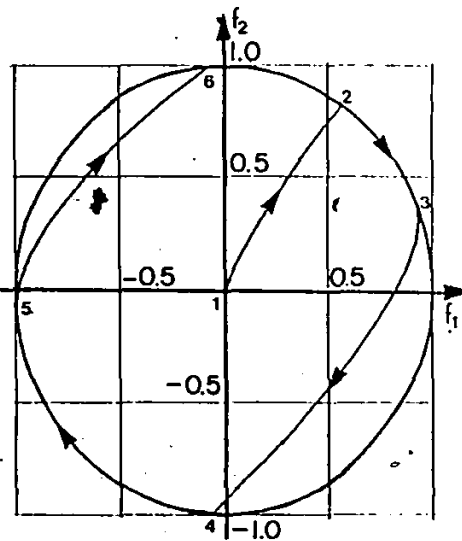
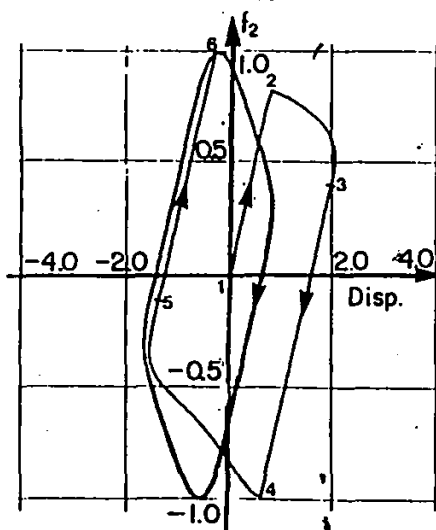


Fig (2.9) Hysteretic Behavior and f_1 - f_2 Response Curve

the stiffness properties of the column in the two directions depending on the relative position of the force vector f from the yield curve. To clarify this dependence, the locus of the tip of the force vector in the f_1 - f_2 space is included in Fig (2.9). While the tip of the force vector remains inside the yield curve, as in segment 1 to 2, the column remains elastic and possesses full elastic stiffness in the two directions. Reaching the yield curve at point 2, the column is said to be in the plastic state and as the force vector slips downward from point 2 to point 3, f_1 increases and f_2 decreases along the curved portions 2-3 in the respective force-displacement diagrams. Once the force vector departs from the yield curve at point 3, the column starts unloading with elastic stiffness indicated in the hysteresis as straight line segments 3 to 4. Similarly, behavior can be interpreted up to point 6 in the figure.

EFFECT OF YIELD CURVES ON THE STEADY STATE RESPONSES

One important effect of shear forces interaction in yielding of the column is the reduction of the force level at which inelastic action is initiated. Using columns modelled with different yield curves and subjected to sinusoidal excitation with phase angle $\rho=0^\circ$, Figure (2.10a) shows the shear force level when the tip of the force vector first reaches the yield curve. For the upper bound yield curve corresponding to the case of no interaction, this force level is given by $f_1=f_2=1$. In other words column will not yield in one direction until its uniaxial yield strength in the same direction is reached. For lower yield curves, this force level decreases being minimum for the lower bound

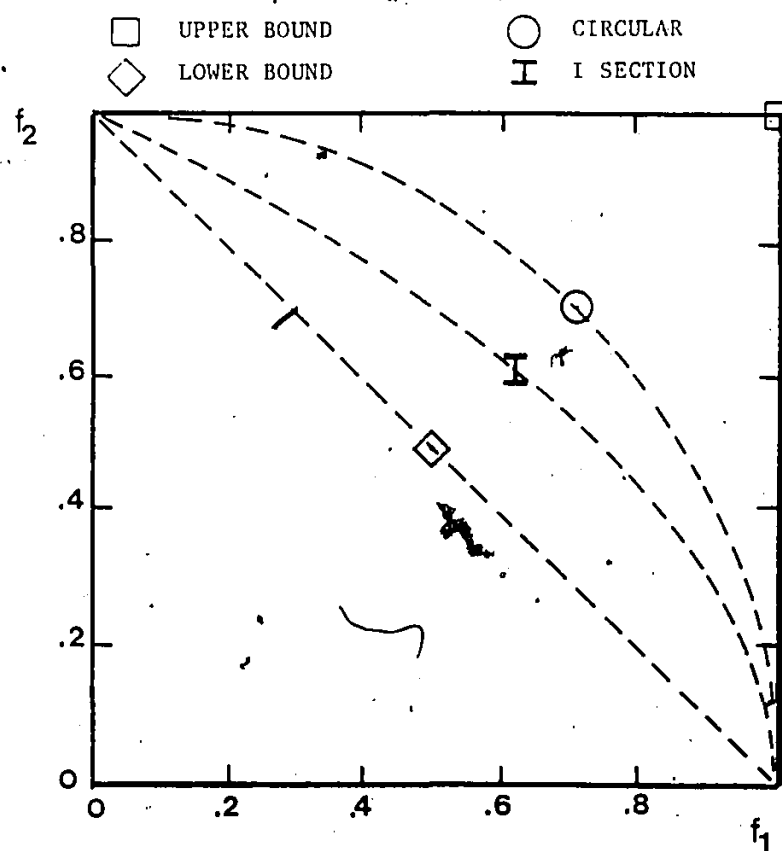


Fig (2.10a). Force Level at First-Time Yield for Different Yield Curves

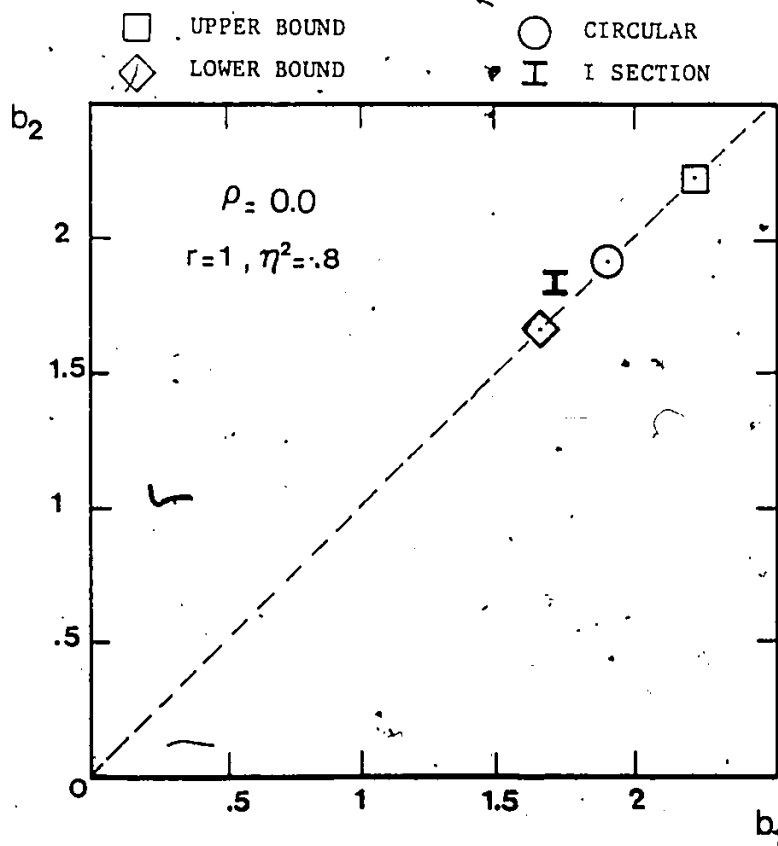


Fig (2.10b) Steady State Displacement Amplitudes b_1 and b_2 ; Phase Angle = 0

yield curve, $f_1=f_2=0.5$. If other parameters of the model are taken to be $\eta^2=0.8$, and $r=1$, Figure (2.10b) shows the steady state displacement amplitudes b_1 and b_2 . It can be seen that displacement response correlates with the yield force level. The lower the yield level, smaller b_1 , b_2 responses become. With the inelastic behavior initiated earlier in the time history of response, more energy is dissipated through hysteretic behavior at earlier stages and the displacement response is eventually reduced.

A more interesting case is provided if the sinusoidal excitation in the 2-2 direction lags the one in the 1-1 direction by $\rho=90^\circ$. For this phase angle and using a circular yield curve, Nigam (34) showed that continuous plastic response will occur. In other words, once the tip of the force vector reaches the yield curve, it will remain thereon indicating that the column top and bottom end sections remain fully plastic for the rest of the excitation. In order to examine the effect of using a different yield curve on this behavior, the f_1 - f_2 response curves for systems with different yield curves are shown in Fig (2.11). One can see that the situation of the continuous plastic response is independent of the shape of the yield curve being used. For the upper bound yield curve, i.e. no interaction, this situation means that the column reaches its plastic capacity in one direction and it remains plastic while the other direction remains elastic and vice versa. Shown in Fig (2.12) are the b_1 and b_2 responses for these cases, and the following observations can be made:

(1) With no interaction, amplitudes b_1 and b_2 remain unchanged as

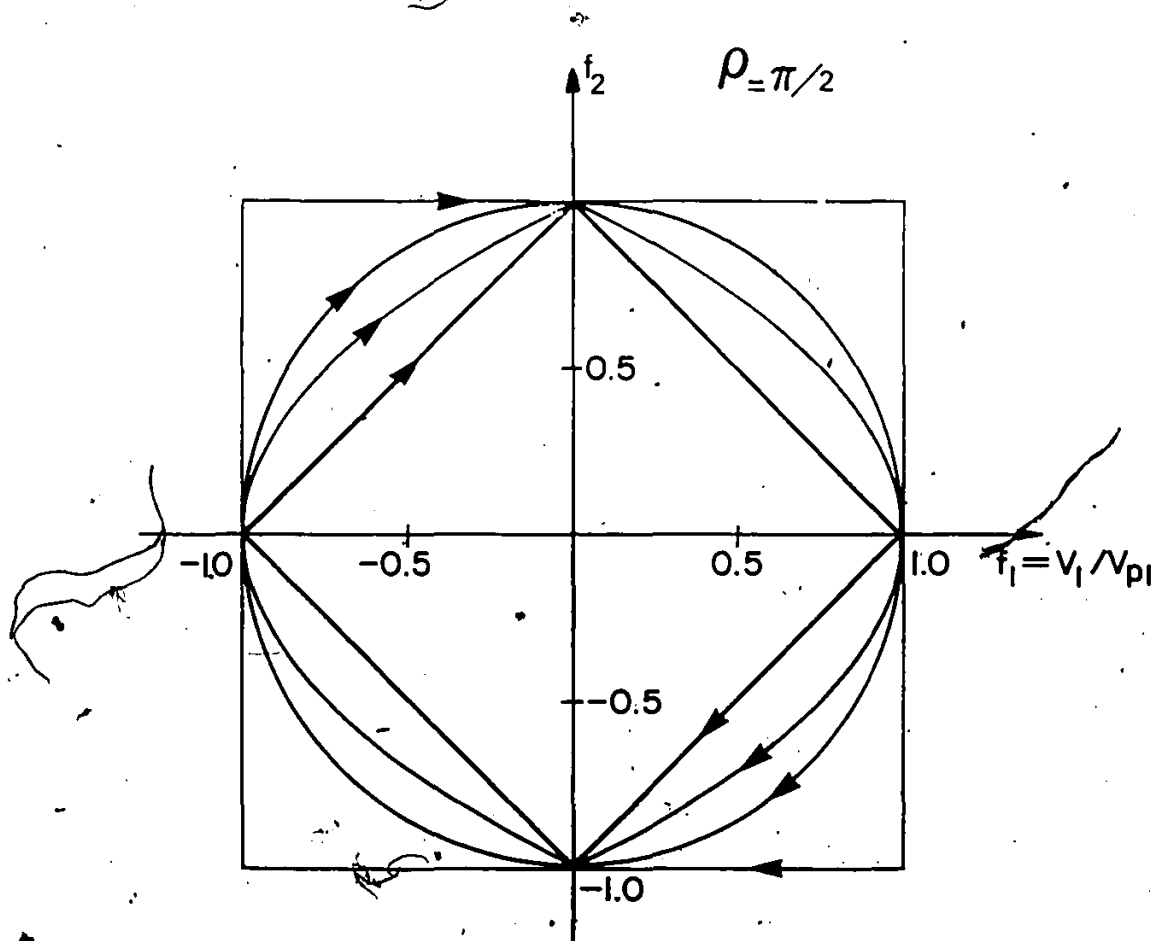


Fig (2.11) f_1 - f_2 Response Curves of Models with Different Yield Curves; Phase Angle=90

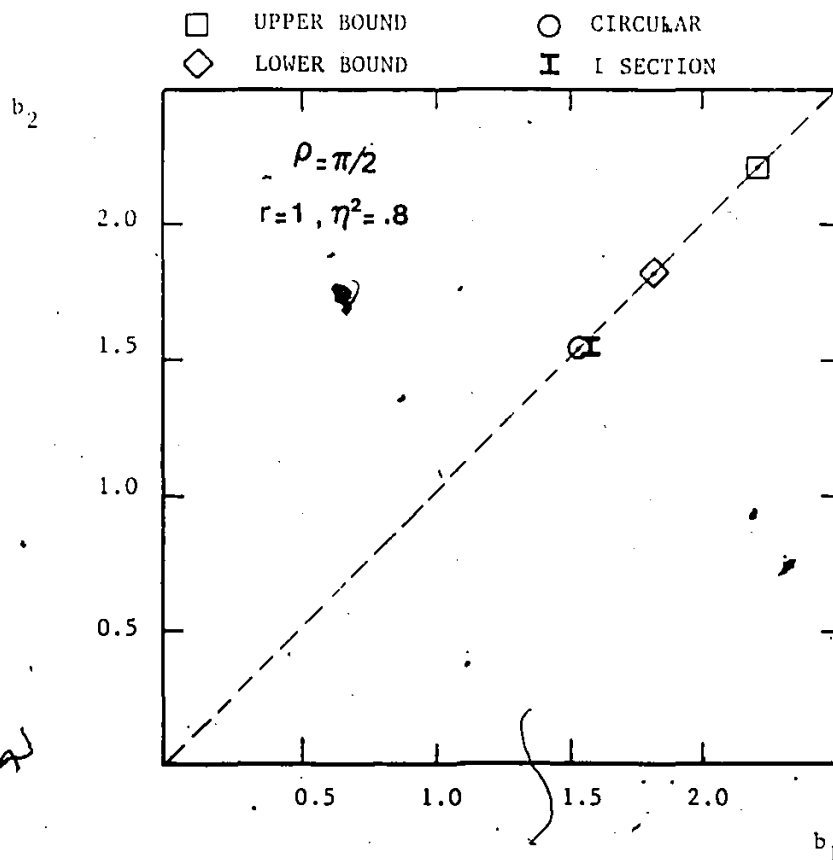


Fig (2.12) Steady State Displacement Amplitudes b_1 and b_2 ; Phase Angle=90

compared to those at $\rho=0^\circ$. In fact, the displacement amplitudes are independent of the phase angle. Varying ρ will only affect the sequence of plastic loading and unloading in the 1-1 and 2-2 directions.

(2) Unlike the case with $\rho=0^\circ$, amplitudes b_1 and b_2 obtained using the lower bound yield curve are higher than those corresponding to columns of circular or I sections. This can be attributed to the observation that if a lower yield curve is being retraced during excitation, as in the situation of continuous plastic loading, this will result in thinner hysteretic loops and in turn a lesser amount of energy can only be dissipated per cycle of loading. This eventually leads to a larger response. This observation is illustrated in Fig (2.13) by showing the steady state hysteretic loops of models with different yield curves. These loops are extracted from the complete hysteretic response calculation. The area enclosed by any of these complete loops is equivalent to the plastic energy dissipated per one cycle of loading (E_p). For each case shown in Fig (2.13), the value of E_p is also presented in the same figure. Comparing these values confirms that the lower bound yield curve leads to the smallest value of energy dissipated per cycle, and in turn to the largest response as compared to those of circular or I-section yield curves.

EFFECTS OF THE EXCITING FREQUENCY AND AMPLITUDE :

So far the discussion has been limited to models with frequency ratio parameter $\eta^2=0.8$, and excitation level $r=1$. However, it can be seen from the normalized equations of motion in Eq (2.19), that the

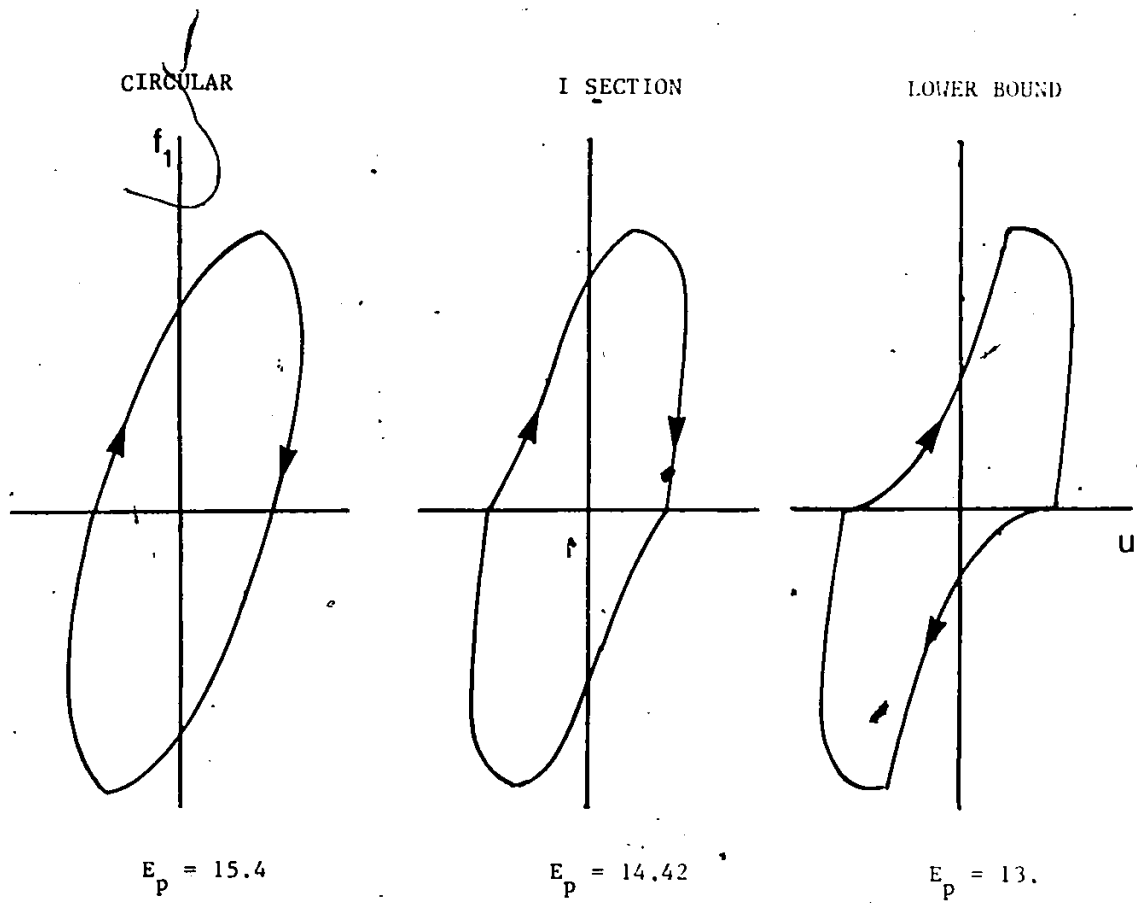


Fig (2.13) Steady State Hysteretic Loops and Plastic Energy Dissipated per Cycle; Phase Angle= 90

response is dependent on these parameters. To examine their effects, the frequency response curves of the displacement amplitudes of models with different yield curves are shown in Fig (2.14). Response curves are shown for two values of the excitation level parameter $r=0.7$ and 1. Phase angle is taken to be 90° , for which case all yield curves will lead to equal displacement amplitudes in the two directions, $b_1=b_2=b$, except for the I-section yield curve. The following observations can be made.

(1) Consider the curves in Fig (2.14a) with $r=0.7$. The model with no interaction shows a typical softening behavior as depicted by the shift of the peak to the left away from $\eta^2=1$. Including interaction enhances the softening effect even further. The peak occurs at a value of η^2 as low as 0.25 for the model with the lower bound yield curve. For the I section model, b_1 is larger than b_2 because the section is more flexible in the 1-1 direction.

(2) Increasing the excitation level to $r=1$, all models with interaction effects included exhibit the unbounded type of response. On the other hand, the one with no interaction still exhibits a curve with bounded response. In fact, it is shown (34) that such a model will exhibit unbounded response at a higher value of excitation level, namely $r=4/\pi$. This shows that including interaction will considerably increase the steady state displacement response in the low frequency ratio range over that of the conventional elasto-plastic model. Again, for this range, the lower bound yield curve leads to the largest responses.

(3) For both values of r , responses of models with circular or I-section yield curves can be conservatively estimated by those obtained using one of the two limiting yield curves, namely the lower and the upper bound

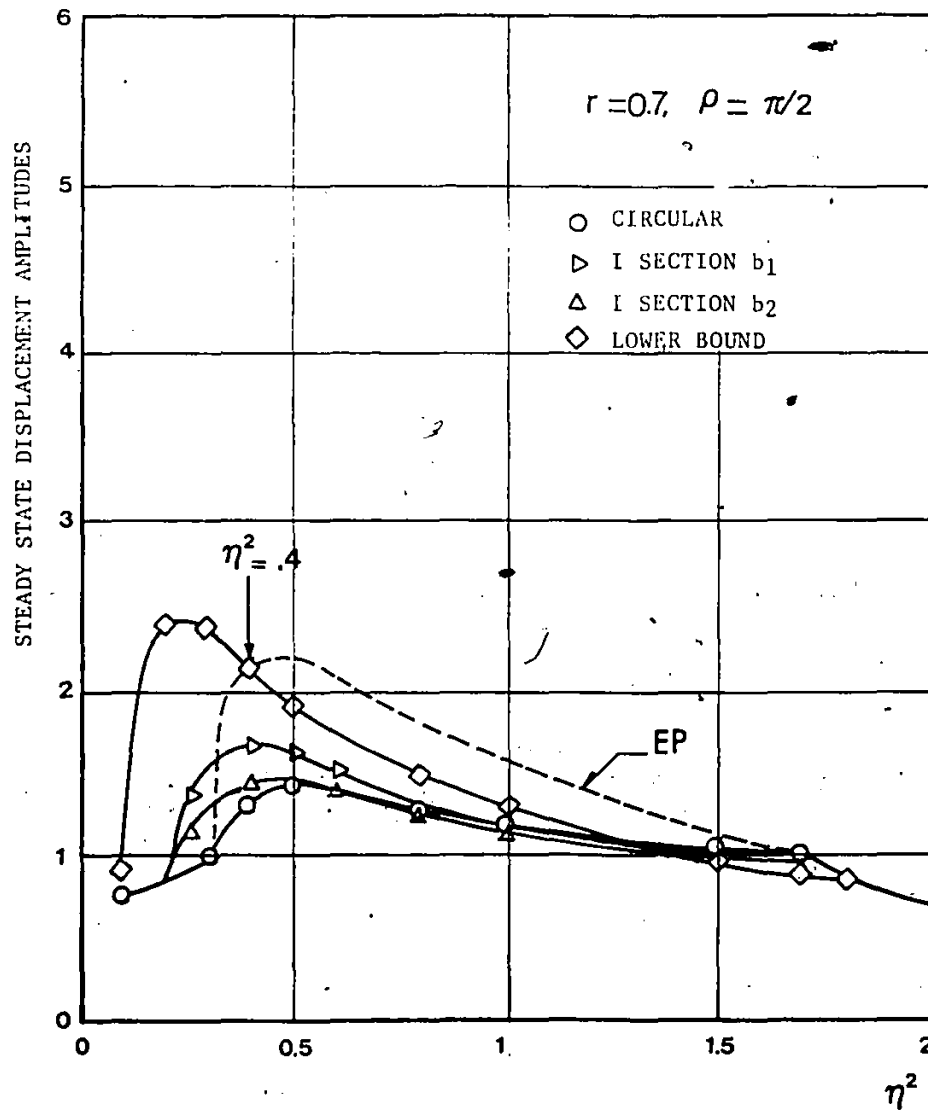


Fig (2.14a) Frequency Response Curves of the Steady State Displacement Amplitudes; $r=0.7$ and $\rho=90$

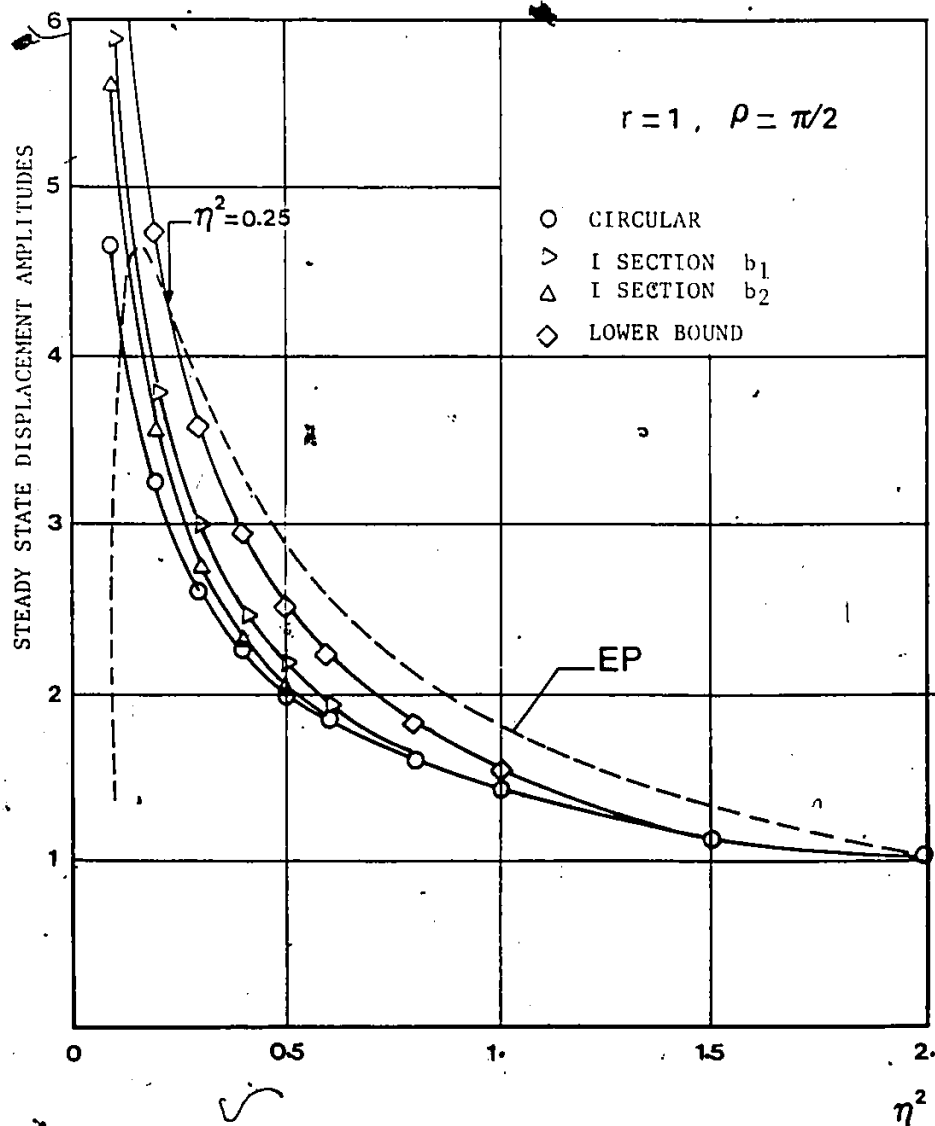


Fig (2.14b) Frequency Response Curves of the Steady State Displacement Amplitudes; $r=1.0$ and $\rho=90$

yield curves, depending on the frequency ratio. For low frequency ratios, displacement responses can be approximated by those based on the lower bound yield curve. For large frequency ratios, an elasto-plastic model with no interaction will lead to a larger response and can be adequately used to approximate the interaction effects. The transition value of η^2 between these two approximations varies depending on the excitation level r . With $r=0.7$, this value is as low as $\eta^2=0.4$ and it becomes even lower for the larger value of $r=1$.

2.3.3 ENERGY INPUT :

Let the sum of the energy input in directions 1-1 and 2-2 during one cycle of loading in the steady state era of response be denoted by E_1 . Figure (2.15) shows the E_1 response curves obtained using different yield curves and with phase angle $\rho=90^\circ$. Response curves are shown for two levels of excitation $r=0.7$ and 1. For both cases, interaction increases the energy input response for low values of ratio η^2 . The largest increase is observed for models with lower bound yield curves. The opposite, however, is true for large values of η^2 . In which cases, ignoring interaction leads to larger energy input per cycle response values. The limits of the frequency ratio ranges for these two situations again vary depending on the excitation level r .

2.3.4 EFFECTS OF PHASE ANGLE ρ :

The variation of the steady state displacement amplitudes b_1 and

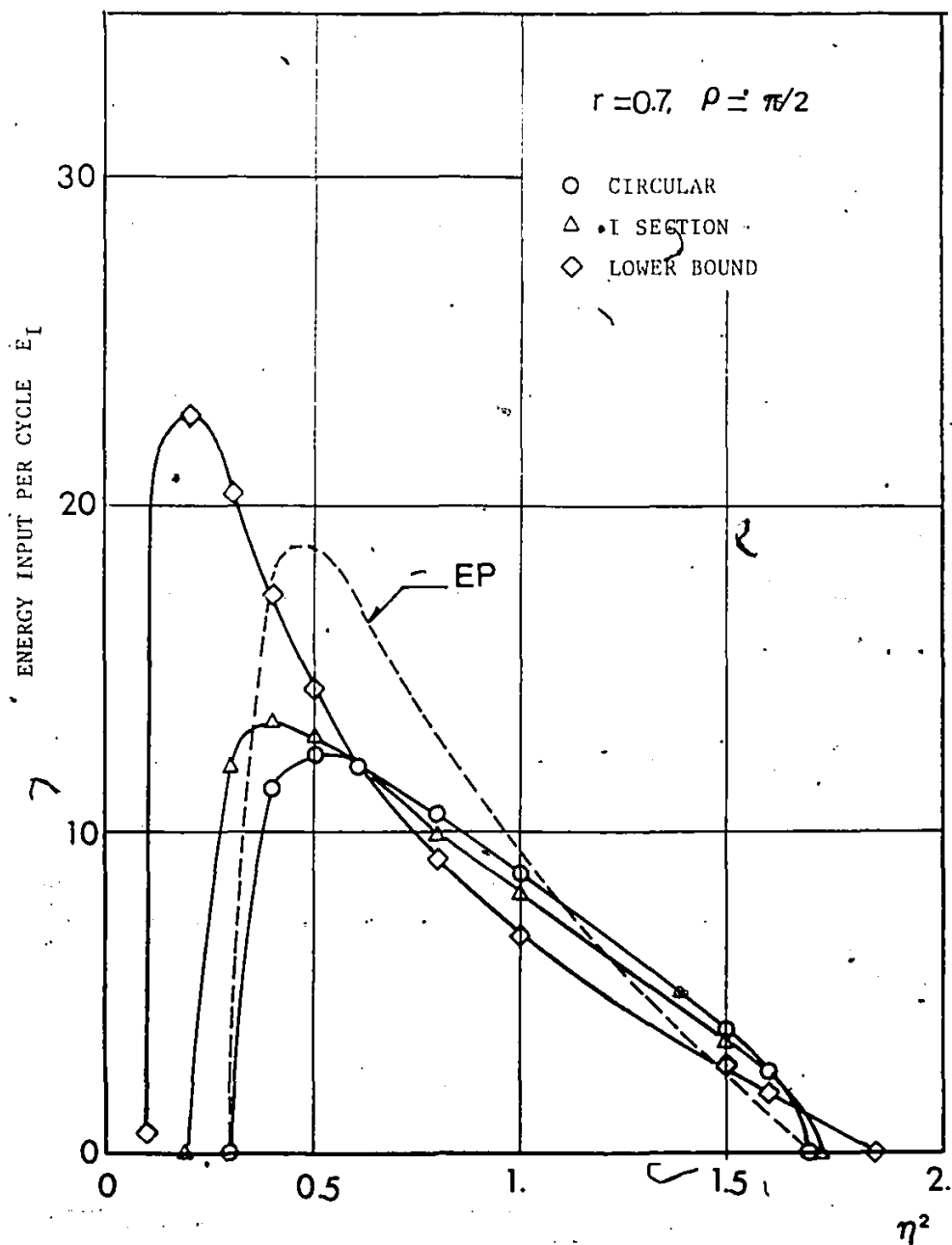


Fig (2.15a) Frequency Response Curves of the Input Energy per Cycle; $r=0.7$ and $\rho=90$

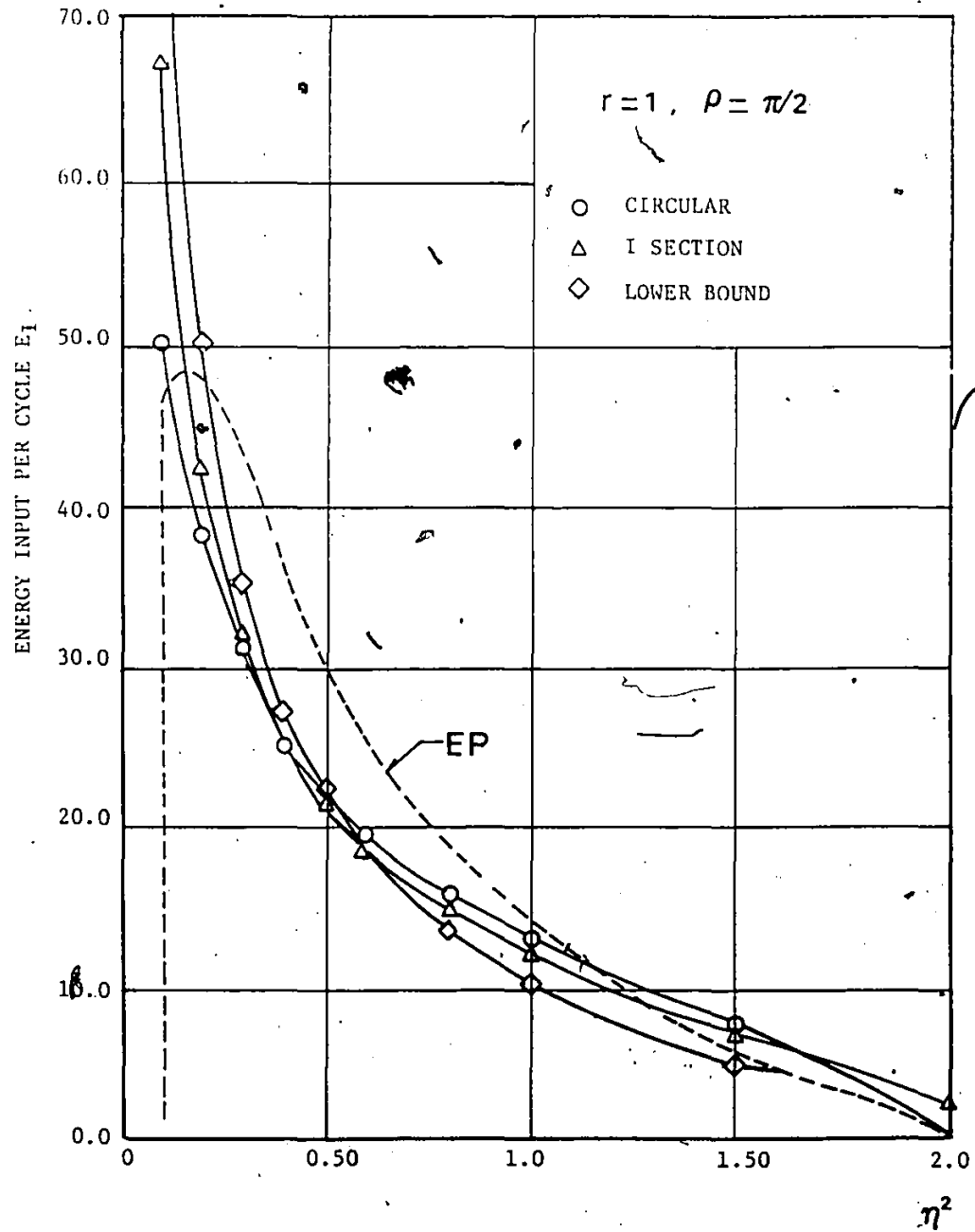


Fig (2.15b) Frequency Response Curves of the Input Energy per Cycle;
 $r=1.0$ and $\rho=90$

b_2 with the phase angle ρ ranging from 0° to 90° is shown in Fig (2.16) for models with $\eta^2=0.8$, and $r=1$. With a circular yield curve, equal amplitudes $b_1=b_2=b$ are observed for the two cases of $\rho=0^\circ$ and 90° .

In the first case, i.e. $\rho=0^\circ$, Nigam (34) pointed out that since identical excitations $r\sin\eta\tau$ being inputted in the 1-1 and 2-2 directions, an equivalent one dimensional problem with excitation equal to $\sqrt{2}r\sin\eta\tau$ along the 45 degree direction will give the same total response as the original bidirectional excitation problem. It is obvious then that the components of this total response along the original axes should be equal.

For the other case with $\rho=90^\circ$, input motions in the 1-1 and 2-2 directions are given by $r\sin\eta\tau$ and $r\cos\eta\tau$ respectively. The resultant excitation is then time invariant and is given by the parameter r . Figure (2.17) shows the locus of the base motion to be a circle of radius r . The two input motions are completely uncorrelated in this case. Also in Fig (2.17), the locus of the top mass motion is shown to be another circle of radius b . It appears that since the input motions in the two directions are completely uncorrelated, there is no redistribution of the energy input, and hence equal responses are obtained in the two directions. For other values of ρ , the input motions are partially correlated and the energy redistribution affects the response by increasing the response in one direction and decreasing it in the other.

Let the radial displacement amplitude b_r be defined as follows

$$b_r = \max [(b_1 \sin\eta\tau)^2 + (b_2 \sin(\eta\tau + \rho))^2]^{1/2}$$

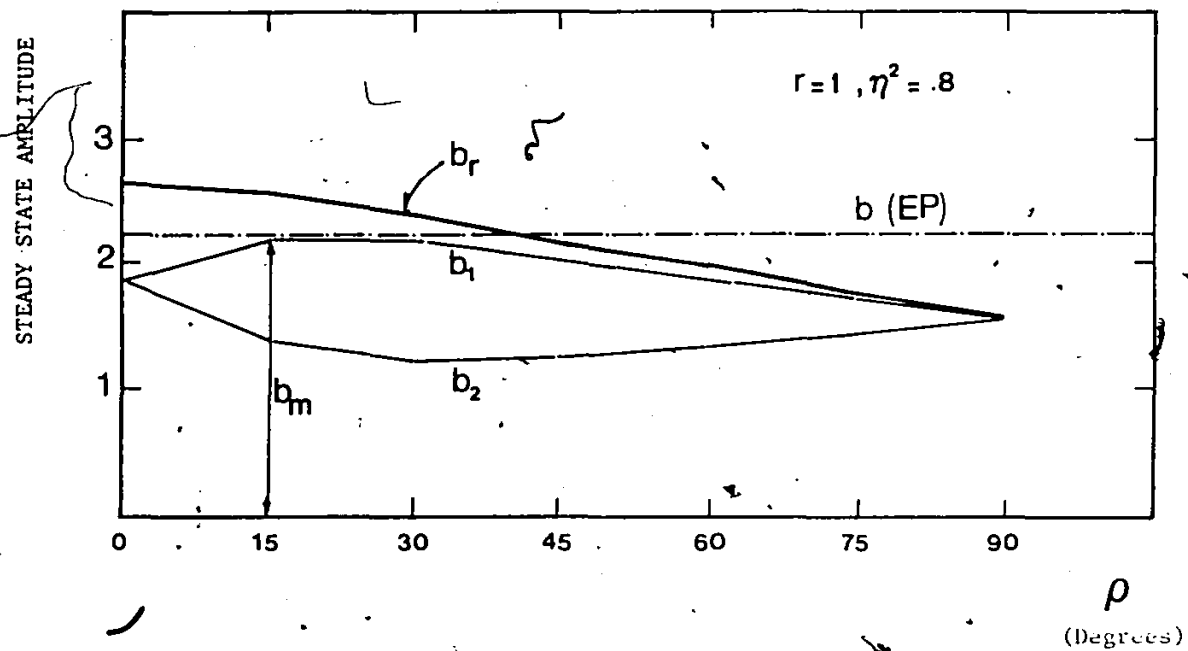


Fig (2.16) Variation of the Steady State Displacement Amplitude Components with ρ ; $r=1.0$ and $\eta^2=0.8$

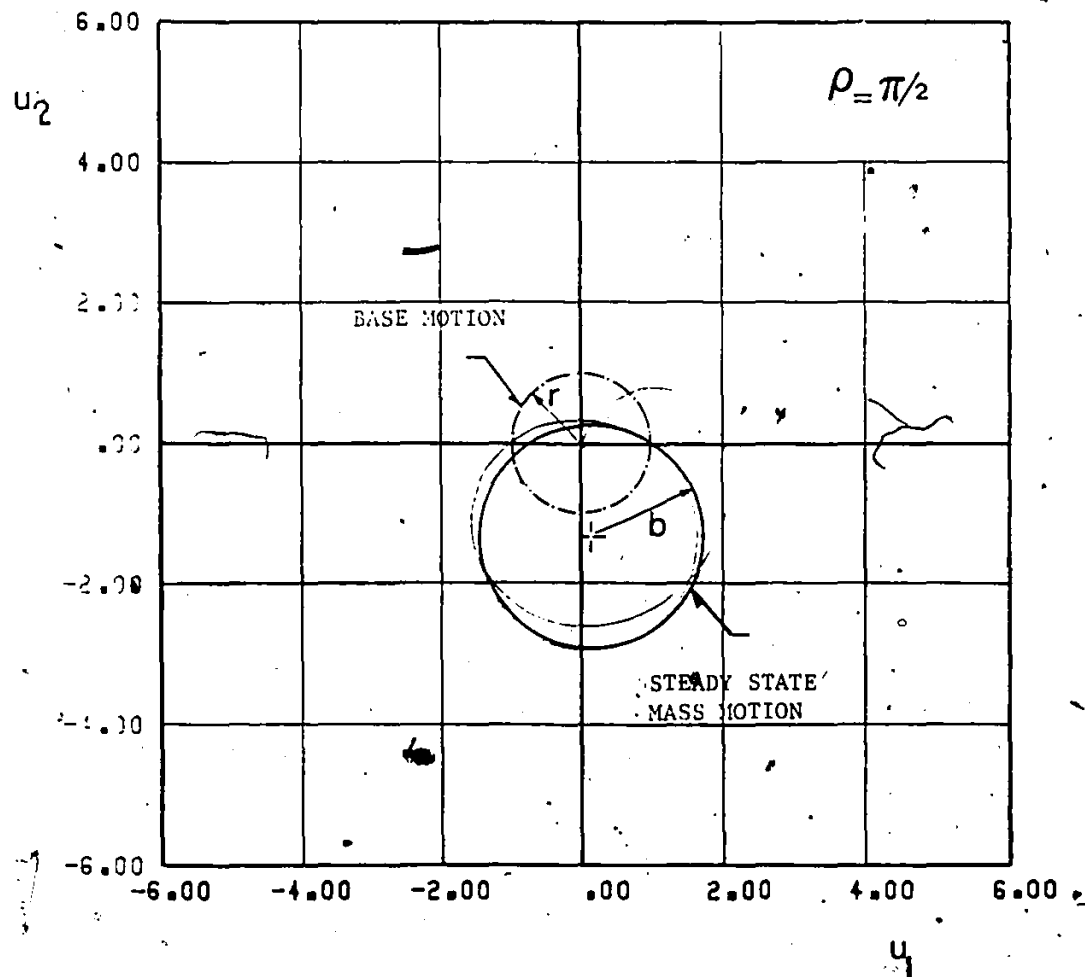


Fig (2.7) Locus of the Base Motion and the Top Mass Motion in Plan.

Using this expression, it can be shown that for $\rho=0^\circ$, or completely correlated motions, $b_r=\sqrt{2}b$, and for $\rho=90^\circ$, or completely uncorrelated motions, $b_r=b$. for intermediate values of ρ , Figure (2.16) shows the radial amplitude b_r to be decreasing function of ρ . This uniform decrease in b_r can be ascribed to the loss of correlation between the input motions as ρ grows from 0° to 90° .

With interaction ignored (EP), amplitude b becomes independent of the phase angle. Its value is found to be larger than the maximum amplitude b_m that an equivalent model with interaction can have over the range of the phase angle ρ from 0° to 90° (see Fig (2.16)). To estimate the maximum steady state amplitude with interaction over this range of the phase angle using the amplitude b , calculated by neglecting interaction, the ratio b_m/b is shown in Fig (2.18) as a function of η^2 for different yield curves. Two useful observations can be made. First, it can be seen that the ratio b_m/b is insensitive to the yield curve used. In other words, the maximum effect of the phase angle on the displacement amplitude is insensitive to the shape of the yield curve. Second, for frequency ratio parameter η^2 greater than 0.6, the ratio b_m/b has values very close to unity. This suggests that for this range of frequency ratios, an elasto-plastic model will give a good estimate of the steady state amplitude.

2.3.5 RESPONSE OF TYPICAL I-SECTIONS :

In designing columns subjected to static biaxial bending effects, design codes (42) suggest to use the straight line strength

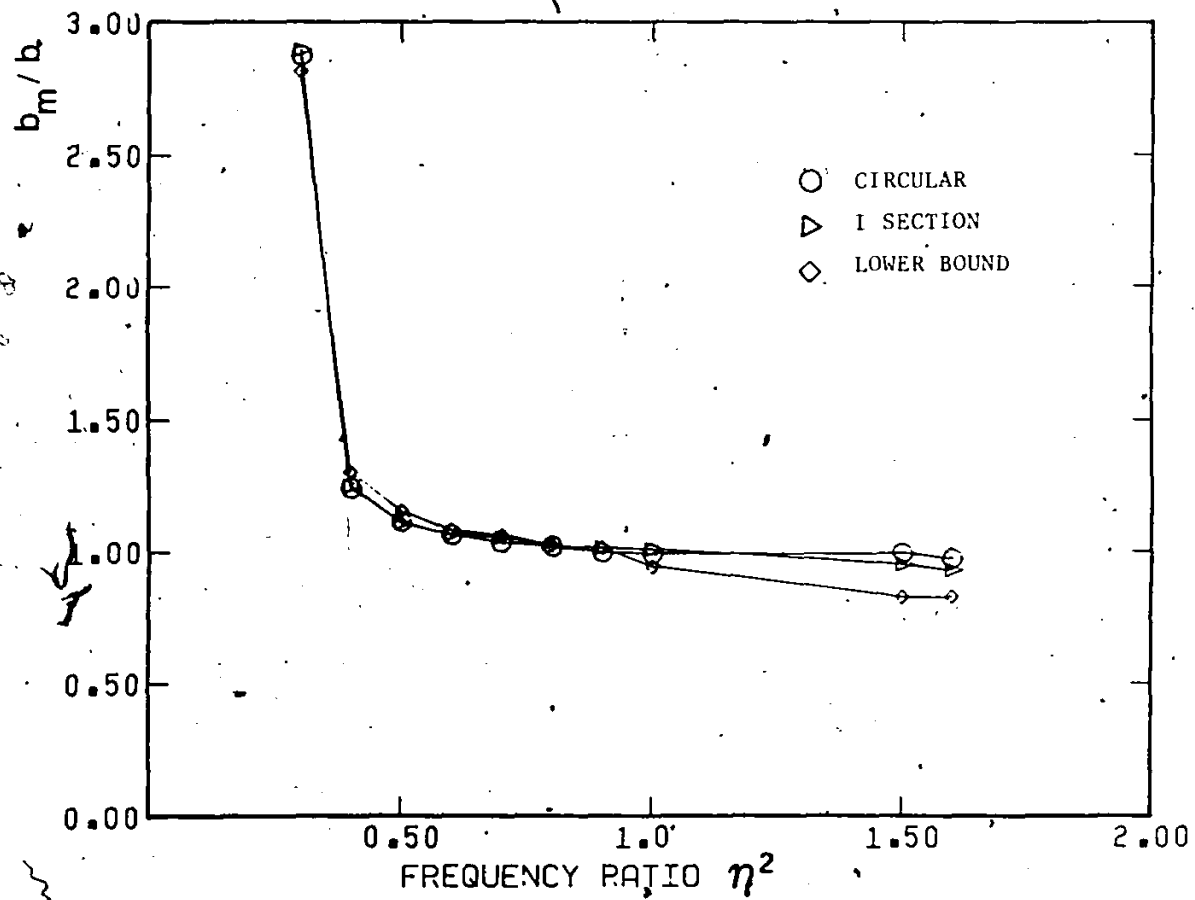


Fig (2.18) Variation of Ratio b_m/b with η^2

interaction formula $f_1 + f_2$ when evaluating the ultimate capacity of the column. This approximate formula is known to result in conservative design of such columns. An equivalent approach in case of dynamic loads is to approximate the plastic capacity of the column in the four quadrants of the force space with the lower bound yield curve. The degree of conservatism of this approach when applied to columns of actual cross sections is examined in the following. Two typical rolled I-sections, a heavy section W14x370, and a light section W14x82, are considered for this purpose. The dimensions of these sections are presented in Table (2.2). The ratio of major to minor plastic capacity (β_c) is 1.99 and 3.06 for the heavy and the light sections respectively. Assuming the same fixed end conditions in the major and the minor directions of the column, the ratio of the stiffnesses in these directions (γ_c) is 2.73 and 5.96 for the heavy and the light sections respectively.

The steady state displacement amplitude b_1 of two columns having these sections as cross sections in response to sinusoidal excitation with $p=0^\circ$, and $r=0.7$ and 1 are shown in Fig (2.19a,b). In this figure, curves obtained using yield curve derived earlier in Section 2.2.1 for the idealized I-section as well as the lower bound yield curve, as an approximate calculation, are presented. Except for the case when $r=1$ together with low frequency ratios, the straight line approximation of the curved I-section yield curve will give a good estimate of the steady state displacement amplitude. For the situation when $r=1$ and η^2 is low, the approximate calculations predict a larger displacement response.

Table 2.2 Dimensions of Two I-Sections (Inches)

	2H	2B	t_f	t_w
W14x82	14.31	10.31	0.85	0.51
W14x370	17.92	16.47	2.66	1.66

2B, t_f = width and depth of the flange;

2H, t_w = height and thickness of the web.

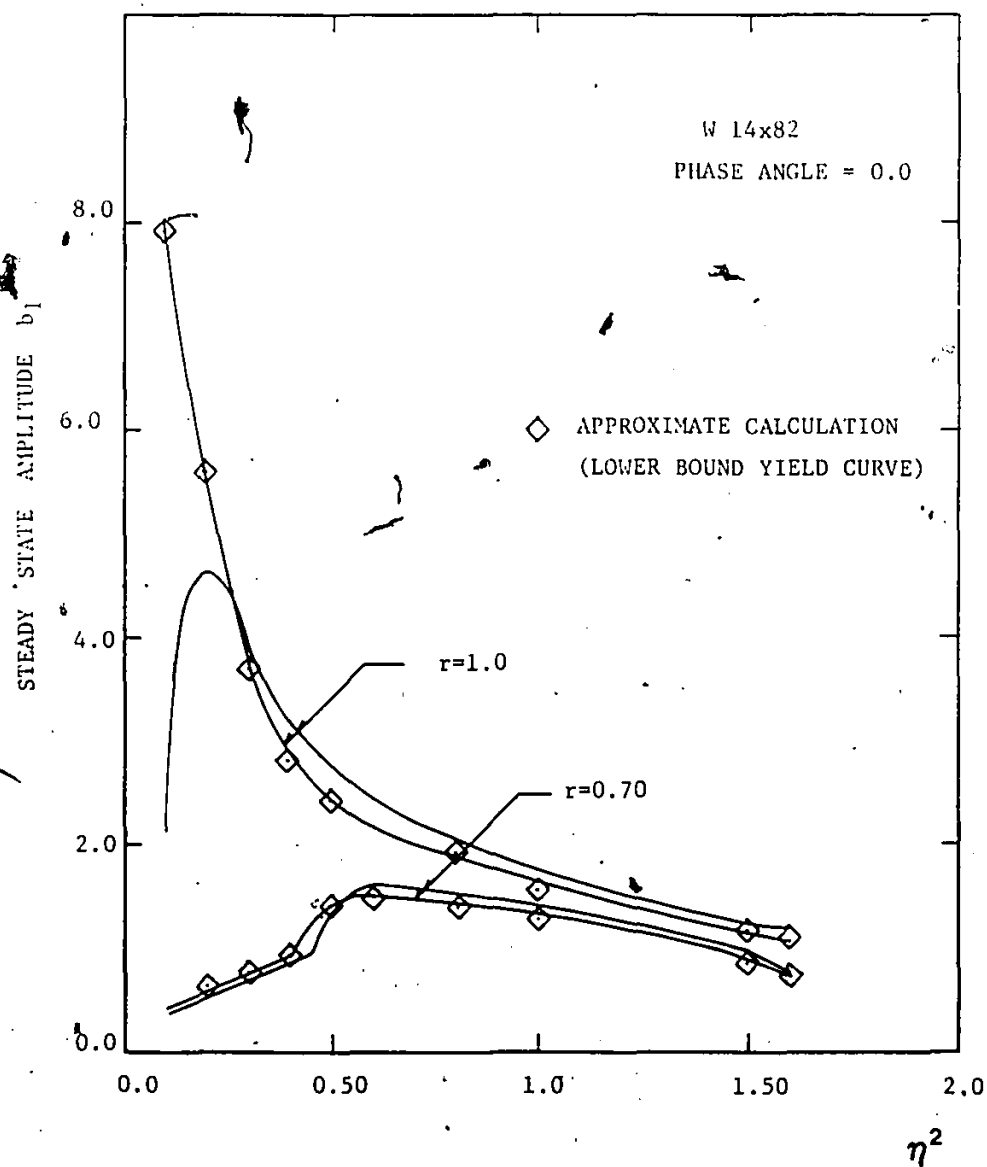


Fig (2.19a) Comparison of Frequency Response Curves of the Light I-Section (W14x82); $r=0.7$, 1.0 and $p=0$

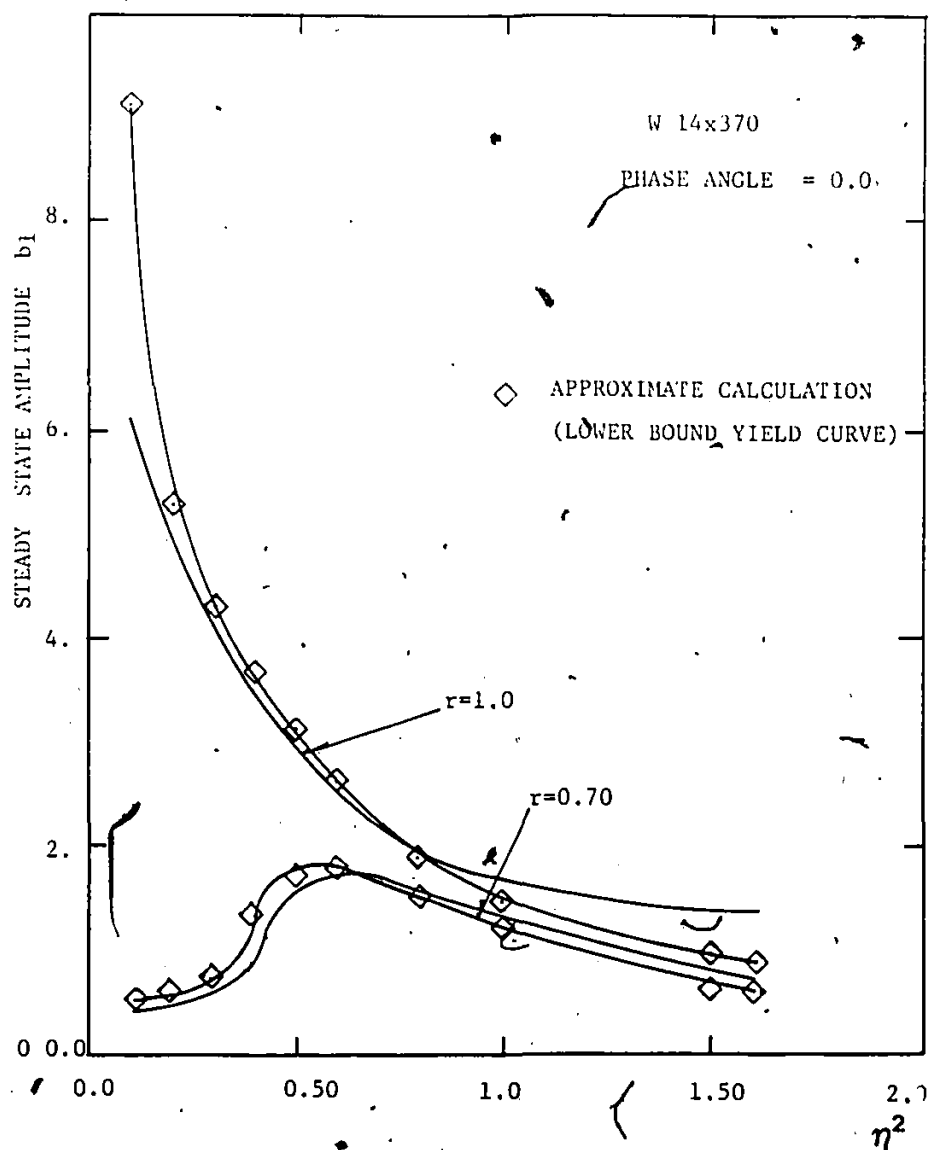


Fig (2.19b) Comparison of Frequency Response Curves of the Heavy I-Section (W14x370); $r=0.7, 1.0$ and $\rho=0$

2.4 SUMMARY AND CONCLUSIONS :

In this chapter, the dynamic response of columns having cross sections with two axes of symmetry and subjected to biaxial bending due to sinusoidal base motions along two orthogonal horizontal directions has been discussed. The intention is to gain insight as to the effects of including interaction in the inelastic analysis of columns under biaxial bending. In addition to circular columns, which were considered by Nigam (34), columns having I sections are studied. An expression of the yield curve for an idealized I-section is derived and compared with other investigators' work. Factors such as the shape of the yield curve assumed and the phase angle between the two input motions are also discussed. Columns are modelled either as two independent elasto-plastic springs in the two lateral directions or a yield curve which accounts for the interaction between the two acting bending moments is assumed. The response parameters are the steady state displacement amplitude and the energy input per cycle of loading. The results are presented in the form of frequency response curves. Based on the results presented in the chapter, the following conclusions can be made.

1. For systems with large ratios of excitation to system frequencies, including the interaction effect has the tendency to reduce the steady state displacement response. For such systems it is adequate to consider the elasto-plastic responses.

2. Interaction becomes significant for systems with low

frequency ratios particularly with high levels of excitation. Including interaction leads to a large increase of the steady state displacement response over that of an elasto-plastic model. For this situation, a conservative estimate of the response can be obtained if the lower bound yield curve, which admits maximum interaction, is assumed for the element considered.

3. Varying the phase angle between the two input sinusoidal waves leads to the redistribution of energy in the two orthogonal directions of the system when the interaction effect is included. The redistribution of energy causes the response in one direction to increase and in the other to decrease. The maximum effect of the phase angle on the displacement amplitude is insensitive to the shape of the yield curve assumed. In addition, an elasto-plastic model will give a good estimate of this maximum displacement amplitude provided the frequencies ratio is large ($\eta^2 > 0.6$).

4. Using a circular yield curve, Nigam (34) showed analytically that a situation of continuous plastic response will occur at a phase angle equal to $\pi/2$. It has been shown numerically that this type of behavior is independent of the shape of the yield curve assumed. When the phase angle is equal to $\pi/2$, the system is subjected to an excitation whose resultant remains constant with time and is equal to the amplitude of the component excitation.

5. For columns under static biaxial bending, the use of an approximate linear strength interaction formula leads to conservative design of such columns. Under dynamic loads, an equivalent approach is

to use the lower bound yield curve to represent the plastic capacity of the element in the force space. Comparing the approximate calculations as applied to two typical rolled I-sections, it is found that the straight line approximation of the curved I-section yield curve gives a good estimate of the steady state displacement amplitude except for the situation of low frequency ratio combined with high excitation levels. In such situations, the approximate estimate can be very conservative compared to the more accurate estimate.

CHAPTER 3
RESPONSE OF SYMMETRIC STRUCTURES TO
EARTHQUAKE EXCITATIONS

3.1 INTRODUCTION :

It is common practice suggested by design codes that a three dimensional structure subjected to multicomponent earthquake ground motions can be analyzed by first considering planar responses to each ground motion component one at a time and then these responses are combined to give the final responses. This procedure greatly simplifies the analysis of a complicated problem and it has its validity based on the superposition principle which applies in the elastic range of response. Although this concept is strictly valid for elastic response conditions, this procedure is often used in analyzing the inelastic responses of structures. Among the primary effects overlooked in applying such a procedure in the inelastic range are: (1) the effect of forces interaction on the yielding properties of the resisting elements (type of the resistance function); and (2) the effect of the simultaneous action of various components of the ground motion (combination schemes).

The consequences of neglecting these effects on the inelastic response are examined in this chapter for structures having two axes of symmetry in plan. Specifically, a symmetric single story model consisting of a rigid slab on four columns, is used for this purpose.

The inelastic behavior of the column is taken to be elasto-plastic when being deformed in one direction, and the yield criterion is prescribed by a circular yield curve when subjected to simultaneous deformations in two horizontal directions. In this way, the effects of forces' interaction on yielding properties of the columns is taken into account. To avoid the conclusions obtained being dependent on the particular ground motion record used, an ensemble of five pairs of orthogonal horizontal components of recorded earthquake records is used as the input ground motions.

After deriving the equations of motion in a form suitable for earthquake response calculations, the effects of force interaction are examined in detail. The response parameters of interest are the ductility demand as defined by the ratio of the maximum displacement to the yield deformation, and the energy input.

Approximate methods to estimate ductility demands are then discussed. One method is to combine the two-planar elasto-plastic responses according to schemes available in literature. Another method which requires only the elastic response of the system is proposed. The accuracy of these methods is examined.

The consequences of difference in natural periods in the two directions are then discussed. It is shown that the orientation of directions of excitation with respect to the structural axes becomes a significant parameter in this case.

3.2 EQUATIONS OF MOTION

Consider a single story structure consisting of a rigid deck of

mass m and of a square shape in plan with dimensions D by D . The deck is supported on four circular section columns on rigid footings located at the extremities of a square of dimensions a by a as shown in Fig (3.1). In this part of the study, the structural model is assumed to have a symmetric configuration so that the center of mass (CM) and the center of stiffness (CS) are coincident. The deformation of the structure is adequately described by q_x and q_y , the two translational displacements at CM relative to the base. The equations of motion of this model when subjected to the two horizontal components of ground motion in the x and y directions, $\ddot{u}_{gx}(t)$ and $\ddot{u}_{gy}(t)$, can be written as follows

$$[M] (\ddot{q}) + [c] (\dot{q}) + \{Q\} = -[M] (\ddot{u}_g(t)) \quad (3.1)$$

where

$$\{q\}^T = \langle q_x, q_y \rangle$$

$$\{\ddot{u}_g(t)\}^T = \langle \ddot{u}_{gx}(t), \ddot{u}_{gy}(t) \rangle$$

$$[M] = m [I]; [I] \text{ is the identity matrix;}$$

$$[C] = 2\xi m \begin{bmatrix} \omega_x & 0 \\ 0 & \omega_y \end{bmatrix}$$

and ξ is the fractional critical damping in both x and y directions.

$\{Q\}$ is the restoring force vector. ω_x and ω_y are the natural frequencies of the model along the x and y directions respectively. ω_y is taken to be proportional to ω_x with a factor of proportionality γ ; in other words, $\omega_y = \gamma \omega_x$.

For inelastic response calculations, the incremental form of Eq

(3.1) is used, namely

$$[M] \Delta(\ddot{q}) + [c] \Delta(\dot{q}) + [K_t] \Delta(q) = -[M] \Delta(\ddot{u}_g(t)) \quad (3.2)$$

where $[K_t]$ is the tangential global stiffness matrix of the system assembled from the individual updated column stiffness matrices $[S]_i$ as follows

$$[K_t] = \sum_{i=1}^4 [S]_i \quad (3.3)$$

The elements of $[S]_i$ depend on the resistance function assumed and the state of stresses as explained earlier in Section 2.3.1.

Equation (3.2) can be put into a dimensionless form as follows

$$\Delta(\ddot{u}) + 2\xi\omega_x \begin{bmatrix} 1 & 0 \\ 0 & \gamma \end{bmatrix} \Delta(\dot{u}) + \omega_x^2 [\bar{K}_t] \Delta(u) = \Delta(\ddot{G}) \quad (3.4)$$

where

$$\{u\}^T = \langle q_x/\delta_x, q_y/\delta_y \rangle;$$

$$[\bar{K}_t] = [K_t]/K_x;$$

$$\Delta(G) = -[\delta]^{-1} \Delta(\ddot{u}_g(t));$$

$$\text{and } [\delta] = \begin{bmatrix} \delta_x & 0 \\ 0 & \delta_y \end{bmatrix}$$

δ_x and δ_y are the overall yield displacement of the system along the x and y axes respectively and given by

$$\delta_x = F_x/K_x; \text{ and } \delta_y = F_y/K_y$$

F_x and F_y are the system yield strength along the x and y axes respectively. The ratio of the yield strength in the y direction to the

one in the x direction is denoted by B .

EXCITATION TERM (G)

To introduce equivalence among responses of structures with different natural periods to ground motion $\ddot{u}_g(t)$ or among responses to different earthquake records, a normalization factor in acceleration units should be applied to $\ddot{u}_g(t)$. Obviously, this normalization factor should be a measure of the strength of the ground excitation. Since there does not exist a unique way to quantify the strength of ground motion, different parameters have been used by different researchers as the normalization factor. These parameters can be grouped into: (i) structural period independent parameters such as the peak ground acceleration \ddot{u}_{gm} or the root mean square acceleration \ddot{u}_{rms} (34), and (ii) structural period dependent parameters such as the elastic spectral acceleration S_a (17, 51) or some derived inelastic spectral acceleration S_{ap} (22, 58) of a specific ground motion. These alternatives are shown in Fig (3.2) for the case of the NS component of the 1940 El Centro earthquake record. The drawback in using parameters in group (i) is that these parameters are structural period invariant. As a result, they tend to overestimate the anticipated earthquake force levels for intermediate and long period systems as compared to those for short period systems. The strength supply necessary to keep the system elastic when subjected to these forces is in turn overestimated. An improvement is achieved by using the spectral acceleration of a specific earthquake. This approach can take into account the specifics of a particular ground motion, however it lacks resemblance to actual design

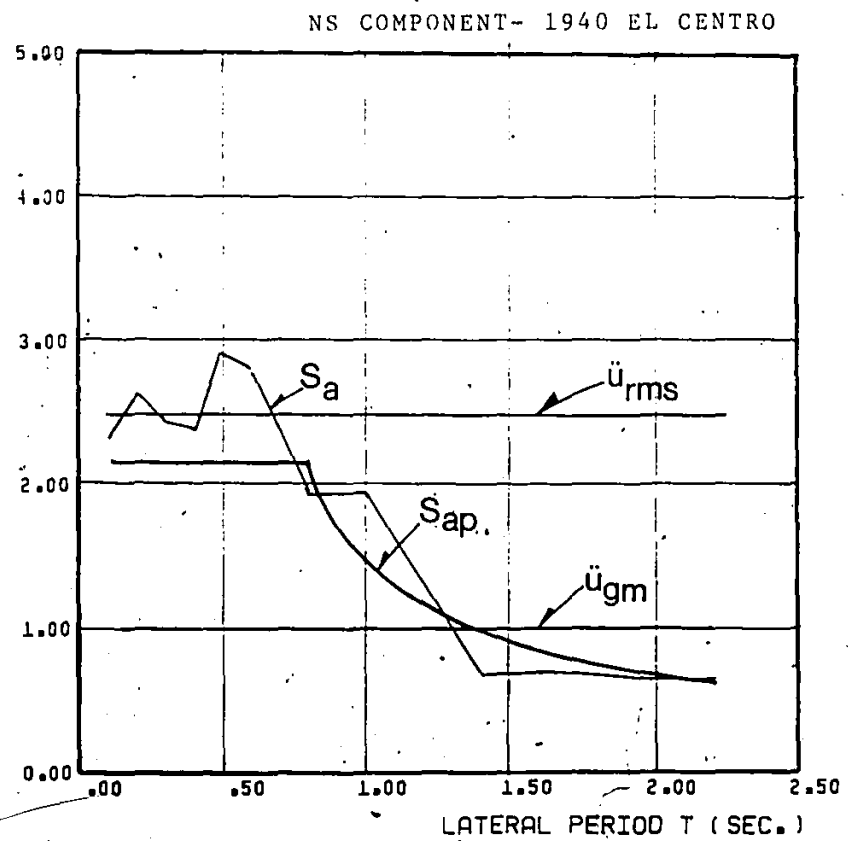


Fig (3.2) Variation of Different Ground Motion Characteristics with Structural Period

practice.

Using a smooth elastic spectrum for normalization purposes would overcome the above mentioned shortcomings. In this study a smooth spectrum S_a^* is used. The shape of S_a^* is such that it is flat for periods $T_x \leq 0.5$ sec and inversely proportional to the period for $T_x > 0.5$ sec. In the flat portion, the ratio S_a^* to the peak ground acceleration \ddot{u}_{gm} is assumed to have a value of 3.68. This value corresponds to the amplification factor suggested by Newmark and Hall (31) for 0.5% critically damped elastic system. The variation of the ratio S_a^*/\ddot{u}_{gm} is shown in Fig (3.3) as a function of natural period T_x .

Writing $\{\ddot{u}_g(t)\} = S_a^* \{\ddot{\ddot{u}}_g(t)\}$, the excitation term $\{G\}$ in Eq (3.4) can be written as

$$\{G\}^T = -R \omega_x^2 \langle \ddot{\ddot{u}}_{gx}(t), 0, (\gamma^2/B) \ddot{\ddot{u}}_{gy}(t) \rangle \quad (3.5)$$

where

$$R = m S_a^* / F_x \quad (3.6)$$

With $R=1$, $m S_a^*$ in Eq (3.6) can be considered as the required strength of a lightly damped simple oscillator so that it will just reach yield, when subjected to a ground motion having a spectral acceleration value of S_a^* . Larger values of R correspond to the case of structures whose design strength capacity is lower than the elastic strength demand and hence these systems will be excited into the inelastic range. Therefore, R can be considered as a strength reduction factor in the design context.

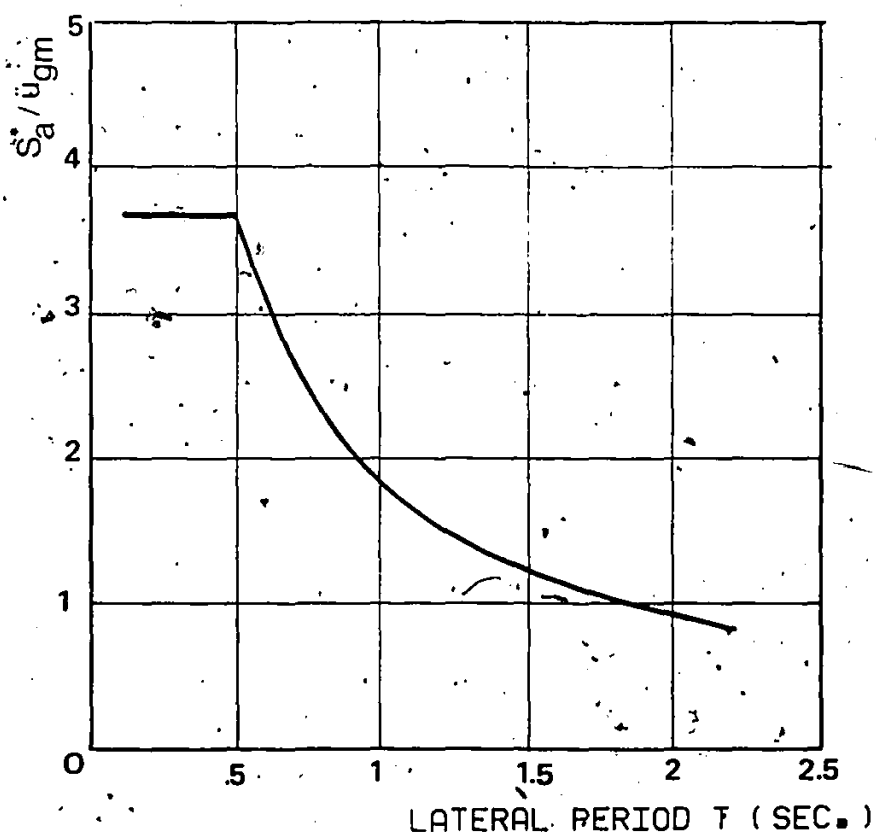


Fig (3.3) Elastic Smooth Spectrum S_a^*/\ddot{u}_{gm}

SYSTEM PARAMETERS :

Unless otherwise mentioned, the symmetric model studied is considered to have identical properties in the x and y directions. In terms of the system parameters, this means

$$F_y = F_x \quad (\beta=1), \quad \omega_y = \omega_x \quad (\gamma=1), \quad \text{and} \quad \delta_y = \delta_x.$$

The lateral period $T_x = 2\pi/\omega_x$ is varied from 0.1 sec to 2.2 sec. 0.5% of critical damping is used to represent the viscous component of energy dissipation mechanism in the system. This value is consistent with the level of viscous damping associated with the selected smooth design spectrum (31).

The responses of elasto-plastic models (EP) and the elasto-plastic models with interaction effects included (EPI) are studied. In the EPI model, yielding properties of columns are prescribed by circular yield curves as discussed in the previous chapter.

Two values of R are used herein, namely R=3 and 5. With R=3, the system has a design strength which is one third of the elastic strength demand and the system will be moderately excited into the inelastic range. The larger value of R indicates that the design strength of the system is considerably lower than the elastic strength demand and the system will be excited well beyond its elastic limit.

NUMERICAL INTEGRATION :

The equations of motion are solved numerically assuming linear variation of the acceleration over a short time increment Δt . To satisfy the stability condition of the numerical method, Δt is taken as

0.02 sec, but not more than 1/30 of the initial elastic period for systems with very short periods, say $T_x < 0.2$ sec. Equilibrium iteration is performed using the Newton-Raphson technique to reduce the unbalanced forces to an acceptably small value. In the case of EPI response, special care is required to prevent any premature unloading off the yield curve. An efficient numerical scheme is used in this regard and the details of this scheme are given in Appendix B.

3.3 ENERGY CALCULATION :

From Eq (3.1), the equilibrium of forces in direction i ($i=x,y$) is given by

$$m\ddot{q}_i + c_i\dot{q}_i + Q_i = -m\ddot{u}_{gi} \quad (3.7)$$

Multiplying Eq (3.7) by dq_i and integrating, one can obtain the energy equation as follows

$$\int_0^{q_i} m\ddot{q}_i dq_i + \int_0^{q_i} c_i\dot{q}_i dq_i + \int_0^{q_i} Q_i dq_i = \int_0^{q_i} -m\ddot{u}_{gi} dq_i \quad (3.8)$$

In this equation, the integrals represent, respectively, the kinetic energy (\bar{E}_{ki}), the energy dissipated by viscous damping (\bar{E}_{vi}), the sum of the strain energy stored (\bar{E}_{si}) plus the energy dissipated by plastic deformation (\bar{E}_{pi}), and the energy imparted to the system (\bar{E}_{li}) in direction i . Changing variables of integration in Eq (3.8), one obtains

$$m \int_0^{\dot{q}_i} \dot{q}_i d\dot{q}_i + c_i \int_0^t \dot{q}_i^2 dt + \int_0^{q_i} (Q_i dq_i^e + Q_i dq_i^p) = \int_0^t -m\ddot{u}_{gi} \dot{q}_i dt \quad (3.9)$$

where dq^e and dq^p are the elastic and plastic components of the

displacement increment dq . Hence it is possible to evaluate \bar{E}_{si} and \bar{E}_{pi} separately. Normalizing Eq (3.9) with respect to the elastic energy capacity in direction i , $E_{ei} = K_i \delta_i^2 / 2$, and recognizing the following relationships

$$\begin{aligned} c_i &= 2m\xi\omega_i, \quad dq_i^e = dQ_i / K_i \\ \bar{u}_{gi} &= S_a^* \bar{u}_{gi}, \quad R = m S_a^* / F_i, \text{ and} \\ \bar{Q}_i &= Q_i / F_i, \end{aligned}$$

then the normalized energy expressions are given by

$$\begin{aligned} E_{ki} &= (\dot{u}_i / \omega_i)^2 \\ E_{vi} &= (4\xi / \omega_i) \int_0^t \dot{u}^2 dt \\ E_{si} &= \bar{Q}_i^2 \\ E_{pi} &= 2 \int_0^{u_i^P} \bar{Q}_i du_i^P \\ E_{ii} &= 2R \int_0^t \bar{u}_{gi} \dot{u} dt \end{aligned} \quad (3.10)$$

The change in these energy quantities over the time interval from t to $t+\Delta t$ is evaluated using the trapezoidal rule as follows

$$\begin{aligned} \Delta E_{ki} &= [\dot{u}^2(t+\Delta t) - \dot{u}^2(t)] / \omega_i^2 \\ \Delta E_{vi} &= [\dot{u}^2(t+\Delta t) + \dot{u}^2(t)] (2\xi \Delta t / \omega_i) \\ \Delta E_{si} &= [\bar{Q}_i^2(t+\Delta t) - \bar{Q}_i^2(t)] \\ \Delta E_{pi} &= [\bar{Q}_i(t+\Delta t) + \bar{Q}_i(t)] [u_i^P(t+\Delta t) - u_i^P(t)] \\ \Delta E_{ii} &= [\bar{u}_{gi}(t+\Delta t) \dot{u}(t+\Delta t) + \bar{u}_{gi}(t) \dot{u}(t)] R \Delta t \end{aligned} \quad (3.11)$$

3.4 EFFECTS OF INTERACTION :

In the following sections, the significance of interaction is examined. Attention is focused on ductility demand, permanent set, and

energy input as the response parameters for comparison.

3.4.1 DUCTILITY RATIO RESPONSES :

Ductility ratio along certain direction is defined herein as the ratio of the absolute maximum displacement to the yield displacement in the same direction. Let μ_x and μ_y be the ductility ratios for the x and y directions. They are defined as

$$\mu_x = \max |u_x(t)|, \quad \mu_y = \max |u_y(t)|$$

Shown in Fig (3.4) is the variation of ductility demand μ_x against lateral period T_x with force interaction included (EPI) and ignored (EP). The two horizontal components of the 1949 Olympia earthquake records are used as input. It can be seen that when the structure has a design strength one fifth of the elastic strength demand ($R=5$), interaction causes significant increase in the ductility ratio μ_x in the short period range, whereas the EP and EPI responses become practically the same in the long period range. This trend can be explained by examining the detailed response characteristics in both ranges. Figures (3.5) through (3.8) show the details of the displacement response of the EP and EPI systems with periods 0.1 and 2.2 sec.

Figure (3.5) shows the time history of displacement response $u_x(t)$ of a long period structure with $T_x=2.2$ sec. Both the EP and EPI responses are shown. In each case, the response is mainly vibrational in nature; the plastic drift contribution is only a minor part of the total displacement. From the similarity between the EP and EPI

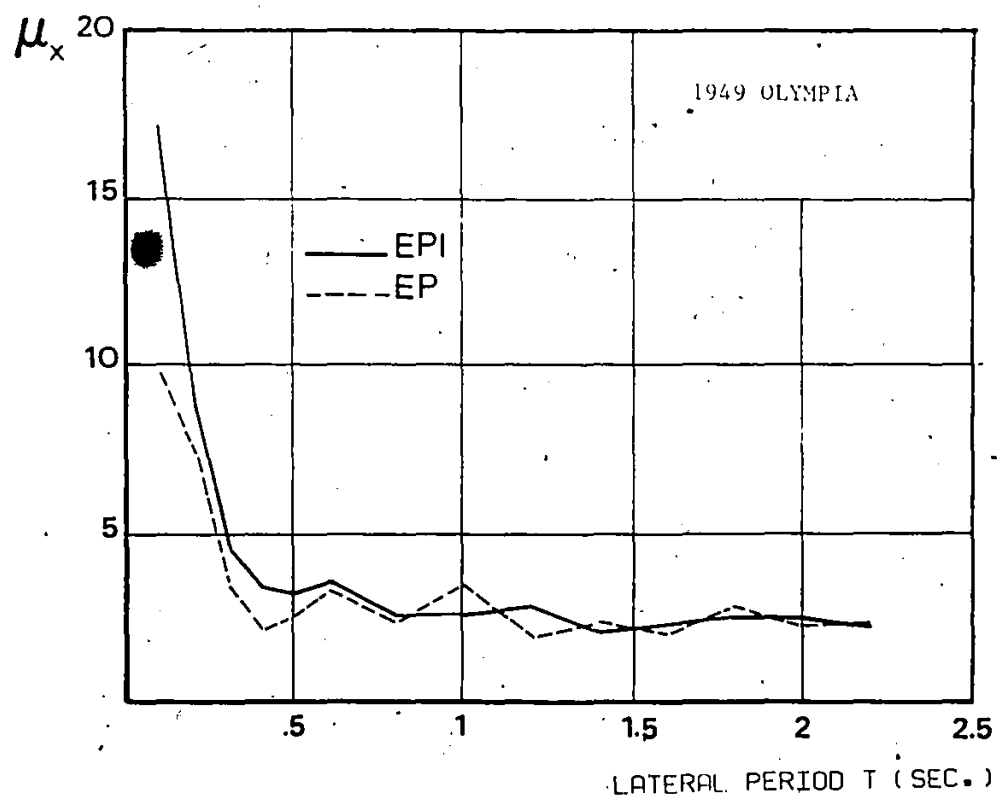


Fig (3.4) Ductility Demand μ_x of the EP and EPI Models; R=5

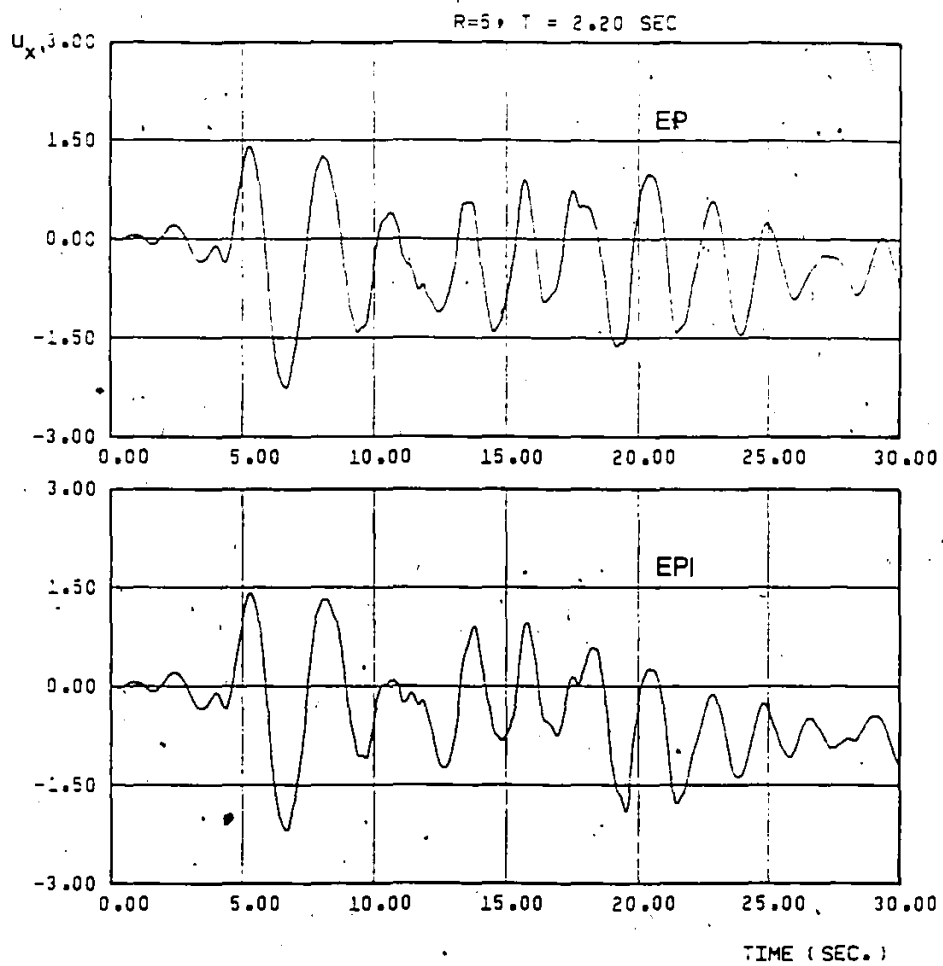


Fig (3.5) Displacement Time History of the EP and EPI Models; $T=2.2$ sec and $R=5$

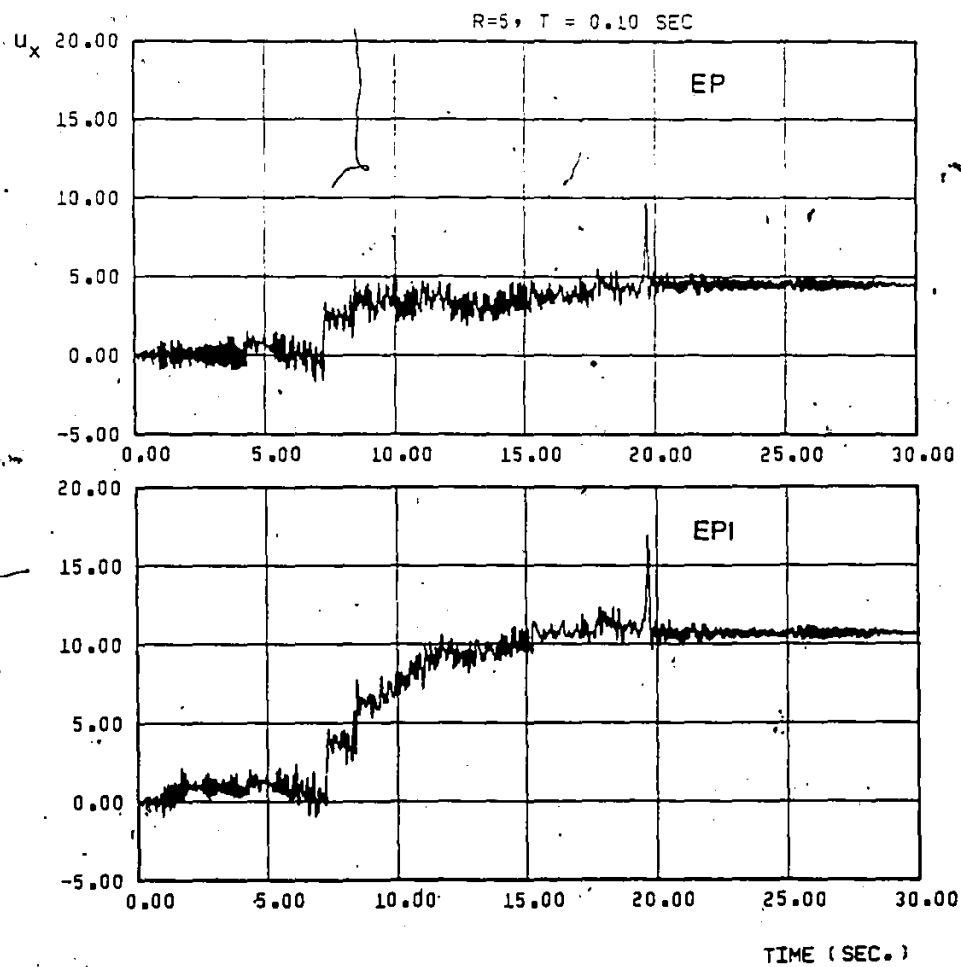


Fig (3.6) Displacement Time History of the EP and EPI Models; $T=0.1$ sec and $R=5$

responses, it appears that a yielding structure with a long period is insensitive to the further reduction in its strength capacity that occurs if interaction is included.

On the other hand, Figure (3.6) shows that a short period structure (0.1 sec) has different response characteristics. First consider the top figure showing the EP response. It can be seen that such a short period structure with low design strength ($R=5$) experiences large plastic drift which constitutes most of the displacement response. The vibrational part of response has only minimal contributions. When interaction effect is included, the plastic drift is substantially increased as shown in the bottom figure in Fig (3.6). While the plastic drift at the end of ground motion is less than five times the yield displacement for the EP system, it is increased to more than ten times when interaction effect is included. Therefore, short period structures with low design strength are prone to exhibit large plastic drift and sensitive to the effect of interaction. Including the interaction effect could lead to substantial increase in response over an equivalent EP response in this situation.

The hysteretic behavior of the above cases is shown in Figs (3.7) and (3.8). For the long period structure with $T_x=2.2$ sec, the hysteretic behavior is characterized by a number of complete wide loops signifying the vibrational type of response as shown in Fig (3.7). Different from the straight elasto-plastic hysteresis developed in the EP system, interaction causes less regular hysteretic behavior as shown in the bottom figure in Fig (3.7). The hysteretic behavior of the short period structure is characterized by a large number of thin hysteretic

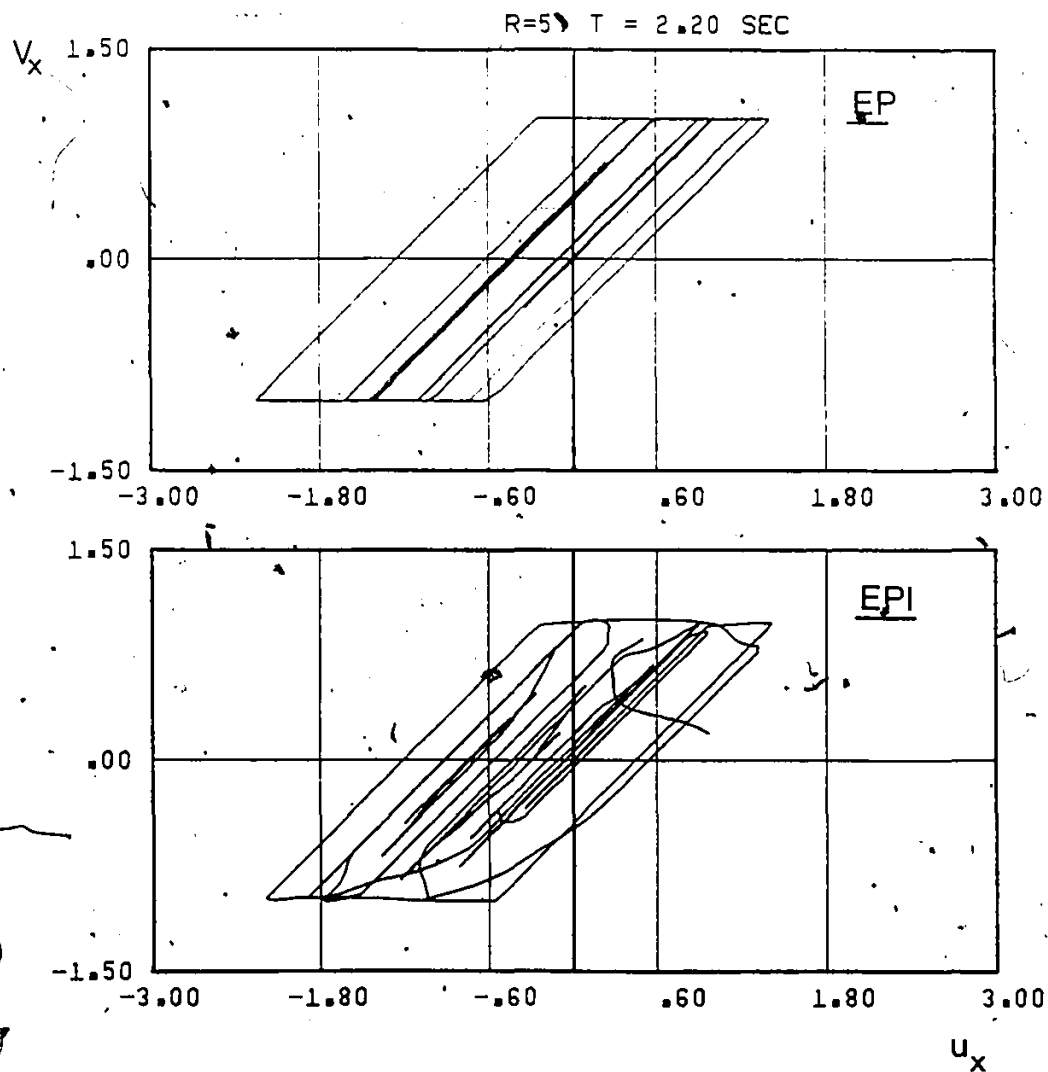


Fig (3.7) Hysteretic Behavior of the EP and EPI models; $T=2.2 \text{ sec}$ and $R=5$

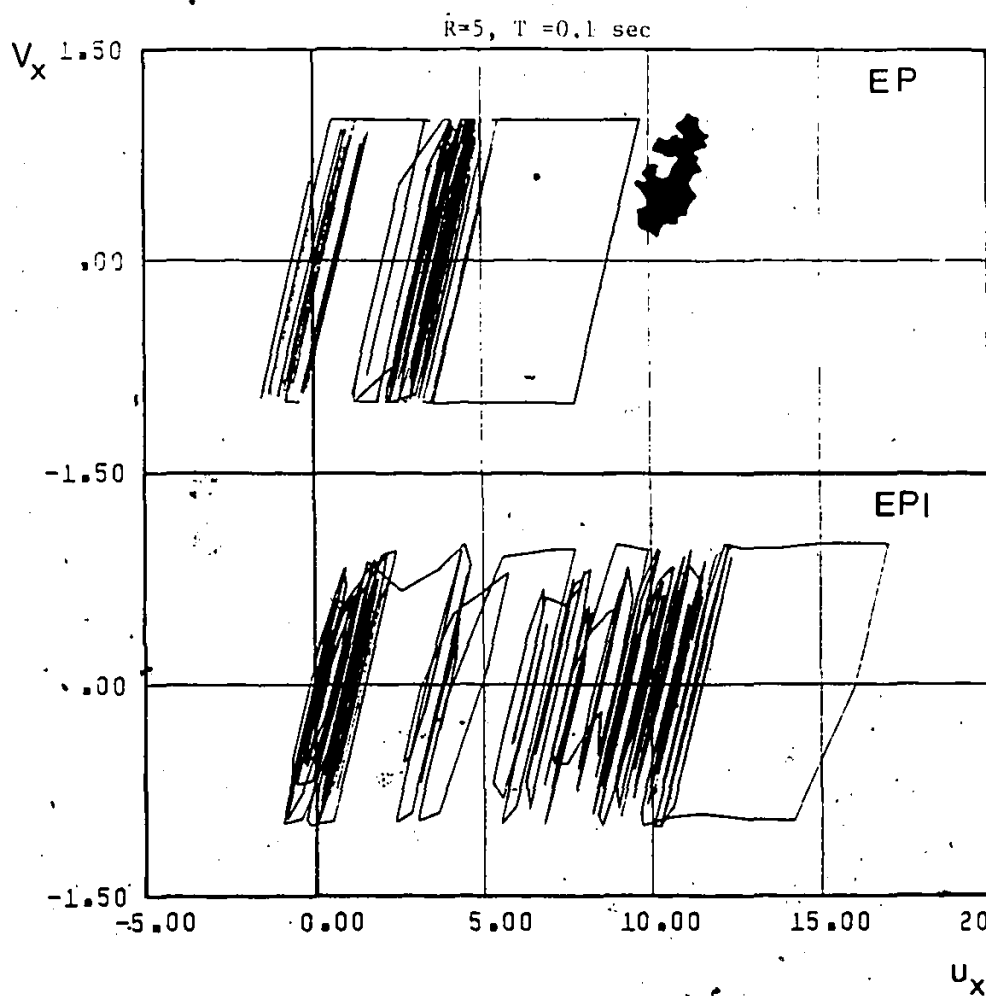


Fig (3.8) Hysteretic Behavior of the EP and EPI Models; $T=0.1 \text{ sec}$ and $R=5$

loops. These small loops are incapable of dissipating much of the energy in the structure. This is compensated by sizable plastic drift as an alternative mechanism of energy dissipation.

So far the effects of interaction on the displacement response are discussed when the structure is excited well into the inelastic range ($R=5$). These effects however are strongly dependent on the level of excitation. The EP and EPI responses to the Olympia ground motion for the case when $R=3$ is shown in Fig (3.9). Compared to the previous case with $R=5$, the displacement response is considerably reduced for the EP system, and is reduced even further due to interaction particularly in the short period range. Therefore, it appears that interaction becomes less significant on the displacement response for moderate levels of excitation.

Energy Transfer :

Allowing interaction in the model means that the behavior in one direction affects the response in the orthogonal direction, and vice versa. One interesting consequence is that part of the energy imparted in one direction can be transferred to the orthogonal direction. An example of the energy transfer is presented in Fig (3.10). It shows the variation of ductility ratio μ_x against T_x for the EP and EPI cases with $R=5$. In each case the NS and EW component of the 1940 El Centro earthquake records are acting along the x and y directions respectively. It can be seen that μ_x for the EPI case is noticeably larger than that of the EP system, even in the long period range. In that period range, the EW component of the El Centro ground motion acting along the y

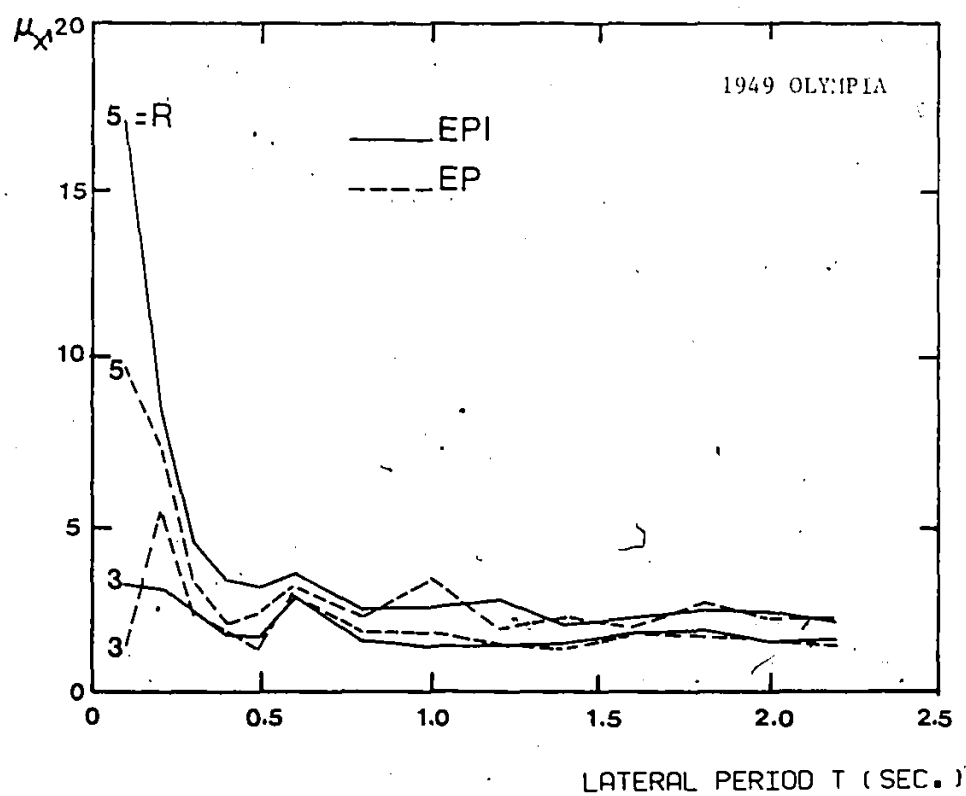


Fig (3.9) Ductility Demand μ_x of the EP and EPI Models;
R=3, 5

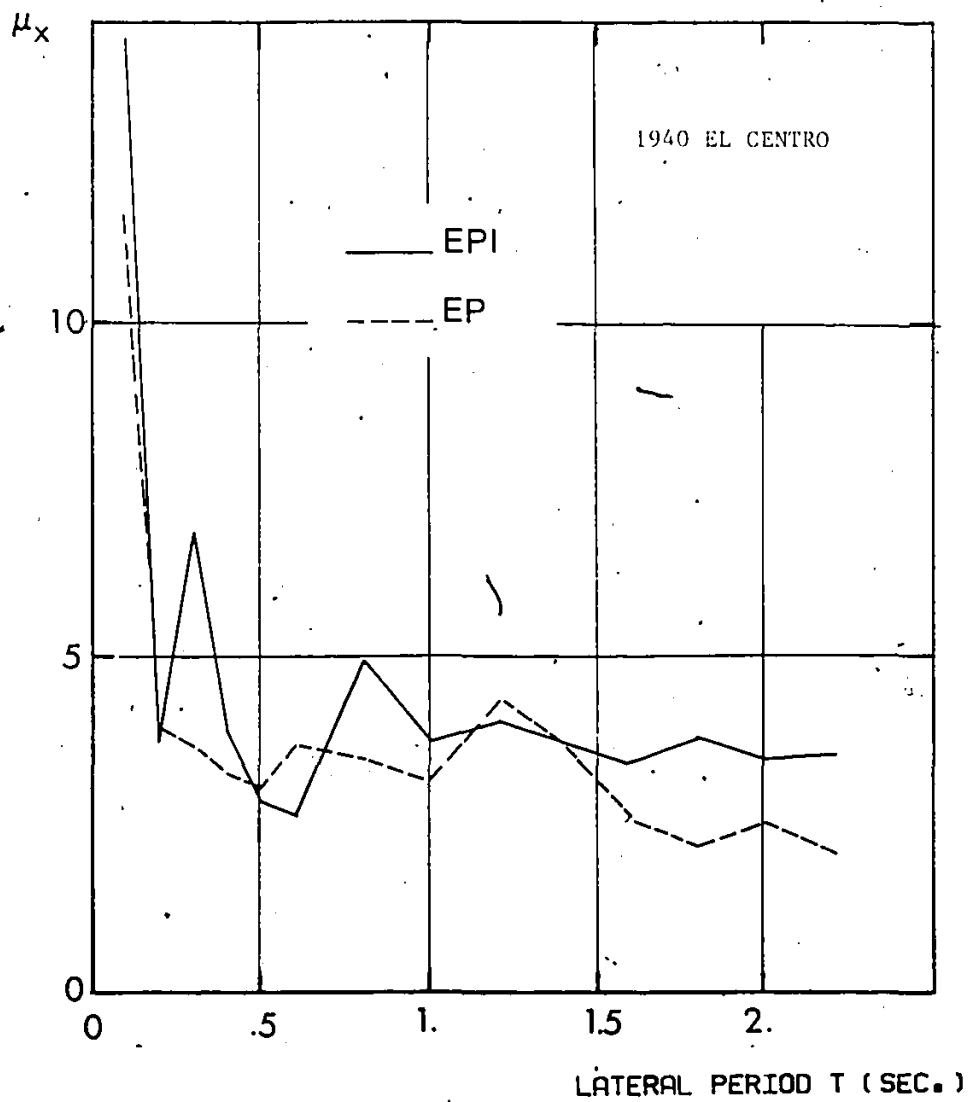


Fig (3.10) Ductility Demand μ_x of the EP and EPI Models; R=5
1940 El Centro Ground Motion

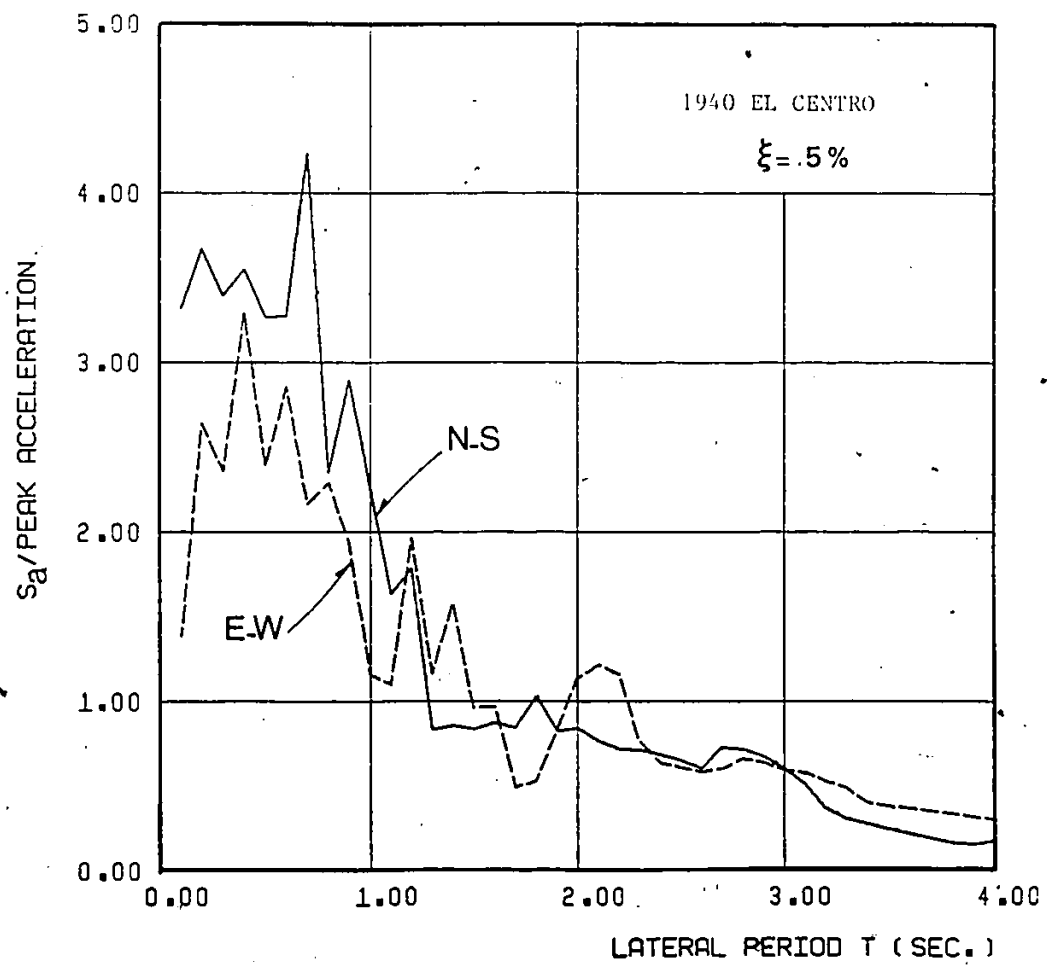


Fig (3.11) Elastic Acceleration Spectrum of the NS and EW Components of the 1940 El Centro Ground Motion; $\xi=0.5\%$

direction becomes stronger than the NS component; as indicated in Fig (3.11). Because of the coupling of motions in the x and y directions due to interaction, the response in the x direction is affected by the EW component. This increases the response of the EPI system over the equivalent EP system.

3.4.2 AXISYMMETRIC PROPERTIES OF THE EPI SYSTEM :

For structures subjected to seismic excitations, the angle of orientation θ_g of the axes of ground motion with respect to the principal structural axes (see Fig (3.12)) is a random parameter. The orientation that gives the maximum value to some response quantity should be considered in design. A related problem is to determine the resistance that can be offered by the structure along directions different from the principal directions. Both stiffness and strength resistance functions need to be considered.

Consider a symmetric structure with identical circular columns. The yielding of each column is described by a circular yield curve. The overall stiffness and strength resistance functions in their respective planes are shown in Fig (3.13). The axisymmetry of the resistance functions of the system implies the axisymmetry of the response. First let us define the normalized radial displacement $u_r(t)$ to be given by $(u_x^2(t) + u_y^2(t))^{1/2}$ and the radial ductility ratio μ_r as the maximum value of the normalized radial displacement, i.e. $\mu_r = \max |u_r(t)|$. It should be noted that the radial displacement does not occur along a fixed direction. In fact its direction varies with time and at any time

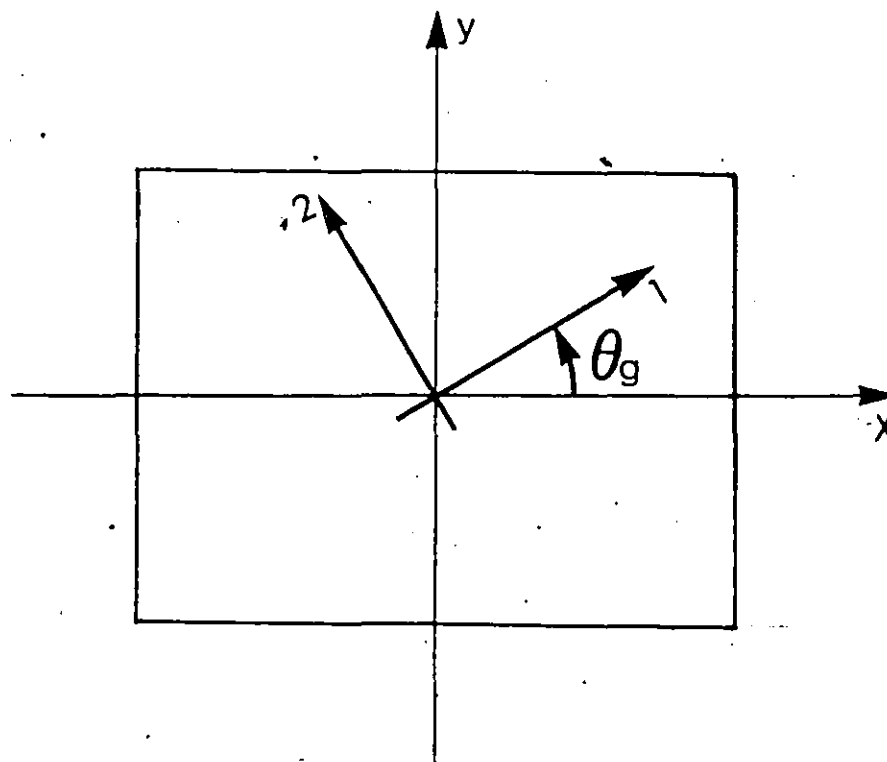


Fig (3.12) Orientation of the Ground Motion Directions Relative to the Structural Axes

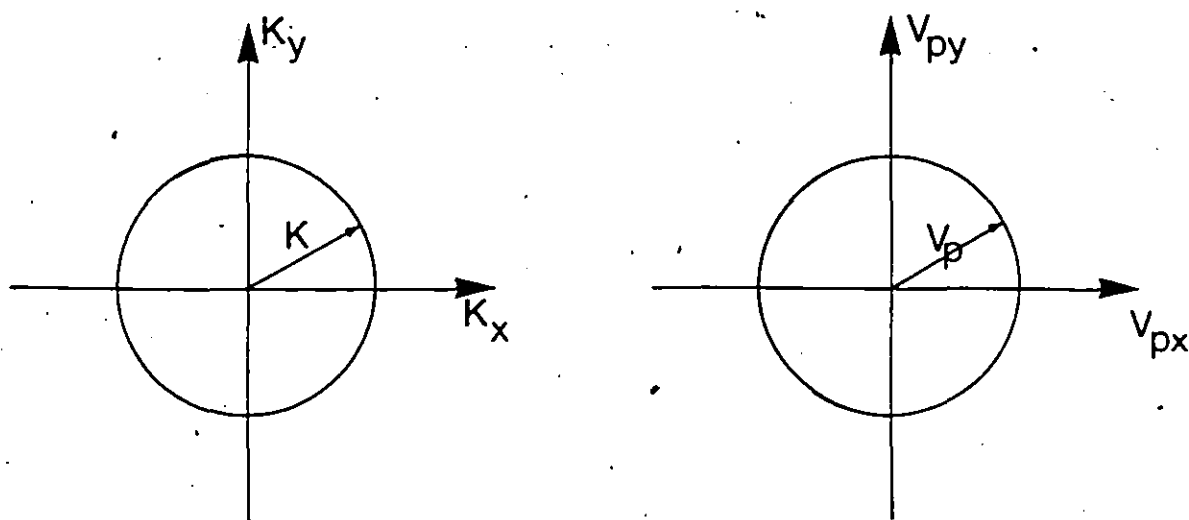


Fig (3.13) Axisymmetric Resistance Functions of Stiffness and Strength

t, it is given by $\arctan(u_y(t)/u_x(t))$. Also, let the resultant of $\ddot{u}_{g1}(t)$ and $\ddot{u}_{g2}(t)$, the 1-1 and 2-2 components of loading be expressed in polar form as $P(t), \theta(t)$ with magnitude and angle given by

$$\begin{aligned} P(t) &= [(\ddot{u}_{g1}(t))^2 + (\ddot{u}_{g2}(t))^2]^{1/2} \\ \theta(t) &= \arctan[\ddot{u}_{g2}(t)/\ddot{u}_{g1}(t)] \end{aligned} \quad (3.12)$$

Now, if this system of loading is assumed to act on the axisymmetric structure at two arbitrarily different orientations, it is expected that the radial response will be identical in both cases. This is due to the well known fact that the radial response of axisymmetric models is independent of the orientation of the applied load provided its magnitude remains unchanged. Therefore, for an axisymmetric structure where identical stiffness in two major axes exist and whose yield properties can be described by a circular yield curve, the radial response should be independent of the orientation of the ground motion axes.

Let us consider the inelastic response of the system with $T_x=1$ sec and $R=5$, when subjected to the two horizontal components of the 1949 Olympia earthquake ground motion. Three values of the orientation angle θ_g are considered, namely 0° , 30° , and 60° . Figure (3.14) shows the displacement response $u_x(t)$ and $u_y(t)$ along the x and y directions respectively. It can be seen that the response along fixed directions such as the principal structural axes is strongly dependent on the orientation of ground motions. In fact, with interaction effects included, the time variations $u_x(t)$ and $u_y(t)$ corresponding to any orientation θ_g can be related to $u_{x0}(t)$ and $u_{y0}(t)$ evaluated for $\theta_g=0^\circ$, by the following rotational transformation

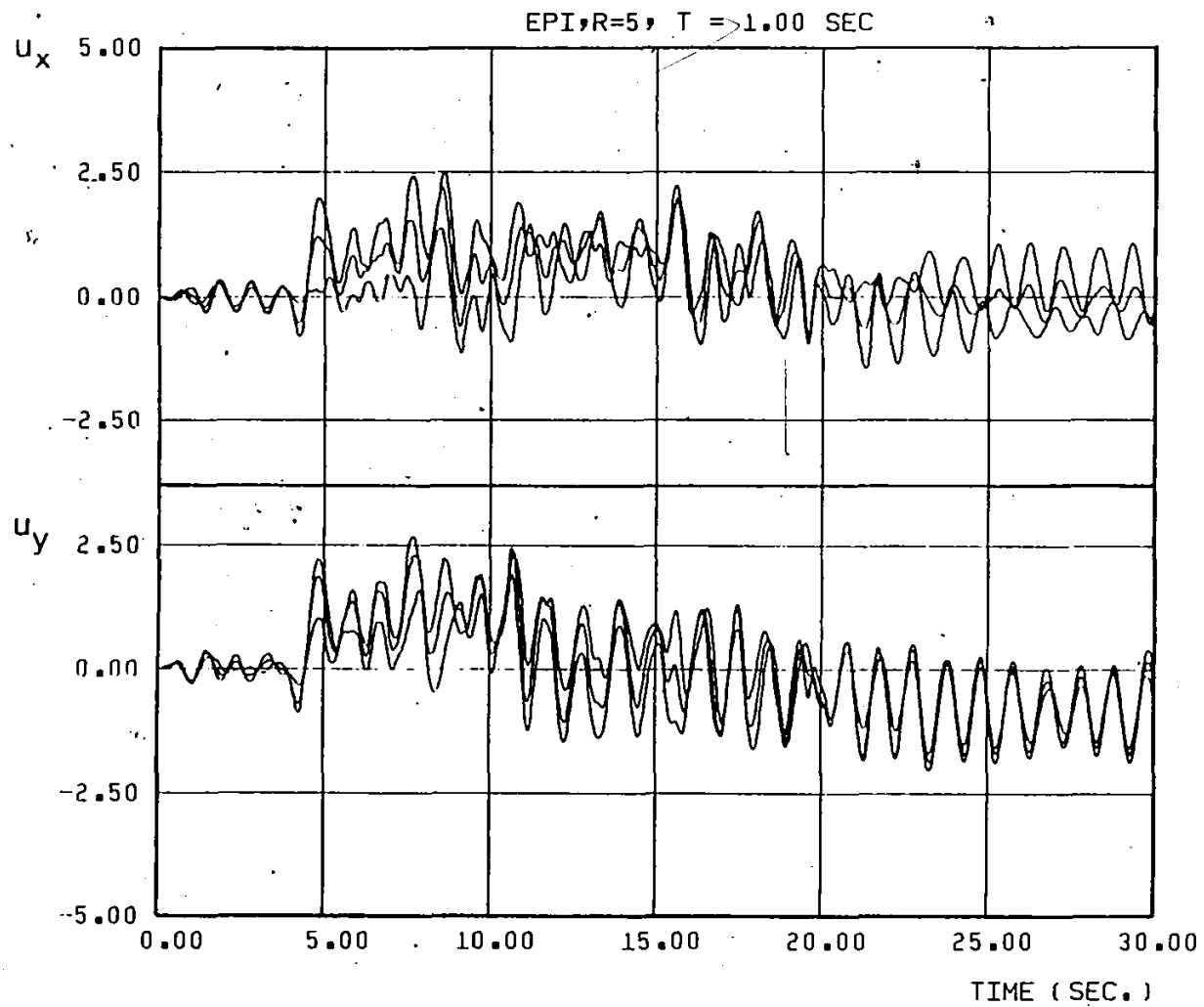


Fig (3.14) Time History of the Displacement Components $u_x(t)$ and $u_y(t)$ of the EPI Model; $\theta_g=0, 30, 60$ and $T=1$ sec

$$\begin{Bmatrix} u_x(t) \\ u_y(t) \end{Bmatrix} = \begin{bmatrix} \cos\theta_g & \sin\theta_g \\ -\sin\theta_g & \cos\theta_g \end{bmatrix} \begin{Bmatrix} u_{x0}(t) \\ u_{y0}(t) \end{Bmatrix} \quad (3.13)$$

On the other hand, identical curves of the radial displacement $u_r(t)$ are obtained for the different values of θ_g , as shown in Fig (3.15a). This calculation confirms that the radial response of the axisymmetric structures is independent of the excitation orientation as expected. However, if the interaction effect is ignored, then the radial response will vary with angle of orientation. Figure (3.15b) shows different curves of $u_r(t)$ for different values of θ_g . This calculation illustrates the illogical consequences of ignoring the interaction effect in computing the overall inelastic response of the system subjected to bidirectional ground motion excitation.

Since $u_r(t)$ is invariant with respect to orientation, it follows that the radial ductility ratio μ_r is also invariant of orientation angle θ_g . Figure (3.16) shows μ_r for models with interaction included (EPI) or ignored (EP) as a function of θ_g ranging from 0° to 90° . While μ_r does vary with θ_g in the EP model, it remains invariant for all θ_g values in the EPI model.

From design point of view, the radial ductility demand μ_r is an important response parameter. Nigam (34) recommended that this quantity be used as a measure of deformation in structures subjected to bidirectional excitations. Moreover, radial ductility ratio provides an upper bound of ductility demand along certain direction due to all possible orientations of ground motion axes. For the x direction, it

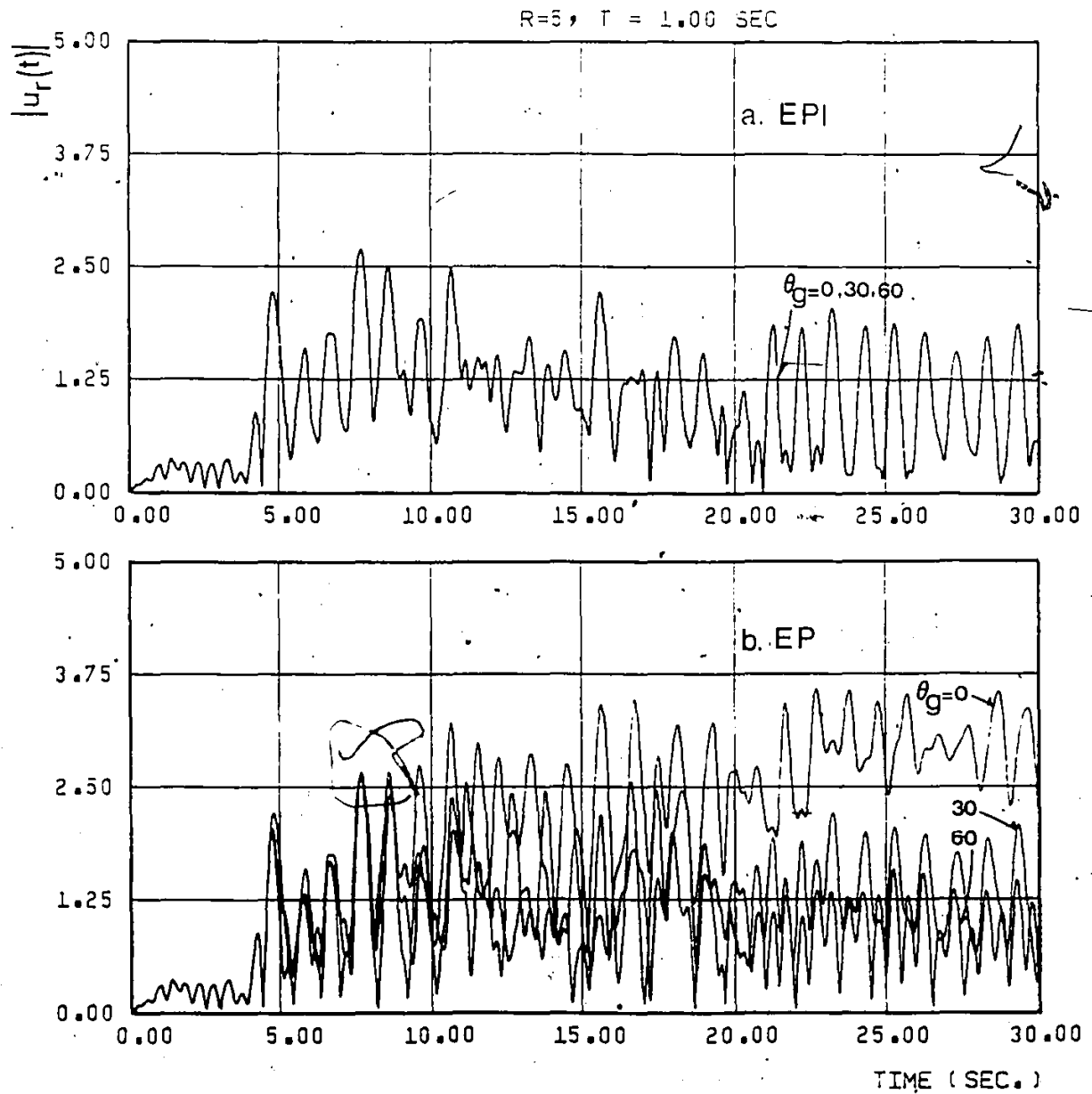


Fig (3.15) Time History of the radial Displacement $|u_r(t)|$ of the EP and EPI Models; $\theta_g = 0, 30, 60$ and $T=1 \text{ sec}$

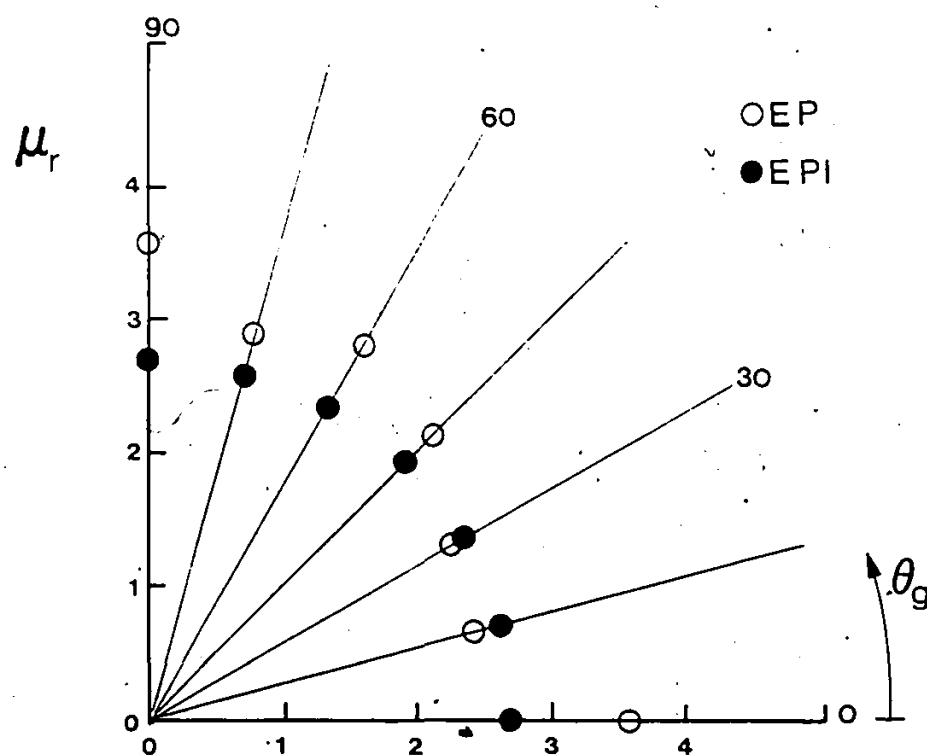


Fig (3.16) Variation of the Radial Ductility Demand μ_r with θ_g in the EP and EPI Models; $R=5$ and $T=1$ sec

can be stated that

$$\max \mu_x(\theta_g) = \mu_r^* \quad (3.14)$$

where μ_r^* is the radial ductility that is invariant with respect to orientation angle, i.e. obtained using the EPI model. μ_r^* can be compared with μ_x evaluated ignoring the interaction effect and orientation of the ground motion input. This comparison shown in Fig (3.17) indicates that ductility demand can be seriously underestimated if these effects are ignored in the analysis, particularly for short period structures.

The axisymmetric property of response for models with identical properties is also reflected in the total energy input response. The time variations of this parameter for models with and without interaction effect taken into account is shown in Fig (3.18a, and b). It can be seen that identical curves are obtained when interaction is included for different values of θ_g . It follows from this, that the value of the energy input at the end of the ground motion is also invariant with respect to θ_g in models with interaction as shown in Fig (3.19).

3.4.3 ENERGY INPUT :

The total energy input E_I^* is defined as the ratio of the sum of energy input in the x and y directions at the end of earthquake excitation to the elastic energy capacity $E_e = F_x \delta_x / 2$. For models with and without interaction, the variation of E_I^* as a function of natural period T_x is shown in Fig (3.20). The two horizontal components of the 1952 Taft earthquake records are used as input ground motion in the

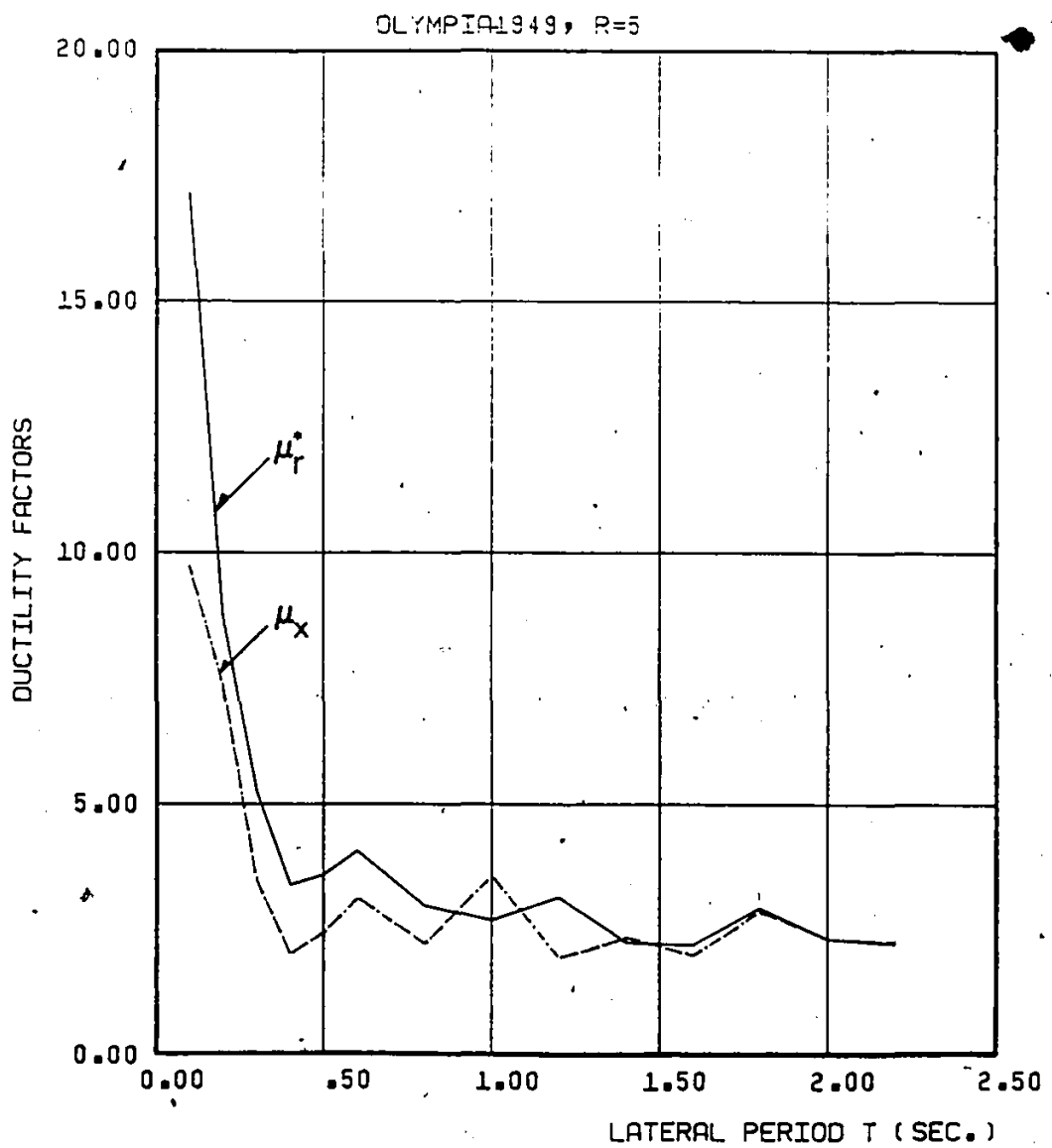


Fig (3.17) Comparison of Ductility Demand Estimates μ_r^* and μ_x ; R=5

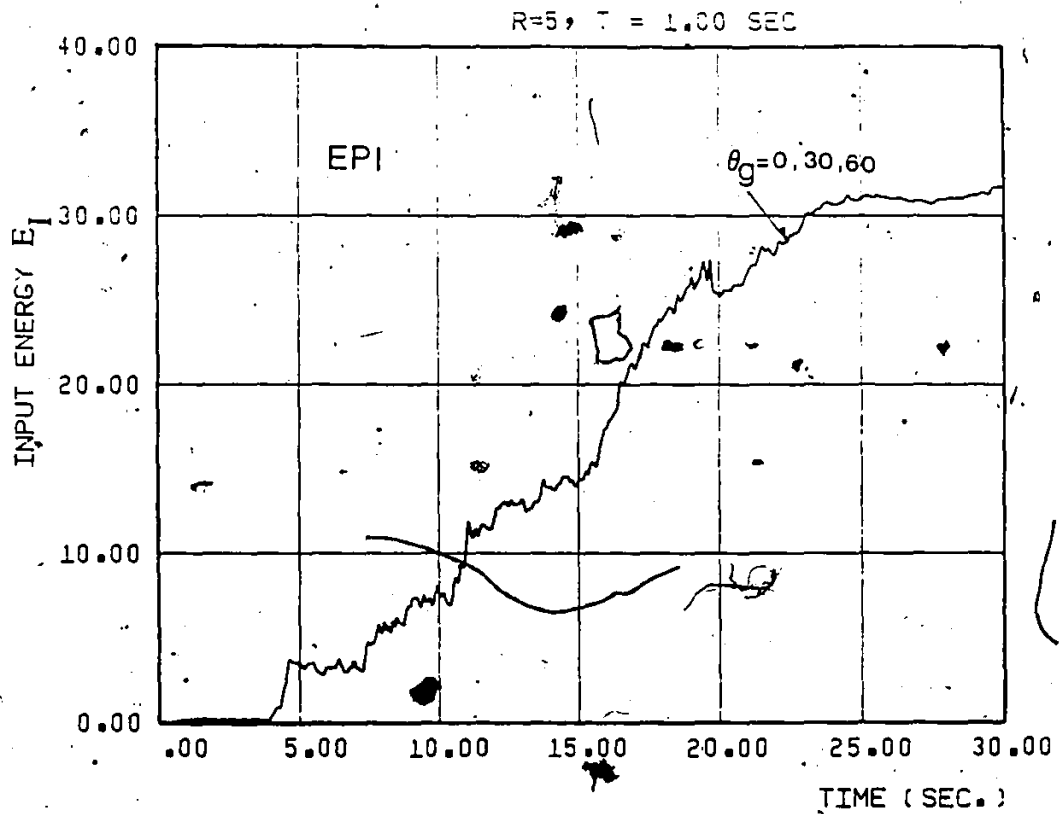


Fig (3.18a) Time History of the Energy Input E_I of the EPI Model;
 $\theta_g=0, 30, 60$ and $T=1 \text{ sec}$

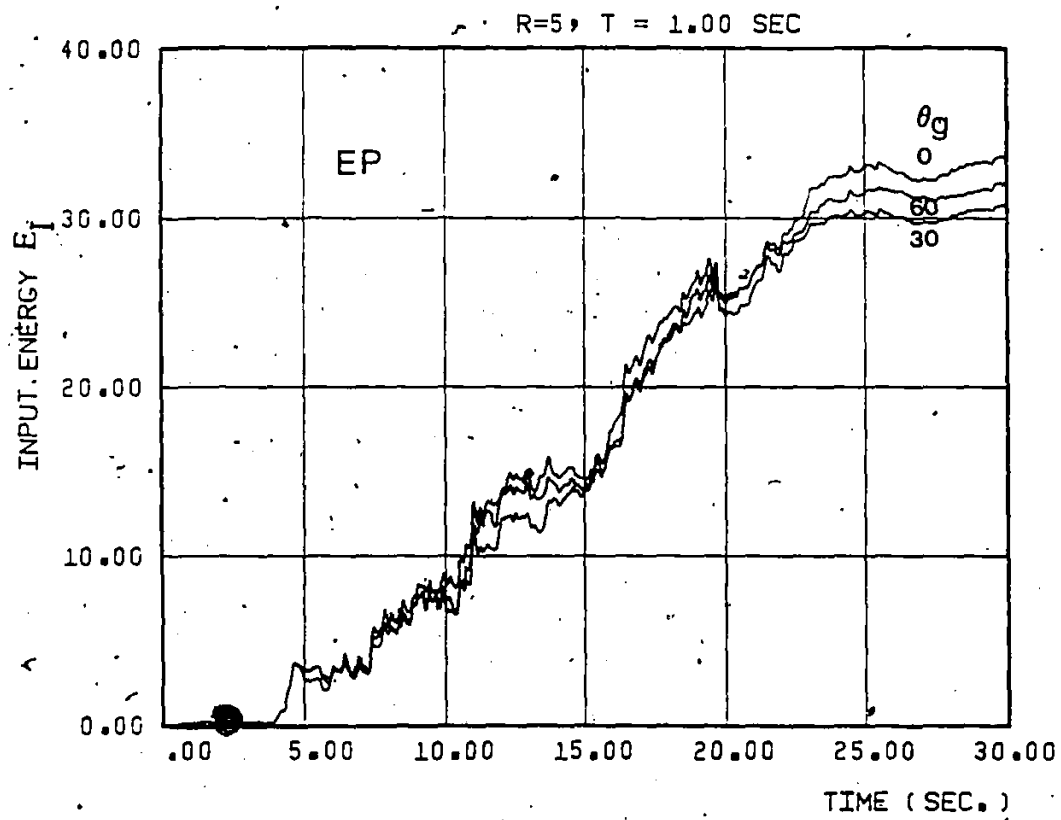


Fig (3.18b) Time History of the Energy Input E_I of the EP Model;
 $\theta_g = 0, 30, 60$ and $T=1 \text{ sec}$

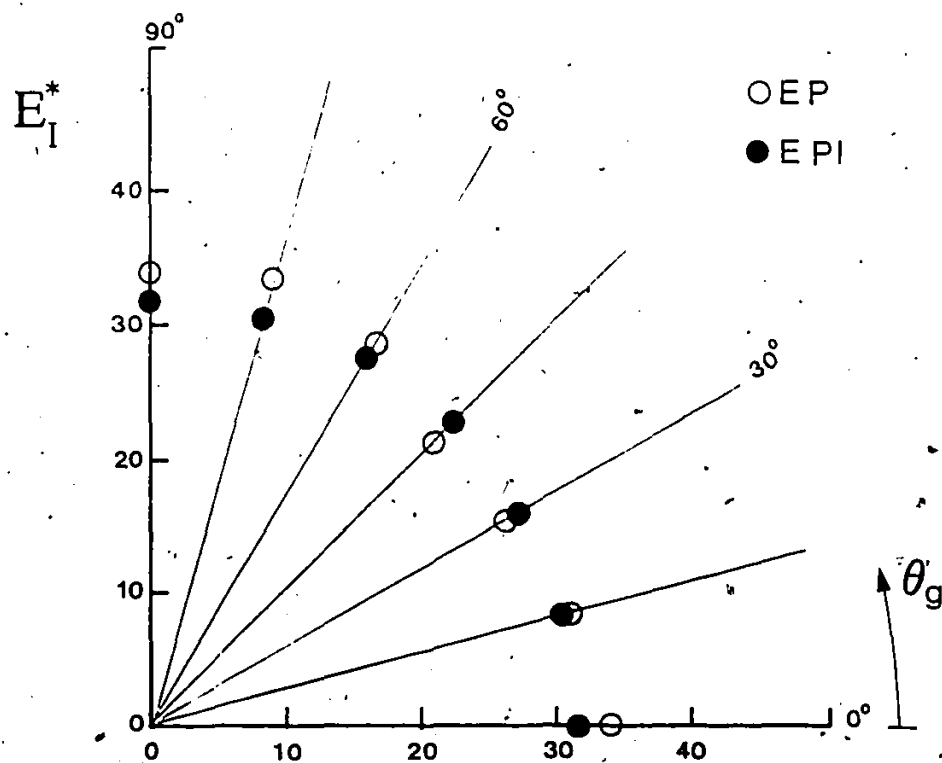


Fig (3.19) Variation of the Energy Input E_I^* with θ_g in the EP and EPI Models; $R=5$ and $T=1$ sec

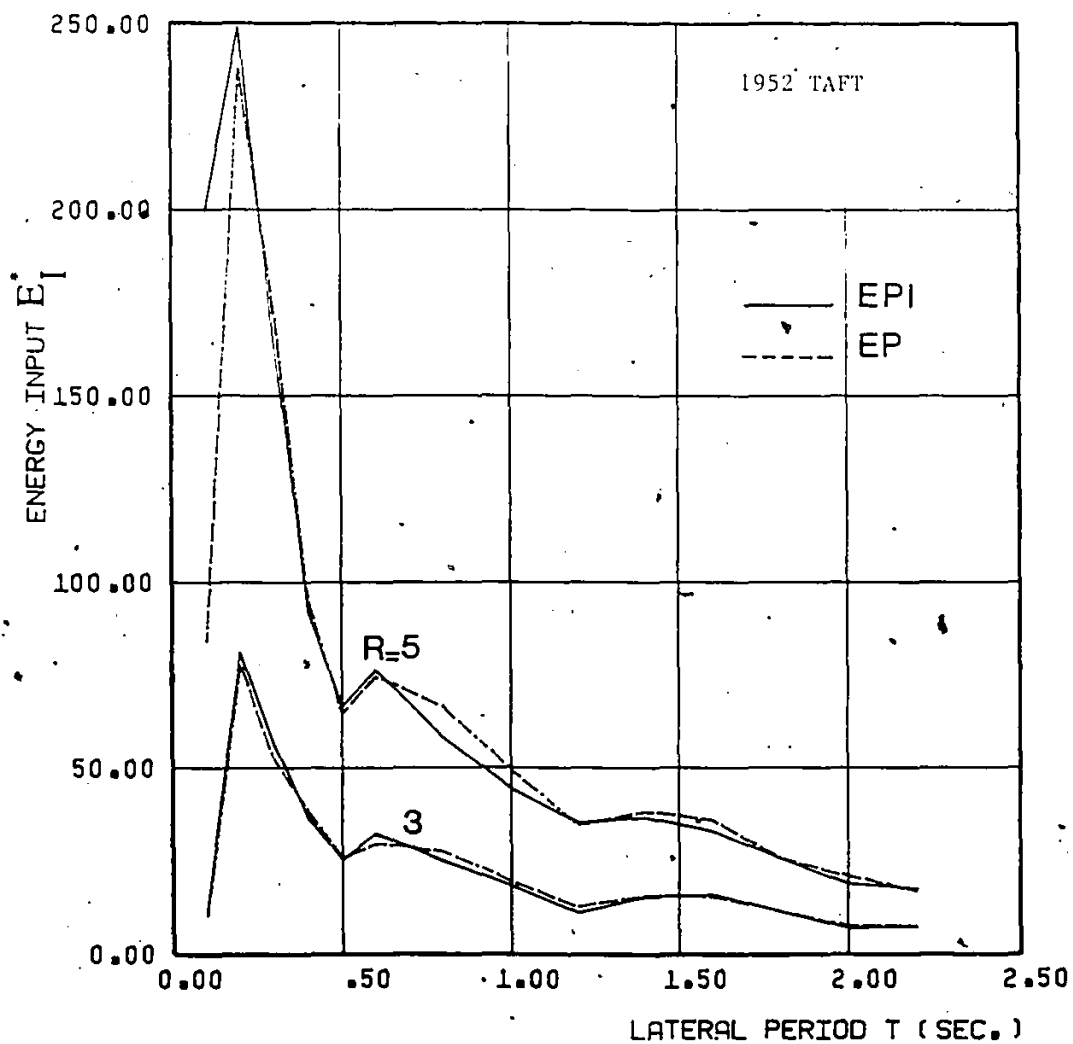


Fig (3.20) Comparison of the Energy Input E_I^* in the EP and EPI Models; $R=3, 5$ and 1952 Taft Ground Motion

calculation. The curves are shown for $R=3$ and 5 . With $R=5$, the energy input response is considerably increased for short period structures with $T_x < 0.2$ sec when the effect of interaction is included. Only a slight increase is observed for structures in this period range for the case when $R=3$. On the other hand, beyond $T_x=0.2$, including interaction hardly affects the energy input responses for both cases of R . Using the Taft earthquake records and considering systems with natural periods ranging from 0.25 to 2.5 sec, Nigam (34) stated that including interaction effect in the model tends to reduce the energy input response by up to 30% as compared to that of an equivalent EP model. Structures with natural period $T_x=0.25$ sec is the lowest period considered by Nigam. It is shown here that for shorter period structures, say $T_x=0.2$ sec, including interaction effect can lead to considerable increases in the energy input responses.

For elastic systems, if the energy input $E_I^*(R_0)$ at an excitation level R_0 is known, then the energy input at another excitation level n times larger, is given by

$$E_I^*(nR_0) = n^2 E_I^*(R_0) \quad (3.15)$$

For inelastic systems, Jennings (18) suggested that the concept of scaling energy by the n^2 factor also be used in an approximate sense. For the inelastic range, the equality in Eq (3.15) becomes

$$E_I^*(nR) < n^2 E_I^*(R) \quad (3.16)$$

In Figure (3.21), the energy input values calculated for models with $R=5$ are compared with those estimated based on the energy input response of

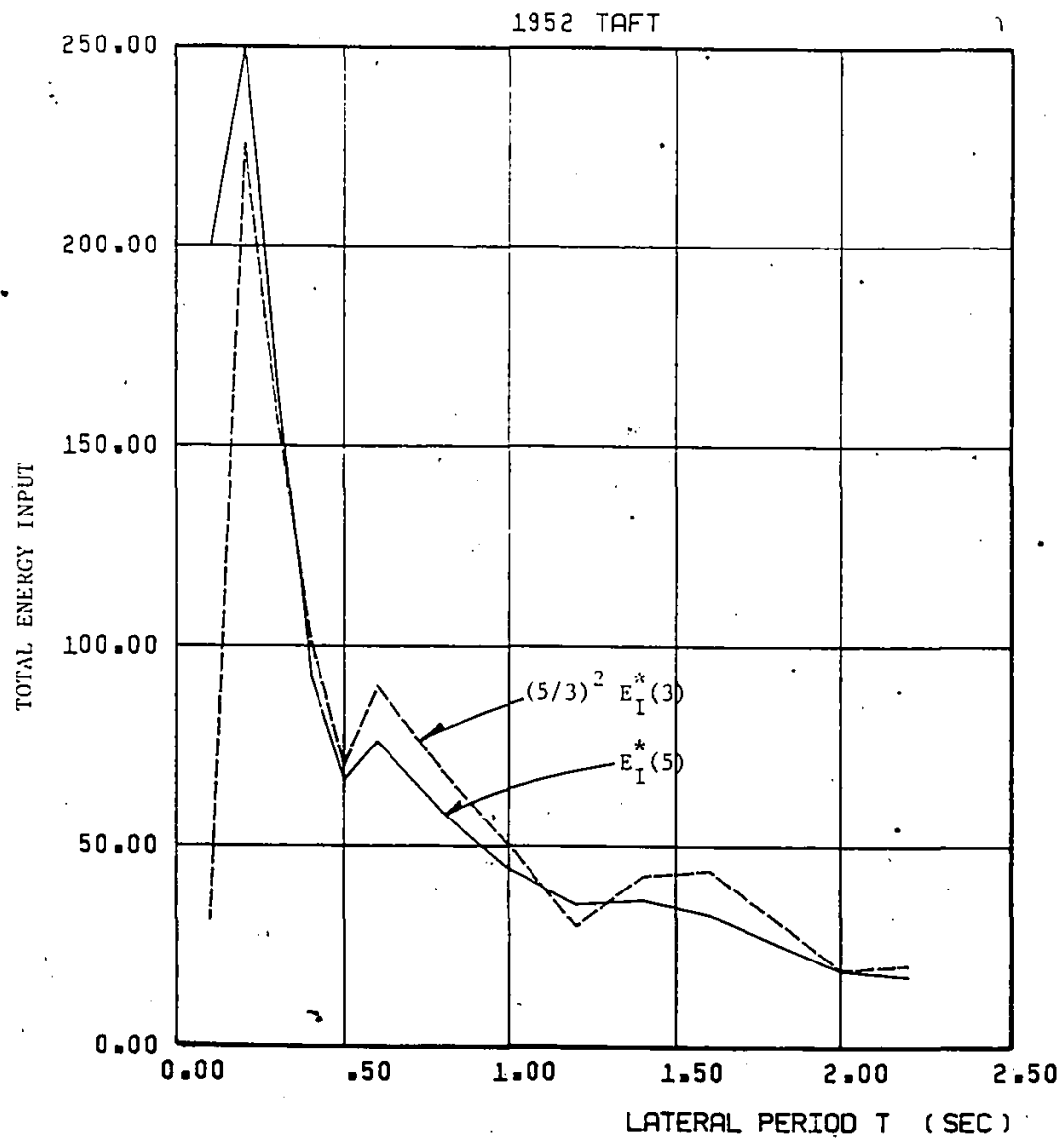


Fig (3.21) Comparison of Estimates of the Energy Input E_I^* , $R=5$ and 1952 Taft Ground Motion

models with $R=3$. In other words, the estimate is given by $(5/3)^2 E_1^*(R=3)$. It can be seen that the estimate is generally conservative for systems with $T_x \geq 0.4$ sec; however for systems with shorter periods, this method seriously underestimates the energy input response.

So far, specific earthquake records (El Centro 1940, Taft 1952, and Olympia 1949) are used to illustrate the effect of interaction on different response parameters of interest. The results obtained are compared with observations made by other investigators. One important observation is that for short period structures ($T_x < 0.25$ sec), the interaction effect is significant and many conclusions obtained by previous investigators do not apply in this short period range. In order to ensure the observations made are not specific to the particular pair of earthquake records used, a statistical approach is used as described in the next section.

3.4.4 RESPONSE TO ENSEMBLE OF EARTHQUAKES :

It is well known that many specifics of an earthquake record cannot be quantified readily. Therefore, any findings based on records of a single instrument during a single earthquake should be taken with caution. Thus to confirm the findings obtained so far using specific earthquake records, it is decided to consider the average responses to an ensemble of earthquakes. Averaging tends to eliminate the specifics and reveal the general trends in the responses. The ensemble used in this study for this purpose is described in the following.

ENSEMBLE OF RECORDED EARTHQUAKES :

The ensemble of ground motions considered consists of the two horizontal components of five actual earthquake recordings. The specifics of these earthquakes are listed in Table (3.1). All earthquake recordings are classified to be strong either in terms of their magnitude, $M_L > 6$, or in terms of peak acceleration.

An important characteristic of the ensemble is the associated elastic response spectra. Shown in Fig (3.22) is the mean acceleration spectrum of the five earthquake records for fractional critical damping $\xi=0.5\%$. In each pair, the stronger component is the one with the larger peak acceleration. This component is scaled to have one g peak acceleration and considered to act in the x direction. The other component is scaled up by the same factor and considered to act in the y direction. It is seen that the mean spectrum, both in the x and y directions, of the ensemble has a similar trend as the smooth spectrum S_a^* used to define the strength of the structure. The S_a^* curve is also shown in the same plots. the coefficients of variation (COV) of the response to these earthquakes in the x and y directions are also shown in Fig (3.23) as a measure of dispersion of results around the average values.

DUCTILITY DEMAND

Figures (3.24), (3.25), and (3.26) show the average curves of ductility demand μ_x , μ_y , and μ_r obtained using the elasto-plastic and

Table 3.1 Information on the Ensemble of Recorded Earthquake Ground Motions.

DATE	EARTHQUAKE	RECORDING SITE	MAGNITUDE M_L	COMPONENT	MAXIMUM ACC. (g)	DURATION (SEC.)
1940 May 18	Imperial Valley	El Centro	6.5	S00E	0.348	30
				S90W	0.214	30
1952 July 21	Kern County	Taft, Lincoln school Tunnel	7.2	S69E	0.179	30
				N21E	0.156	30
1934 Dec. 30	Lower California	El Centro Imperial Valley	7.1	S90W	0.183	30
				S00W	0.160	30
1949 Apr. 13	Western Washington	Olympia, Hwy. Test Lab	6.5	N86E	0.280	30
				N04W	0.165	30
1971 Feb. 9	San Fernando	Caltech Seismological Lab	6.3	S90W	0.192	20
				S00W	0.089	20

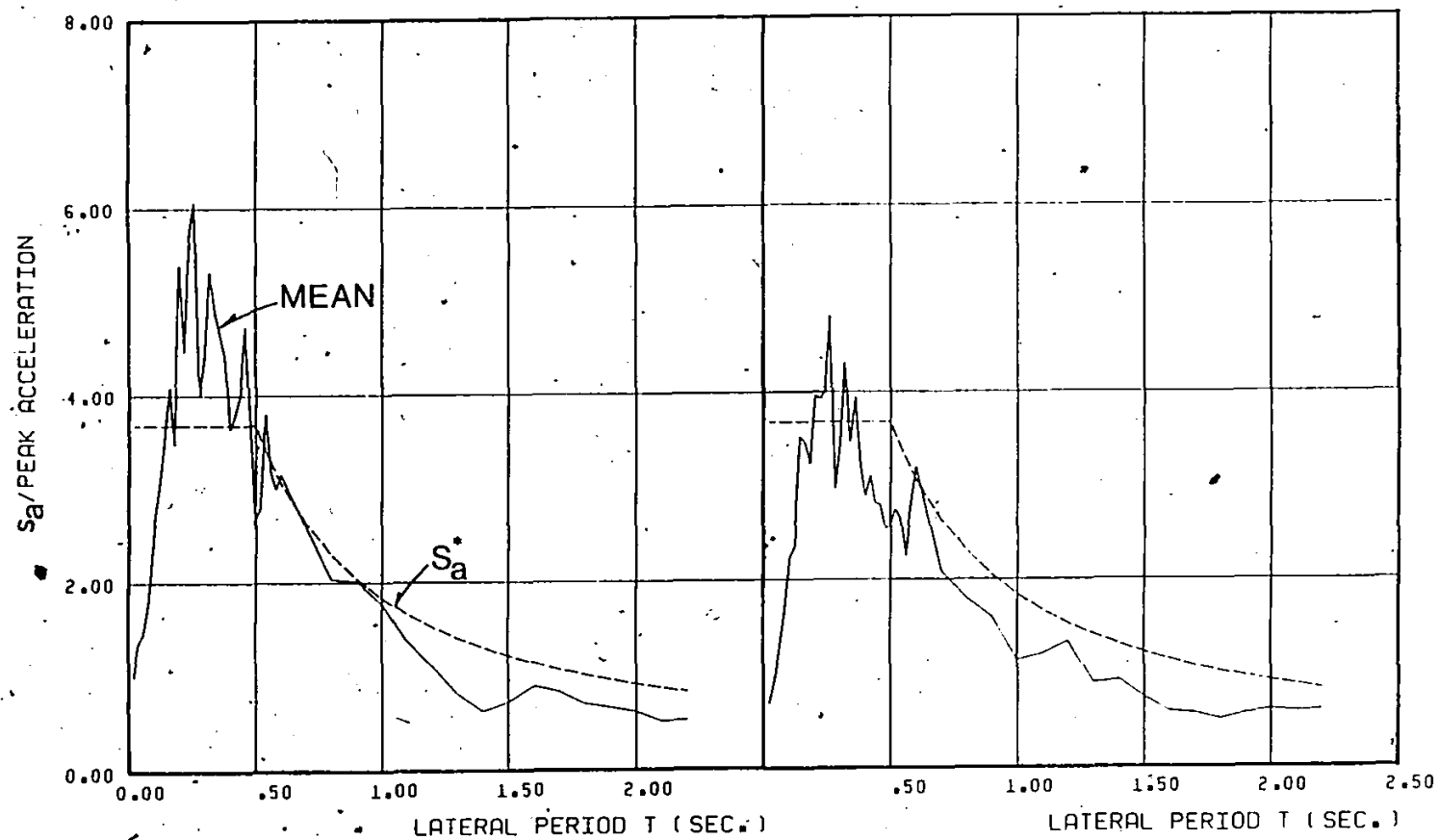


Fig (3.22) Mean Elastic Acceleration Spectrum of the Ensemble of Earthquakes Records; $\xi=0.5\%$

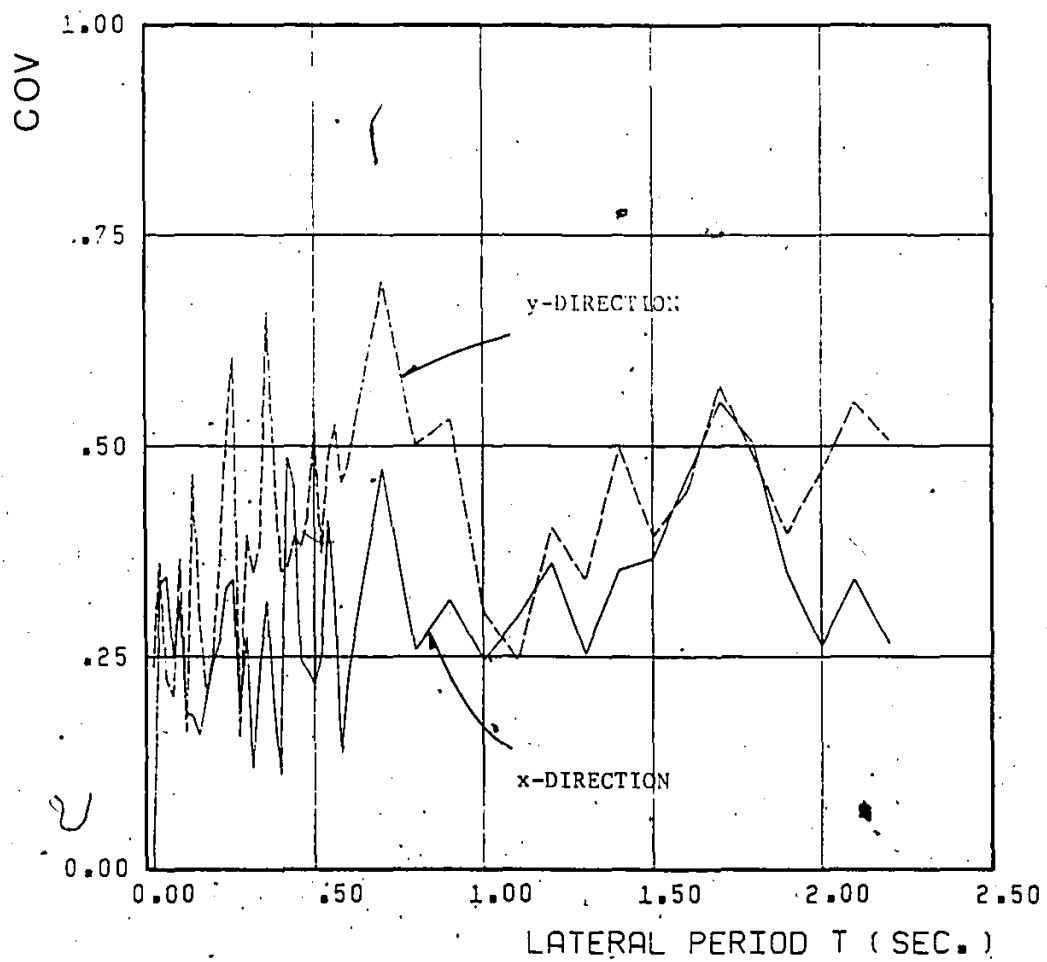


Fig (3.23) C.O.V. of the Elastic Responses to the Ensemble of the Earthquakes Records

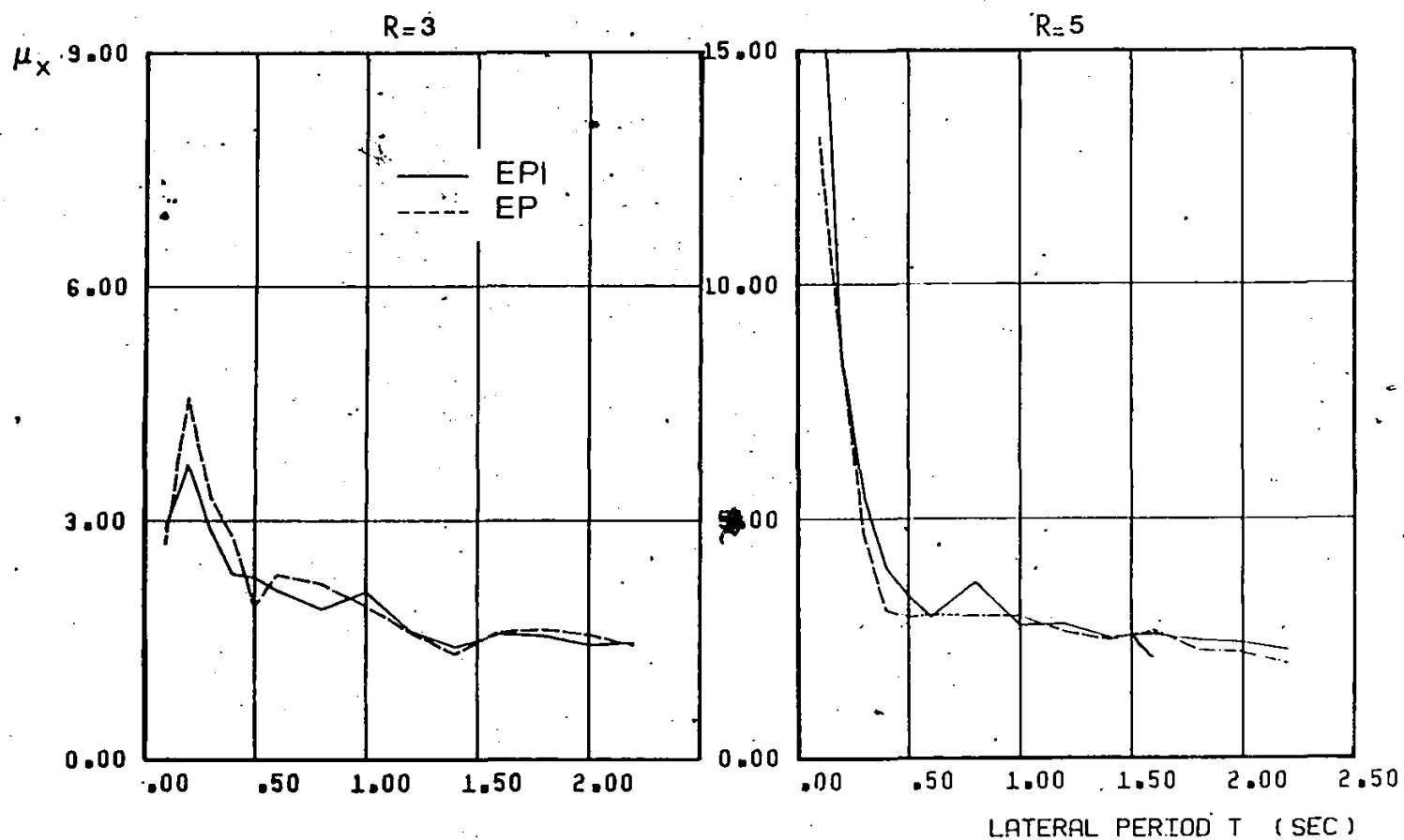


Fig (3.24) Average Ductility Demand μ_x in the EP and EPI Models; $R=3,5$

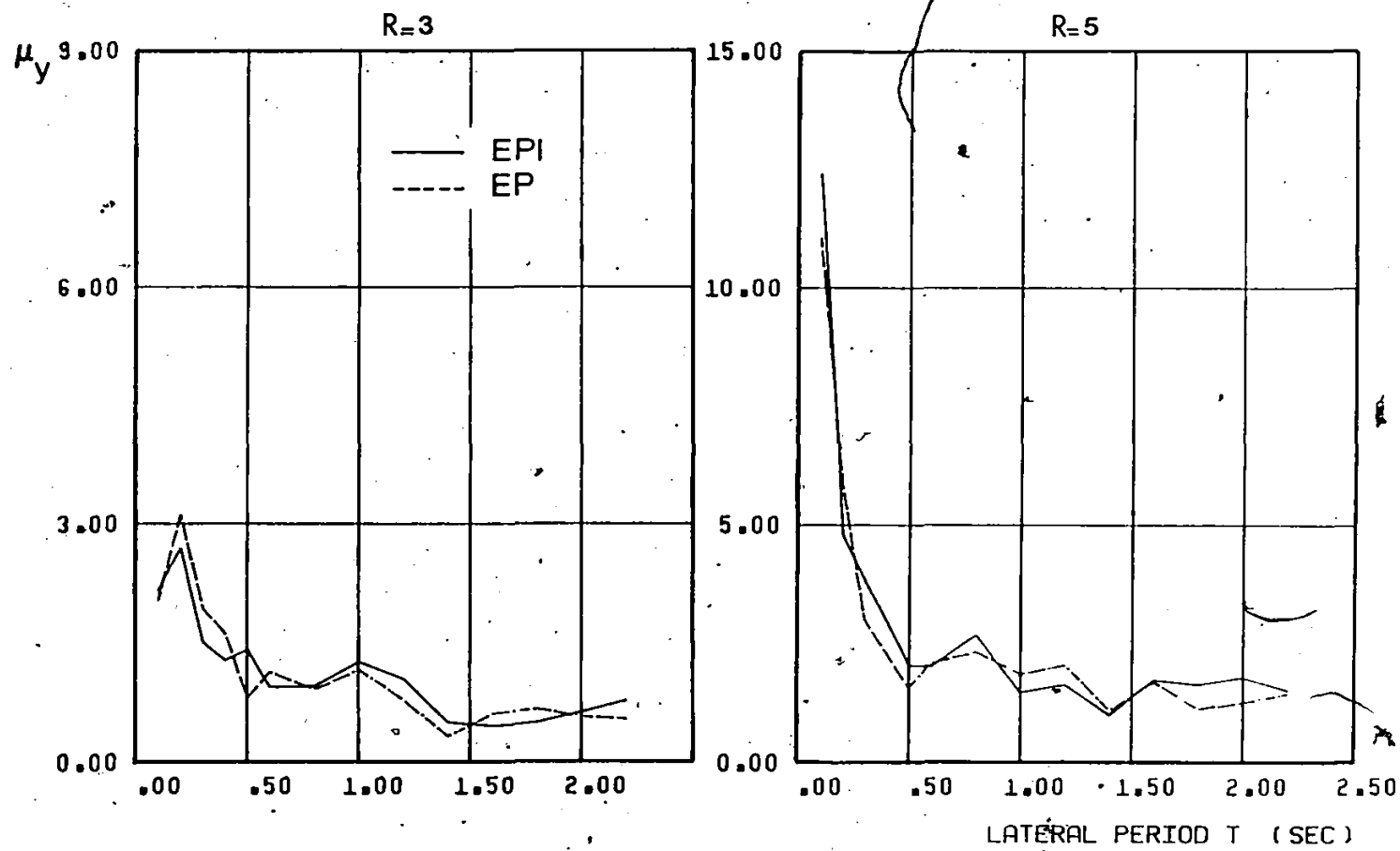


Fig (3.25) Average Ductility Demand μ_y in the EP and EPI Models; R=3,5

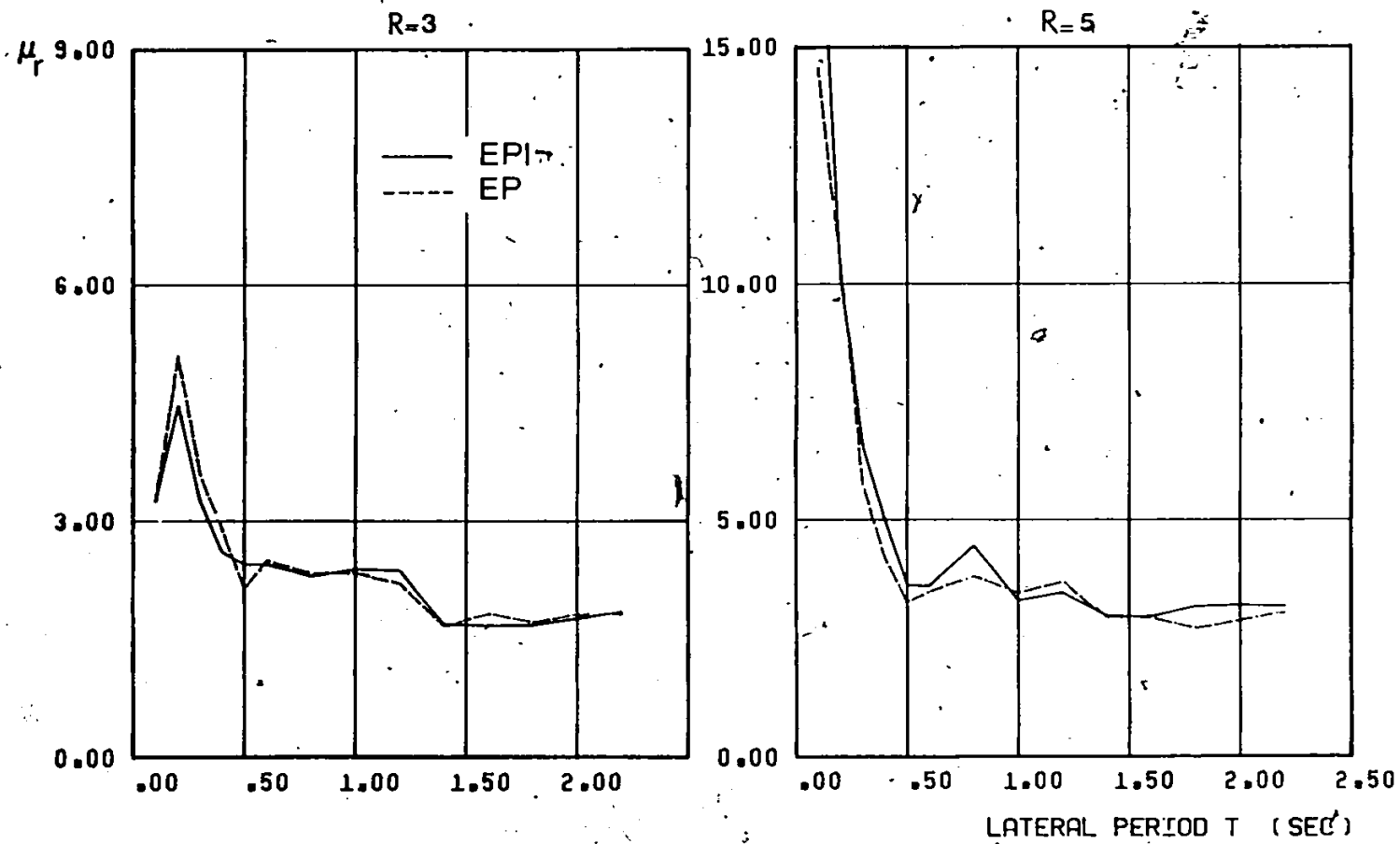


Fig (3.26) Average Ductility Demand μ_T in the EP and EPI Models; $R=3,5$

the elasto-plastic with interaction models for two values of reduction factor $R=3$ and 5. Trends of the average curves are in agreement with those observed earlier for the 1949 Olympia earthquake records. Hence the effects of interaction on ductility demand can be summarized as follows:

1. Including interaction in the inelastic analysis of long period structures ($T_x > 0.5$ sec) has a minor effect on ductility demand response. This holds true for all levels of yield strength relative to the elastic strength demand, in other words for all values of the reduction factor R .

2. For short period structures ($T_x < 0.5$ sec) with moderate yield strength ($R=3$), interaction favorably reduces the displacement response. Therefore, for this class of structures, an elasto-plastic analysis is expected to give conservative values of ductility demand.

3. Short period structures ($T_x < 0.5$ sec) with low yield strength ($R=5$) exhibit large values of ductility demand based on elasto-plastic analysis with unidirectional excitation. For such structures, including interaction increases ductility demand even further. The increase becomes very substantial for very short period structures ($T_x=0.1$ sec).

THRESHOLD YIELD STRENGTH LEVEL

Yield strength capacity has a remarkable effect on ductility demand of very short period structures ($T_x=0.1$ sec). Figure (3.26) shows the variation of average ductility with period for the cases $R=3$ and

$R=5$. The μ - T curves are remarkably different in the short period range. In the left figure ($R=3$), the μ - T curve has a major peak at $T_x=0.2$ sec, then it decreases for smaller periods. A μ - T curve with this feature is denoted as the "bounded" type. For the case $R=5$, the μ - T curve does not show any peak at $T_x=0.2$ sec and the values increase monotonically for decreasing periods. This behavior will be referred to as the "unbounded" type. This distinction suggests the existence of a threshold level of yield strength of structures that separates the two types of behavior. The ductility response of a structure in the short period range is characterized by the bounded or the unbounded type curves depending on its yield strength capacity being greater or lower than the threshold level respectively. The practical significance of the threshold level of yield strength is that one can avoid the very high ductility demand in the very short period structures by providing a yield strength capacity that is larger than the threshold value.

The ductility demand μ_x obtained using the elasto-plastic model with $T_x=0.1$ sec is shown in Fig (3.27) for the ensemble of earthquake records. Models are assumed to have different yield strength levels relative to the elastic strength demand as indicated by values of the reduction factor R ranging from 1 to 6. In the figure, the occurrence of the bounded and unbounded types of ductility demand curves is identified by the open and solid markers, respectively. The following observations can be made.

1. Yield strength which is as low as one third to one fourth of the elastic strength demand seems to be a reasonable estimate of the threshold level of yield strength capacity. These values correspond to values of the reduction factor R between 3 and 4.

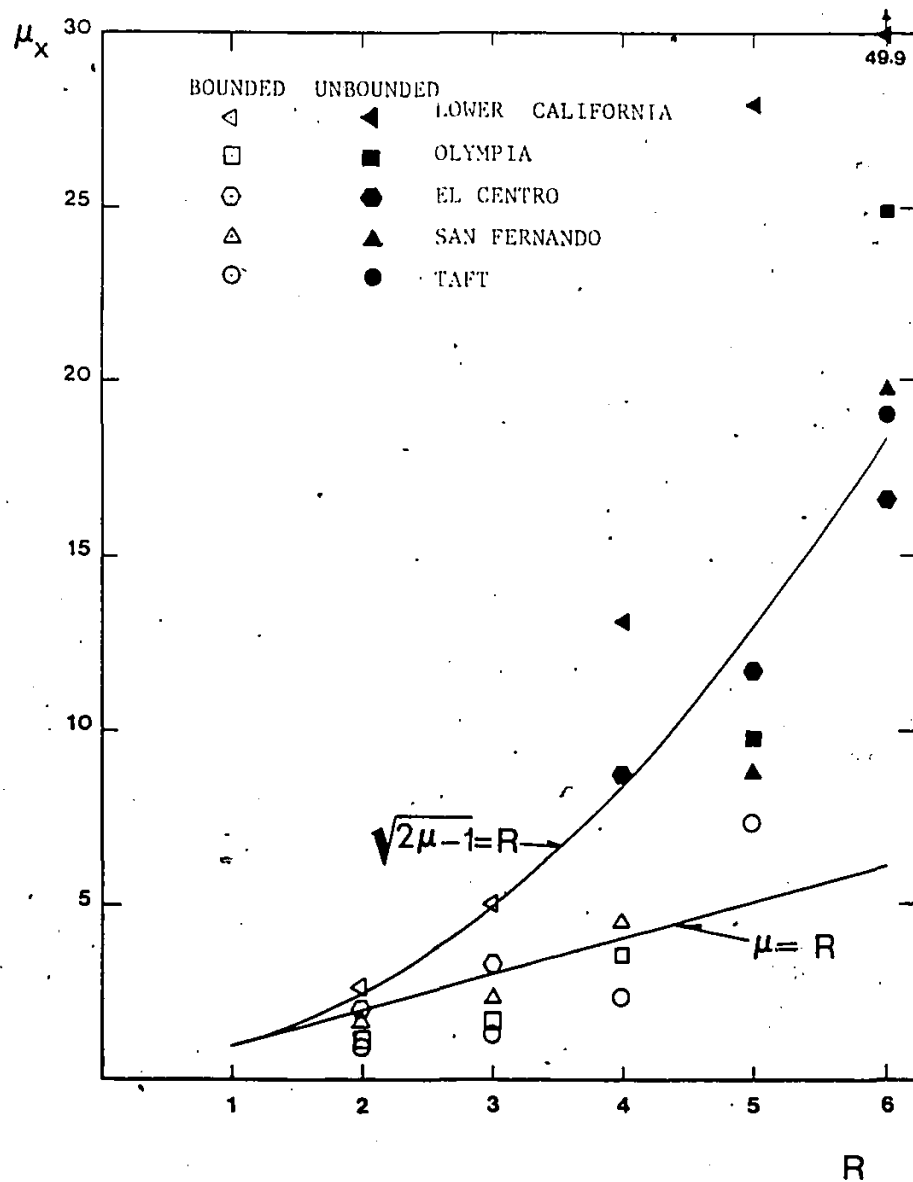


Fig (3.27) Variation of the Ductility Demand μ_x with Reduction Factor R in the EP Model; $T=0.1$ sec

2. For structures whose yield strength capacity are lower than the threshold value (i.e. $R > 3$), substantial values of ductility demand are observed. They even exceed the relation $\sqrt{2\mu - 1} = R$ suggested in (55).
3. Based on the current study it would be prudent to design very stiff structures with yield strength no less than one third of the elastic strength demand to avoid excessive ductility demand on the elements.

RADIAL PERMANENT SET

The permanent set is the nonrecoverable plastic deformation at the end of excitation. This parameter is important in determining repairing costs and the feasibility of restoring a damaged structure. Let μ_{px} and μ_{py} be the permanent deformation in the x and y directions respectively. Then the radial permanent set μ_p is given by $(\mu_{px}^2 + \mu_{py}^2)^{1/2}$. The average curves of μ_p are shown in Fig (3.28). The trends of these curves are similar to those of the ductility demand curves. Also it can be seen that short period structures with low yield strength ($R=5$) are particularly prone to substantial permanent deformation. The inclusion of interaction effect will further increase such permanent deformation. The permanent set constitutes most of the ductility demand of short period structures as shown in Fig (3.6).

DISPERSION OF RESULTS :

Figure (3.29) shows the coefficient of variation (COV) associated with the mean responses of ductility demand μ_x , μ_y , and μ_r .

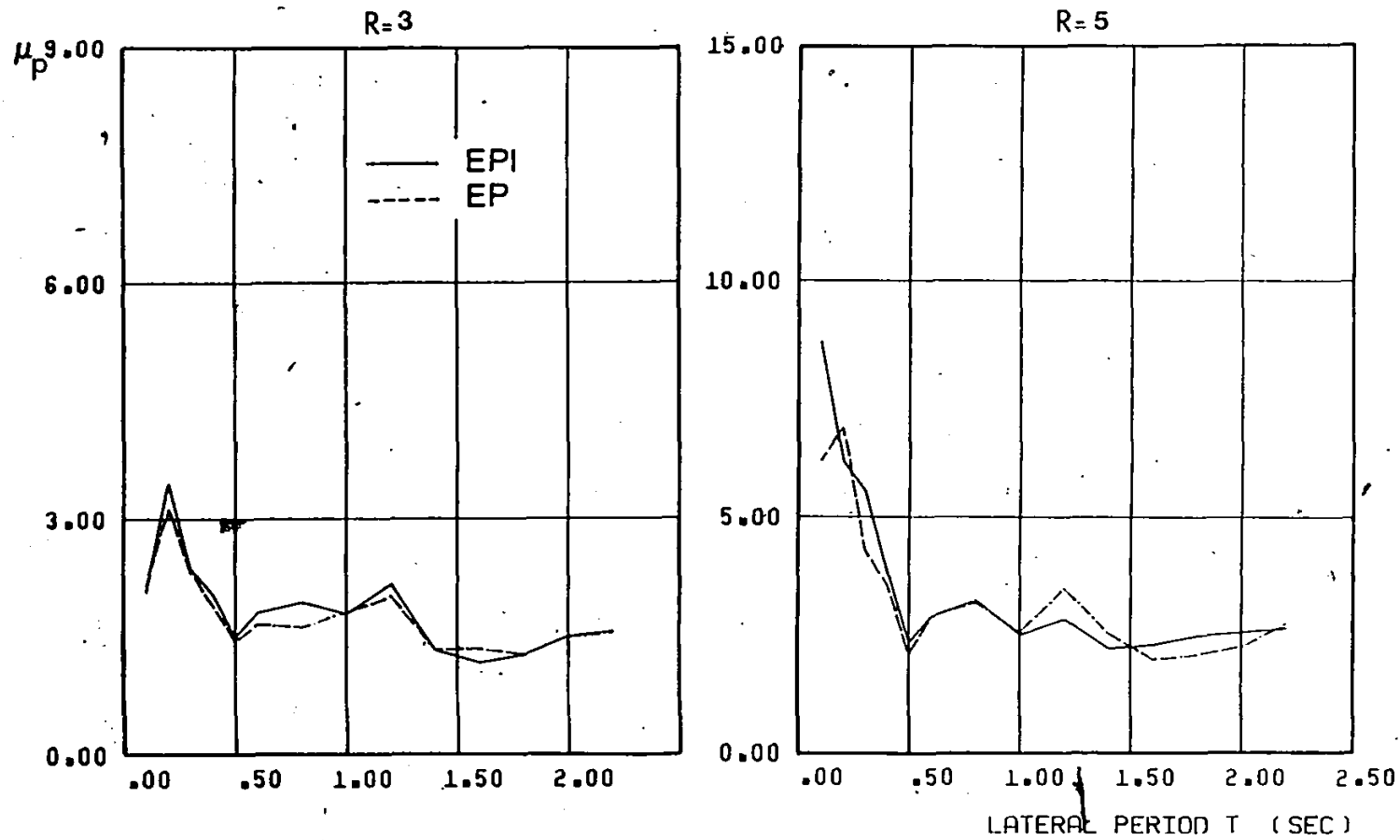


Fig (3.28). Average Radial Permanent Set μ_p in the EP and EPI Models;
 $R=3,5$

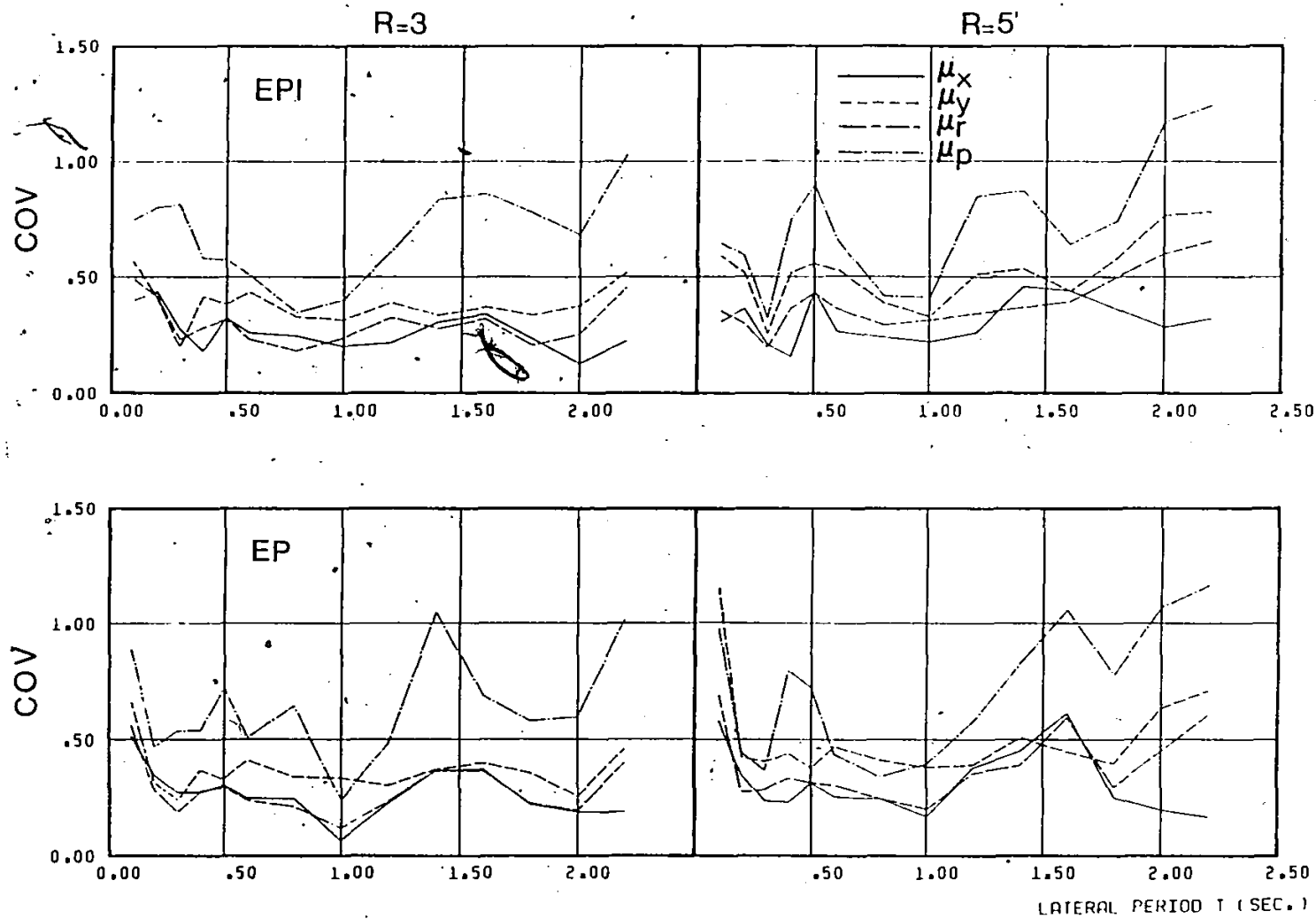


Fig (3.29) C.O.V. of the Inelastic Responses to the Ensemble of the Earthquakes Records; $R=3, 5$

and permanent set μ_p for models with interaction effect included or ignored. Also the average values of COV over the period range are presented in Table (3.2). Based on the values in Table (3.2), including interaction has little effect on the scatter of response. Also it can be observed that the permanent set μ_p shows the largest scatter. This indicates the sensitivity of permanent set to the particular records used.

RELIABILITY OF INELASTIC DESIGN METHODS :

Mahin et al (26) assessed the reliability of the inelastic design method suggested by ATC (48). In their assessment, a single degree of freedom model of either elastoplastic or stiffness degrading behavior is subjected to unidirectional excitations consisting of an ensemble of ten earthquake records. Attention is focused on the reliability of the method to limit the ductility demand to the specified values. It is found that this method fails to limit the ductility demand for structures with short period and low design strength. The results of that study can be complemented by the findings of the present study in which the model used is more realistic in two ways. First, the interaction effect is included in column yielding and second, the simultaneous action of bidirectional excitations is considered. Let μ_{x0} denote the ductility demand obtained using the elasto-plastic model and correspond to Mahin's results, and the radial ductility μ_r^* denote the ductility demand obtained with interaction effect included. The variation of the average ratio μ_r^*/μ_{x0} with natural period T_x is shown in Fig (3.30) for models with $R=3$ and 5. This ratio averages over the

Table 3.2 Average Values of COV of Different Response Parameters

	R=3		R=5	
	EP	EPI	EP	EPI
μ_x	0.27	0.27	0.31	0.31
μ_y	0.37	0.38	0.51	0.52
μ_r	0.28	0.30	0.38	0.39
μ_p	0.64	0.68	0.71	0.73

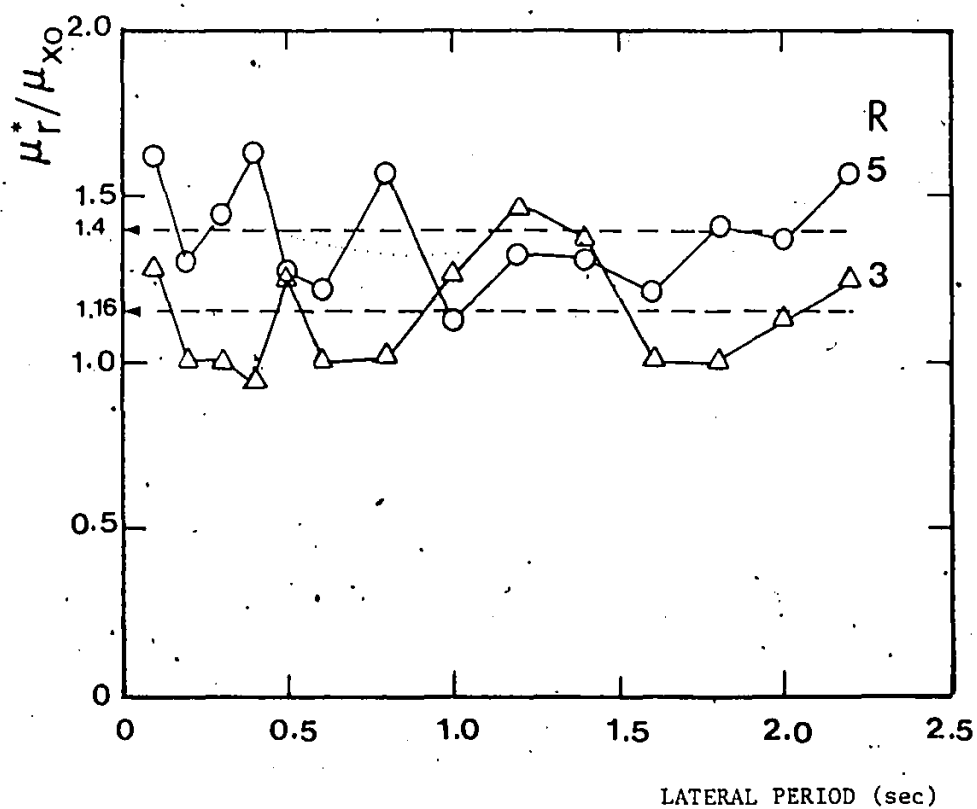


Fig (3.30) Mean Values of the Ratio of Ductility Estimates (μ_r^*/μ_x);
 $R=3, 5$

entire period range a value of 1.16 for $R=3$, and 1.40 for $R=5$. Thus the realistic estimate of ductility which accounts for interaction effects and bidirectionality of excitation, can be up to 40% larger than the values calculated otherwise.

TOTAL ENERGY INPUT :

The mean values of the ratio of total energy input E_I^* obtained with interaction effect included to that of an equivalent elasto-plastic model are shown in Fig (3.31). For models with $R=3$, the average curve fluctuates very close to unity throughout the period range. The same observation holds true for models with $R=5$ except in the short period range where there is a substantial increase in the total energy input to the system when interaction effect is taken into account. This confirms the findings based on the 1952 Taft earthquake records which indicate that for a short period structure with low yield strength, interaction causes the input energy response to increase. This increase is on the average about 50% over that when interaction is neglected.

3.5 APPROXIMATE ESTIMATES OF DUCTILITY DEMAND :

An elaborate inelastic analysis of structures which takes into account force interaction effect is complex and often costly. Therefore it is very desirable to have simple approximate methods to estimate the inelastic response of structures. The usefulness of any approximate method is assessed on basis of two criteria. First, the effort required to obtain the initial approximate value or the

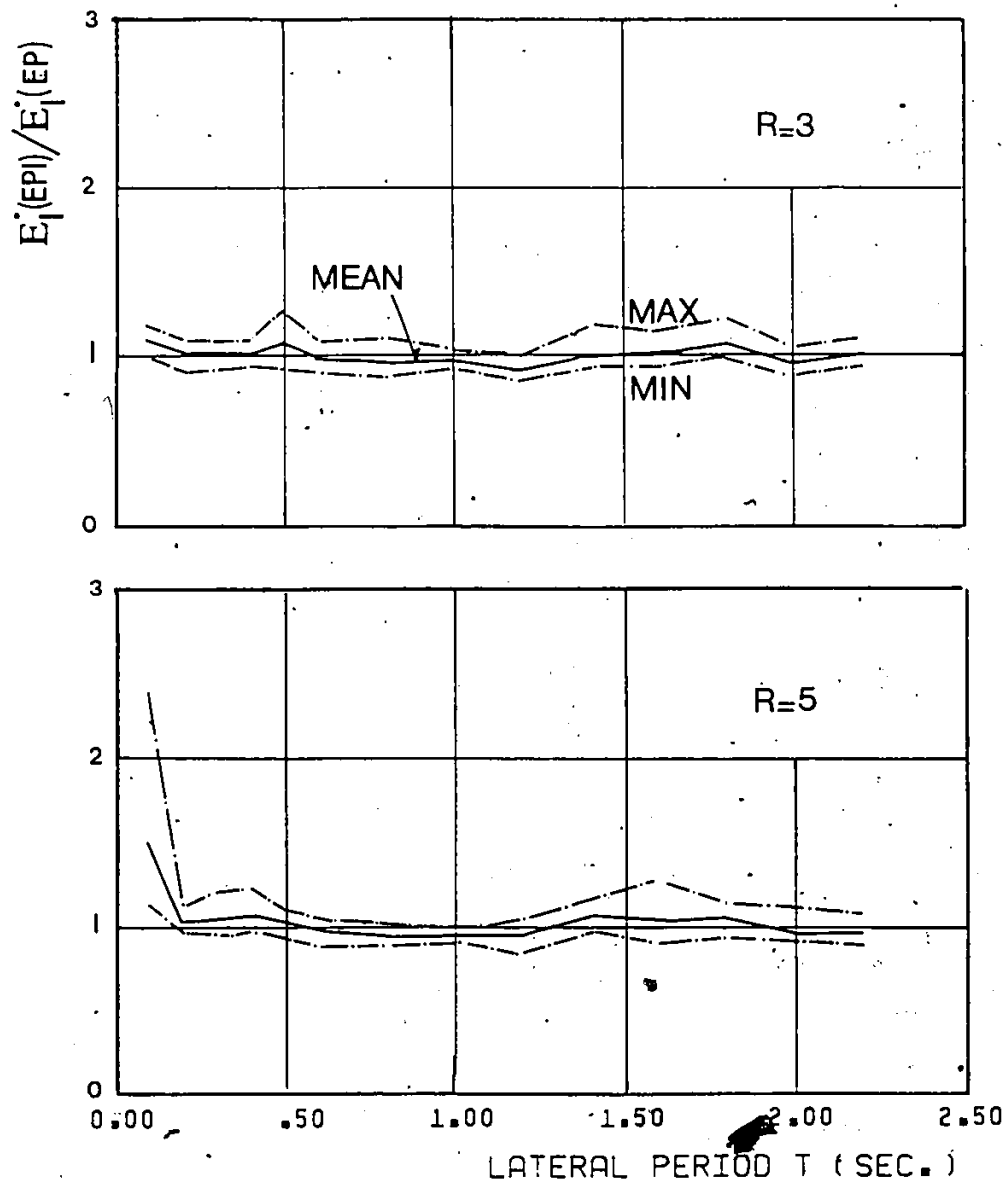


Fig (3.31) Ratio of the Energy Input E_1 in the EPI and EP Models;
 $R=3,5$

"estimator", and second, the degree of conservatism relative to the "true" values.

In the following, two approximate methods are given to estimate the ductility demand of single story structures with identical properties along two principal directions. The distinction between the two methods is based on the nature of the "estimator". In the first method, the elasto-plastic response is used as the estimator. Attention is focused on available formulae in literature (33, 44, 48). It is denoted as the EP-estimator method. In the second method, a scheme is proposed in which only the elastic response is required. Hence it is denoted as the E-estimator method.

In both methods, the best estimated values of ductility demand are defined to be those calculated using models with interaction effect included and are invariant to the orientations of ground motion axes relative to the structural axes, namely the radial ductility μ_r^* .

3.5.1 EP-ESTIMATOR :

The radial ductility μ_r^* can be estimated by combining the ductility demand μ_x and μ_y based on the EP planar responses to the two horizontal components of ground motion acting one at a time. Two combination schemes are attempted herein, namely

1. Newmark (33):

$$\mu_{E1} = \sqrt{2} \mu_x \quad (3.17)$$

2. ATC3-06 (48):

$$\mu_{E2} = \mu_x + 30\% \mu_y \quad (3.18)$$

Ratios μ_r^*/μ_{E1} and μ_r^*/μ_{E2} are calculated using the ensemble of earthquakes records. Figure (3.32) shows the variation of the mean values and the range of these ratios as function of systems period. Values are shown for models with $R=3$ and 5. The following observations can be made.

1. The curves of the mean values of the ratios for the two schemes are very similar. They both fluctuate close to unity. Then on an average basis, both schemes are considered to be equally successful.
2. A careful comparison of the ranges associated with the two schemes indicates that using the second scheme, which considers the responses to both components, tends to reduce the dispersion of results for both values of R .

3.5.2 E-ESTIMATOR :

Newmark and Hall (32) proposed a method to derive the inelastic design spectrum from the elastic design response spectrum. They proposed to deamplify the smooth elastic response spectrum using period dependent factors $\phi(u)$ defined as follows:

Short period range,

$$\phi_1(u) = 1/\sqrt{2u-1} \quad (3.19)$$

Long period range,

$$\phi_2(u) = 1/u \quad (3.20)$$

The inelastic spectrum so obtained if used in analysis is expected to limit the values of ductility demand to the specified value u .

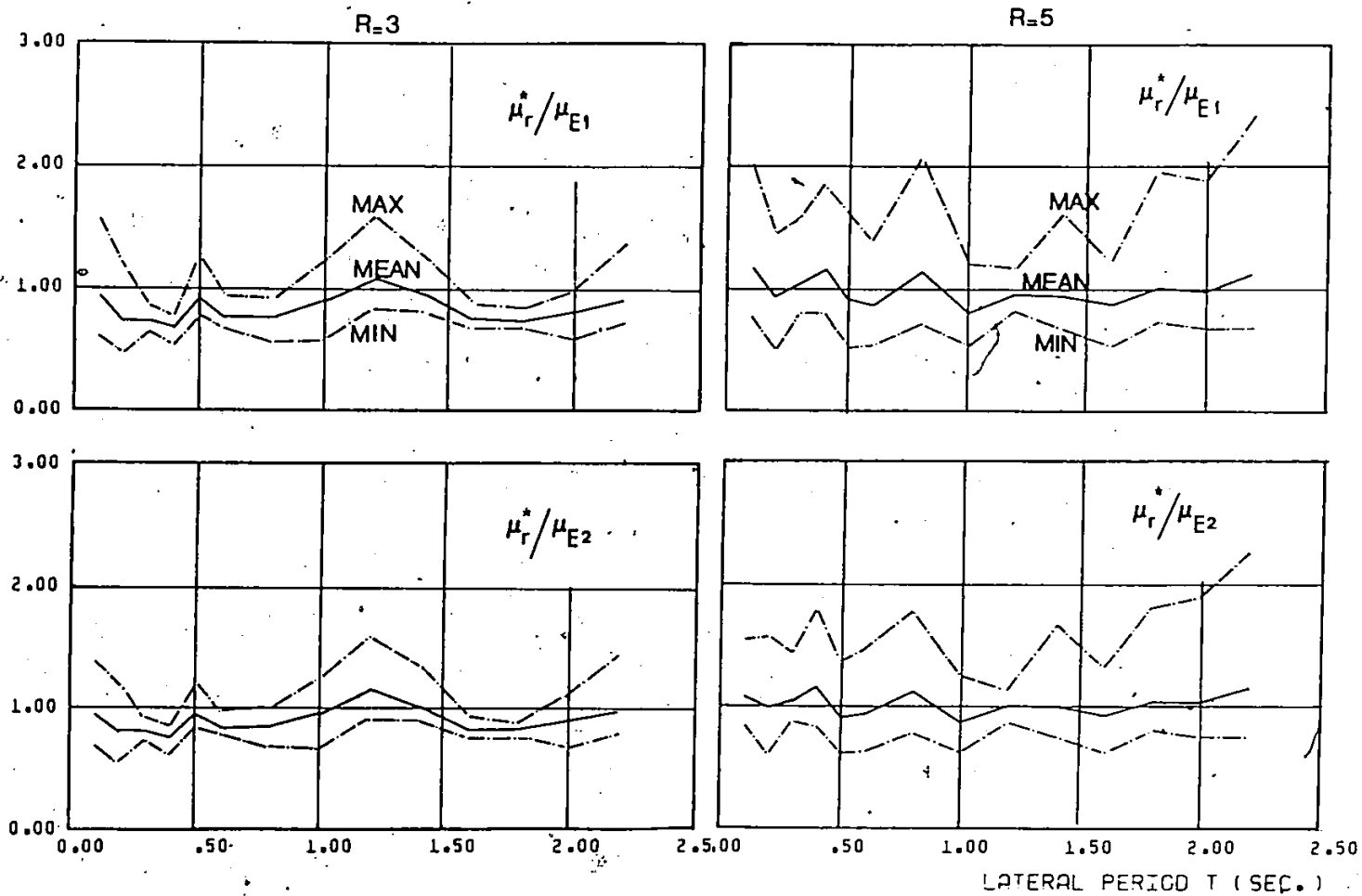


Fig (3.32) Ratio of Accurate to Approximate Estimates of Ductility Demand (EP-Estimator); $R=3, 5$

In the following, the $\Phi(\mu)$ factors are further modified. the modified factors, denoted as Γ , when applied to the elastic displacement response, i.e. with reduction factor $R_0=1$, will give an estimate of the ductility demand of a structure whose design strength is R_n times lower than the elastic strength demand. Γ factors are derived in the following for different period ranges. The limits of these ranges are determined based on the trends observed for the mean displacement response curves obtained herein.

1. Short Period Structures ($T < 0.2$ sec)

Let μ_0 be the elastic response corresponding to $R=R_0$, and μ_n be the response that needs to be estimated when $R=R_n$, then according to (32)

$$R_0 = \sqrt{2\mu_0 - 1} ; \text{ and } R_n = \sqrt{2\mu_n - 1}$$

Therefore,

$$\left(\frac{R_n}{R_0} \right)^2 = \frac{2\mu_n - 1}{2\mu_0 - 1}$$

dividing denominator and numerator of the R.H.S. term in the above equation by $2\mu_0$ and setting $R_n/R_0 = n$, gives

$$n^2(1 - 0.5\mu_0) = (\mu_n/\mu_0) - (1/2\mu_0)$$

$(\mu_n/\mu_0) = \Gamma(n)$ is the required amplification factor which is dependent on ratio n . Since R_0 is equal to unity for elastic response design, it is reasonable to assume the associated ductility μ_0 to be equal to unity. Substituting $\mu_0=1$ and dropping the remaining $1/2$ term on the R.H.S., the above expression reduces to

$$\Gamma(n) = n^2/2. \quad (3.21)$$

II. Long Period Structures ($T > 0.5$ sec)

$$\Gamma(n) = R_n / R_0$$

$$= n$$

(3.22)

III. Intermediate Period Structures ($0.2 < T < 0.5$)

A linear variation of $\Gamma(n)$ is assumed between the two expressions obtained at $T=0.2$ sec and $T=0.5$ sec.

The variation of $\Gamma(n)$ with period of this proposed scheme for two values of $n=3$ and 5 is shown in Fig (3.33).

TEST CASES :

The amplification factors Γ for $n=3$ and 5 are applied to the elastic radial displacement response spectrum obtained using the 1940, El Centro and 1952 Taft earthquake ground motions. The obtained estimate of ductility demand is compared with the radial ductility μ_r response of systems with design strength equal to one third and one fifth of the elastic strength demand. The comparison is shown in Figs (3.34) and (3.35). The estimated values are in general reasonably conservative. However, for systems with very short period ($T_x=0.1$ sec) and low design strength ($R=5$), ductility demand can be seriously underestimated by the proposed scheme. This is a manifestation of the problem of high inelastic response of very stiff structures with low yield strength which was observed earlier.

Another inelastic feature which is not taken into account here is the period shift due to yielding. The apparent shift between the two curves of the estimated and actual ductilities in the left figure of Fig

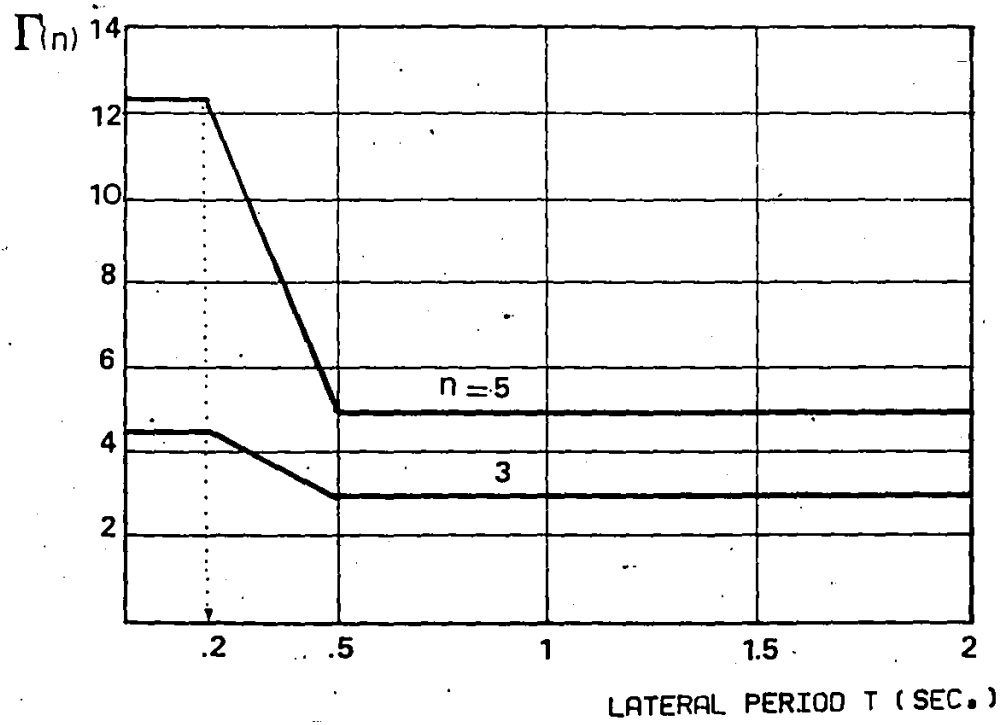


Fig (3.33) Variation of the Amplification Factor $\Gamma(n)$ with Lateral Period T ; $n=3, 5$

R=3

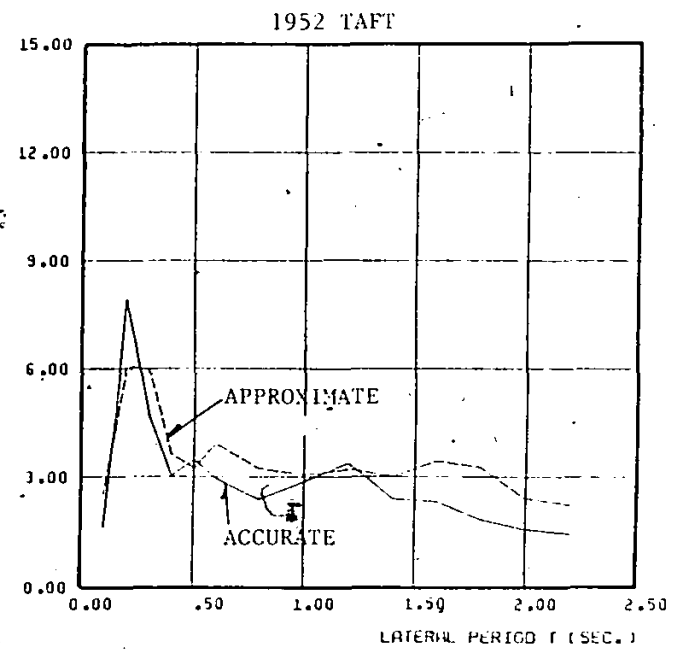
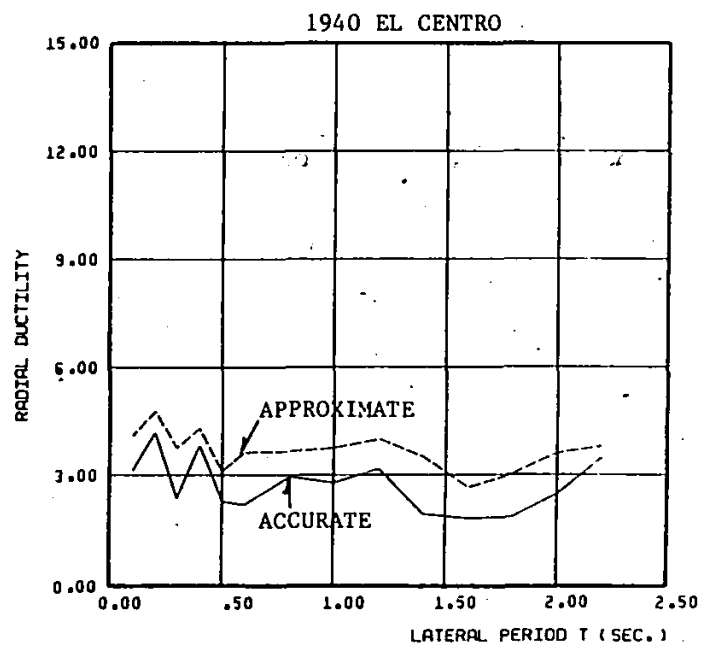


Fig (3.34) Comparison of the Accurate and Approximate Estimates of Ductility Demand (E-Estimator); R=3

R=5

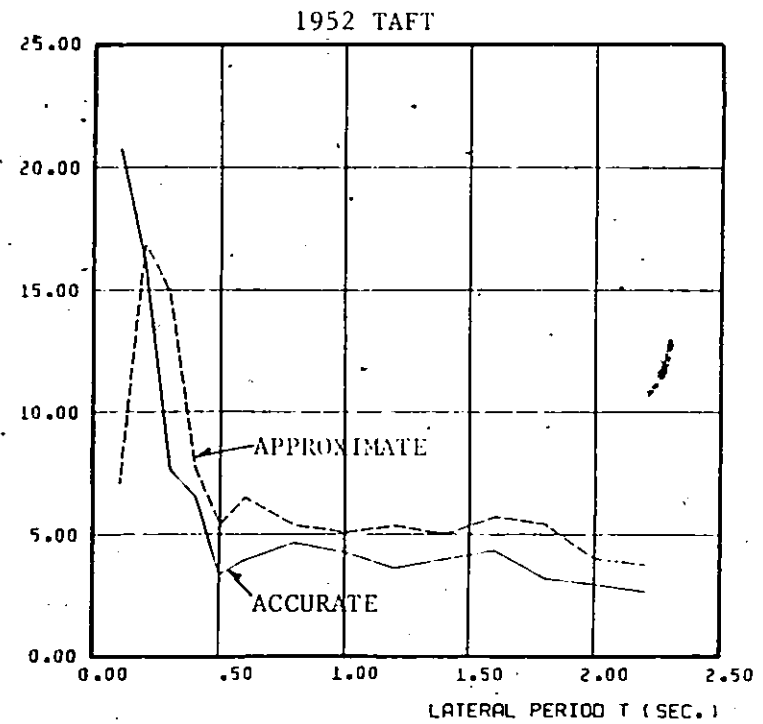
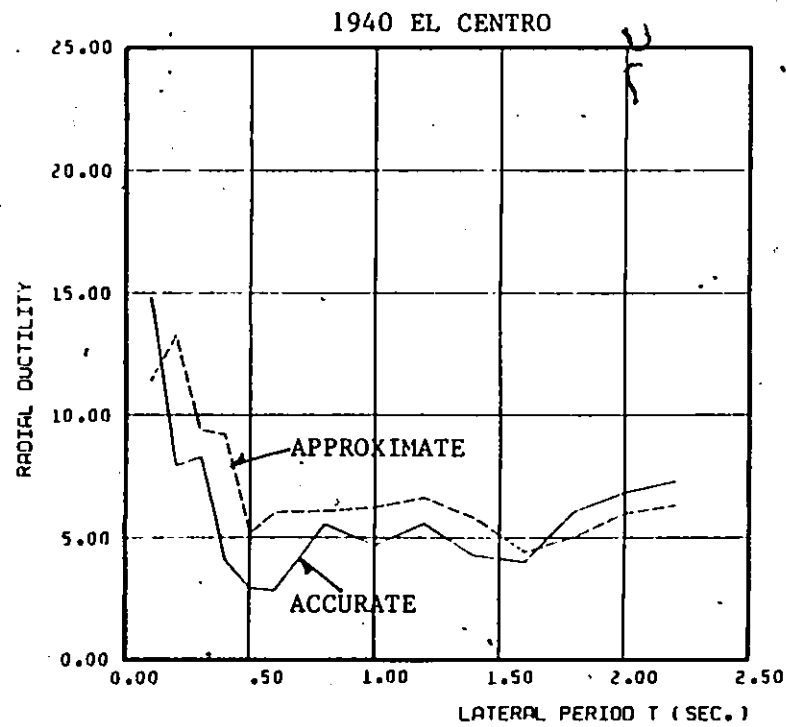


Fig (3.35) Comparison of the Accurate and Approximate Estimates of Ductility Demand (E-Estimator); $R=5$

(3.35) is a clear example.

Except for the situation of very stiff structures with low yield strength, the accuracy of the proposed scheme can be considered reasonable in view of the already existing dispersion of results of the inelastic responses from individual pair of records.

3.6 SYMMETRIC STRUCTURES WITH UNEQUAL PERIODS ALONG TWO PRINCIPAL DIRECTIONS :

So far, discussion has been limited to symmetric structures having identical natural periods along the x and y directions. It is however useful to consider systems with unequal periods, being representative of most actual structures.

3.6.1 EFFECT ON DUCTILITY DEMAND μ_x :

In order to examine the effect of the natural period in the y direction being different from that in the x direction on the ductility demand in the x direction, two models are defined: (i) A model with period in the y direction lower than that in the x direction and they are related by $T_y = (2/3)T_x$; and (ii) in the other model, the period in the y direction is greater than that in the x direction, $T_y = (4/3)T_x$. In both models, T_y is different from T_x by a factor of one third.

Figure (3.36) shows the ductility demand μ_x obtained using these models as a function of T_x . The two horizontal components of the 1940 El Centro and the 1952 Taft earthquakes records are used as ground motions with the stronger component in each case acting along the x

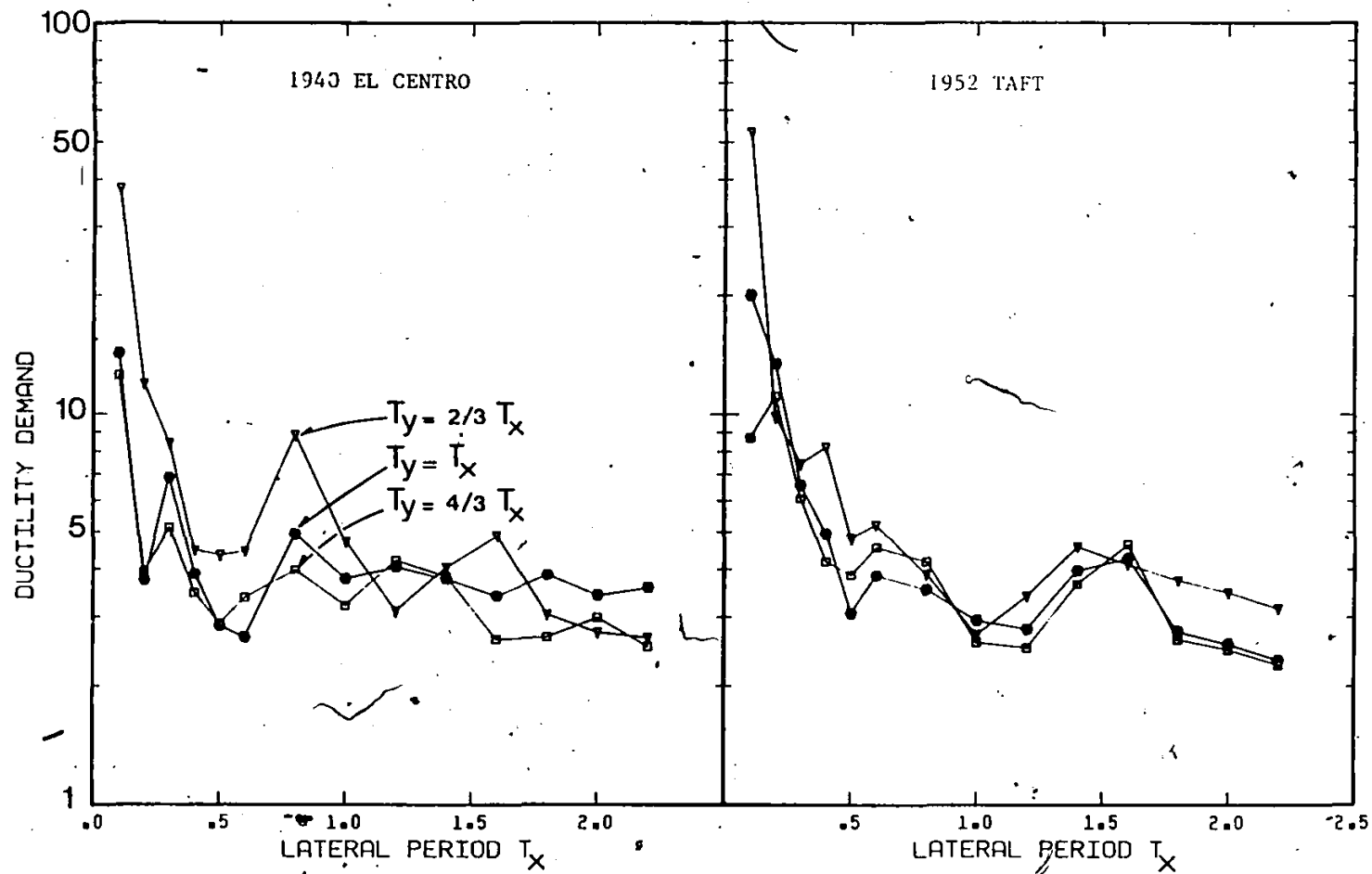


Fig (3.36) Ductility Demand μ_x of the EPI Models ; $T_y = T_x$, $T_y = (2/3)T_x$, and $T_y = (4/3)T_x$; $R=5$

direction. The elasto-plastic response with interaction effect included is calculated for models with yield strength equal to one fifth of the elastic strength demand ($R=5$). For purposes of comparison, equivalent curves obtained using axisymmetric models with $T_y=T_x$ are also included. It can be seen that curves labelled $T_y=(4/3)T_x$ are not much different from those of the axisymmetric model in the long period range of T_x . For low values of T_x , ductility demand obtained using the model with $T_y=(4/3)T_x$ can be significantly lower than those of the axisymmetric model. Reductions up to 50% from the axisymmetric model values are encountered. On the other hand, making the system stiffer in the y direction has a more profound effect of increasing ductility demand in the x direction, μ_x , particularly for low values of T_x . Ductility μ_x in the model with $T_y=(2/3)T_x$ is only 40% to 80% larger than those of equivalent axisymmetric models for $T_x > 0.5$ sec whereas ductility values can be three times as large as those of the axisymmetric model for low values of T_x (0.1 sec). This increase can be attributed to the fact that making the structure stiffer in one direction, i.e. with a shorter period, leads to a further reduction in the combined overall period of the system.

3.6.2 ORIENTATION OF GROUND MOTION :

For systems with unequal periods in the x and y directions, the radial displacement response is dependent on the orientation of the ground motion axes because the system stiffness function is no longer axisymmetric. To examine the effect of orientation angle θ_g on the

radial response of such systems, it is sufficient to consider any of the two models defined in the previous section. The model with $T_y = (2/3)T_x$ is considered for this purpose. Henceforth in this section, the x and y directions are referred to as the long and short period directions respectively.

Figure (3.37) shows the radial ductility μ_r as a function of θ_g ranging from 0° to 180° with intervals of 15° . The model has the following properties: $T_x = 1$ sec, $T_y = 0.67$ sec, and $R = 5$. Orientation angle is said to be zero when the stronger component of the ground motion (NS component of the 1940 El Centro and S69E component of the 1952 Taft) is acting along the long period direction, then θ_g is increased in an anticlockwise sense. The figure shows that the radial ductility is no longer independent of the orientation angle θ_g , since the system lacks the stiffness axisymmetry. Values of μ_r show considerable variation for different values of θ_g . This variation is also dependent on the ground motion used. Consider the radial ductility $\mu_r^{(45)}$ and $\mu_r^{(135)}$ corresponding to $\theta_g = 45^\circ$ and 135° respectively. It can be seen that $\mu_r^{(45)} < \mu_r^{(135)}$ for the case of the El Centro ground motion while $\mu_r^{(45)} > \mu_r^{(135)}$ for the other ground motion (Taft). This can be interpreted by considering the frequency content of the effective response spectra $S_a^{(45)}$ and $S_a^{(135)}$ in each case. The effective response spectrum associated with an orientation angle θ_g is obtained by first resolving the two components of ground motion along the structural short and long period directions then the effective spectrum is the one associated with the component along the short period direction. Figure (3.38) shows the elastic acceleration spectra $S_a^{(45)}$ and $S_a^{(135)}$ for the

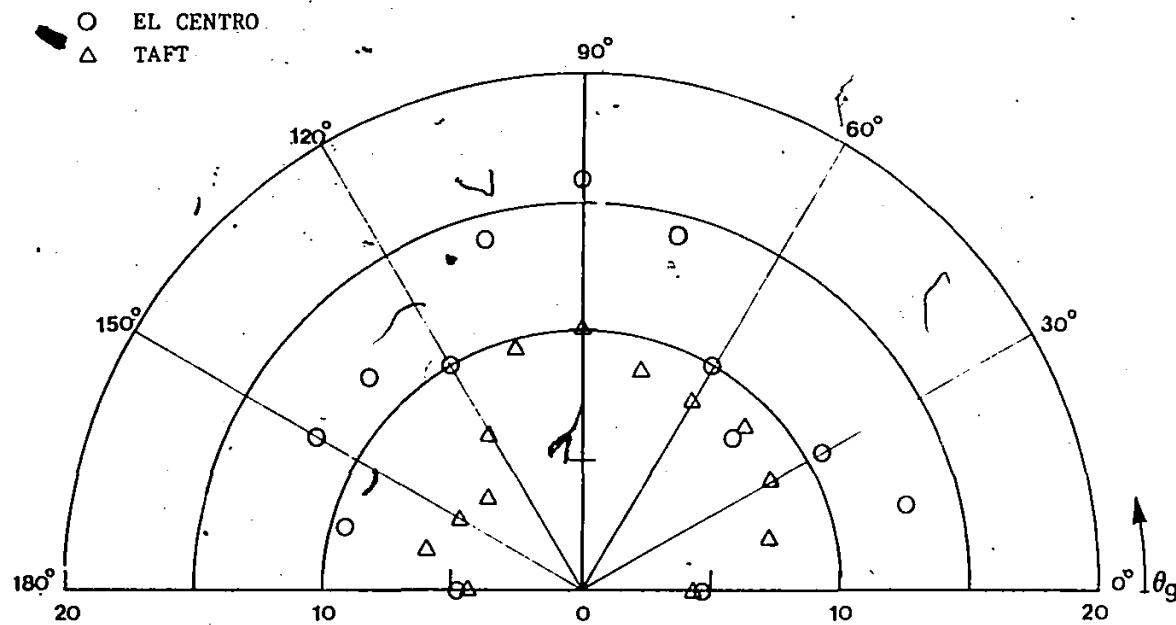


Fig (3.37) Variation of the Radial Ductility Demand with θ_g in the EPI Model; $T_x=1$ sec and $T_y=0.67$ sec

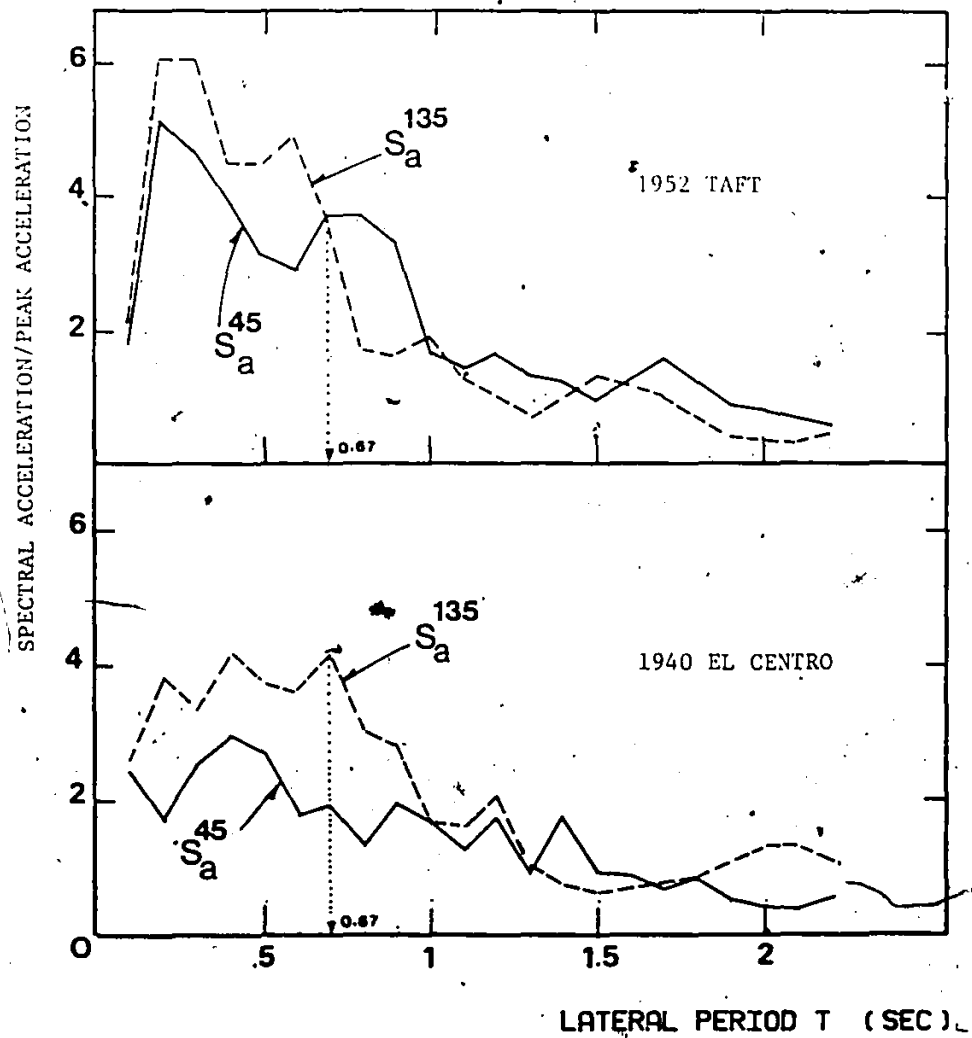


Fig (3.38) Comparison of the Effective Elastic Spectra at $\theta_g=45$ and 135 ; 1940 El Centro and 1952 Taft; $\xi=0.5\%$

two ground motions. The relative values of ductility correlate well with the relative frequency content in the response spectra beyond $T=0.67$ sec. In other words, for El Centro

$$\mu_r^{(45)} < \mu_r^{(135)}$$

$$S_a^{(45)}(T>0.67) < S_a^{(135)}(T>0.67)$$

and for Taft,

$$\mu_r^{(45)} > \mu_r^{(135)}$$

$$S_a^{(45)}(T>0.67) > S_a^{(135)}(T>0.67)$$

Among all possible values of θ_g , the two cases $\theta_g=0^\circ$ and 90° are of practical significance since the ground motion axes coincide with the principal structural axes. And it is the case with $\theta_g=90^\circ$ that will most likely give larger response, $\mu_r^{(90)}$, since the orientation is such that the stronger component is acting along the short period direction. To assess the validity of assuming $\mu_r^{(90)}$ as an upper limit of response parameter μ_r for different θ_g , consider the variation of the ratio $\mu_r^{(\theta_g)}/\mu_r^{(90)}$ with θ_g as shown in Fig (3.39). Using the El Centro and Taft ground motions and with $R=5$, ratio $\mu_r^{(\theta_g)}/\mu_r^{(90)}$ is shown for selected values of system period, $T_x=0.2, 0.5$, and 1 sec. For most cases $\mu_r^{(90)}$ is larger than ductilities associated with other orientations. In some cases, this ratio is larger than unity by at most 20%. This observation suggests that a reasonable estimate of ductility demand in structures with unequal periods in two directions can be obtained by considering the response when the stronger component is acting along the short period direction and the other component is acting in the long period direction.

○ 1940 EL CENTRO

△ 1952 TAFT

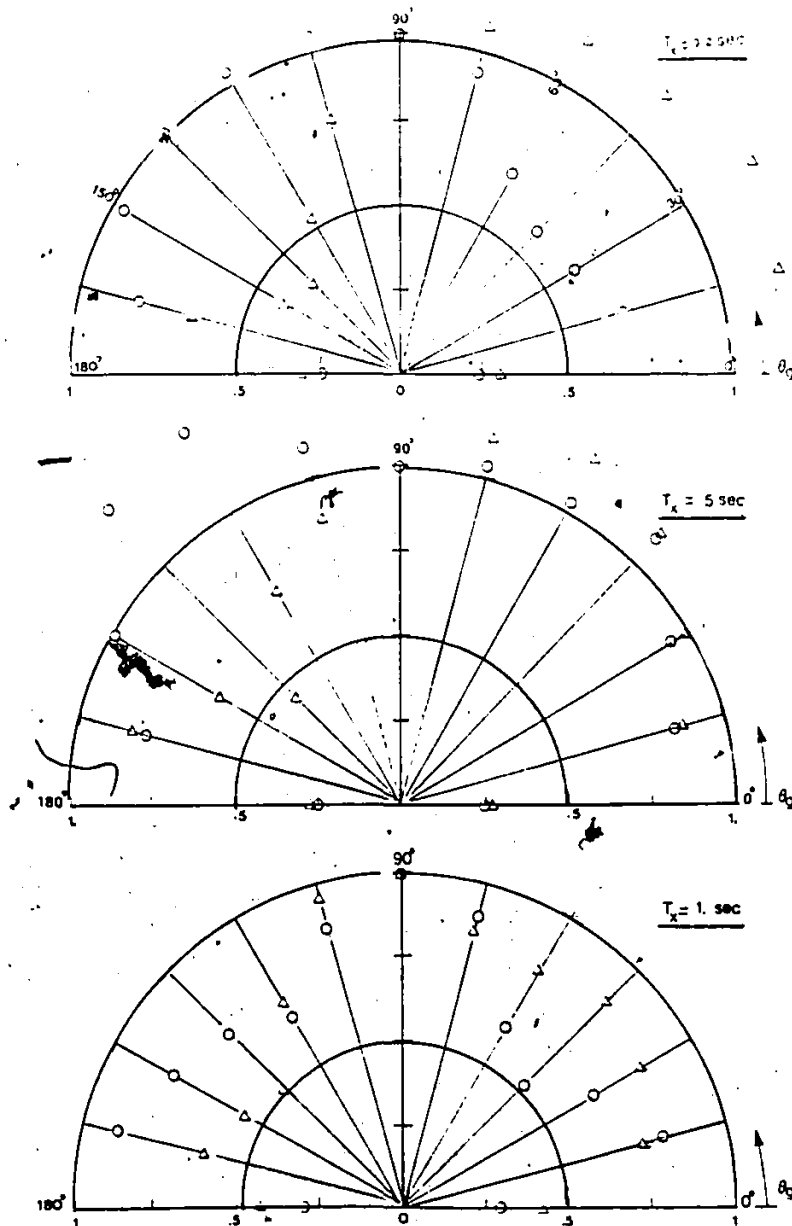


Fig (3.39) Ratio $\mu_r/\mu_r^{(90)}$ in the EPI Models; $T_y = (2/3)T_x$; $R=5$

APPROXIMATE RULES :

The approximate schemes discussed in Section 3.5.1 are used in this section to estimate the ductility demand in the long and short period directions. As mentioned earlier, these schemes require the EP planar responses to each component of the ground motion to be independently calculated. In addition, two orientations of the ground motion are taken into account in the estimate, namely $\theta_g = 0^\circ$, and 90° which correspond to the cases when the stronger component is either acting in the long or short period directions respectively. According to these schemes, the estimates of the ductility demand in the long and short period directions are given in the following.

Long Period Direction :

Scheme I

$$\mu_{xE1} = \max \begin{cases} 1.40 \mu_x^0 \\ 1.40 \mu_x^{90} \end{cases}$$

Scheme II

$$\mu_{xE2} = \max \begin{cases} \mu_x^0 + 0.3 \mu_y^0 \\ \mu_x^{90} + 0.3 \mu_y^{90} \end{cases}$$

Short Period Direction :

Scheme I

$$\mu_{yE1} = \max \begin{cases} 1.40 \mu_y^0 \\ 1.40 \mu_y^{90} \end{cases}$$

Table 3.3 Ratios of Accurate Estimate of the Ductility Demand
Approximate Estimate

LONG PERIOD DIRECTION				
T_x (sec)	SCHEME (I)		SCHEME (II)	
	ELCENTRO	TAFT	ELCENTRO	TAFT
0.2	1.74	1.62	0.96	1.07
0.5	1.13	0.76	0.84	0.62
0.8	1.49	0.92	1.29	0.72
1.0	1.76	0.83	0.96	0.61
1.5	1.32	0.84	0.73	0.93
2.0	0.85	1.00	0.83	0.88

SHORT PERIOD DIRECTION				
T_x (sec)	SCHEME (I)		SCHEME (II)	
	ELCENTRO	TAFT	ELCENTRO	TAFT
0.2	0.68	1.05	0.88	1.36
0.5	0.89	0.79	1.18	1.04
0.8	1.22	0.64	1.49	0.80
1.0	0.70	0.58	0.92	0.73
1.5	0.65	0.75	0.87	0.95
2.0	0.97	0.80	1.24	1.04

Scheme II

$$\mu_{yE2} = \max \begin{cases} \mu_y^0 + 0.3 \mu_x^0 \\ \mu_y^{90} + 0.3 \mu_x^{90} \end{cases}$$

The best estimate of ductility demand in each direction, μ_x^* and μ_y^* , are obtained using the model with interaction effect included and defined to be the actual maximum value over the entire range of θ_g .

The ratio of the accurate to the approximate estimates of the ductility demand in the long and the short period directions are presented in Table (3.3) for selected values of T_x . In the long period direction, ductility demand is best estimated by scheme (ii), for which ratios in Table (3.3) are close to unity. Approximate estimates by scheme (i) are exceeded by up to 70%. In the short period direction, scheme (i) seems to give reasonable estimates of the ductility demand. It may be noted that the ductility demand in either directions is best estimated by the scheme that includes a larger contribution of the uniaxial response in the short period direction.

3.7. SUMMARY AND CONCLUSIONS :

The inelastic response of symmetric structures to earthquake excitations is examined in this chapter. The main objective of the study is to assess the significance of including the interaction effect in the inelastic analysis of symmetric structures. For this purpose, the elasto-plastic response of a single mass symmetric structural model with interaction effect included or ignored is considered. The two horizontal components of ground motions are taken to act simultaneously

on the model. An ensemble of five pairs of recorded earthquakes ground motions is used as input and the mean values of responses are presented. The effects of interaction are discussed in detail and the response parameters of interest are taken to be the displacement ductility demand, permanent deformations, and the total energy input to the system. Buildings with identical or different properties in the two lateral directions are considered in the study. Based on the results and discussion presented in the chapter, the following conclusions can be drawn.

1. Including the interaction effect has only a minor effect on the inelastic response for long period structures (say $T > 0.5$ sec) or short period structures excited moderately into the inelastic range. Therefore, an elasto-plastic analysis without taking the yield interaction effect into account will be sufficient for determining ductility demand estimates for these classes of structures.

2. Stiff structures ($T < 0.5$ sec) with low yield strength, hence those excited well into the inelastic range, are shown to exhibit large values of ductility demand based on elasto-plastic analysis. For such structures, the interaction effect is significant and it further increases the ductility demand. The increase becomes substantial for very stiff structures ($T < 0.2$ sec). This observation is significant on two counts. First, it points out the inadequacy of planar inelastic analyses to estimate the ductility demand for stiff structures excited well into the inelastic range. Second, it shows that the ductility demand for such structures can be exceedingly high. Therefore, very stiff structures should be designed so that the expected

earthquake disturbance will not cause the structure to be excited well into the inelastic range. In other words, it is prudent to design very stiff structures to remain elastic or almost elastic when subjected to the probable earthquake excitation. Since none of the existing studies on effects of interaction considered structures in this period range, this effect has been overlooked before.

3. The radial ductility ratio in systems with identical properties along the two lateral directions of resistance is invariant to the orientation of the ground motion directions relative to the structural axes provided the interaction effect is included in the inelastic analysis. Such quantity can be used as an index of ductility demand in structures subjected to bidirectional excitations, and should be used in ductility estimates for design purposes.

4. A more realistic estimate of ductility demand which takes into account the effect of interaction and the bidirectionality of excitation can be, on the average, up to 40% larger than estimates calculated otherwise. Such an estimate can be derived using the elastoplastic uniaxial responses of the system by approximate rules. These rules are either (i) increasing the uniaxial response to the stronger component by 40% or (ii) as the sum of the uniaxial response to the stronger component plus 30% of the response to the other component.

5. An approximate estimate of the ductility demand of symmetric structures based on amplifying the elastic response with a period dependent factor is proposed. These factors are related to those proposed in (32) to derive inelastic response spectra from elastic

smooth spectra. Except for very stiff structures with low yield strength, this approximate method seems to be satisfactory.

6. For systems with unequal periods in the two lateral directions, the radial ductility ratio shows considerable variations with the angle of orientation of ground motions even if the interaction effect is taken into account. The maximum radial ductility ratio over the entire range of the angle of orientation can be reasonably estimated by orienting the pair of ground motions such that the stronger component is acting along the shorter period direction.

7. The maximum effect of the orientation of ground motion components on the ductility demand in the longer period direction can be estimated by the 30% rule, i.e. the sum of the maximum uniaxial response in the longer period direction plus 30% of that in the shorter period direction. And to account for this effect in the shorter period direction, it is sufficient to increase the maximum uniaxial response in this direction by 40%.

29

CHAPTER 4
RESPONSE OF ECCENTRIC STRUCTURES TO
EARTHQUAKE EXCITATIONS

4.1 INTRODUCTION :

A detailed analysis of inelastic response of asymmetric structures is carried out in this chapter for the following reasons. First, most of structures have some asymmetry in plan due to architectural or functional reasons. Even in nominally symmetric structures, asymmetry is inevitable due to uncertainty of live load distributions or imperfections in material which can cause variation in true stiffness distribution. Second, it is not economical to design ordinary buildings, residential, offices, and warehouses, etc., to remain elastic under the action of severe earthquakes because of the prohibitive cost. In addition, there are specific motives behind the present study of asymmetric structures, namely

(1) In asymmetric structures, yielding that occurs along one of the principal directions of structural resistance, affects the response in the orthogonal direction because of torsional coupling. It follows that it is important to consider the effect of forces interaction on columns yielding along with the simultaneous action of the two horizontal components of ground motion in the analysis of inelastic asymmetric systems. Very little information on the effects of interaction in the inelastic analysis of asymmetrical systems is found

In the literature. The reader is referred to Section 1.2.4 in Chapter 1 for more discussion on this subject. In the present study, the horizontal ground motions are considered to come from two orthogonal directions, and the effect of forces interaction in yielding of columns is included in evaluation of the responses of asymmetric structures under such bidirectional ground motion excitations.

(2) Existing studies on inelastic torsional responses contain apparently conflicting remarks regarding the importance of some parameters on inelastic response of asymmetrical buildings. As an example, structural eccentricity which is considered as the most important parameter in elastic response studies, received different comments in inelastic response studies by different investigators. The comments vary from "insignificant" (16) to "response varies linearly with eccentricity" (58). In this chapter, a new concept of eccentricity based on the yield properties of the system is proposed. It is shown that this new eccentricity is a better index to characterize the inelastic torsional effect on ductility demands.

4.2 FORMULATION AND MODEL PARAMETERS :

Consider the monosymmetric configuration of the structural model described in Section 3.2, by assuming the center of mass (CM) and the center of stiffness (CS) to be noncoincident along the y direction. The offset is denoted by the nominal eccentricity e_y . The additional rotational deformation q_θ needs to be incorporated into the equations of motion. The dynamic equilibrium equations with reference to CM can be

written as follows.

$$\begin{bmatrix} m & 0 & 0 \\ 0 & m & 0 \\ 0 & 0 & m \end{bmatrix} \begin{Bmatrix} \ddot{q}_x \\ r\ddot{q}_\theta \\ \ddot{q}_y \end{Bmatrix} + 2\xi m \begin{bmatrix} \omega_x & 0 & 0 \\ 0 & \omega_\theta & 0 \\ 0 & 0 & \omega_y \end{bmatrix} \begin{Bmatrix} \dot{q}_x \\ r\dot{q}_\theta \\ \dot{q}_y \end{Bmatrix} + \begin{Bmatrix} Q_x \\ Q_\theta \\ Q_y \end{Bmatrix} = -m \begin{Bmatrix} \ddot{u}_{gx}(t) \\ 0 \\ \ddot{u}_{gy}(t) \end{Bmatrix} \quad (4.1)$$

In addition to the symbols defined earlier in Section 3.2, r is the radius of gyration of the rigid slab about CM, Q_θ is the restoring torque, and ω_θ is the torsional frequency given by $\sqrt{K_\theta/mr^2}$, where K_θ is the torsional stiffness of the system. The incremental restoring forces and deformations are related by the tangential stiffness matrix $[K_t]$

$$\Delta\{Q\} = [K_t] \Delta\{q\} \quad (4.2)$$

The system stiffness matrix is assembled using the updated elements stiffness matrices $[S]_i$ as follows

$$[K_t] = \sum_{i=1}^4 [D]_i [S]_i [D]_i \quad (4.3)$$

where $[S]_i$ is the element stiffness matrix in the global x and y coordinates. $[S]_i$ can be written in the form

$$[S]_i = \begin{bmatrix} s_x & s_{xy} \\ s_{xy} & s_y \end{bmatrix}$$

and is related to the one in local coordinates, defined earlier, as follows

$$[S]_i = [L]_i^T [S]_{li} [L]_i$$

If θ_i is the inclination between local and global coordinates for column i , the matrix $[L]_i$ is given by

$$[L]_i = \begin{bmatrix} \cos \theta_i & \sin \theta_i \\ -\sin \theta_i & \cos \theta_i \end{bmatrix}$$

For the i th column with position coordinates (x_i, y_i) with respect to CM, the position matrix $[D]_i$ is given by

$$[D]_i = \begin{bmatrix} 1 & -y_i/r & 0 \\ 0 & x_i/r & 1 \end{bmatrix} \quad (4.4)$$

Hence, the elements of matrix $[K_t]$ in general are given by

$$\begin{aligned} K_x(t) &= \sum_i s_x ; \quad K_y(t) = \sum_i s_y \\ K_\theta(t) &= \sum_i s_x (y_i/r)^2 + s_y (x_i/r)^2 - \underline{2s_{xy}(y_i/r)(x_i/r)} \\ K_{xy}(t) &= K_{yx}(t) = \sum_i \underline{s_{xy}} \\ K_{\theta x}(t) &= K_{x\theta}(t) = \sum_i \underline{-s_x(y_i/r) + s_{xy}(x_i/r)} \\ K_{\theta y}(t) &= K_{y\theta}(t) = \sum_i \underline{-s_y(x_i/r) - s_{xy}(y_i/r)} \end{aligned} \quad (4.5)$$

The underlined terms in Equations (4.5) are those terms that appear only when interaction is included but vanish otherwise.

In the elastic range, the stiffness matrix reduces to the following

$$[K] = K_x \begin{bmatrix} 1 & -e_y & 0 \\ -e_y & \Omega^2 & 0 \\ 0 & 0 & \gamma^2 \end{bmatrix} \quad (4.6)$$

Thus there are only three system parameters which affect the response of the system in the elastic range. They are (i) eccentricity e_y , (ii) torsional to lateral frequency ratio $\Omega = \omega_\theta / \omega_x$, and (iii) lateral frequency ratio $\gamma = \omega_y / \omega_x$.

In the inelastic response with interaction ignored (EP), the stiffness matrix $[K_t]$ still has the same form as in Eq (4.6), however its coefficients become time variants

$$[K_t] = K_x(t) \begin{bmatrix} 1 & -e_y(t) & 0 \\ -e_y(t) & \Omega^2(t) & 0 \\ 0 & 0 & \gamma^2(t) \end{bmatrix} \quad (4.7)$$

Since the stiffness value of an elasto-plastic element is either the initial elastic stiffness or zero, then it is expected that significant variations do occur in the system parameters from their respective initial values when the system is excited into the inelastic range. As a result, there is no a priori reason to believe that these parameters will influence the inelastic response in the same capacity that they are known to do to the elastic case.

Upon including the interaction effect in the inelastic response of the system (EPI), further complications are introduced to the coefficients of the matrix $[K_t]$ due to the presence of the additional terms underlined in Eq (4.5).

NORMALIZED EQUATIONS OF MOTION :

Equations (4.1) can be put into a nondimensional form as follows

$$\begin{Bmatrix} \ddot{u}_x \\ \ddot{u}_\theta \\ \ddot{u}_y \end{Bmatrix} + 2\xi\omega_x \begin{bmatrix} 1 & 0 & 0 \\ 0 & \Omega & 0 \\ 0 & 0 & \gamma \end{bmatrix} \begin{Bmatrix} \dot{u}_x \\ \dot{u}_\theta \\ \dot{u}_y \end{Bmatrix} + \omega_x^2 \begin{Bmatrix} \bar{Q}_x \\ \Omega^2 \bar{Q}_\theta \\ \gamma^2 \bar{Q}_y \end{Bmatrix} = -R\omega_x^2 \begin{Bmatrix} \ddot{u}_{gx}(t) \\ 0 \\ (\gamma^2/\beta)\ddot{u}_{gy}(t) \end{Bmatrix} \quad (4.8)$$

where

$$u_x, u_\theta, u_y = q_x/\delta_x, r q_\theta/\delta_\theta, q_y/\delta_y$$

$$\bar{Q}_x, \bar{Q}_\theta, \bar{Q}_y = Q_x/F_x, Q_\theta/F_\theta, Q_y/F_y$$

- where δ_θ is the torsional yield deformation, and F_x , and F_y are the system yield strength in lateral deformations. F_θ is the system yield strength under pure torque.

To investigate the inelastic behavior of the model, the inelastic responses were computed considering the following model parameters.

1. Lateral period $T_x = 2\pi/\omega_x$ ranges from 0.1 to 2.2 sec.
2. Torsional to lateral frequency ratio $\Omega = 1$. The spacing between columns, a , in the model is adjusted so that the torsional and lateral frequencies are equal. In general, buildings having the resisting elements uniformly distributed in plan can be shown also to have a frequency ratio of unity.
3. Nominal eccentricity e_y ; unless other wise mentioned, the eccentricity e_y is taken to be equal to one fifth of the plan dimension D , i.e. $e_y = 0.2 D$. This value corresponds to buildings with large eccentricities.

The study is confined to systems with identical stiffness and

strength properties in the two lateral directions. In other words, $\gamma=1$ and $\beta=1$. This leads to equal yield deformations of the system in translations and rotation, i.e. $\delta_x=\delta_y=\delta_\theta$.

4.3 EFFECTS OF INTERACTION :

To assess the significance of interaction in the presence of eccentricity as compared to that in the symmetric case, the symmetric and monosymmetric configurations of a single mass model are considered as shown in Fig (4.1). The monosymmetric configuration in Fig (4.1b) is obtained from its symmetric counterpart by shifting CM of the rigid slab along the y axis, and leaving the four column arrangement unchanged. This introduces an eccentricity e_y to the system. Figure (4.2) shows the elasto-plastic response with interaction ignored (EP) and included (EPI) of both models when subjected to the two horizontal components of the 1952 Taft ground motion. Models have their yield strength equal to one fifth of the elastic strength demand, i.e. $R=5$. Curves show the variation of ductility demand of column 1, μ_{x1} , with lateral period T_x . While columns in the symmetric model are equally stressed, column 1 is the most stressed column in the eccentric model. It is seen that the increase in response due to interaction from the response ignoring interaction is larger when the model is symmetrical. This observation is generally applicable for periods $T_x < 0.5$ sec, and most pronounced for $T_x < 0.3$ sec.

To make the comparison more transparent, the ratio of ductility demand μ_{x1} with and without interaction is replotted in Fig (4.3) for both the symmetric and monosymmetric structures. For this comparison,

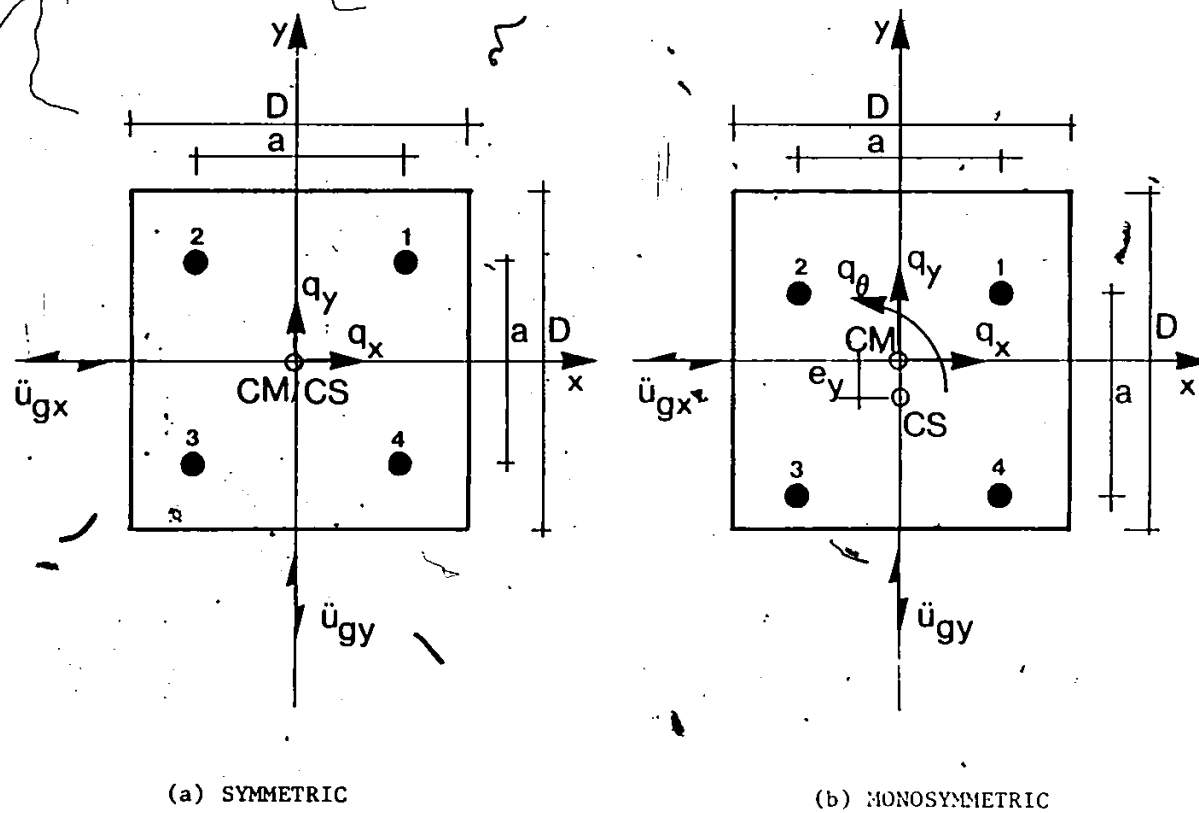


Fig (4.1) Symmetric and Monosymmetric Single Mass Structural Models

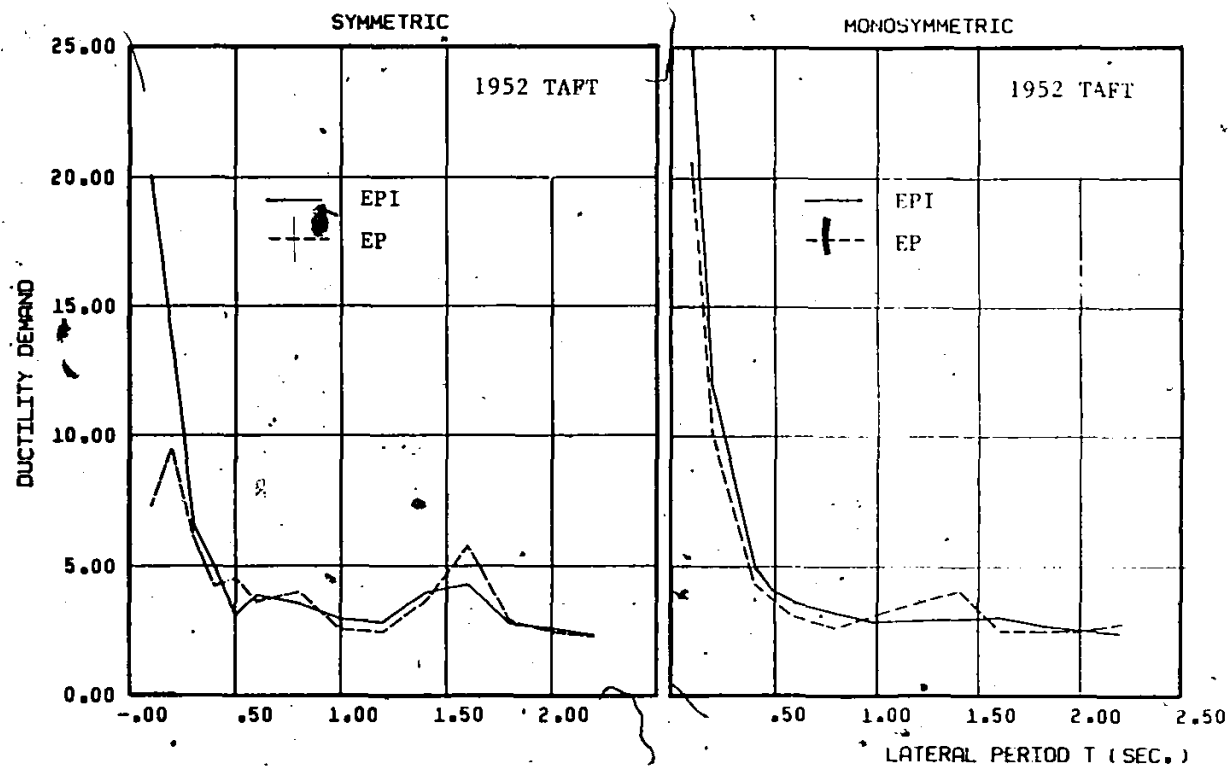


Fig (4.2) Ductility Demand on Column 1 in Symmetric and Monosymmetric Configurations of the EP and EPI Models; $R=5$; 1952 Taft Ground Motion

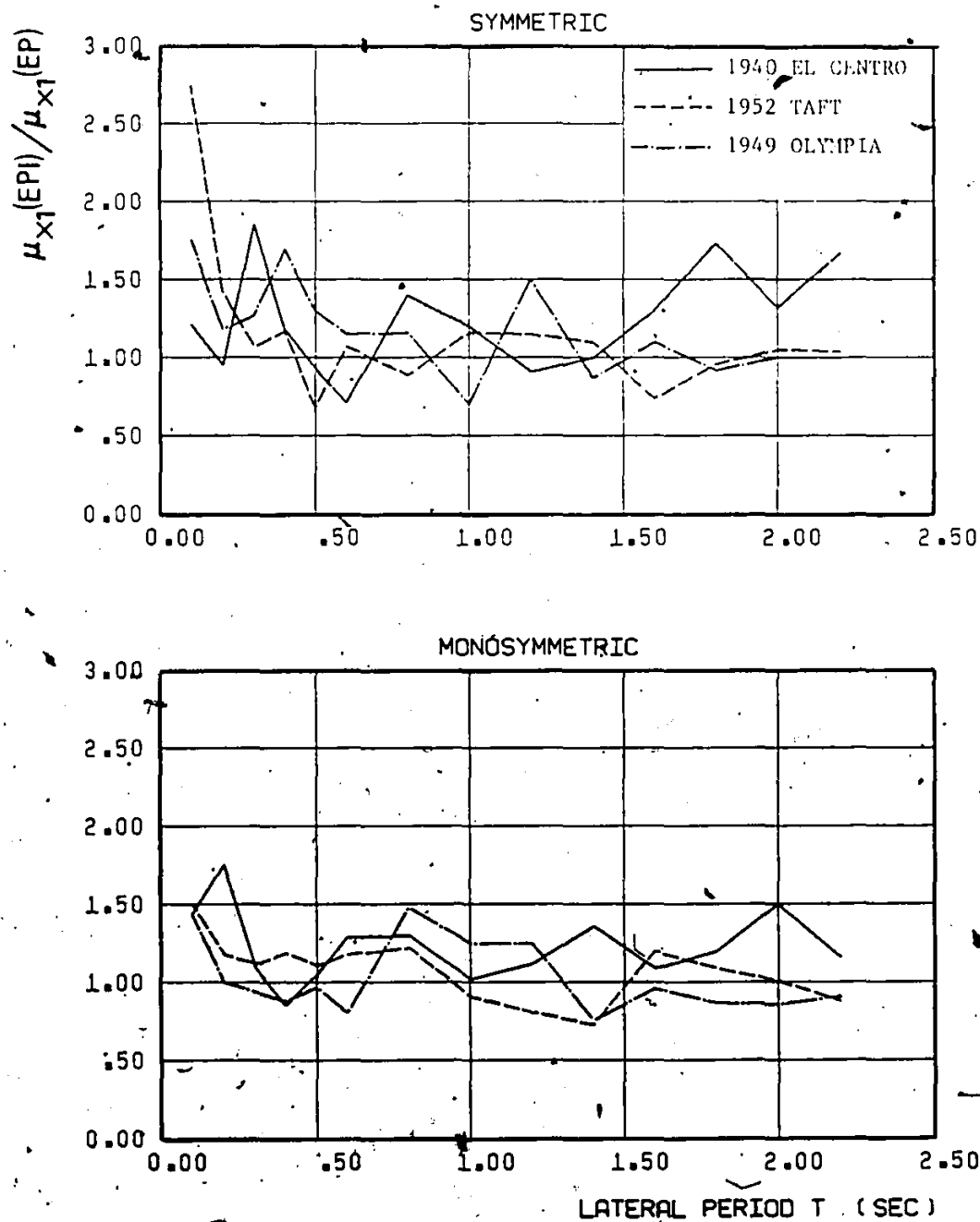


Fig (4.3) Ratio of the Ductility Demand on Column 1 in the EPI Model to that in the EP Model; Symmetric and Monosymmetric Configurations; R=5

the 1940 El Centro and the 1949 Olympia ground motions are used in addition to the 1952 Taft earthquake records. Comparing the top and bottom plots, one can see that this ratio is higher for the symmetric model than that for the eccentric model in general. While this ratio reaches up to a value of 2.75 for the symmetric model, a maximum value of only 1.75 is encountered for the eccentric model. Based on these observations, one can conclude that (1) ductility demand is higher if interaction effect is taken into account, and (2) interaction affects the displacement response of eccentric structures to a lesser extent than it does to that of symmetric structures.

To explain such behavior, consider the interrelationships between the two lateral components of deformations of a column located in a symmetric and in an eccentric structures. In symmetric structures, the response in one direction is independent of that in the other direction if elastic or elasto-plastic behavior is assumed. Including the interaction between lateral forces is the only mechanism which accounts for the response in one direction being affected by the response in the other direction. On the other hand, in eccentric systems, responses in the two lateral directions are interdependent even without considering interaction because of torsional coupling. Not only the overall system's deformations $u_x(t)$, $u_y(t)$, and $u_\theta(t)$ are dependent because of the simultaneous solution of their dynamic equilibrium equations but also the columns' deformations $v_x(t)$, $v_y(t)$ in the two lateral directions are interdependent since the rotational component $u_\theta(t)$ contributes to both components as given by

$$v_x(t) = u_x(t) - u_\theta(t) (y/r)$$

$$v_y(t) = u_y(t) + u_\theta(t) (x/r)$$

Therefore, the eccentric structure already has some of the effects that inelastic interaction might have on the response by virtue of torsional coupling, namely (i) the transfer of energy input between the principal structural directions, and (ii) yielding in one direction affects the response in the other direction. As a result, including the interaction effect in eccentric systems produces less dramatic change than for the case of symmetric systems.

Since interaction has less effect on asymmetrical systems, it is decided to neglect the interaction effect in the elasto-plastic response calculation of eccentric systems for the remaining part of this chapter. While neglecting the interaction makes the modelling less realistic, one can focus better the torsional coupling effect on the inelastic response of eccentric systems.

4.4 PLASTIC ECCENTRICITY CONCEPT :

4.4.1 BACKGROUND :

In torsionally coupled systems, the amount of rotation is usually governed by the offset of the center of load application from the center of rigidity. In earthquake excitation, applied forces are acting through the center of mass. The center of rigidity refers to the point in the floor plan through which if a lateral load is applied then the floor will only translate with no rotation. In elastic response

analyses, the resistance is offered by the stiffness properties of elements. Therefore, the definition of eccentricity is based on the relative location of the center of stiffness with respect to the center of mass.

This definition however becomes inconsistent when the structure is assumed to be excited well into the inelastic range. At this stage, since most if not all the elements have reached their yield strength limits, resistance is better characterized by the strength distribution rather than by the stiffness distribution within the system. The inadequacy of such elastic definition of eccentricity is also evident from the conflicting findings of the available studies on the inelastic torsional responses as indicated in Section 4.1. The substantial dispersion of conclusions suggests the need of a better index to estimate the ductility demand for eccentric structures. One such index is to give an alternative definition of eccentricity based on the yield strength properties of the resisting elements.

This idea was touched upon in two of the earliest papers on inelastic torsional response. Tanabashi in 1960 (47) studied an eccentric single story model consisting of a rigid slab on two parallel frames with one stiffer than the other. Using idealized ground motions, he stated that "we shall need to make the rigidity of structures distributed as uniformly as possible in regard to the ultimate state rather than the elastic range of stiffness members." And in 1969, Shibata et al (45) studied a similar model and they emphasized the importance of the yield strength of columns by stating that "the distribution of strength as well as of stiffness has significant

influence on the nonlinear response." Although these studies pointed out the significance of the strength distribution on nonlinear response, no specific guidelines were given as to incorporate this information when specifying the eccentric model for inelastic response analyses. Moreover, the results of these studies are limited since they are based on idealized ground motions.

4.4.2 DEFINITION :

Consider the i th resisting element in a structure. Its effect on the response calculation can be described by its load-deflection curves along the x and y directions. In each direction, the elastoplastic idealization is assumed. These load deflection curves are characterized by the elastic stiffness k_{xi} and k_{yi} and the yield strength V_{pxi} and V_{pyi} . According to the definition of the elastic eccentricity, it is the distance between location of the center of stiffness from CM. The coordinates of the center of stiffness can be evaluated as follows

$$\begin{aligned} x_s &= \frac{\sum_i k_{yi} x_i}{\sum_i k_{yi}} \\ y_s &= \frac{\sum_i k_{xi} y_i}{\sum_i k_{xi}} \end{aligned} \quad (4.9)$$

In a similar manner, the center of yield strengths can be found as follows

$$\begin{aligned}
 x_p &= \frac{\sum_i V_{pyi} x_i}{\sum_i V_{pyi}} \\
 y_p &= \frac{\sum_i V_{pxi} y_i}{\sum_i V_{pxi}}
 \end{aligned}
 \tag{4.10}$$

Coordinates x_p and y_p define the center of strength (CP) which represents the point of action of the resultant of the resisting yield forces. The plastic eccentricity (e_p) is then defined as the offset of this center of strength (CP) from the center of mass CM. The relative location of the center of strength CP depends on the strength distribution of the resisting elements. The structure is considered to have uniform strength distribution if the center of strength CP and the center of mass CM are coincident, i.e. the plastic eccentricity e_p is equal to zero. It is then expected that such structure will experience less rotational deformations in its post-yield response as compared to that of an equivalent structure but with a nonuniform strength distribution, i.e. the plastic eccentricity e_p is not equal to zero.

Before examining the influence of the plastic eccentricity on dynamic inelastic response of asymmetric structures, it is instructive to give an example to show its effect to induce rotational deformations. For this purpose, consider a single story structure supported on four columns which are symmetrically arranged and assumed to have identical stiffnesses. Thus the center of stiffness coincides with CM. However let columns 1 and 2 have lower yield strength than those of columns 3 and 4. This leads the center of strength CP to be offset from CM. The

($e = 0.00$, $e_p = 0.20D$)

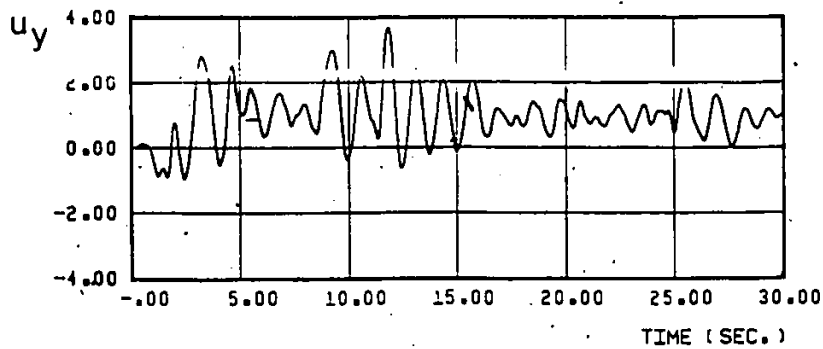
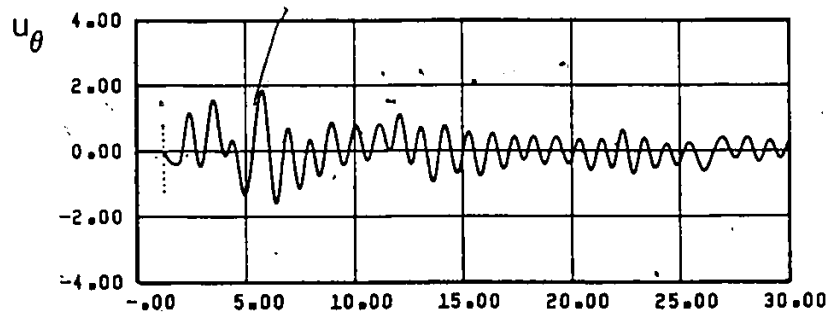
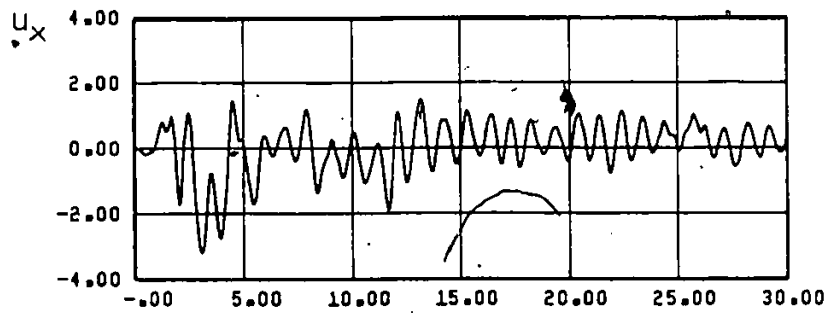


Fig (4.4) Time History of the Deformation Components at CM; System Properties: $e_p=0.20$, $e=0$, $T_x=1.0$ sec, and $R=5$

difference in strength levels is adjusted so that the plastic eccentricity e_p is equal to 0.2D. This initially symmetric structure is subjected to the NS and EW components of the 1940 El Centro earthquake records along the x and y directions respectively. The other parameters of the model are: $T_x = T_y = 1$ sec, and $R = 5$. Figure (4.4) shows the time variations of the deformation components at CM, namely $u_x(t)$, $u_y(t)$, and $u_\theta(t)$. It can be seen that the model initially behaves in a symmetric fashion with the rotational component $u_\theta(t)$ is equal to zero. Once yielding is initiated with columns reaching their yield strength, then the uneven distribution of strength influences the response and rotation is induced and it persists till the end of the excitation. This is due to the complicated pattern of yielding and unloading sequence of the four columns. This example shows that the presence of the plastic eccentricity will induce rotation in the post yield era of response of structures known to be symmetric in the elastic sense.

4.4.3 EFFECTS ON ASYMMETRIC STRUCTURES :

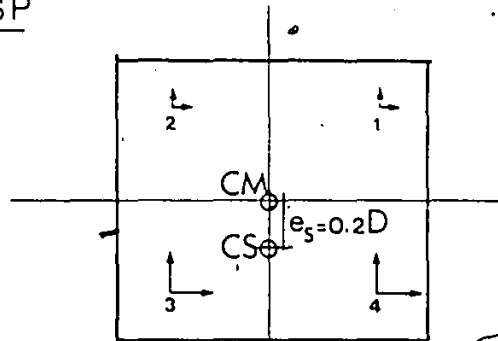
To assess the significance of the plastic eccentricity in the inelastic response of asymmetric structures consider the following two models (see Fig (4.5)) consisting of a rigid slab on four columns and having the following properties.

MODEL SP :

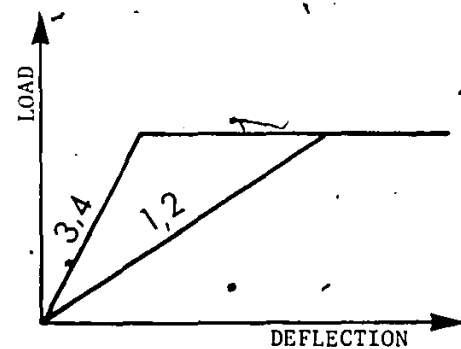
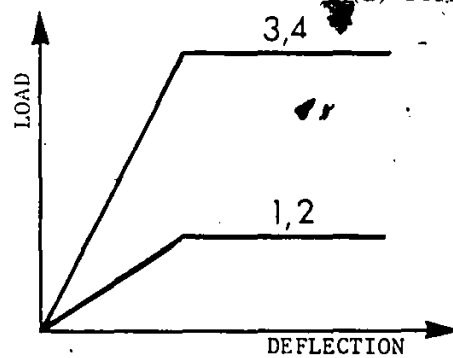
The stiffnesses of columns 3 and 4 are larger than those of columns 1 and 2 and the difference is adjusted so that the offset of the center of stiffness from CM is one fifth of the plan dimension. Since the asymmetry in the elastic sense is due to the uneven distribution of

MODEL SP

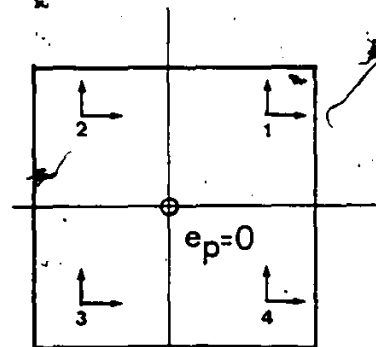
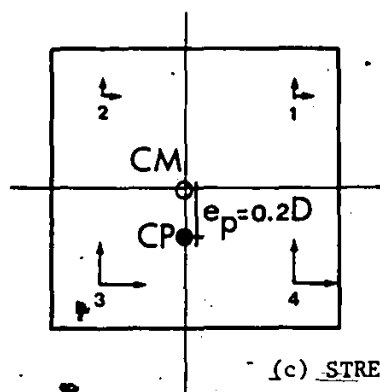
MODEL S



(a) STIFFNESS DISTRIBUTION



(b) LOAD-DEFLECTION CURVES OF COLUMNS



(c) STRENGTH DISTRIBUTION

Fig (4.5) Properties of the S and SP Models

stiffness, the eccentricity obtained is referred to as the stiffness eccentricity (e_s). If the yield strength of the columns are taken to be proportional to their stiffness values as shown in Fig (4.5b), then the center of strength CP is offset from CM and the value of the plastic eccentricity along the y axis is $e_p=0.2D$. The y axis remains an axis of symmetry.

MODEL S :

In this model, the stiffness distribution is the same as model SP. However columns are assumed to have identical yield strength irrespective of their stiffness values. By so doing, the center of strength CP coincides with CM and the plastic eccentricity vanishes ($e_p=0$).

The inelastic response of the two models are compared in Figures (4.6), (4.7), and (4.8). These response parameters are $u_{\theta m}$ and u_{xm} defined as the maximum absolute values of rotation and translation, respectively, at CM and the ductility demand on column 1. In each case, the system yield strength is equal to one fifth of the elastic strength demand ($R=5$). The two components of the 1940 El Centro and the 1952 Taft earthquakes records are used as input. The following observations can be made.

1. Comparing the broken and solid lines in Fig (4.6) shows that the rotational deformation $u_{\theta m}$ is considerably reduced in the S model which does not contain plastic eccentricity. This observation is quite evident for short period structures with $T_x < 0.2$ sec. Reductions in $u_{\theta m}$ of up to 75% are obtained at $T_x=0.1$ sec. For other period values

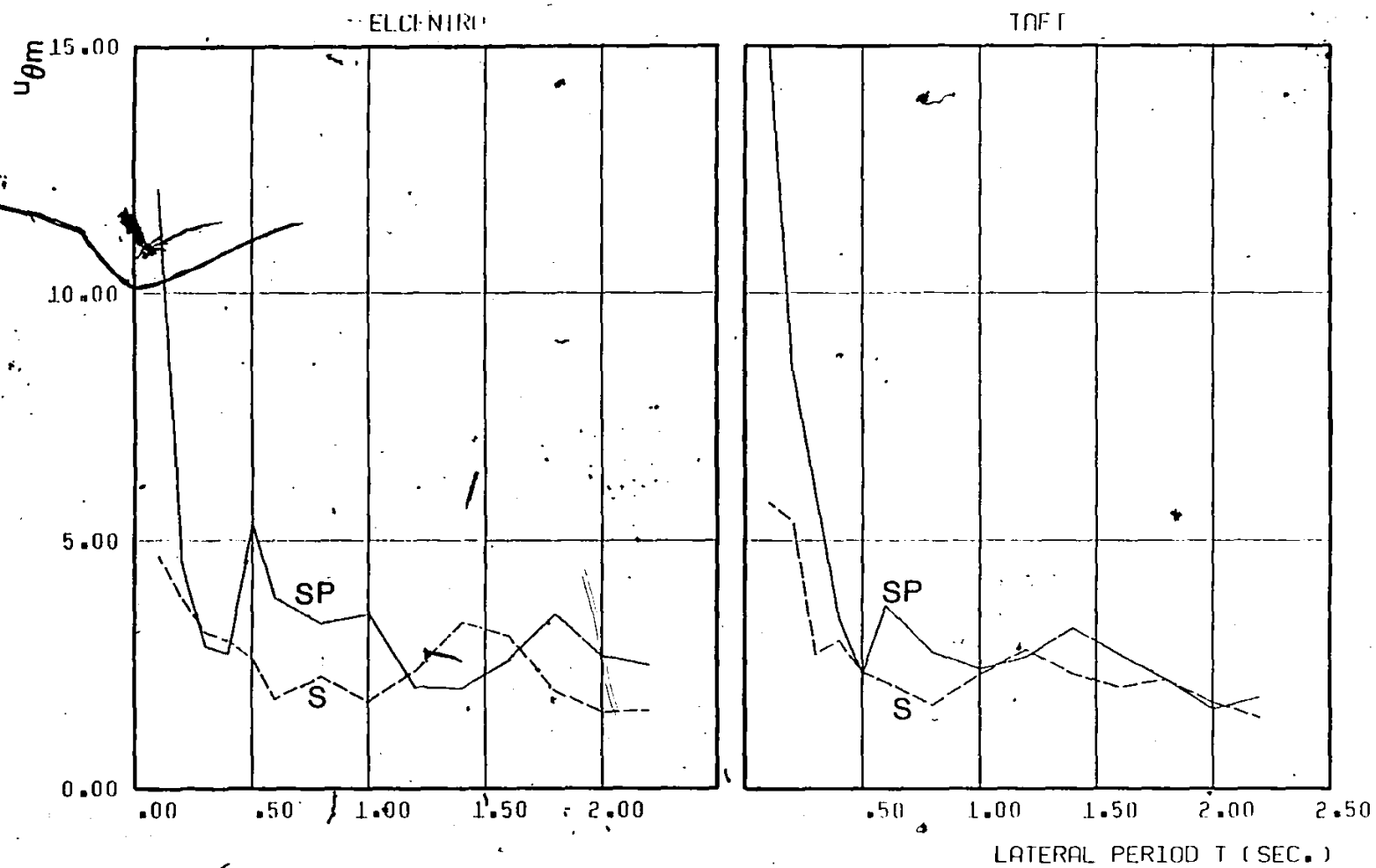


Fig (4.6) Comparison of Rotation $u_{\theta m}$ in the S and SP Models; $R=5$

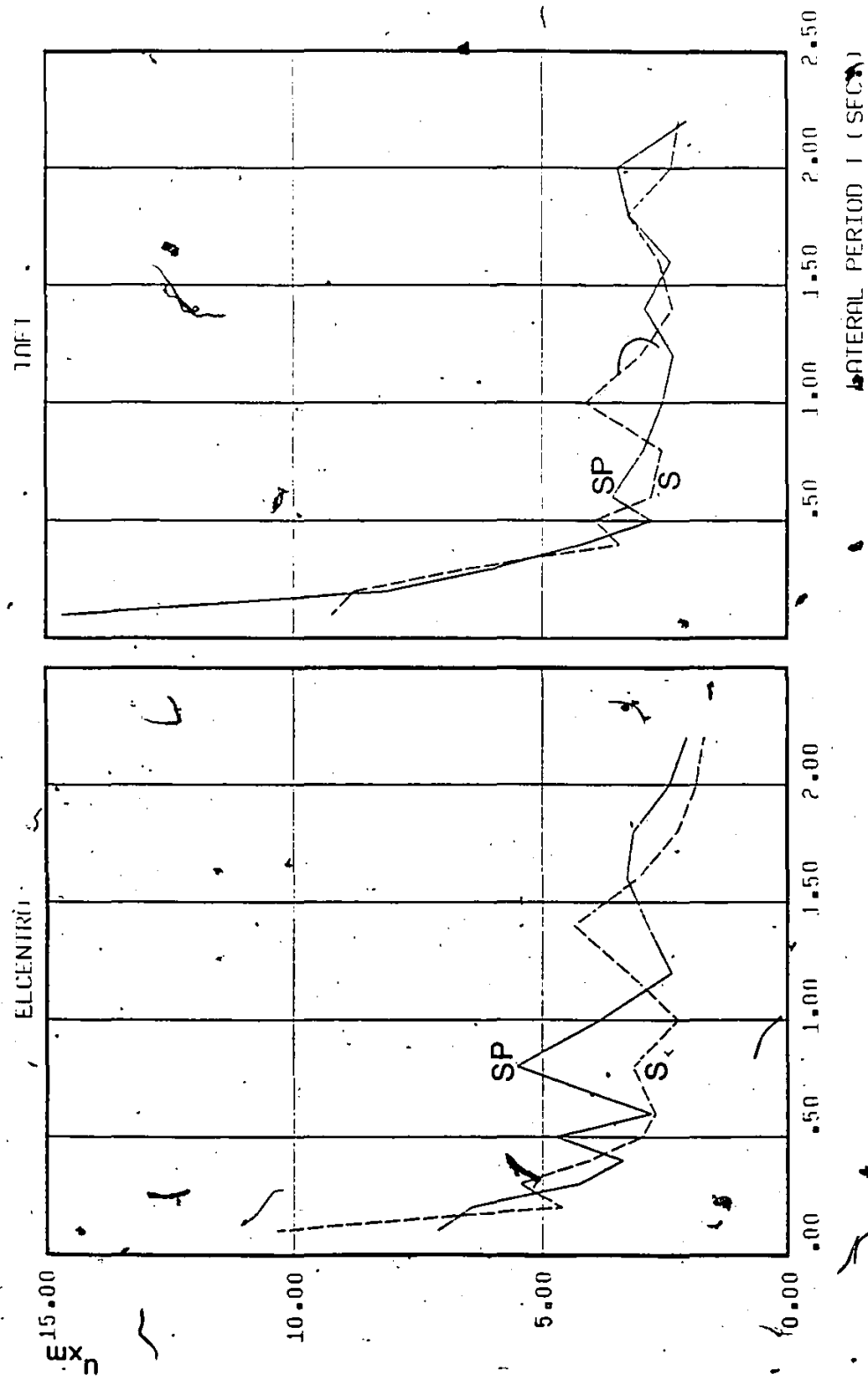


Fig (4.7) Comparison of Translation u_{xm} in the S and SP Models; $R=5$

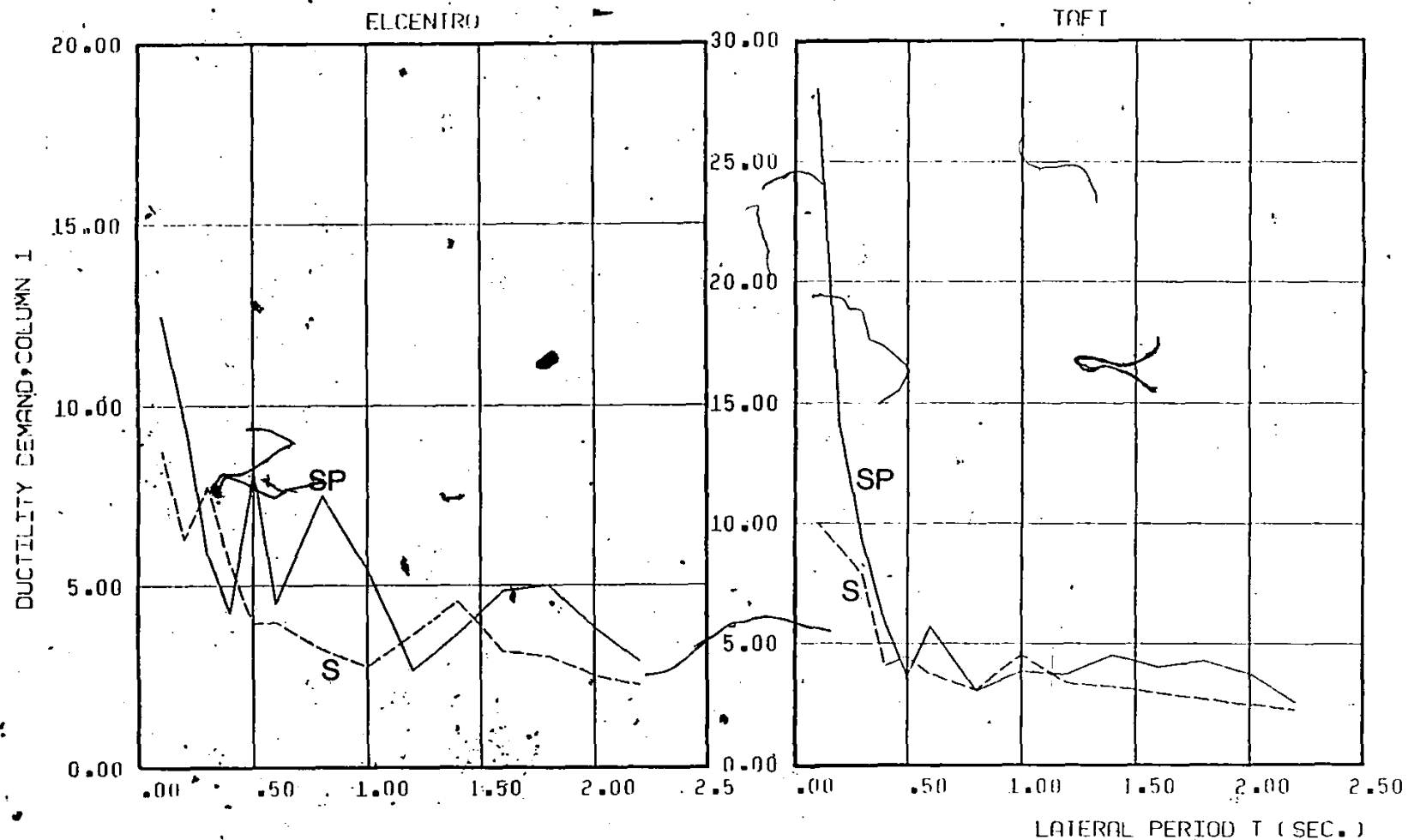


Fig (4.8) Comparison of the Ductility Demand on Column 1 in the S and SP Models; R=5

reductions of 50% are not uncommon.

ii. Figure (4.7) shows that the translational component u_{xm} is not systematically affected by changing the value of the plastic eccentricity.

iii. The ductility demand on the most stressed column, number 1, combines the effects of the rotational and translational displacements. The ductility demand is defined by

$$\mu_x = \max |u_x(t) - [u_0(t)/r](a/2)| \quad (4.11)$$

The influential effect that the plastic eccentricity has on the response is evident by comparing the solid and broken lines corresponding to models with and without plastic eccentricity, respectively, in Fig (4.8). By eliminating the plastic eccentricity, as in the model S, it is possible to limit the ductility demand for short period structures to values less than ten while for the other model, ductility demand can be as large as 28.

These observations indicate that although the two models used are equivalent in the elastic sense, their responses are significantly different by the virtue of differences in the strength distribution. The one that has nonuniform strength distribution exhibited larger rotational deformations and consequently larger ductility demands. A structure attains its maximum deformations during the strong shaking era of the excitation. At this stage the structure is excited well into the inelastic range and it is the strength distribution rather than the stiffness distribution that governs the response. Therefore, a structure with uniform strength distribution will behave more like a

symmetric structure with less rotation and more uniform distribution of ductility demand on the elements across the plan.

In the foregoing discussion, models with large values of plastic eccentricity as well as stiffness eccentricity have been used. It is useful however to see how sensitive structures, which are excited well into the inelastic range, will be to variations in the value of the eccentricity of both types. This is achieved as follows. On one hand the response of structures having identical values of stiffness eccentricity ($e_s=0.20$) but with different values of plastic eccentricity ($e_p=0, 0.10, 0.20$) are considered. On the other hand the responses of structures having identical values of plastic eccentricity ($e_p=0.20$) are considered for different values of stiffness eccentricity ($e_s=0, 0.10, 0.20$). These response curves are shown in Figs (4.9) and (4.10) for the 1952 Taft and 1940 El Centro ground motions. Figures (4.9a) and (4.9b) show the variation of the maximum rotation θ_{max} against lateral period T_x . The spread of the curves in the left plot, corresponding to different values of e_p , shows that the structure is sensitive to variations in the magnitude of the plastic eccentricity. This sensitivity is particularly significant for short period structures ($T_x < 0.5$ sec). The rotational response is considerably reduced with decreasing values of the plastic eccentricity. On the other hand the right plots in Figs (4.9a) and (4.9b) show that the rotational response is insensitive to variations in the value of the stiffness eccentricity. All curves have steep slopes in the short period range with substantial values of deformations. This indicates that regardless

1952 TAFT

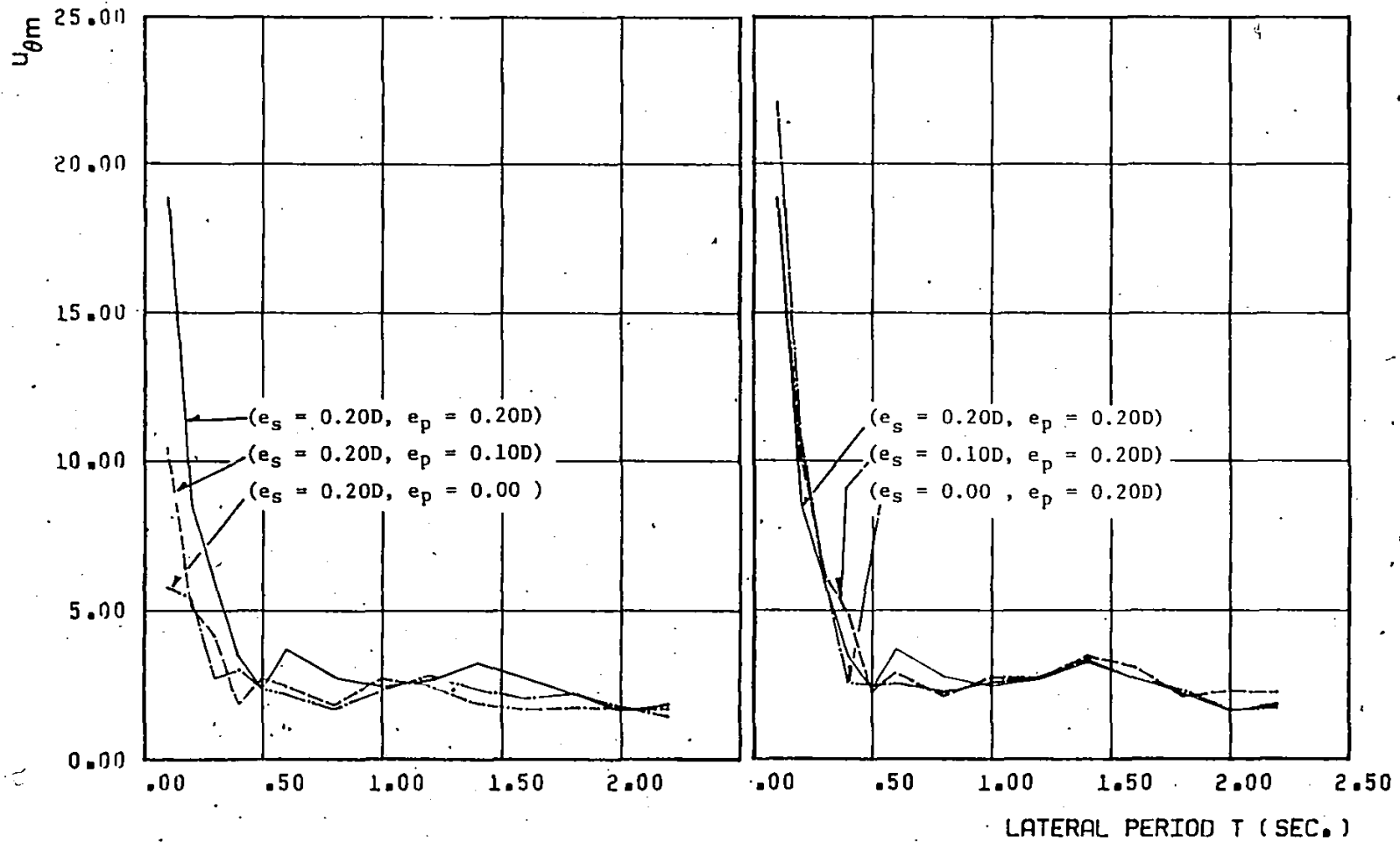


Fig (4.9a) Comparison of Rotation $u_{\theta m}$ of Models with Different Values of e_p and e_s ; Left: $e_s = 0.20$ and $e_p = 0, 0.10, 0.20$; Right: $e_p = 0.20$ and $e_s = 0, 0.10, 0.20$; $R=5$; 1952 Taft

1940 EL CENTRO

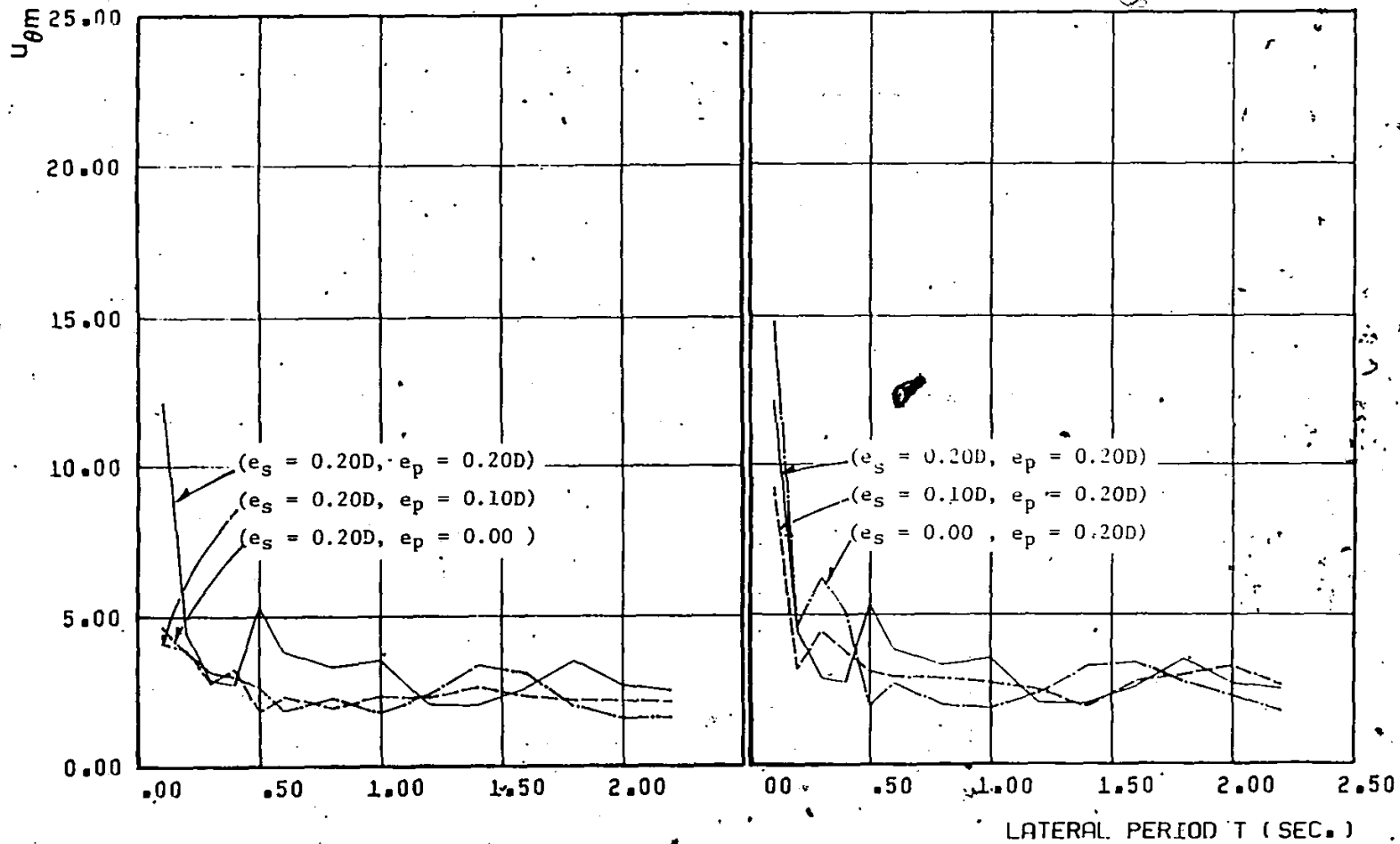


Fig (4.9b) Comparison of Rotation $u_{\theta m}$ of Models with Different Values of e_p and e_s ; Left: $e_s=0.20$ and $e_p=0, 0.10, 0.20$; Right: $e_p=0.20$ and $e_s=0, 0.10, 0.20$; $R=5$; 1940 El Centro.

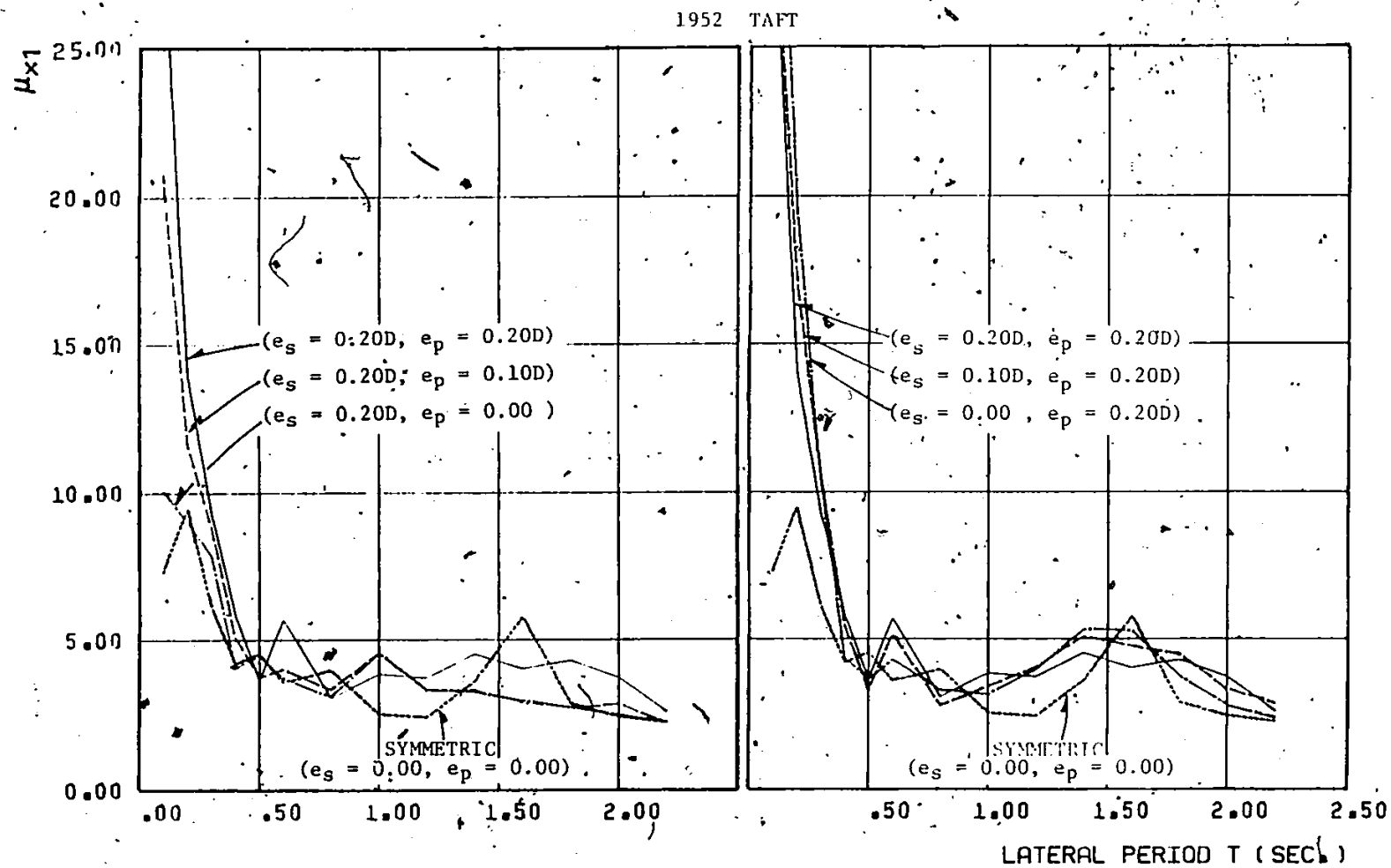


Fig (4.10a) Comparison of Ductility Demand on Column 1 in Models with Different Values of e_p and e_s , Including the Symmetric Case ($e_p = e_s = 0$); $R=5$; 1952 Taft

1940 EL CENTRO

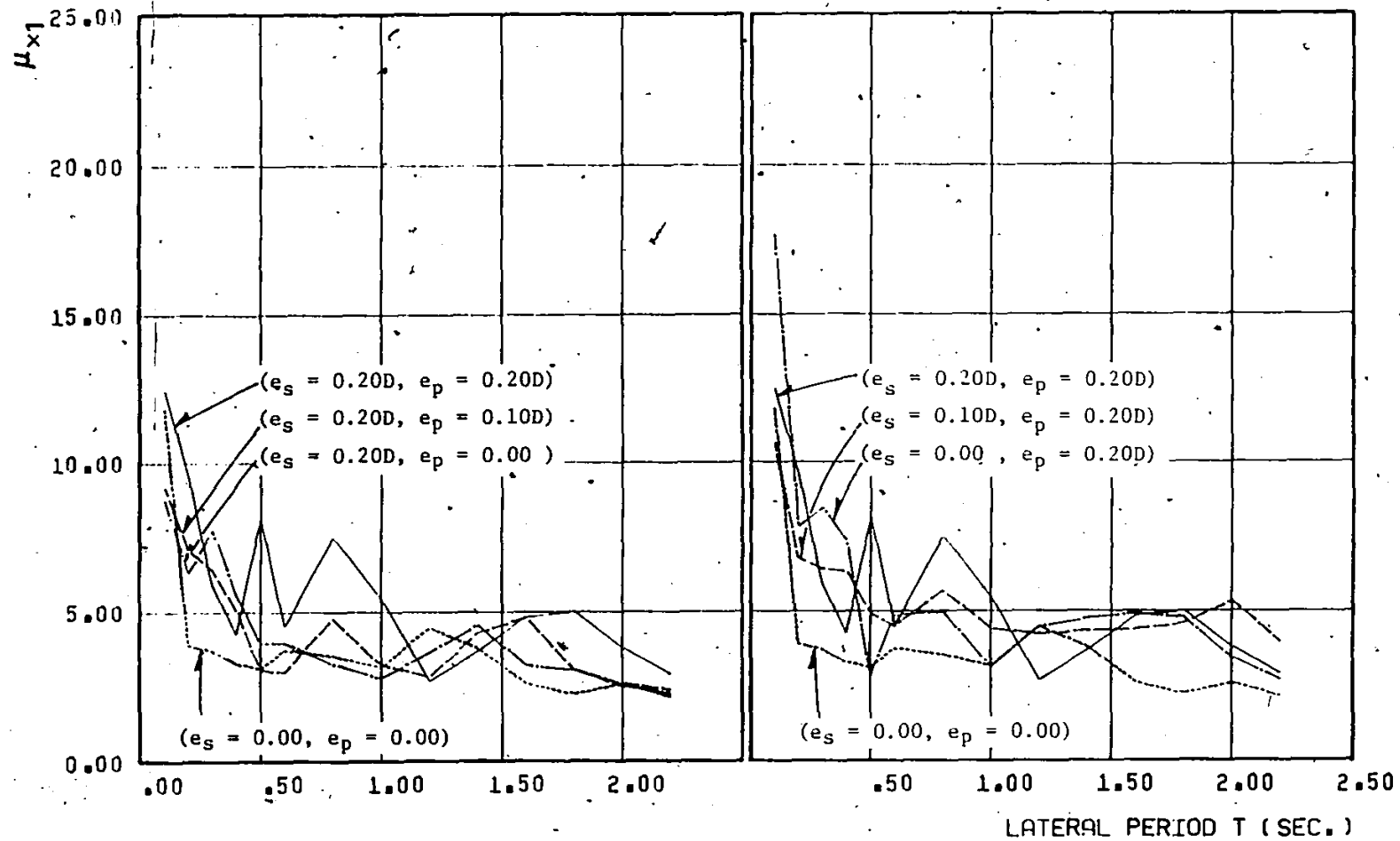


Fig (4.10b) Comparison of the Ductility Demand on Column I in Models with Different Values of e_p and e_s Including the Symmetric Case ($e_p=e_s=0$); R=5, 1940 El Centro

of the magnitude of the stiffness eccentricity, response is controlled by the plastic eccentricity.

This observation is true also for ductility demand responses on the critical column as shown in Figs (4.10a) and (4.10b). In addition to the curves of the different asymmetric models, curves corresponding to the true symmetric case, i.e. $e_p=e_s=0$, are also included. In the left figure, it can be seen that the two curves of the symmetric and asymmetric case with zero plastic eccentricity are very close even in the short period range. Thus by aiming towards a uniform distribution of yield strength, it is possible to effectively reduce the additional ductility demand due to stiffness asymmetry. This effect is particularly useful in view of the findings of the present study and the related studies⁽⁶⁾ indicating that short period structures are vulnerable to the combined effect of inelasticity and asymmetry. In the right figure, all asymmetric models curves are substantially larger than that of the symmetric case. This shows the consequences of having different strategies of stiffness distribution, including the one of uniform distribution ($e_s=0$). Even with no elastic eccentricity, it fails to reduce the additional ductility demand due to asymmetry because of the influential effect of the large plastic eccentricity common in these models.

The usefulness of the plastic eccentricity is based on two assumptions. First, all resisting elements are assumed to have reached their yield strength capacity. Second, the load deflection curve of any element participating in the lateral resistance is idealized by the elastic-perfectly-plastic relationship. The first assumption

corresponds to the case of structures being excited well into the inelastic range either due to severe excitations or when the design strength of a structure is well below the anticipated elastic seismic forces. In this range, the strength distribution controls the response as indicated earlier. However, if the structure is only moderately excited into the inelastic range, the strength as well as the stiffness distributions interact in a complicated way to control the response. Therefore, neither the stiffness eccentricity nor the plastic eccentricity alone will be an adequate index for torsion. The second assumption is the elasto-plastic idealization of the elements resistance functions. Although this idealization approximates actual behavior only in limited cases, it has been widely used in nonlinear analyses. This idealization is a special case of the more general bilinear curve with the yielding branch having a nonzero slope. For the bilinear idealization, the specification of the plastic eccentricity is still simple because the yielding branch is also a straight line. The extension of the plastic eccentricity concept to the more complicated nonlinear curves will require additional work and it is considered beyond the scope of the present study.

In the parameteric study of the plastic eccentricity and the elastic eccentricity, it has been assumed that they are independent parameters. In other words, even if the elastic eccentricity is dictated for example by the architectural considerations, one can still minimize the magnitude of the plastic eccentricity and hence reduce the rotational deformations should inelastic response occurs. To a limited

extent, this assumption is valid as shown below. Consider the two structural plans shown in Fig (4.11). One consists of a rigid slab supported on two open frames parallel to the direction of excitation. The frame to the right has larger beam and columns than those of the one to the left. For this system, both types of eccentricity are expected to be of similar magnitudes. The other system has its slab supported on an open frame and an infilled frame as shown in Fig (4.11b). While the infilled frame is stiffer than the open frame and hence the center of stiffness is offset from CM, the ultimate strength of the two structural elements are almost the same since the infilled wall fails in a brittle manner once the strain exceeds the critical value. Therefore, the center of strength coincides with CM and $e_p=0$ in this second structure. This example demonstrates the independence of the concept of elastic eccentricity and plastic eccentricity for certain types of structures.

4.5 MASS VS STIFFNESS UNBALANCED ECCENTRIC STRUCTURES :

So far, discussion has been limited to models whose elastic asymmetry, i.e. the relative location of CS from CM, is due to stiffness unbalance. Asymmetry can also be introduced in structures due to the uneven distribution of masses. Structures with irregularly shaped slabs or uneven distribution of the live loads are typical examples in which the center of mass may be shifted off the center of stiffness. Such asymmetry is said to be due to mass unbalance.

Asymmetric structures with either mass or stiffness unbalances will give the same overall elastic response provided the system parameters are identical. However, their inelastic responses will be

O.F. OPEN FRAME

I.F. INFILLED FRAME

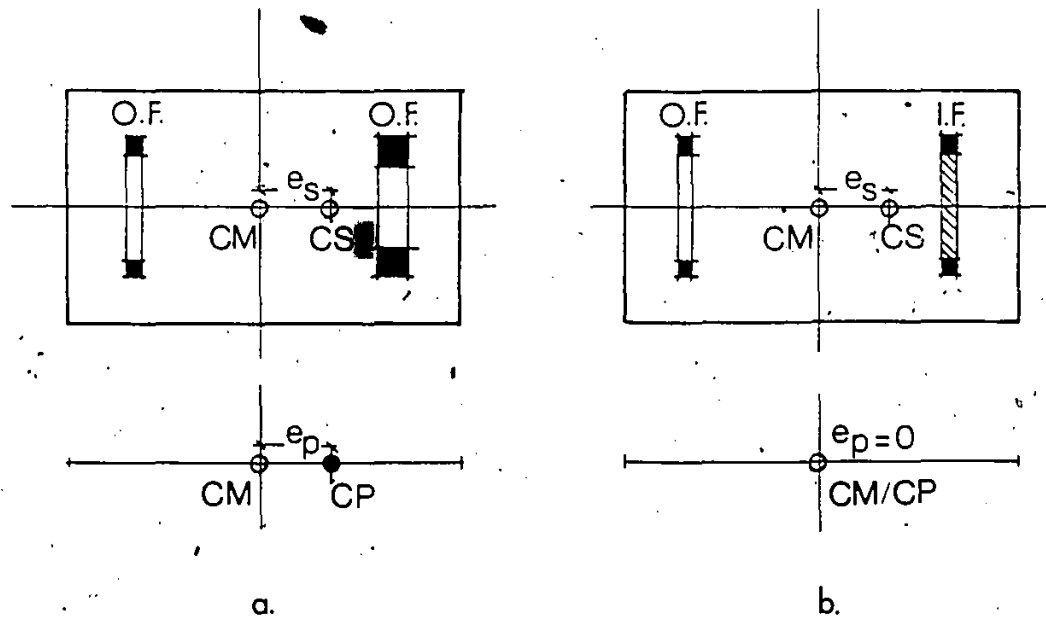
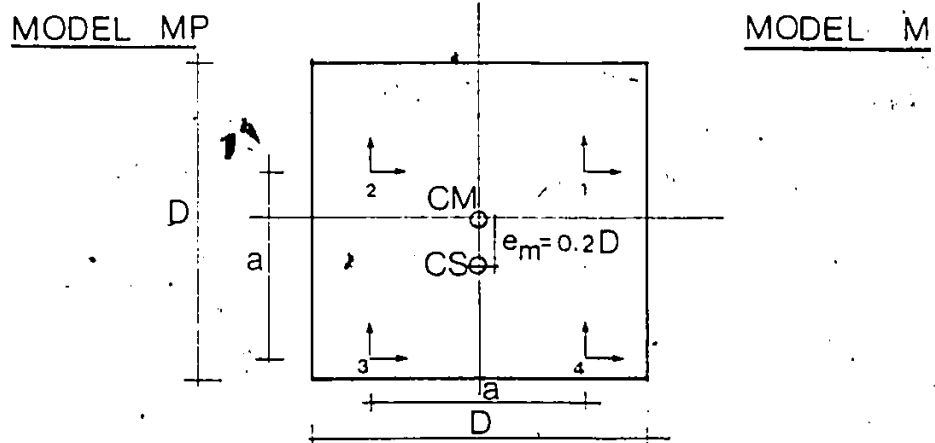


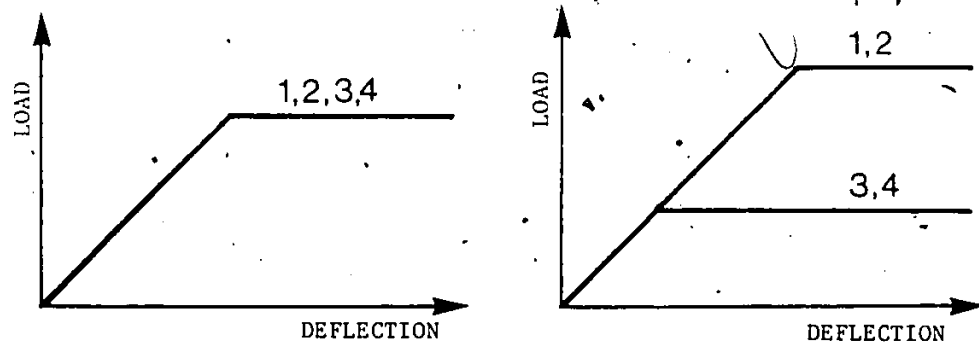
Fig (4.11) Structural Plans

different since in this range the response depends on the details of the structure. A model with mass unbalance is shown in Fig.(4.12). It consists of a rigid slab on four identical columns symmetrically arranged and the CM of the slab is shifted along the y direction. This eccentricity is referred to as the mass eccentricity (e_m) and is taken to be equal to one fifth of the plan dimension D ($e_m=0.2D$). Taking the first moment of yield forces about CM, it can be shown that the center of strength coincides with the center of stiffness, hence the plastic eccentricity of the system is given by $e_p=0.2D$. This model will be referred to as the MP model. The inelastic response of this model ($e_m=0.2D$, $e_p=0.2D$) is compared with that of the SP model ($e_s=0.2D$, $e_p=0.2D$) in the following way. The ratio of rotation $u_{\theta m}$ and translation u_{xm} of the MP model to those of the SP model are shown in Fig (4.13) using the 1940 El Centro and 1952 Taft ground motions. It can be seen that the translational component is insensitive to the type of eccentricity as indicated by the ratios being little different from unity. However the rotational deformations of the MP model are less than those of the SP model by a factor of 30% on the average.

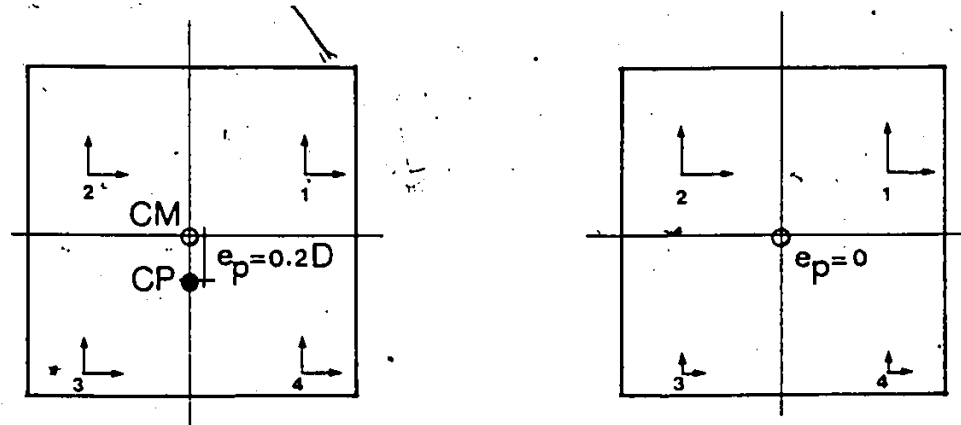
The ratios of ductility demand of Column 1 in the two models are shown in Fig (4.14). The ratios are clearly below unity. Thus the ductility demand on the most stressed column in asymmetric structures with mass unbalance is smaller than that in an equivalent system but with stiffness unbalance. This is not only because of the smaller rotational deformations but also the rotational component contributes less to the column ductility in the mass unbalance model since the



(a) STIFFNESS DISTRIBUTION



(b) LOAD-DEFLECTION CURVES OF COLUMNS



(c) STRENGTH DISTRIBUTION

Fig (4.12) Properties of the M and MP Models

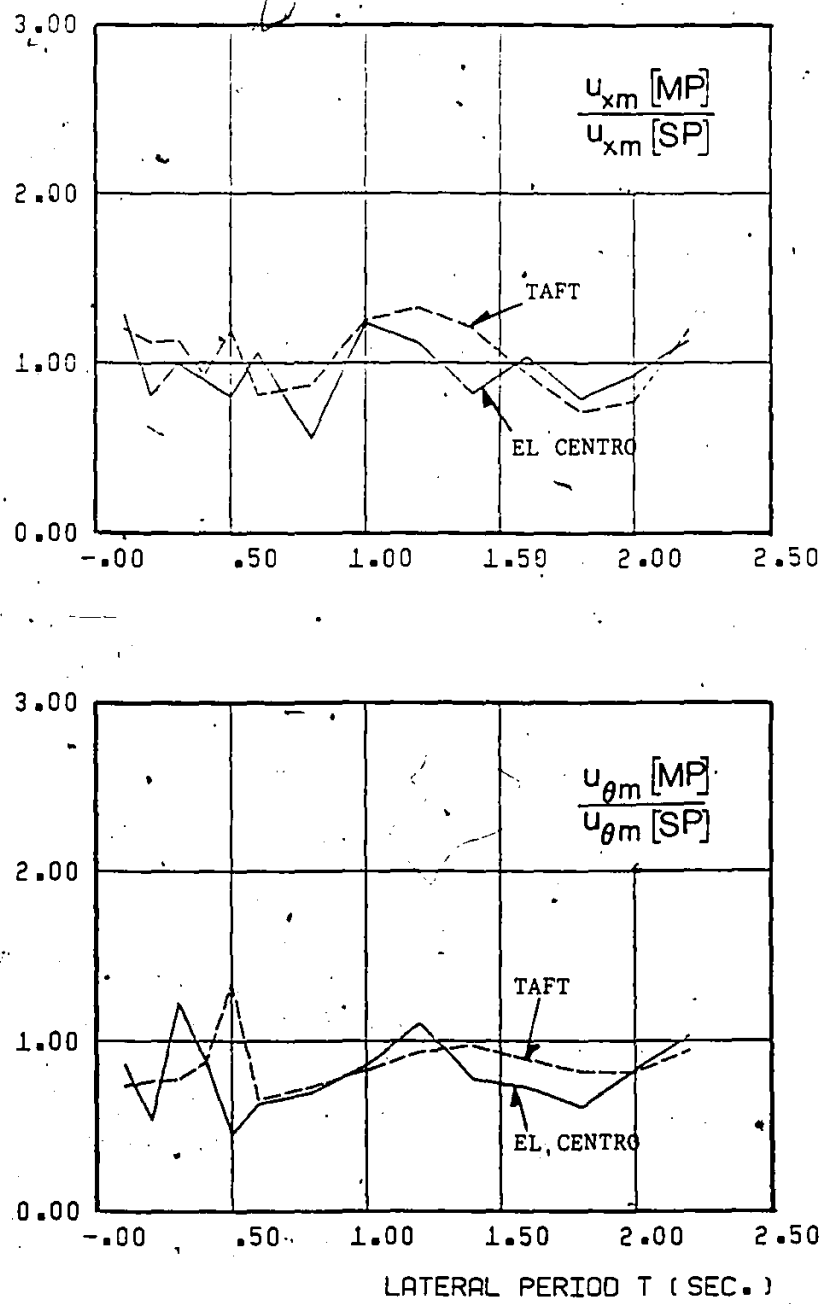


Fig (4.13) Comparison of Translation u_{xm} and Rotation $u_{\theta m}$ of the MP and SP Models; $R=5$; 1940 El Centro and 1952 Taft

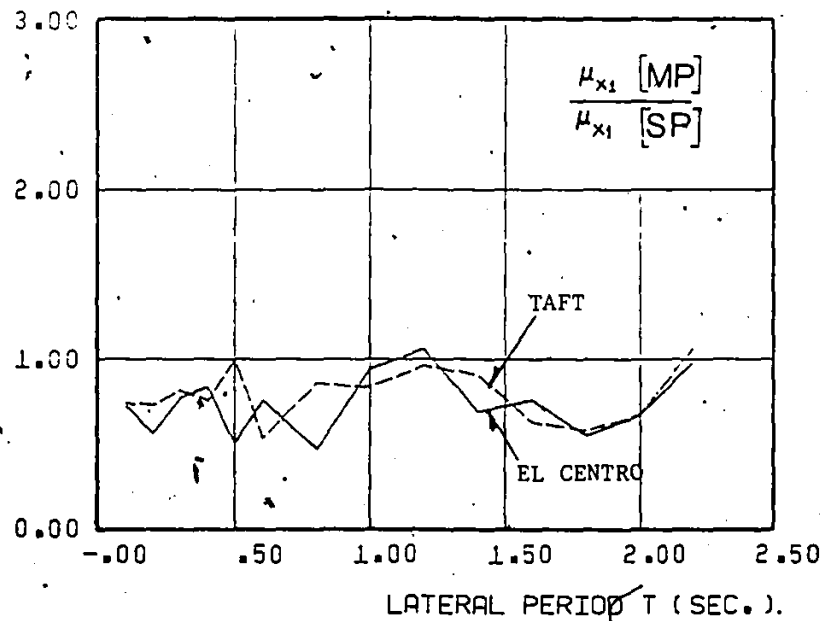


Fig (4.14) Comparison of the Ductility Demand on Column 1 in the MP and SP Models; $R=5$; 1940 El Centro and 1952 Taft

column is located closer to CM as compared to the case of stiffness unbalance. Column 1 is located at a distance $a/2$ or $(a/2)-e_m$ away from CM in the stiffness or mass unbalance models respectively.

4.6 EDGE DISPLACEMENT :

The edge displacement of the floor slab serves as measure of the nonstructural damage potential. The positive edge displacement Δ_x is defined as the absolute maximum displacement of the edge of the slab furthest away from the initial center of stiffness CS, in other words

$$\Delta_x = \max |\Delta_x(t)| \quad (4.12)$$

where

$$\Delta_x(t) = u_x(t) - (u_0(t)/r)(D/2)$$

Since the relative location of this point is invariant in all the asymmetric models considered herein, the edge displacement Δ_x is a useful parameter of comparison. The information on the edge displacement is normalized with respect to Δ_{x0} which is the edge displacement of an equivalent symmetric model. The ratio Δ_x/Δ_{x0} represents the asymmetry effect, in other words the additional deformations introduced due to asymmetry. The variation of this ratio against lateral period is shown in Figs (4.15a, and b). Ratios are obtained using asymmetric models with uniform and nonuniform strength distributions and asymmetry is either due to stiffness or mass unbalances. The following observations can be made.

- i. Asymmetry effects are substantially reduced in the stiffness unbalance models if a uniform strength distribution is provided, while

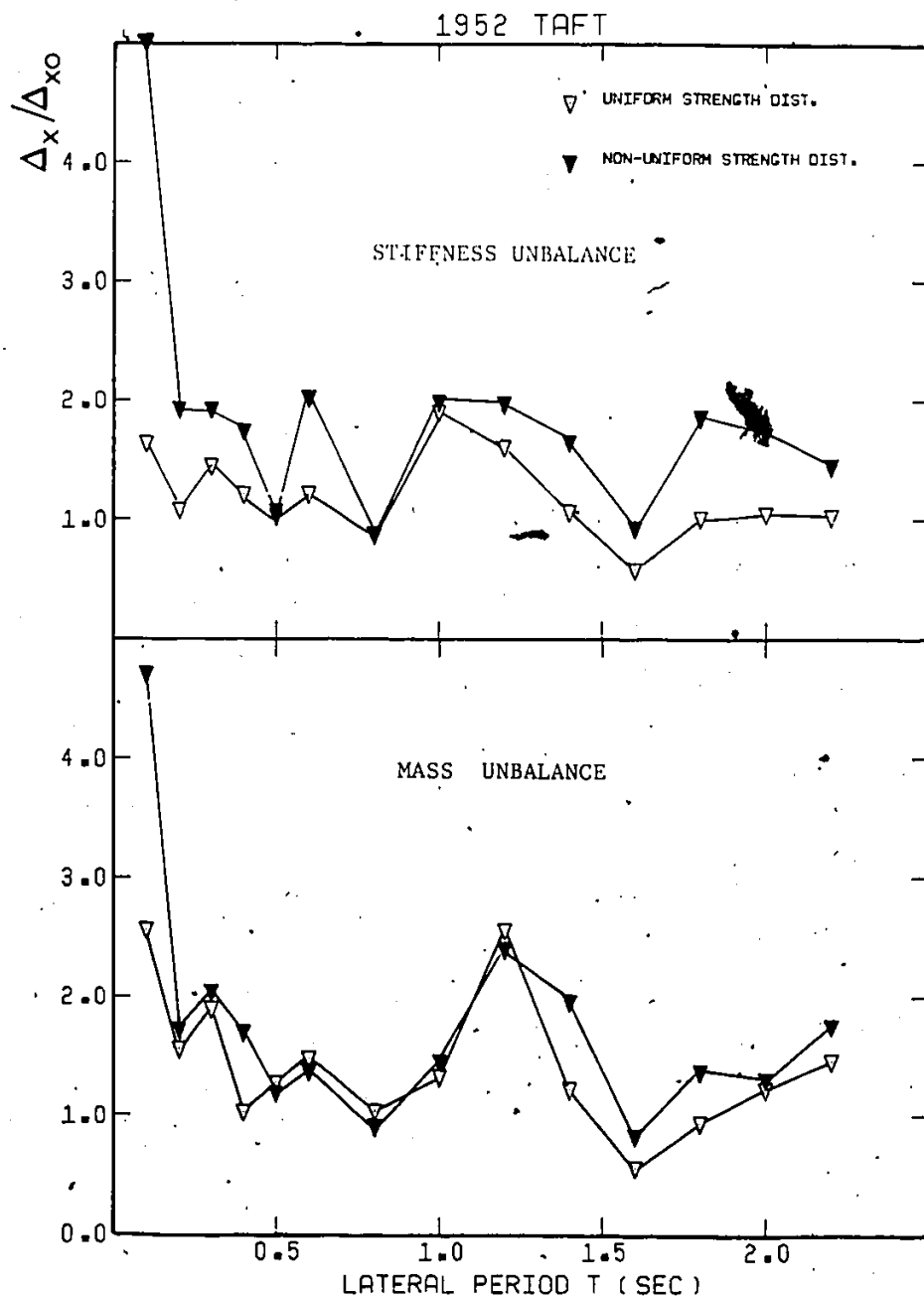


Fig. (4.15a) Comparison of the Ratio ($\Delta x / \Delta x_0$) of Stiffness or Mass Unbalanced Models with Uniform or Nonuniform Strength Distributions; R=5; 1952 Taft

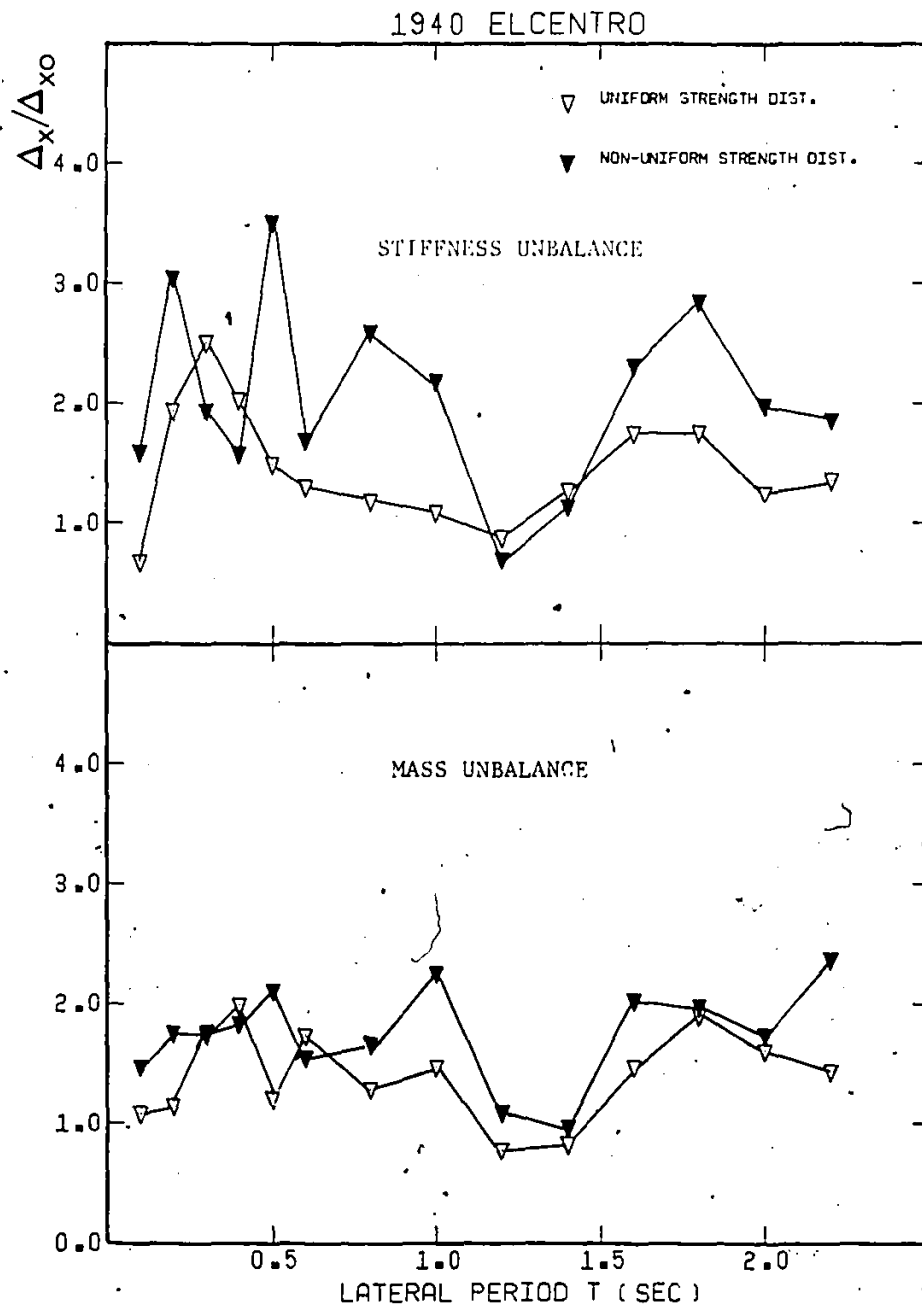


Fig (4.15b) Comparison of the Ratio ($\Delta x / \Delta x_o$) of Stiffness or Mass Unbalanced Models with Uniform or Nonuniform Strength Distributions; $R=5$; 1940 El Centro

the ratio Δ_x/Δ_{x0} can be as large as 5 for the nonuniform strength distribution case, its value is kept below 2 for the other case.

ii. Strength distribution affects the mass unbalance models to a lesser extent than it does to the stiffness unbalance models. This can be explained by recalling that the rotational component of deformation is less in the mass unbalance systems as shown earlier. Since the plastic eccentricity essentially affects the rotational deformations of the system, it is expected that eliminating the plastic eccentricity in the mass unbalance system will affect the total displacement response to a lesser extent.

iii. Independent of the type of the elastic eccentricity, mass or stiffness types, asymmetry effects can be limited to values between one and two over the entire period range by proportioning strength for uniform distributions.

4.7 SUMMARY AND CONCLUSIONS:

The effects of asymmetry on the inelastic response of structures have been discussed. The prime concern of this study is regarding the role of "eccentricity" in the inelastic response of asymmetric structures. For this purpose a single mass monosymmetric structural model subjected to the two horizontal components of ground motions is used. A number of models are used to represent a variety of buildings with different stiffness as well as strength distributions among the resisting elements. To limit the size of the study, only buildings with identical properties in the two lateral directions are considered.

Moreover, the torsional to lateral frequencies ratio is assumed to have a value of unity in all models. The response parameters of interests are the rotational and lateral deformation components at the center of mass, the ductility demand on the most stressed column, and the edge displacement. Having analyzed the results, it is possible to make the following conclusions.

(A) Effects of Interaction:

1. Including interaction between the two lateral components of shear in yielding of columns affects the inelastic response of asymmetric systems to a lesser extent than it does to the symmetric case. This can be attributed to the presence of torsional coupling. It introduces to the asymmetric system some features that interaction is known to have, namely the allowance of transfer of energy between the two lateral directions.

(B) Plastic Eccentricity Concept:

1. An alternative definition of eccentricity based on the ultimate strength properties is proposed as a better index to denote the severity of torsion on the inelastic response of asymmetric structures. The proposed plastic eccentricity is defined as the offset of the center of strength from the center of mass of the system. The center of strength can be obtained by taking the first moment of the yield forces in the resisting elements about any arbitrary point in the floor plan.

2. Different from the experience with the elastic eccentricity (the offset of the center of stiffness from CM), the rotational response

of asymmetric structures excited well into the inelastic range is found to be strongly correlated with the magnitude of the plastic eccentricity. Structures with uniform strength distributions, or zero plastic eccentricity, are expected to experience considerably less rotational deformations in their inelastic response as compared to the case of structures with nonuniform strength distributions. The reduction in rotational deformations and consequently in the elements ductility demand is particularly evident for stiff structures.

3. The plastic eccentricity concept helps in understanding the nature of the inelastic torsional responses. Under severe excitations, most and if not all the resisting elements reach their strength limits and the rigidity of the system is best characterized by its strength properties. The response in these situations is controlled by the strength distribution. Structures having uniform distributions of strength will behave more like symmetric systems in ductility demand estimates.

4. Stiff structures with yield strength well below the elastic strength demand are known to be vulnerable to the effect of asymmetry (6). By providing a uniform strength distribution, it is possible to effectively reduce the rotational response as well as the elements ductility demand for structures under strong earthquake excitations. The ductility demands of asymmetric structures with uniform strength distribution are found to be not much different from those of a completely symmetric structure (both in stiffness and strength distributions).

(C) Mass versus Stiffness Eccentricities:

1. Within the elastic definition of eccentricity, asymmetry can be due to either uneven distributions of stiffness or mass. This distinction is useful only in the case of inelastic response since it is model specific. Comparing the inelastic response of structures of both types shows that while the lateral component of deformation at CM is insensitive to the type of asymmetry, the rotational component is found to be less in the mass eccentric systems as compared to that of the stiffness eccentric systems. This observation is in agreement with the findings in (49).

(D) Edge Displacement:

1. For a structure with uniform strength distribution, asymmetry can only increase the displacement of the edge furthest away from the initial center of stiffness by 100% at most over that of the symmetric case. This information would be useful in the design of nonstructural elements such as claddings at the perimeter of the building envelope.

CHAPTER 5

SUMMARY AND CONCLUSIONS

5.1 SUMMARY :

In this investigation, a study has been made of the inelastic seismic response of single story structures having symmetrical as well as asymmetrical configurations and subjected to bidirectional excitations. The intent of this investigation was (i) to assess the significance of forces interaction in yielding of columns in the analysis of inelastic structures, (ii) to provide guidelines as how to account for the bidirectionality of the ground motion, and (iii) to clarify the role of "eccentricity" in the lateral-torsional response of inelastic asymmetrical systems.

To gain insight as to the effects of including forces interaction, the dynamic response of inelastic columns subjected to biaxial bending due to sinusoidal base motions along two orthogonal directions is discussed. The elasto-plastic responses with interaction effect included or ignored are presented. Columns having either circular or I sections are considered in the discussion.


The inelastic response of single story structural model subjected to the simultaneous action of the two horizontal components of earthquake ground motions is then discussed. An ensemble of five pairs of recorded earthquakes ground motions is used as input and the mean values of responses are presented. Attention is focused on the

displacement ductility demand responses. In this part of the study, buildings with identical or different properties in the two lateral directions are considered. The effects of the orientation of the ground motion components with respect to the structural axes are examined. Approximate methods to estimate the peak ductility demand are presented. One method which requires only the elastic response of the system is proposed.

Finally, the effects of asymmetry on the inelastic response of structures are examined using a single mass monosymmetrical structural model subjected to bidirectional earthquake ground motions. The significance of the interaction effect is assessed for such torsionally coupled system. The prime concern in this part of the study is regarding the role of "eccentricity" in the inelastic response of eccentric structures. A new concept of eccentricity based on the yield properties of the resisting elements is proposed. The adequacy of the proposed eccentricity as a measure of the rotational response of inelastic eccentric systems is examined. The response parameters of interest are the ductility demand on the most stressed column and the edge displacement.

5.2 CONCLUSIONS :

By the end of each of chapters 2, 3, and 4, related conclusions are included. In addition, the outstanding conclusions are presented in the following to help gain an overall view of the findings of the present work.



Based on the discussion in chapter 2 on the effects of interaction for inelastic columns subjected to biaxial bending due to sinusoidal input motion, the following conclusions can be made.

1. For systems with large ratios of excitation to system frequencies, including the interaction effect has the tendency to reduce the steady state displacement response. For such systems it is adequate to consider the elasto-plastic responses.

2. Interaction becomes significant for systems with low frequency ratios particularly with high levels of excitation. Including interaction leads to a large increase of the steady state displacement response over that of an elasto-plastic model. For this situation, a conservative estimate of the response can be obtained if the lower bound yield curve, which admits maximum interaction, is assumed for the element considered.

3. Varying the phase angle between the two input sinusoidal waves leads to the redistribution of energy in the two orthogonal directions of the system when the interaction effect is included. The redistribution of energy causes the response in one direction to increase and in the other to decrease. The maximum effect of the phase angle on the displacement amplitude is insensitive to the shape of the yield curve assumed. In addition, an elasto-plastic model will give a good estimate of this maximum displacement amplitude provided the frequencies ratio is large ($\eta^2 > 0.6$).

Based on the inelastic analysis of symmetrical structures subjected to bidirectional earthquake ground motions presented in chapter 3, the following conclusions were reached.

(A) Effects of Interaction :

1. Including the interaction effect has only a minor effect on the inelastic response for long period structures (say $T > 0.5$ sec) or short period structures excited moderately into the inelastic range. Therefore, an elasto-plastic analysis without taking the yield interaction effect into account will be sufficient for determining ductility demand estimates for these classes of structures.

2. Stiff structures ($T < 0.5$ sec) with low yield strength, hence those excited well into the inelastic range, are shown to exhibit large values of ductility demand based on elasto-plastic analysis. For such structures, the interaction effect is significant and it further increases the ductility demand. The increase becomes substantial for very stiff structures ($T < 0.2$ sec). This observation is significant on two counts. First, it points out the inadequacy of planar inelastic analyses to estimate the ductility demand for stiff structures excited well into the inelastic range. Second, it shows that the ductility demand for such structures can be exceedingly high. Therefore, very stiff structures should be designed so that the expected earthquake disturbance will not cause the structure to be excited well into the inelastic range. In other words, it is prudent to design very stiff structures to remain elastic or almost elastic when subjected to the probable earthquake excitation. Since none of the existing studies on

effects of interaction considered structures in this period range, this effect has been overlooked before.

3. The radial ductility ratio in systems with identical properties along the two lateral directions of resistance is invariant to the orientation of the ground motion directions relative to the structural axes provided the interaction effect is included in the inelastic analysis. Such quantity can be used as an index of ductility demand in structures subjected to bidirectional excitations, and should be used in ductility estimates for design purposes.

4. A more realistic estimate of ductility demand which takes into account the effect of interaction and the bidirectionality of excitation can be, on the average, up to 40% larger than estimates calculated otherwise. Such an estimate can be derived using the elastoplastic uniaxial responses of the system by approximate rules. These rules are either (i) increasing the uniaxial response to the stronger component by 40% or (ii) as the sum of the uniaxial response to the stronger component plus 30% of the response to the other component.

(B) Approximate Estimate of Ductility:

1. An approximate estimate of the ductility demand of symmetric structures based on amplifying the elastic response with a period dependent factor is proposed. These factors are related to those proposed in (32) to derive inelastic response spectra from elastic smooth spectra. Except for very stiff structures with low yield strength, this approximate method seems to be satisfactory.

For symmetric structures with unequal periods in the two lateral directions, the following conclusions were specifically stated.

1. The radial ductility ratio shows considerable variations with the angle of orientation of ground motions even if the interaction effect is taken into account. The maximum radial ductility ratio over the entire range of the angle of orientation can be reasonably estimated by orienting the pair of ground motions such that the stronger component is acting along the shorter period direction.

2. The maximum effect of the orientation of ground motion components on the ductility demand in the longer period direction can be estimated by the 30% rule, i.e. the sum of the maximum uniaxial response in the longer period direction plus 30% of that in the shorter period direction. And to account for this effect in the shorter period direction, it is sufficient to increase the maximum uniaxial response in this direction by 40%.

Examining the inelastic response of the single mass monosymmetrical models subjected to the two horizontal components of earthquake ground motions, the following conclusions were drawn.

(A) Effects of Interaction:

1. Including interaction between the two lateral components of shear in yielding of columns affects the inelastic response of asymmetric systems to a lesser extent than it does to the symmetric case. This can be attributed to the presence of torsional coupling. It introduces to the asymmetric system some features that interaction is

known to have, namely the allowance of transfer of energy between the two lateral directions.)

(B) Plastic Eccentricity Concept:

1. An alternative definition of eccentricity based on the ultimate strength properties is proposed as a better index to denote the severity of torsion on the inelastic response of asymmetric structures. The proposed plastic eccentricity is defined as the offset of the center of strength from the center of mass of the system. The center of strength can be obtained by taking the first moment of the yield forces in the resisting elements about any arbitrary point in the floor plan.

2. Different from the experience with the elastic eccentricity (the offset of the center of stiffness from CM), the rotational response of asymmetric structures excited well into the inelastic range is found to be strongly correlated with the magnitude of the plastic eccentricity. Structures with uniform strength distributions, or zero plastic eccentricity, are expected to experience considerably less rotational deformations in their inelastic response as compared to the case of structures with nonuniform strength distributions. The reduction in rotational deformations and consequently in the elements ductility demand is particularly evident for stiff structures.

3. The plastic eccentricity concept helps in understanding the nature of the inelastic torsional responses. Under severe excitations, most and if not all the resisting elements reach their strength limits and the rigidity of the system is best characterized by its strength properties. The response in these situations is controlled by the

strength distribution. Structures having uniform distributions of strength will behave more like symmetric systems in ductility demand estimates.

4. Stiff structures with yield strength well below the elastic strength demand are known to be vulnerable to the effect of asymmetry (6). By providing a uniform strength distribution, it is possible to effectively reduce the rotational response as well as the elements ductility demand for structures under strong earthquake excitations. The ductility demands of asymmetric structures with uniform strength distribution are found to be not much different from those of a completely symmetric structure (both in stiffness and strength distributions).

5. For a structure with uniform strength distribution, asymmetry can only increase the displacement of the edge furthest away from the initial center of stiffness by 100% at most over that of the symmetric case. This information would be useful in the design of nonstructural elements such as claddings at the perimeter of the building envelope.

The above favorably indicates that the proposed plastic eccentricity is a useful index of the severity of rotational response of structures excited well into the inelastic range. However, if the structure is only moderately excited into the inelastic range, neither the elastic eccentricity nor the plastic eccentricity alone will be an adequate index for torsional response. Moreover, the plastic eccentricity is introduced herein based on the elasto-plastic idealization of the inelastic behavior of resisting elements. It is

desirable to extend such a useful concept to the case of more elaborate idealizations of the inelastic behavior of elements.

(C) Mass versus Stiffness Eccentricities:

1. Within the elastic definition of eccentricity, asymmetry can be due to either uneven distributions of stiffness or mass. This distinction is useful only in the case of inelastic response since it is model specific. Comparing the inelastic response of structures of both types shows that while the lateral component of deformation at CM is insensitive to the type of asymmetry, the rotational component is found to be less in the mass eccentric systems as compared to that of the stiffness eccentric systems. This observation is in agreement with the findings in (49).

REFERENCES

1. Aktan, A.E., Pecknold, D.A.W., and Sozen, M.A., "Effects of Two-Dimensional Earthquake Motion on a Reinforced Concrete Column", Civil Engineering Studies, Structural Research Series No. 399, University of Illinois, Urbana, May 1973.
2. Aktan, A.E., Pecknold, D.A.W., and Sozen, M.A., "R/C Column Earthquake Response in Two Dimensions", J. Struct. Div., ASCE, Vol. 100, No. ST 10, October 1974, pp. 1999-2015.
3. Aktan, A.E., Pecknold, D.A.W., "Response of a Reinforced Concrete Section to Two Dimensional Curvature Histories", J. Am. Conc. Inst., Title No. 71-16, May 1974, pp. 246-250.
4. Anagnostopoulos, S.A., "Response Spectrum Techniques for Three-Component Earthquake Design," Earthq. Eng. Struct. Dyn., Vol. 9, 1981, pp. 459-476.
5. Anagnostopoulos, S.A., Roesset, J.M., and Biggs, J.M., "Nonlinear Dynamic Analysis of Buildings with Torsional Effects," Proc. of the 5th Wld. Conf. Earthq. Eng., Vol. 2, Rome, Italy, June 1973, pp. 1822-1825.
6. Bozorgnia, Y., and Tso, W.K., "Inelastic Earthquake Response of Monosymmetric Structures," Submitted to J. Struct. Div., ASCE.
7. Caughey, T.K., "Sinusoidal Excitation of a System With Bilinear Hysteresis," J. Appl. Mech., Vol. 27, No. 4, December 1960, pp. 640-643.
8. Chen, W.F., and Atsuta, T., "Interaction Equations of Biaxially Loaded Sections," J. Struct. Div., ASCE, Vol. 98, No. ST5, May 1972, pp. 1035-1052.
9. Chopra, A.K., and Kan, C.L., "Effects of Stiffness Degradation on Earthquake Ductility Requirements for Multistory Buildings," Earthq. Eng. Struct. Dyn., Vol. 2, No. 1, 1973, pp. 35-45.
10. Clough, R.W., and Benuska, K.L., "Nonlinear Earthquake Behavior of Tall Buildings," J. Eng. Mech. Div., ASCE, Vol. 93, No. EM3, July 1967, pp. 129-146.
11. Clough, R.W., and Johnston, S.B., "Effects of Stiffness Degradation on Earthquake Ductility Requirements," Proc., Japan Earthquake Engineering Symposium, Tokyo, Japan, October 1966, pp. 227-232.

12. Drucker, D.C., "A Definition of Stable Inelastic Material," J. Appl. Mech., Vol. 26, March 1959, pp. 101-106.
13. Erdik, M.O., "Torsional Effects in Dynamically Excited Structures," Ph.D. Thesis, Rice University, Houston, Texas, May 1975.
14. Hart, G.C., DiJulio, R.M., Jr., and Lew, M., "Torsional Response of High Rise Buildings," J. Struct. Div., ASCE, Vol. 101, No. ST2, February 1975, pp. 397-416.
15. Hodge, P.G., Jr., "Plastic Analysis of Structures," McGraw-Hill Book Co., Inc., New York, 1959.
16. Irvine, H.M., and Kountouris, G.E., "Peak Ductility Demands in Simple Torsionally Unbalanced Building Model Subjected to Earthquake Excitation," Proc. of the 7th Wld. Conf. Earthq. Eng., Vol. 4, Istanbul, Turkey, September 1980, pp. 117-120.
17. Irvine, H.M., and Kountouris, G.E., "Inelastic Seismic Response of a Torsionally Unbalanced Single-Story Building Model," Report No. R79-31, Department of Civil Engineering, Massachusetts Inst. of Technology, Cambridge, Mass., 1979.
18. Jennings, P.C., "Earthquake Response of a Yielding Structure," J. Eng. Mech. Div., ASCE, Vol. 91, No. EM4, August 1965, pp. 41-68.
19. Jennings, P.C., and Husid, R., "Collapse of Yielding Structures During Earthquakes," J. Eng. Mech. Div., ASCE, Vol. 94, No. EM4, October 1968, pp. 1045-1065.
20. Kan, C.L., and Chopra, A.K., "Effects of Torsional Coupling on Earthquake Forces in Buildings," J. Struct. Div., ASCE, Vol. 103, No. ST4, April 1977, pp. 805-819.
21. Kan, C.L., and Chopra, A.K., "Coupled Lateral Torsional Response of Buildings to Ground Shaking," Report No. EERC 76-13, Earthquake Engineering Center, University of California, Berkeley, California, May 1976.
22. Kan, C.L., and Chopra, A.K., "Torsional Coupling and Earthquake Response of Simple Elastic and Inelastic Systems," J. Struct. Div., ASCE, Vol. 107, No. ST8, August 1981, pp. 1569-1588.
23. Kan, C.L., and Chopra, A.K., "Simple Model for Earthquake Response Studies of Torsionally Coupled Buildings," J. Eng. Mech. Div., ASCE, Vol. 107, No. EM5, October 1981, pp. 935-951.
24. Kobori, T., Minai, R., and Fujiwara, T., "Earthquake Response of Frame Structures Composed of Inelastic Members," Proc. of the 5th

- Wld. Conf. Earthq. Eng., Vol. 2, Rome, Italy, June 1973, pp. 1772-1781.
25. Lopez, O.A., and Chopra, A.A., "Studies of Structural Response to Earthquake Ground Motion," Report No. UCB/EERC-78/07, University of California, Berkeley, California, April 1978.
 26. Mahin, S.A., and Bertero, V.V., "An Evaluation of Inelastic Seismic Design Spectra," J. Struct. Div., ASCE, Vol. 107, No. ST9, September 1981, pp. 1777-1795.
 27. Morris, N.F., "Dynamic Analysis of Elasto-plastic Space Frames," Proc. of the International Symposium on Earthquake Structural Engineering, Vol. 2, St. Louis, Missouri, August 1976, pp. 285-298.
 28. Mosaddad, B., and Powell, G.H., "Computational Models for Cyclic Plasticity, Rate Dependence, and Creep in Finite Element Analysis," Report No. UCB/EERC-82/26, University of California, Berkeley, California, November 1982, pp. 6-12.
 29. Newmark, N.M., "Current Trends in the Seismic Analysis and Design of High-Rise Structures," Earthquake Engineering, Prentice-Hall, Englewood Cliffs, New Jersey, 1970, pp. 403-424.
 30. Newmark, N.M., "Torsion in Symmetrical Buildings," Proc. of the 4th Wld. Conf. Earthq. Eng., Vol. 2, Santiago, Chile, January 1969, pp. A3-19 to A3-32.
 31. Newmark, N.M., and Hall, W.J., "Earthquake Spectra and Design," Earthquake Engineering Research Institute, Berkeley, California, 1982.
 32. Newmark, N.M., and Hall, W.J., "Procedures and Criteria for Earthquake Resistant Design," Building Practices for Disaster Mitigation, National Bureau of Standards, Building Science Series No. 46, 1973.
 33. Newmark, N.M., and Rosenblueth, E., "Fundamentals of Earthquake Engineering," Prentice-Hall, Englewood Cliffs, New Jersey, 1971, pp. 236-241.
 34. Nigam, N.C., "Inelastic Interactions in the Dynamic Response of Structures," Ph.D. Thesis, California Institute of Technology, Pasadena, California, June 1967.
 35. Nigam, N.C., "Yielding in Framed Structures under Dynamic Loads," J. Eng. Mech. Div., ASCE, Vol. 96, No. EM5, October 1970, pp. 687-709.
 36. Nigam, N.C., and Housner, G.W., "Elastic and Inelastic Response

- of Framed Structures during Earthquakes," Proc. of the 4th Wld. Conf. Earthq. Eng., Vol. 2, Santiago, Chile, January 1969, pp. A4-89 to A4-104.
37. Pecknold, D.A., "Inelastic Structural Response to 2D Ground Motion," J. Eng. Mech. Div., ASCE, Vol. 100, No. EM5, October 1974, pp. 949-963.
 38. Pecknold, D.A., and Sozen, M.A., "Calculated Inelastic Structural Response to Uniaxial and Biaxial Earthquake Motions," Proc. of the 5th Wld. Conf. Earthq. Eng., Vol. 2, Rome, Italy, June 1973, pp. 1792-1795.
 39. Padilla-Mora, R., "Nonlinear Response of Framed Structures to Two-Dimensional Earthquake Motion," Ph.D. Thesis, University of Illinois at Urbana-Champaign, Illinois, June 1974.
 40. Penzien, J., "Elasto-Plastic Response of Idealized Multi-Story Structures Subjected to a Strong Motion Earthquake," Proc. of the 2nd Wld. Conf. Earthq. Eng., Vol. 11, Tokyo and Kyoto, Japan, July 1960, pp. 739-760.
 41. Penzien, J., and Watabe, M., "Characteristics of 3-Dimensional Earthquake Ground Motions," Earthq. Eng. Struct. Dyn., Vol. 3, 1975, pp. 365-373.
 42. Plastic Design in Steel- A Guide and Commentary, Manual 41, 2nd Ed., Welding Research Council and ASCE, 1971, pp. 165-166.
 43. Riddell, R., and Newmark, N.M., "Statistical Analysis of the Response of Nonlinear Systems subjected to Earthquakes," Civil Engineering Studies, Structural Research Series No. 468, University of Illinois, Urbana, Illinois, 1979.
 44. Rosenblueth, E., and Contreras, H., "Approximate Design for Multicomponent Earthquakes," J. Eng. Mech. Div., ASCE, Vol. 103, No. EM5, October 1977, pp. 881-893.
 45. Shibata, A., Onose, J., and Shiga, T., "Torsional Response of Buildings to Strong Earthquake Motions," Proc. of the 4th Wld. Conf. Earthq. Eng., Vol. 2, Santiago, Chile, January 1969, pp. A4-123 to A4-138.
 46. Takizawa, H., and Aoyama, H., "Biaxial Effects in Modelling Earthquake Response of R/C Structures," Earthq. Eng. Struct. Dyn., Vol. 4, 1976, pp. 523-552.
 47. Tanabashi, R., "Nonlinear Transient Vibrations of Structures," Proc. of the 2nd Wld. Conf. Earthq. Eng., Vol. 11, Tokyo and Kyoto, Japan, July 1960, pp. 1223-1238.

48. Tentative Provisions for the Development of Seismic Regulations for Buildings, ATC 3-06, Applied Technology Council, Palo Alto, California, 1978.
49. Tso, W.K., and Bozorgnia, Y., "Effective Eccentricity for Inelastic Seismic Response of Buildings," (submitted), Earthq. Eng. Struct. Dyn.
50. Tso, W.K., and Dempsey, K.M., "Seismic Torsional Provisions for Dynamic Eccentricity," Earthq. Eng. Struct. Dyn., Vol. 8, 1980, pp. 275-289.
51. Tso, W.K., and Sadek, A.W., "Inelastic Response of Eccentric Structures," Proc. of the 4th Canad. Conf. Earthq. Eng., Vancouver, Canada, 1983, pp. 261-270.
52. Tso, W.K., and Sadek, A.W., "Inelastic Response of Eccentric Buildings Subjected to Bidirectional Ground Motions," Proc. of the 8th Wld. Conf. Earthq. Eng., Vol. IV, San Francisco, California, 1984, pp. 203-210.
53. Tso, W.K., and Sadek, A.W., "Inelastic Seismic Response of Simple Eccentric Structures," Earthq. Eng. Struct. Dyn., Vol. 13, 1985, pp. 255-269.
54. Veletsos, A.S., and Newmark, N.M., "Effect of Inelastic Behavior on the Response of Simple Systems to Earthquake Motions," Proc. of the 2nd Wld. Conf. Earthq. Eng., Vol. II, Tokyo and Kyoto, Japan, July 1960, pp. 885-912.
55. Veletsos, A.S., Newmark, N.M., and Chelapati, C.V., "Deformation Spectra for Elastic and Elastoplastic Systems Subjected to Ground Shock and Earthquake Motions," Proc. of the 3rd Wld. Conf. Earthq. Eng., Vol. II, Auckland and Wellington, New Zealand, January 1965, pp. 663-682.
56. Wen, R.K., and Farhoomand, F., "Dynamic Analysis of Inelastic Space Frames," J. Eng. Mech. Div., ASCE, Vol. 96, No. EM5, October 1970, pp. 667-686.
57. Wilson, E.L., Der Kiureghian, A., and Bayo, E.P., "A Replacement for the SRSS Method in Seismic Analysis," Earthq. Eng. Struct. Dyn., Vol. 9, 1981, pp. 187-194.
58. Yamazaki, Y., "Inelastic Torsional Response of Structures Subjected to Earthquake Ground Motions," Report No. UCB/EERC-80/07, Earthquake Engineering Research Center, University of California, Berkeley, California, April 1980.

APPENDIX A

DERIVATION OF STIFFNESS MATRIX $[S]^{ep}$ OF AN ELASTO-PLASTIC ELEMENT WITH INTERACTION EFFECT

The following formulation was originally presented by Nigam (34) and is given here for completeness.

The incremental forces $\Delta\{Q\}$ and incremental displacements $\Delta\{q\}$ are related by the general element stiffness matrix $[S]$ as follows

$$\Delta\{Q\} = [S] \Delta\{q\} \quad (A.1)$$

The incremental displacement of an element undergoing inelastic deformations can be decomposed into elastic and plastic components

$$\Delta\{q\} = \Delta\{q\}^e + \Delta\{q\}^p \quad (A.2)$$

The elastic component $\Delta\{q\}^e$ obeys Hooke's law and it is responsible for changing the force level as given by

$$\Delta\{Q\} = [S]^e \Delta\{q\}^e \quad (A.3)$$

where $[S]^e$ is the elastic stiffness matrix of the element and is given by

$$[S]^e = \begin{bmatrix} k_1 & 0 \\ 0 & k_2 \end{bmatrix} \quad (A.4)$$

where k_1 and k_2 are the element elastic stiffnesses along its orthogonal principal axes of resistance.

The plastic component $\Delta\{q\}^p$ follows the plastic flow rule. For a stable plastic material, there exists a yield curve ϕ whose expression

is a function of the generalized forces simultaneously acting on the element, namely Q_1 and Q_2 . An associated flow rule states that the incremental plastic displacement vector $\Delta\{q\}^P$ lies along the outer normal to the yield curve, or in a mathematical form

$$\Delta\{q\}^P = \lambda \left\{ \frac{\partial \phi}{\partial \{Q\}} \right\} \quad (A.5)$$

where λ is a positive scalar. Moreover, for a perfectly plastic material, the incremental force vector $\Delta\{Q\}$ should be tangential to the yield curve since the growth or the translation of the yield curve in the force space is not allowed. Hence the normality rule holds true and it states that the inner product of $\Delta\{q\}^P$ and $\Delta\{Q\}$ should vanish or

$$(\Delta\{Q\}, \Delta\{q\}^P) = 0 \quad (A.6)$$

In other words, the increments of the plastic displacement and the force vector are orthogonal.

Rewriting Eq (A.3) as follows

$$\Delta\{Q\} = [S]^e (\Delta\{q\} - \Delta\{q\}^P) \quad (A.7)$$

and substituting Eqs (A.7) and (A.5) into the normality rule in Eq (A.6), one can obtain an expression for the scalar λ

$$\lambda = \frac{\Delta\{q\}^T [S]^e \left\{ \frac{\partial \phi}{\partial \{Q\}} \right\}}{\left\{ \frac{\partial \phi}{\partial \{Q\}} \right\}^T [S]^e \left\{ \frac{\partial \phi}{\partial \{Q\}} \right\}} \quad (A.8)$$

Substituting Eq (A.5) and Eq (A.8) into Eq (A.7) gives

$$\Delta\{Q\} = [S]^e \left\{ \Delta\{q\} - \frac{\Delta\{q\}^T [S]^e \left\{ \frac{\partial \phi}{\partial \{Q\}} \right\}}{\left\{ \frac{\partial \phi}{\partial \{Q\}} \right\}^T [S]^e \left\{ \frac{\partial \phi}{\partial \{Q\}} \right\}} \left\{ \frac{\partial \phi}{\partial \{Q\}} \right\} \right\} \quad (A.9)$$

Performing the inner multiplication and rearranging, Eq (A.9) becomes

$$\Delta\{Q\} = [S]^e - \frac{1}{k_1 \left(\frac{\partial \phi}{\partial Q_1} \right)^2 + k_2 \left(\frac{\partial \phi}{\partial Q_2} \right)^2} \begin{bmatrix} k_1^2 \left(\frac{\partial \phi}{\partial Q_1} \right)^2 & k_1 k_2 \left(\frac{\partial \phi}{\partial Q_1} \right) \left(\frac{\partial \phi}{\partial Q_2} \right) \\ k_1 k_2 \left(\frac{\partial \phi}{\partial Q_1} \right) \left(\frac{\partial \phi}{\partial Q_2} \right) & k_2^2 \left(\frac{\partial \phi}{\partial Q_2} \right)^2 \end{bmatrix} \Delta\{q\} \quad (A.10)$$

or

$$\Delta\{Q\} = [S]^{ep} \Delta\{q\}$$

where

$$[S]^{ep} = [S]^e - [S]^p \quad (A.11)$$

and

$$[S]^p = \frac{1}{k_1 \left(\frac{\partial \phi}{\partial Q_1} \right)^2 + k_2 \left(\frac{\partial \phi}{\partial Q_2} \right)^2} \begin{bmatrix} k_1^2 \left(\frac{\partial \phi}{\partial Q_1} \right)^2 & k_1 k_2 \left(\frac{\partial \phi}{\partial Q_1} \right) \left(\frac{\partial \phi}{\partial Q_2} \right) \\ k_1 k_2 \left(\frac{\partial \phi}{\partial Q_1} \right) \left(\frac{\partial \phi}{\partial Q_2} \right) & k_2^2 \left(\frac{\partial \phi}{\partial Q_2} \right)^2 \end{bmatrix} \quad (A.12)$$

APPENDIX B
NUMERICAL INTEGRATION

B.1 NUMERICAL INTEGRATION :

The equations of motion of a system whose deformation is described by displacement vector $\{u\}$ and acted upon by $\{P(t)\}$ are given by

$$[M]\{\ddot{u}\} + [C]\{\dot{u}\} + \{F\} = \{P(t)\} \quad (B.1)$$

where $[M]$ and $[C]$ are the mass and damping matrices respectively, and $\{F\}$ is the restoring force vector. Equation (B.1) can be written in incremental form as follows.

$$[M]\Delta\{\ddot{u}\} + [C]\Delta\{\dot{u}\} + [K]\Delta\{u\} = \Delta\{P(t)\} \quad (B.2)$$

where $[K]$ is the tangential stiffness matrix. The equations of motion can be numerically solved assuming the properties of the structure to remain unchanged during a short time interval Δt . Assuming the acceleration vector to vary linearly within the time increment, the following recurrence relationships can be obtained

$$\Delta\{\ddot{u}\} = (6/\Delta t^2)\Delta\{u\} - (6/\Delta t)\{\dot{u}(t)\} - 3\{\ddot{u}(t)\} \quad (B.3)$$

$$\Delta\{\dot{u}\} = (3/\Delta t)\Delta\{u\} - 3\{\dot{u}(t)\} - (\Delta t/2)\{\ddot{u}(t)\} \quad (B.4)$$

Substituting Eq (B.3) and Eq (B.4) into Eq (B.2), the following pseudo static equilibrium equation is obtained

$$[K^*]\Delta\{u\} = \Delta\{P^*\} \quad (B.5)$$

where $[K^*]$ is the effective dynamic stiffness matrix and $\Delta\{P^*\}$ is the

effective load vector and they are given by

$$[K^*] = [K] + (6/\Delta t^2)[M] + (3/\Delta t)[C] \quad (B.6)$$

$$\begin{aligned} \Delta(P^*) = \Delta(P) + ((6/\Delta t)(\dot{u}(t)) + 3(\ddot{u}(t)))[M] \\ + (3(\dot{u}(t)) + (\Delta t/2)(\ddot{u}(t)))[C] \end{aligned} \quad (B.7)$$

The change in displacement vector, $\Delta(u)$, is obtained by solving the set of algebraic equations in Eq (B.5). Then using Eq (B.4), the change in the velocity vector, $\Delta(\dot{u})$, can be obtained. The total displacement and velocity vectors at the end of the current time step are given by

$$\{u(t+\Delta t)\} = \{u(t)\} + \Delta(u)$$

$$\{\dot{u}(t+\Delta t)\} = \{\dot{u}(t)\} + \Delta(\dot{u})$$

To avoid the accumulation of the error due to considering the equilibrium of the incremental forces, the acceleration vector $\{\ddot{u}(t+\Delta t)\}$ can be found so as to satisfy the equilibrium of total forces as follows

$$\{\ddot{u}(t+\Delta t)\} = [M]^{-1}(\{P(t+\Delta t)\} - \{F_D(t+\Delta t)\} - \{F(t+\Delta t)\}) \quad (B.8)$$

where $\{F_D(t+\Delta t)\}$ and $\{F(t+\Delta t)\}$ are the total damping and restoring forces, respectively, at the end of the time step.

B.2 STATE TRANSITIONS IN ELEMENTS WITH INTERACTION EFFECT INCLUDED :

(i) ELASTIC TO PLASTIC

The element is said to change from the elastic state to the plastic state if the value of ϕ , based on the forces at the end of the time step, is equal to or larger than unity. Should ϕ become larger than unity, which may very well occur, the incremental displacement vector $\Delta(u)$ is applied in two portions, the first portion $\epsilon\Delta(u)$ is applied such that the element will just reach yield and the second

portion $(1-\epsilon)\Delta(u)$ is then applied assuming the element in the plastic range.

(ii) PLASTIC TO PLASTIC

To ensure the continuation of the plastic loading, two conditions are examined.

1. The incremental plastic work Δw^P should be positive. Δw^P is a scalar quantity given by the scalar product of the total force vector $\{f(t)\}$ and the incremental plastic component of displacement vector $\Delta\{u^P\}$, or in short

$$\Delta w^P = \{f(t)\}^T \Delta\{u^P\}$$

$$\Delta w^P > 0$$

2. For a specified displacement increment $\Delta\{u\}$, a force increment $\Delta\{f\}^e$ is calculated assuming elastic conditions, i.e.

$$\Delta\{f\}^e = [S]^e \Delta\{u\}$$

If the new force vector $\{f(t)\} + \Delta\{f\}^e$ moves outside the yield curve, then the elastic state is incorrect and the plastic loading should continue. Equivalently, continued plastic loading occurs if

$$\{n\}^T \Delta\{f\}^e > 0$$

where $\{n\}$ is the vector normal to the yield curve at the position of the force vector (see Fig (B.1)).

Implementing condition 1 only, as suggested in (34,58), was found in the course of this study to require very small values of time interval Δt (0.001 sec) in order to prevent the occurrence of premature unloading off the yield curve. On the other hand, implementing both conditions was found to be efficient in eliminating the possibility of

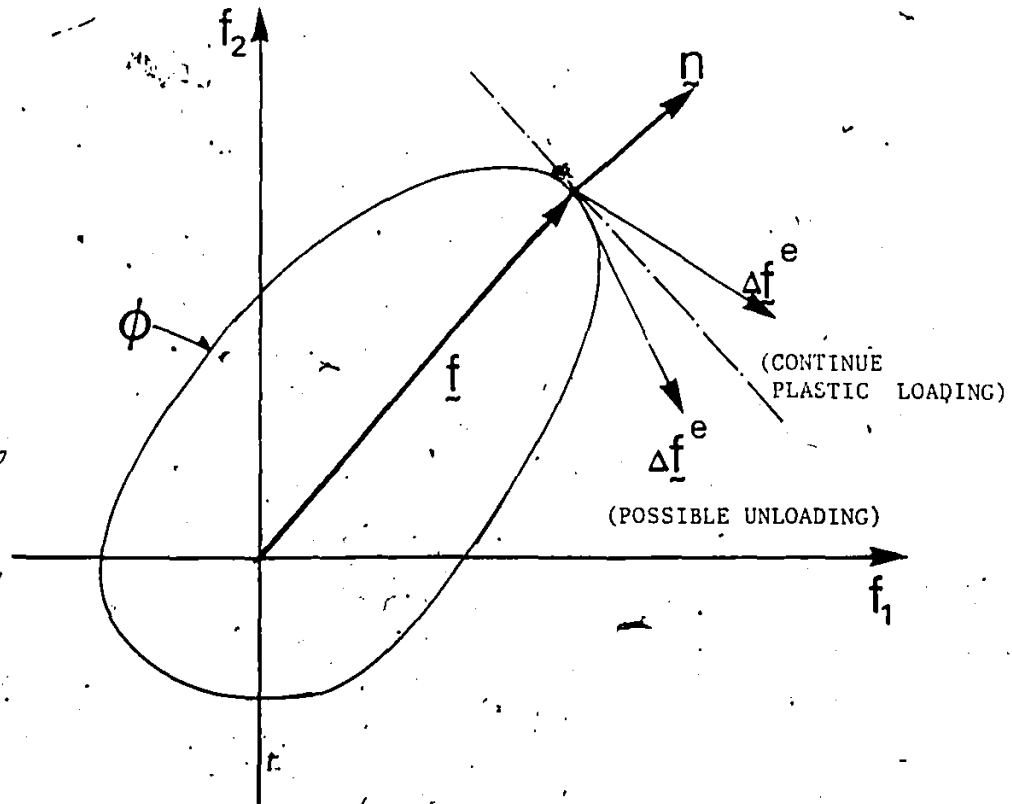


Fig (B.1) positions of vector $\Delta \underline{f}^e$ to check unloading

premature unloading even at a larger time interval $\Delta t = 0.02$ sec. Hence, the following conditional states are implemented in the algorithm

Plastic-Plastic:

$$\Delta w^P \geq 0 \quad \text{AND/OR} \quad \{n\}^T \Delta \{f\}^e \geq 0 \quad (B.9)$$

Plastic-Elastic (Unloading):

$$\Delta w^P < 0 \quad \text{AND} \quad \{n\}^T \Delta \{f\}^e < 0 \quad (B.10)$$

B.3 EQUILIBRIUM ITERATIONS :

In the process of the numerical integration, a number of factors give rise to unbalanced forces. An iterative scheme is required to keep these forces within acceptably small values. The following describes significant sources of such forces.

1. The step-by-step integration scheme assumes the properties of the structure to remain unchanged within the time interval of integration. However, in time increments in which the stiffness of an element changes due to yielding or unloading, equilibrium is disturbed and unbalanced forces are introduced.

2. When the element is said to be plastic, the change in the force vector due to a specified change in displacement is evaluated using the updated stiffness matrix $[S]^{ep}$ as follows

$$\Delta \{f\} = [S]^{ep} \Delta \{v\}$$

The tip of the new total force vector may very well lie outside the yield curve, in other words

$$\phi(\{f(t)\} + \Delta \{f\}) > 1$$

Since these situations are not admissible, the force vector needs to be

pulled back onto the yield curve. This in turn will introduce unbalance in the forces equilibrium.

The resulting unbalanced forces are treated using the Newton-Raphson iteration scheme. The iteration algorithm can be written as follows

$$[K^*] \Delta(u)^{(k+1)} = \Delta(F_U)^{(k)} \quad (B.11)$$

where $\Delta(u)^{(k+1)}$ is the change of displacement vector due to applying the unbalanced forces vector $\Delta(F_U)^{(k)}$ resulting from the k th iteration. The iteration is repeated until the following condition is satisfied

$$\|\Delta(F_U)^{(k)}\| \leq 0.001 \quad (B.12)$$

Two cycles of iterations were found sufficient for this purpose. The true incremental displacement vector is given by

$$\Delta(u) = \Delta(u)^0 + \sum_{k=1}^N \Delta(u)^{(k)} \quad (B.13)$$

where

$$\Delta(u)^0 = [K^*]^{-1} \Delta(P^*) \quad (B.14)$$

B.4 VERIFICATION OF THE PROGRAM :

The developed program is verified by comparing the numerical results of sinusoidal excitation of elasto-plastic systems with and without interaction against corresponding analytical results presented in (34). The comparison is shown in Fig (B.7). Based on the excellent agreement observed between the numerical and analytical results, the developed program is considered reliable.

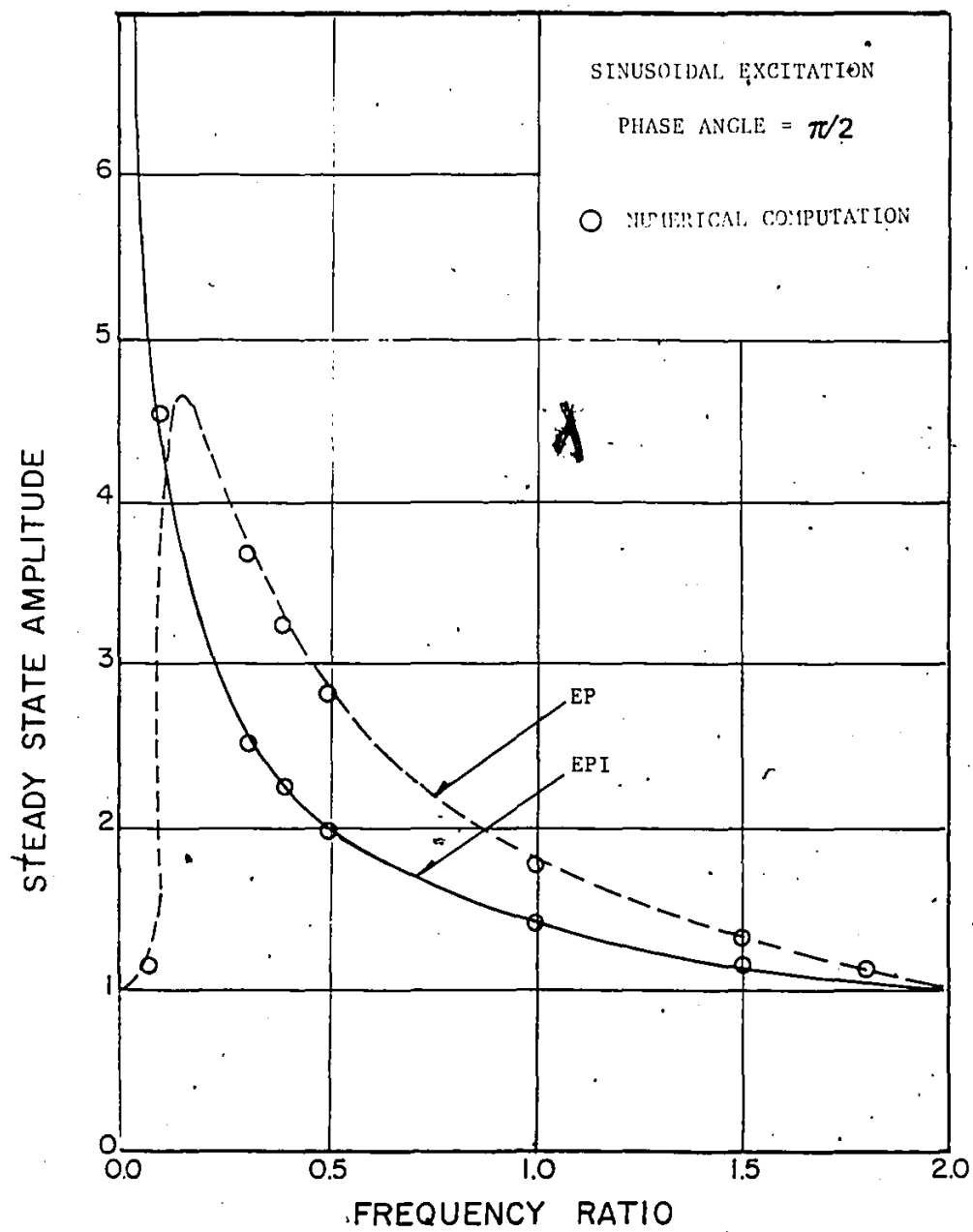


Fig (B.2) Comparison of Numerical Results and Analytical Results in Ref(34)